Encapsulation in liposomes of active agents in free- and cyclodextrin/guest inclusion complex forms : applications to essential oil constituents

Zahraa Hammoud

▶ **To cite this version:**

Zahraa Hammoud. Encapsulation in liposomes of active agents in free- and cyclodextrin/guest inclusion complex forms : applications to essential oil constituents. Biochemistry, Molecular Biology. Université de Lyon, 2020. English. NNT : 2020LYSE1263 . tel-03613194

HAL Id: tel-03613194
https://theses.hal.science/tel-03613194

Submitted on 18 Mar 2022

HAL is a multi-disciplinary open access archive for the deposit and dissemination of scientific research documents, whether they are published or not. The documents may come from teaching and research institutions in France or abroad, or from public or private research centers.

L'archive ouverte pluridisciplinaire **HAL**, est destinée au dépôt et à la diffusion de documents scientifiques de niveau recherche, publiés ou non, émanant des établissements d'enseignement et de recherche français ou étrangers, des laboratoires publics ou privés.

N°d'ordre NNT :
2020LYSE1263

THESE de DOCTORAT DE L'UNIVERSITE DE LYON
opérée au sein de
L'Université Claude Bernard Lyon 1

Ecole Doctorale N° 206
Ecole Doctorale de Chimie de Lyon
Spécialité de doctorat : Pharmacotechnique
Discipline : Biochimie/Biotechnologie

Soutenue publiquement le 07/12/2020, par :
Zahraa HAMMOUD

Encapsulation dans les liposomes d'agents actifs libres et sous forme de complexe d'inclusion dans les cyclodextrines : applications aux constituants d'huiles essentielles

Devant le jury composé de :

M. JADA Amane, CR1-HDR-CNRS, Institut de Sciences Des Matériaux De Mulhouse	Rapporteur
Mme. GOUHIER Geraldine, Pr, Université de Rouen	Rapporteure
M. FESSI Hatem, Pr, Université Lyon 1	Examinateur
M. EL-RASSY Houssam, Pr. Associé, Université Américaine de Beyrouth	Examinateur
Mme. MEDIOUNI BEN JEMAA Jouda, Pr, Université de Carthage	Examinatrice
Mme. KHREICH Nathalie, Pr. Associé, Université Libanaise	Examinatrice
M. ELAISSARI Abdelhamid, DR-CNRS, Université Lyon 1	Directeur de thèse
Mme. GREIGE-GERGES Hélène, Pr, Université Libanaise	Directrice de thèse

Université Claude Bernard - LYON 1

Administrateur provisoire de l'Université	M. Frédéric FLEURY
Président du Conseil Académique	M. Hamda BEN HADID
Vice-Président du Conseil d'Administration	M. Didier REVEL
Vice-Président du Conseil des Etudes et de la Vie Universitaire	M. Philippe CHEVALLIER
Vice-Président de la Commission de Recherche	M. Jean-François MORNEX
Directeur Général des Services	M. Pierre ROLLAND

COMPOSANTES SANTE

Département de Formation et Centre de Recherche en Biologie Humaine	Directrice : Mme Anne-Marie SCHOTT
Faculté d'Odontologie	Doyenne : Mme Dominique SEUX
Faculté de Médecine et Maïeutique Lyon Sud - Charles Mérieux	Doyenne : Mme Carole BURILLON
Faculté de Médecine Lyon-Est	Doyen : M. Gilles RODE
Institut des Sciences et Techniques de la Réadaptation (ISTR)	Directeur : M. Xavier PERROT
Institut des Sciences Pharmaceutiques et Biologiques (ISBP)	Directrice : Mme Christine VINCIGUERRA

COMPOSANTES & DEPARTEMENTS DE SCIENCES & TECHNOLOGIE

Département Génie Electrique et des Procédés (GEP)	Directrice : Mme Rosaria FERRIGNO
Département Informatique	Directeur : M. Behzad SHARIAT
Département Mécanique	Directeur M. Marc BUFFAT
Ecole Supérieure de Chimie, Physique, Electronique (CPE Lyon)	Directeur : Gérard PIGNAULT
Institut de Science Financière et d'Assurances (ISFA)	Directeur : M. Nicolas LEBOISNE
Institut National du Professorat et de l'Education	Administrateur Provisoire : M. Pierre CHAREYRON
Institut Universitaire de Technologie de Lyon 1	Directeur : M. Christophe VITON
Observatoire de Lyon	Directrice : Mme Isabelle DANIEL
Polytechnique Lyon	Directeur : Emmanuel PERRIN
UFR Biosciences	Administratrice provisoire : Mme Kathrin GIESELER
UFR des Sciences et Techniques des Activités Physiques et Sportives (STAPS)	Directeur : M. Yannick VANPOULLE
UFR Faculté des Sciences	Directeur : M. Bruno ANDRIOLETTI

Acknowledgements

Before everything, I would like to thank GOD for granting me the patience, strength, good health and determination in order to finish this work. Indeed, this thesis becomes a reality with the kind support and help of many individuals. I would like to extend my sincere thanks to all of them.

Words cannot express how grateful I am to my supervisor Pr. Hélène GREIGE-GERGES for her professional guidance, discussions, valuable suggestions, encouragement and support during these three years. It is my tremendous honor to complete this work under her supervision where her advice has extended far beyond the technical field. I am especially grateful for her confidence and the freedom she gave me to do this work. Also, I would like to express great gratitude to Pr. Abdelhamid ELAISSARI for accepting the responsibility to supervise my thesis at the University of Lyon 1. I wish to thank him from the core of my heart for his friendship, kindness, encouragement, and support. It was a great pleasure to work under his supervision.

I am deeply grateful to all members of the jury for agreeing to read the manuscript and to participate in the defense of this thesis. I would like to thank Pr. Geraldine GOUHIER and Pr. Amane JADA who accepted to be reviewers for this work. Many thanks also to Pr. Hatem FESSI, Pr. Houssam EL-RASSY, Pr. Jouda MEDIOUNI BEN JEMAA, and Pr. Nathalie KHREICH for examining my PhD manuscript.

I extend my sincere thanks to all members of the Doctoral School of Science and Technology (Hadath, Lebanon), Doctoral School of Science and Technology (Fanar, Lebanon) and the Laboratory of Automation and Engineering Processes (LAGEPP) (Lyon, France) for their help and support. Additionally, I am immensely grateful to Pr. Sophie Fourmentin for her kind support in conducting the release studies, to Dr. Riham Gharib for her help in conducting most of the experiments and to Dr.

Lizette Auezova for her kind help in proofreading the first review article presented in this manuscript. Moreover, I would like to thank all of my colleagues: Ghenwa, Sanaa, Carla, Tracy, Lamia, Aline, Sara, Samar, Joyce, Elissa, Jad and Mohammad for their welcome, help and support during my thesis study.

My deep appreciation goes to the "Agence Universitaire de la Francophonie (AUF), Projet de Coopération Scientifique Inter-Universitaire (PCSI) for funding my travel and stay in France. My thanks also go to the "Islamic Center Association for Guidance and Higher Education" for providing me the doctoral scholarship.

Finally, I am highly indebted to my family members (my father, my mother, my sisters and my brother) for their unbelievable support, sacrifices, prayers, unconditional love and care.

Table of contents

Résumé

Les huiles essentielles présentent des fonctions biologiques importantes et sont connues comme des agents antimicrobiens et des insecticides. Leurs diverses applications sont limitées par leur volatilité, leur faible solubilité dans l'eau, et leur instabilité chimique. Pour pallier à ces inconvénients précités, notre travail de thèse se concentre sur la préparation et la caractérisation des liposomes conventionnels et des liposomes contenant des complexes d'inclusion cyclodextrine-composant d'huiles essentielles (DCLs). La chromatographie liquide à haute performance et la méthode d'extraction d'espace de tête multiple ont été utilisées pour la caractérisation de l'encapsulation et de la libération d'huiles essentielles, respectivement. L'effet de la structure chimique des composants des huiles essentielles sur les caractéristiques des liposomes et des DCLs, ainsi que leur solubilité dans l'eau, leur coefficient de partage octanol/eau (log P), et la constante de Henry sont investigués. Le phospholipide de soja insaturé (Lipoid S100) et le cholestérol (CHOL) ont été utilisés pour préparer les liposomes par la méthode d'injection d'éthanol. Une série des huiles essentielles (alpha-pinène, camphor, estragole, eucalyptol, isoeugénol, pulegone, terpinéol, et thymol) est sélectionnée. Nos resultats ont montré que l'incorporation dans les liposomes conventionnels est favorisée par la présence d'un groupement hydroxyle, une faible constante de Henry, et une faible solubilité aqueuse. La taille et la composition des vésicules affectent la libération des molécules des liposomes. D'un autre côté, différents paramètres conditionnent l'encapsulation dans les DCLs comme la présence d'un groupement propényl ou d'un groupement hydroxyle, et la valeur élevée de log P d'un constituant d'huile essentielle. En outre, une relation négative a été établie entre l'efficacité d'encapsulation des molécules et le taux de cholestérol membranaire dans les vésicules de type DCLs. La libération d'huiles essentielles des DCL est contrôlée par leur efficacité d'encapsulation dans les formulations. De plus, l'effet de l'hydroxypropyl-β-cyclodextrine (HP-β-CD) et des complexes d'inclusion cyclodextrine-huiles essentielle sur la taille et la composition membranaire des liposomes composés de Lipoid S100 ou Phospholipon 90H a été évalué.

Les résultats ont montré que l'HP-β-CD est capable de moduler la distribution de taille des vésicules. Dans nos conditions expérimentales, ce type de CD réduit l'incorporation des phospholipides dans les deux types de membranes étudiées par contre, il réduit l'incorporation de CHOL uniquement dans les membranes formées de Phospholipon 90H et de CHOL. En conclusion, les liposomes conventionnels et les DCL pourraient être considérés comme des systèmes prometteurs d'encapsulation des huiles essentielles. Les formulations développées dans la présente étude pourraient être considérées comme futurs ingrédients dans des préparations alimentaires, agricoles et pharmaceutiques.

Mots clés : complexe d'inclusion, drug-in-cyclodextrin-in-liposomes, encapsulation, huiles essentielles, hydroxypropyl-β-cyclodextrine, libération; liposomes conventionnels, membrane.

Abstract

Essential oil (EO) components possess important biological functions including antimicrobial and insecticidal properties. However, their industrial application is limited due to their volatility, poor water solubility and chemical instability. To solve the aforementioned drawbacks, our thesis work focuses on the preparation and characterization of conventional liposomes (CLs) and drug-in-cyclodextrin-in-liposomes (DCLs) carrying several EO components. Characterization of EO encapsulation and release was performed using High Performance Liquid Chromatography and multiple headspace extraction method, respectively. The effect of the chemical structure, the aqueous solubility, the octanol/ water partition coefficient (log P), and the Henry's law constant (H_c) on the characteristics of CLs and DCLs was investigated. The non-hydrogenated soybean phospholipid (Lipoid S100) was used in combination with cholesterol (CHOL) to prepare the liposomes by the ethanol injection method. A series of EO components was considered including: α-pinene, camphor, estragole, eucalyptol, isoeugenol, pulegone, terpineol, and thymol. Entrapment in CLs was more efficient for the EO components presenting a hydroxyl group in their structure and for those exhibiting a low H_c as well as a low aqueous solubility value. The size and the composition of vesicles were shown to influence the release of components from liposomes. The factors related to EO properties that favor their encapsulation in DCLs were: the presence of a propenyl tail or a hydroxyl group in the structure as well as possessing a high log P value. Besides, a negative relationship was established between the encapsulation efficiency of EO components into DCLs and the CHOL membrane content of vesicles. The release of components from DCLs depends on their encapsulation efficiency into the formulations. Moreover, the interaction of hydroxypropyl-β-cyclodextrin (HP-β-CD) and HP-β-CD/drug inclusion complex with Lipoid S100:CHOL- and Phospholipon 90H:CHOL liposomes was studied where their effects on the size and the membrane composition of vesicles were examined. Results demonstrated that the incorporation of

HP-β-CD in the internal aqueous compartment of the liposomes modified the size distribution of vesicles. In addition, HP-β-CD reduced phospholipids incorporation into both types of membranes while reduced CHOL incorporation only for Phospholipon 90H:CHOL vesicles. In conclusion, liposomes and DCLs could be considered as promising carrier systems for EO components. The developed formulations may find wide applications in food, agricultural and pharmaceutical fields.

Keywords: conventional liposomes; drug-in-cyclodextrin-in-liposomes; encapsulation; essential oil component; hydroxypropyl-β-cyclodextrin; inclusion complex; membrane; release.

List of abbreviations

Alpha-PIN	Alpha-pinene
CAM	Camphor
CD	Cyclodextrin
CHOL	Cholesterol
CL	Conventional liposome
DCL	Drug-in-cyclodextrin-in-liposome
DPPC	Dipalmitoylphosphatidylcholine
EE	Encapsulation efficiency
EO	Essential oil
EST	Estragole
EUC	Eucalyptol
Hc	Henry's law constant
HP-β-CD	Hydroxypropyl-ß-cyclodextrine
IR	Incorporation rate
ISOEUG	Isoeugenol
K_f	Formation constant
LR	Loading rate
MT	Monoterpene
PL	Phospholipid
PP	Phenylpropene
PUL	Pulegone
TER	Terpineol
THY	Thymol

General Introduction

Insect pests cause heavy damage to agricultural crops and stored products, thereby leading to severe economic loss. Controlling of these insects relies on the use of synthetic insecticides such as organophosphates and pyrethroids. The overuse of synthetic pesticides has caused significant environmental damage and serious health hazards to humans and animals due to their toxic and non-biodegradable properties and to the accumulation of residues in soil, water and food. Thus, the number of studies focusing on alternatives to synthetic pesticides has increased in recent years. Natural insecticides based on essential oils (EOs) appear to be suitable for controlling insect pests due to their eco-friendly and biodegradable nature, effectiveness, multiple modes of action, and low toxicity to non-target organisms (Mossa, 2016; Pavela and Benelli, 2016).

EOs are volatile, natural and complex compounds characterized by a strong odor and are formed by aromatic plants as secondary metabolites. In the last few decades, much more importance has been given to EOs from different plant species due to the increasing interest in their antimicrobial, antifungal, insecticidal and antioxidant properties. Hence, they have gained remarkable attention in the food, cosmetics, agricultural and pharmaceutical industries (Bakkali et al., 2008). In this work, the phenylpropanoids (PP): estragole (EST) and isoeugenol (ISOEUG), and the monoterpenes (MTs): alpha-pinene (α-PIN), camphor (CAM), eucalyptol (EUC), pulegone (PUL), terpineol (TER) and thymol (THY) were considered. The selected EO components differ with respect to their aqueous solubility, octanol/water partition coefficient (log P) and Henry's law constant (Hc) values. According to the literature (Pubchem), log P values vary between 2.38 and 4.83 for CAM and α-PIN, respectively. Their aqueous solubility ranges between 2.5 mg/L for α-PIN and 7100 mg/L for TER. Despite their remarkable properties, their low aqueous solubility, high volatility and sensitivity to light, temperature and oxygen limit their wide applications (Turek and Stintzing, 2013). The encapsulation of EO components in carrier systems like cyclodextrins, liposomes and drug-in-cyclodextrin-in-liposomes can

be considered as a potential solution to overcome the drawbacks of components, thereby extending their shelf life and activity.

Cyclodextrins (CDs) are cyclic oligosaccharides that possess a truncated shape with a hydrophilic external surface and a hydrophobic cavity. Thus, they can encapsulate guests partially or entirely leading to the formation of an inclusion complex. The native CDs α-, β-, and γ-CDs consist of six, seven, or eight subunits of α-1,4-linked D-glucopyranose, respectively. However, their use is generally limited due to their low aqueous solubility. Chemical modification of CDs allows obtaining derivatives with improved aqueous solubility compared to the native CDs (Szejtli, 1998). We specifically selected, herein, hydroxypropyl-β-CD (HP-β-CD) owing to its high aqueous solubility (> 500 mg/mL) and strong complexing ability with the selected EO components. Previous studies investigated the formation of inclusion complexes between HP-β-CD and the selected PPs and MTs and determined the stability constants of these complexes (Ciobanu et al., 2013; Kfoury et al., 2014b, 2014a).

Liposomes are spherical vesicles consisting of one or more lipid bilayers surrounding an inner aqueous compartment. This structure makes liposomes suitable for encapsulating both hydrophilic and hydrophobic molecules. Water-soluble drugs can be encapsulated in the inner aqueous compartment, whereas lipid-soluble drugs can be embedded within the liposome bilayers (Gharib et al., 2015). However, the incorporation of a highly hydrophobic drug into lipid bilayers may lead to the alteration of the membrane integrity, causing a rapid release of the drug from the bilayer (Kirby and Gregoriadis, 1983).

Liposomes and CDs are viewed as attractive materials by the food, cosmetics and pharmaceutical industries. They have been extensively used to improve the aqueous solubility, the bioavailability, and the stability of poorly water-soluble drugs. Moreover, they could allow a controlled release of bioactive

agents (Del Valle, 2004; Kfoury et al., 2016; Reza Mozafari et al., 2008; Sebaaly et al., 2015; Zylberberg and Matosevic, 2016). Nevertheless, CDs are able to extract lipid components from biomimetic and biological membranes. Also, they can influence the fluidity and permeability of membranes under definite conditions. The CD effect on membranes is mediated by several factors including the membrane structure and composition as well as the CD type and the CD concentration (Denz et al., 2016; Hatzi et al., 2007; Ohvo-Rekilä et al., 2000; Puglisi et al., 1996).

The drug-in-cyclodextrin-in-liposome" (DCLs) system was proposed by McCormack B and Gregoriadis G in 1994 (McCormack and Gregoriadis, 1994). DCLs are based on the entrapment of CD/drug inclusion complexes in the inner aqueous core of liposomes. This system combines the advantages of both carriers (CD and liposome) and limits their disadvantages (Gharib et al., 2015).

Several studies have already prepared and characterized EO-loaded liposomes and DCLs. However, to the best of our knowledge, the effect of drug properties on liposome and DCL characteristics has not been previously discussed. Furthermore, the factors that influence the encapsulation of EO components into liposomes and DCLs cannot be estimated from literature data since the liposome formulations, which were characterized in the different studies, were prepared under different experimental conditions. Hence, the first part in this work aims to investigate the impact of the chemical structure, the aqueous solubility and the log P values of EO components on their encapsulation in liposomes and DCLs as well as on their release from these systems. For this purpose, conventional liposome (CL) and DCL formulations containing EST, EUC, ISOEUG, PUL, TER and THY were prepared by the ethanol injection method under the same experimental conditions. We used spectroscopic, analytical and microscopic techniques to characterize the various formulations. In the next step, the EO components α-PIN and CAM were considered due to their interesting insecticidal properties. Their encapsulation into

CLs and DCLs was investigated, and the best encapsulation system could be later selected for its potential use in agriculture and food products.

This manuscript is divided into four chapters. In the first chapter, we review the literature concerning the interaction of CDs with biomimetic and biological membranes. The second chapter presents an overview of the various systems used for the delivery of natural insecticides and their characteristics. The third chapter consists of two research articles. The first article discusses the impact of the chemical structure and the physicochemical properties of EO components on CL characteristics. The second article sheds light on the factors influencing DCL characteristics. The fourth chapter also consists of two research articles. The first one presents the results regarding the characteristics of liposomes and DCLs loading α-PIN. The second one concerns the characteristics of CAM-loaded liposomes and DCLs. This manuscript ends with a general discussion and perspectives for continuing this work.

References

Bakkali, F., Averbeck, S., Averbeck, D., Idaomar, M., 2008. Biological effects of essential oils – A review. Food Chem. Toxicol. 46, 446–475.

Ciobanu, A., Landy, D., Fourmentin, S., 2013. Complexation efficiency of cyclodextrins for volatile flavor compounds. Food Res. Int. 53, 110–114.

Del Valle, E.M.M., 2004. Cyclodextrins and their uses: a review. Process Biochem. 39, 1033–1046.

Denz, M., Haralampiev, I., Schiller, S., Szente, L., Herrmann, A., Huster, D., Müller, P., 2016. Interaction of fluorescent phospholipids with cyclodextrins. Chem. Phys. Lipids 194, 37–48.

Gharib, R., Greige-Gerges, H., Fourmentin, S., Charcosset, C., Auezova, L., 2015. Liposomes incorporating cyclodextrin–drug inclusion complexes: Current state of knowledge. Carbohydr. Polym. 129, 175–186.

Hatzi, P., Mourtas, S., G. Klepetsanis, P., Antimisiaris, S.G., 2007. Integrity of liposomes in presence of cyclodextrins: Effect of liposome type and lipid composition. Int. J. Pharm. 333, 167–176.

Kfoury, M., Auezova, L., Fourmentin, S., Greige-Gerges, H., 2014a. Investigation of monoterpenes complexation with hydroxypropyl-β-cyclodextrin. J. Incl. Phenom. Macrocycl. Chem. 80, 51–60.

Kfoury, M., Hădărugă, N.G., Hădărugă, D.I., Fourmentin, S., 2016. Cyclodextrins as encapsulation material for flavors and aroma, in: Encapsulations. Elsevier, pp. 127–192.

Kfoury, M., Landy, D., Auezova, L., Greige-Gerges, H., Fourmentin, S., 2014b. Effect of cyclodextrin complexation on phenylpropanoids' solubility and antioxidant activity. Beilstein J. Org. Chem. 10, 2322–2331.

Kirby, C., Gregoriadis, G., 1983. The effect of lipid composition of small unilamellar liposomes containing melphalan and vincristine on drug clearance after injection into mice. Biochem. Pharmacol. 32, 609–615.

McCormack, B., Gregoriadis, G., 1994. Drugs-in-cyclodextrins-in liposomes: a novel concept in drug delivery. Int. J. Pharm. 112, 249–258.

Mossa, A.-T.H., 2016. Green Pesticides: Essential Oils as Biopesticides in Insect-pest Management. J. Environ. Sci. Technol. 9, 354–378.

Ohvo-Rekilä, H., Akerlund, B., Slotte, J.P., 2000. Cyclodextrin-catalyzed extraction of fluorescent sterols from monolayer membranes and small unilamellar vesicles. Chem. Phys. Lipids 105, 167–178.

Pavela, R., Benelli, G., 2016. Essential Oils as Ecofriendly Biopesticides? Challenges and Constraints. Trends Plant Sci. 21, 1000–1007.

Puglisi, G., Fresta, M., Ventura, C.A., 1996. Interaction of Natural and Modified β-Cyclodextrins with a Biological Membrane Model of Dipalmitoylphosphatidylcholine. J. Colloid Interface Sci. 180, 542–547.

Reza Mozafari, M., Johnson, C., Hatziantoniou, S., Demetzos, C., 2008. Nanoliposomes and Their Applications in Food Nanotechnology. J. Liposome Res. 18, 309–327.

Sebaaly, C., Jraij, A., Fessi, H., Charcosset, C., Greige-Gerges, H., 2015. Preparation and characterization of clove essential oil-loaded liposomes. Food Chem. 178, 52–62.

Szejtli, J., 1998. Introduction and General Overview of Cyclodextrin Chemistry. Chem. Rev. 98, 1743–1754.

Turek, C., Stintzing, F.C., 2013. Stability of Essential Oils: A Review: Stability of essential oils…. Compr. Rev. Food Sci. Food Saf. 12, 40–53.

Zylberberg, C., Matosevic, S., 2016. Pharmaceutical liposomal drug delivery: a review of new delivery systems and a look at the regulatory landscape. Drug Deliv. 23, 3319–3329.

Bibliography

Chapter 1

Interaction of cyclodextrins with biomimetic and biological membranes

Introduction

DCLs are drug carriers comprising one or more phospholipid (PL) bilayers and an aqueous internal cavity where a CD/drug inclusion complex is loaded. It has been proposed as an effective carrier system to prolong drug release when compared to CLs and CDs (Gharib et al., 2015). For DCLs preparation, an overall understanding of the interaction between CDs and liposomes is necessary and valuable.

In this review, published in the International Journal of Pharmaceutics, we focus on the interaction of CDs with biomimetic and biological membranes considering the factors that may affect this interaction such as the type and the concentration of CDs as well as the membrane structure and composition. In addition, the effect of CDs on the membrane properties, mainly fluidity and permeability, is highlighted.

CDs are used to prepare lipid asymmetric membranes and to modify the composition of synthetic and biological membranes (Huang and London, 2013; Li et al., 2016). Additionally, CDs (Gharib et al., 2018; Madison et al., 2013; Zeng and Terada, 2000) and cholesterol-loaded CDs (Salmon et al., 2016) are able to maintain the integrity of a membrane during freeze-drying, thereby ensuring its protection. The secondary effects of CDs are due to their ability to extract membrane constituents (PL, cholesterol (CHOL) and proteins) (Denz et al., 2016; Milles et al. 2013; Motoyama et al., 2006).

The basic structural and functional properties of membranes and CDs are given at first for being essential to deeply understand the CD-membrane interaction. A wide range of techniques has been developed to study CD-membrane interaction, and these techniques are introduced in the review. For instance, the effect of CDs on the fluidity of lipid membranes was evaluated using differential scanning calorimetry, fluorescence anisotropy, and electron spin techniques. Similarly, the effect of CDs on the liposome membrane permeability for fluorescent dyes was presented. This review presents five recapitulative tables summarizing the literature data on: (1) the impact of CDs on the thermotropic

parameters of membranes determined by DSC; (2) the CD-induced membrane extraction; (3) the CD-induced lipid exchange between membranes; (4) the CD-induced protein extraction; (5) and the effect of CDs on membrane permeability. Additionally, the mechanisms by which CDs cause signaling pathway changes are described. The cryoprotective properties of CDs and CD/CHOL inclusion complexes are highlighted. Finally, recent data on DCL development are discussed.

References

Denz, M., Haralampiev, I., Schiller, S., Szente, L., Herrmann, A., Huster, D., Müller, P., 2016. Interaction of fluorescent phospholipids with cyclodextrins. Chem. Phys. Lipids. 194, 37–48.

Gharib, R., Greige-Gerges, H., Fourmentin, S., Charcosset, C., Auezova, L., 2015. Liposomes incorporating cyclodextrin–drug inclusion complexes: Current state of knowledge. Carbohydr. Polym. 129, 175–186.

Gharib, R., Greige-Gerges, H., Fourmentin, S., Charcosset, C., 2018. Hydroxypropyl-ßcyclodextrin as a membrane protectant during freeze-drying of hydrogenated and non-hydrogenated liposomes and molecule-in-cyclodextrin-in-liposomes: application to trans-anethole. Food Chem. 267, 67–74.

Huang, Z., London, E., 2013. Effect of cyclodextrin and membrane lipid structure upon cyclodextrin-lipid interaction. Langmuir 29, 14631–14638.

Li, G., Kim, J., Huang, Z., St. Clair, J.R., Brown, D.A., London, E., 2016. Efficient replacement of plasma membrane outer leaflet phospholipids and sphingolipids in cells with exogenous lipids. Proc. Natl. Acad. Sci. 113, 14025–14030.

Madison, R.J., Evans, L.E., Youngs, C.R., 2013. The effect of 2-hydroxypropyl-β-cyclodextrin on post-thaw parameters of cryopreserved jack and stallion semen. J. Equine Vet. Sci. 33, 272–278.

Milles, S., Meyer, T., Scheidt, H.A., Schwarzer, R., Thomas, L., Marek, M., Szente, L., Bittman, R., Herrmann, A., Günther Pomorski, T., Huster, D., Müller, P., 2013. Organization of fluorescent cholesterol analogs in lipid bilayers – lessons from cyclodextrin extraction. Biochim. Biophys. Acta 1828, 1822–1828.

Motoyama, K., Arima, H., Toyodome, H., Irie, T., Hirayama, F., Uekama, K., 2006. Effect of 2,6-di-O-methyl-α-cyclodextrin on hemolysis and morphological change in rabbit's red blood cells. Eur. J. Pharm. Sci. 29, 111–119.

Salmon, V.M., Leclerc, P., Bailey, J.L., 2016. Cholesterol-loaded cyclodextrin increases the cholesterol content of goat sperm to improve cold and osmotic resistance and maintain sperm function after cryopreservation1. Biol. Reprod. 94.

Zeng, W., Terada, T., 2000. Freezability of boar spermatozoa is improved by exposure to 2-hydroxypropyl-beta-cyclodextrin. Reprod. Fertil. Dev. 12, 223–228.

International Journal of Pharmaceutics 564 (2019) 59–76

Contents lists available at ScienceDirect

International Journal of Pharmaceutics

journal homepage: www.elsevier.com/locate/ijpharm

Review

Cyclodextrin-membrane interaction in drug delivery and membrane structure maintenance

Zahraa Hammoud[a,c], Nathalie Khreich[a], Lizette Auezova[a], Sophie Fourmentin[b], Abdelhamid Elaissari[c], Hélène Greige-Gerges[a,*]

[a] Bioactive Molecules Research Laboratory, Doctoral School of Sciences and Technologies, Faculty of Sciences, Section II, Lebanese University, Lebanon
[b] Unité de Chimie Environnementale et Interactions sur le Vivant (UCEIV, EA 4492), SFR Condorcet FR CNRS 3417, ULCO, F-59140 Dunkerque, France
[c] Univ Lyon, University Claude Bernard Lyon-1, CNRS, LAGEP-UMR 5007, F-69622 Lyon, France

ARTICLE INFO

Keywords:
Cholesterol
Cyclodextrin
Liposome
Membrane
Phospholipid

ABSTRACT

Cyclodextrins (CDs) are cyclic oligosaccharides able to improve drug water solubility and stability by forming CD/drug inclusion complexes. To further increase drug entrapment and delay its release, the CD/drug inclusion complex can be embedded in the aqueous phase of a liposome, a lipid vesicle composed of phospholipid bilayer surrounding an aqueous compartment. The resulting carrier is known as drug-in-cyclodextrin-in-liposome (DCL) system. CDs and DCLs are recognized as effective drug delivery systems; therefore, understanding the interaction of CDs with liposomal and biological membranes is of great importance. CDs are able to extract phospholipids, cholesterol, and proteins from membranes; the effect depends on the membrane structure and composition as well as on the CD type and concentration. Under definite conditions, CDs can affect the membrane fluidity, permeability, and stability of liposomes and cells, leading to the leakage of some of their internal constituents. On the other side, CDs demonstrated their beneficial effects on the membrane structure, including preservation of the membrane integrity during freeze-drying. In this paper, we review the literature concerning the interaction of CDs with biomimetic and biological membranes. Moreover, the impact of CDs on the membrane properties, mainly fluidity, stability, and permeability, is highlighted.

1. Introduction

Liposomes are phospholipid (PL) vesicles containing one or more lipid bilayers and an aqueous internal cavity. They can encapsulate hydrophilic and hydrophobic drugs in their aqueous core and lipid bilayer, respectively, constituting an effective drug delivery system (Gharib et al., 2015).

Another drug delivery system is based on cyclodextrins (CDs), oligosaccharides formed of glucopyranose units. CDs have a truncated funnel shape with a hydrophobic internal cavity and a hydrophilic outer surface (Gharib et al., 2015). Thus, CDs can entrap hydrophobic drugs in their cavities forming CD/drug inclusion complexes that improve drug solubility and bioavailability, enhance physical and thermal stability of drugs, and limit drug toxic effects (Baek et al., 2013; Loftsson and Masson, 2001; Zhang et al., 2013).

Drug-in-CD-in-liposome (DCL), a combined system made of CD and liposome, was proposed by McCormack and Gregoriadis (1994) to increase loading rates of hydrophobic molecules and to provide their prolonged release compared to conventional liposomes and CD/drug inclusion complexes. In DCL, hydrophobic drugs are loaded into the aqueous phase of liposome in the form of CD/drug inclusion complex.

CDs boost drug delivery by interacting with membrane components (Babu and Pandit, 2004; Mura et al., 2014; Nakanishi et al., 1992; Tilloy et al., 2006; Ventura et al., 2001). This interaction may induce a perturbation in the lipid bilayer affecting the membrane properties such as fluidity (Gharib et al., 2018a; Grammenos et al., 2010) and permeability (Piel et al., 2007; Wang et al., 2011). A deep understanding of CD interaction with biomimetic, i.e. liposomal, and biological membranes is crucial in pharmacology for controlling CD-mediated drug delivery and release.

Freeze-drying of liposomes is essential to extend their shelf life (Gharib et al., 2018b). Also, sperm cryopreservation has been extensively applied in artificial insemination programs (Mocé et al., 2010). However, the freezing process can cause membrane damage (Drobnis et al., 1993); therefore, suitable cryoprotectants should be added. CDs are able to form hydrogen bonds with polar groups of membrane lipids, thereby stabilizing the ordered conformation of liposomes and spermatozoa during freeze-drying. Furthermore, CD/

* Corresponding author at: Bioactive Molecules Research Laboratory, Faculty of Sciences, Lebanese University, B.P. 90656, Jdaidet El-Matn, Lebanon.
E-mail address: hgreige@ul.edu.lb (H. Greige-Gerges).

https://doi.org/10.1016/j.ijpharm.2019.03.063
Received 27 December 2018; Received in revised form 28 March 2019; Accepted 29 March 2019
Available online 05 April 2019
0378-5173/ © 2019 Elsevier B.V. All rights reserved.

cholesterol inclusion complexes serve as cholesterol (Chol) donors to load membranes with Chol for membrane stabilization. Consequently, free CDs (Gharib et al., 2018b; Madison et al., 2013; Zeng and Terada, 2000) and Chol-loaded CDs (Salmon et al., 2016) are capable to maintain the integrity of a membrane during freeze-drying, thereby ensuring its protection.

To the best of our knowledge, this is the first review that focuses on CD interaction with biomimetic and biological membranes considering the factors that may affect this interaction such as the type and concentration of CD as well as the membrane structure and composition. The main techniques applied to study the CD-membrane interaction are introduced, and the literature data are resumed into conclusive tables. Furthermore, the literature data on CD-mediated extraction of membrane components (PLs, Chol, and proteins) are discussed. We also summarize the effects of CDs on the membrane properties such as permeability, fluidity, and stability. In addition, an overview of the beneficial effects of CDs as membrane cryoprotectants is presented. The last section of this review discusses recent data on DCLs development.

2. Biological membranes

2.1. Membrane structure based on fluid mosaic model

The fluid mosaic model of cell membranes is a fundamental concept in membrane biology. According to this model, the basic structure of a biological membrane is a lipid bilayer associated with proteins, often glycosylated (Singer and Nicolson, 1972). The variety of lipids and proteins experience both rotational and translational freedom within the bilayer plane and are asymmetrically distributed between the membrane leaflets (Holthuis and Levine, 2005).

2.2. Membrane composition

2.2.1. Phospholipids and sphingolipids

PLs are amphiphilic molecules comprising a glycerol backbone esterified at first and second positions with two fatty acids; the third alcohol of glycerol is esterified by a phosphoric acid which, in turn, is esterified by a polar group such as choline, ethanolamine, glycerol, inositol, or serine. The membrane surface charge depends on the polar head groups of PLs and sphingolipids constituting the membrane. The PLs phosphatidylcholine (PC) and phosphatidylethanolamine (PE) containing, respectively, positively charged groups choline and ethanolamine, are neutral. On the contrary, when the polar group is zwitterionic (serine) or non-ionizable (glycerol, hydrogen, or inositol), the resulting PL is negatively charged. Furthermore, the fatty acids which esterify the primary and secondary alcohols of glycerol vary in their length and degree of saturation (Li et al., 2015). Like PLs, sphingolipids are composed of a polar head group and a nonpolar moiety, which is a fatty acid linked to a long-chain amino alcohol, sphingosine. They include sphingomyelins (SM) and glycosphingolipids: cerebrosides, sulfatides, globosides, and gangliosides. Gangliosides and sulfatides are negatively charged due to the presence of sialic acid and sulfate groups, respectively, contributing to the global membrane charge. Sphingolipids have generally much more saturated hydrocarbon chains than PLs allowing them to be packed tightly together (Brown and London, 2000).

The structure of a lipid influences its geometry and membrane curvature. Thus, PC and SM both possess a cylindrical shape based on the head-to-tail ratio (the same head and tail cross sectional areas) resulting in a lamella (bilayer) when mixed in an aqueous medium. However, lysophosphatidylcholine (LPC) and phosphatidylinositol (PI) are of inverted conical shape (higher head-to-tail ratio) and form micelles in an aqueous environment. Conversely, PE, phosphatidic acid (PA), and phosphatidylserine (PS), containing relatively small head groups, are cone-shaped lipids which adopt in water an inverted micellar structure. The fact that biological membranes have a lamellar structure explains the choice of PC for the preparation of biomimetic lipid bilayers.

As mentioned earlier, membrane components are asymmetrically distributed between the inner and outer leaflets of membrane. In general, the inner leaflet is rich in PLs containing amine or serine moieties and the signaling lipids such as PI and PA, whereas PC and SM are densely located in the outer leaflet (Zalba and ten Hagen, 2017).

2.2.2. Cholesterol

Cellular membranes contain up to 40% sterols (Chol in mammals) in relation to the total membrane lipids. Chol has a four-ring nucleus with a double bond between C-5 and C-6, an iso-octyl side chain at C-17, two methyl groups at C-18 and C-19, and a hydroxyl group at C-3. Its hydroxyl group is oriented toward the aqueous phase while the hydrophobic moiety is located alongside PL acyl chains. Chol plays an essential role in controlling membrane fluidity, permeability, receptors function, and ion transport (Burger et al., 2000; Cooper, 1978; Kaddah et al., 2018; Simons and Toomre, 2000).

2.2.3. Proteins

Membrane proteins are classified into integral (or intrinsic) and peripheral (or extrinsic). Integral proteins intercalate into the membrane hydrophobic matrix where they are tightly bound by hydrophobic interactions. Integral proteins are also suggested to be amphipathic with their hydrophobic domains embedded in the hydrophobic interior and their hydrophilic domains protruding from the hydrophobic region of the lipid bilayer into the surrounding aqueous environments. Peripheral proteins are loosely bound to hydrophilic parts of membranes by electrostatic and other non-hydrophobic interactions (Nicolson, 2014).

2.2.4. Lipid rafts

Lipids are not only asymmetrically distributed between the membrane leaflets but also heterogeneously dispersed within a single layer. Cellular membranes contain highly ordered stable structures called “lipid rafts” surrounded by a liquid disordered matrix. Lipid rafts are small-sized domains rich in sphingolipids and Chol, closely packed, functional, and dynamic. They are resistant to solubilization by mild detergents (Brown and London, 1998; Simons and Ikonen, 1997). Also, rafts contain a specific group of membrane proteins linked to saturated acyl chains either using glycosylphosphatidylinositol (GPI) anchor or through acylation with myristate or palmitate (Brown and London, 1998). Lipid rafts were proved to be implicated in many cellular processes such as sorting of lipids and proteins (McIntosh et al., 2003), signal transduction and trafficking (Hanzal-Bayer and Hancock, 2007; Stauffer and Meyer, 1997), and transmission of viral and bacterial infections (Wang et al., 2009).

3. Biomimetic membranes

Due to the complex organization of biological membranes, simple biomimetic membranes are used as models. In the case of CD–membrane interaction studies, lipid monolayers and liposomes are utilized (Grauby-Heywang and Turlet, 2008; Milles et al., 2013; Ohvo-Rekilä et al., 2000).

3.1. Lipid monolayers

Lipid monolayers, also referred as Langmuir monolayers, are formed by spreading amphiphilic molecules at the surface of a liquid; they consist of a single lipid type or a mixture of lipids. This system displays many advantages in comparison with other biomimetic membranes allowing control of parameters such as temperature, nature and packing of lipids, and compositions of the liquid medium (pH, ionic strength) (Maget-Dana, 1999).

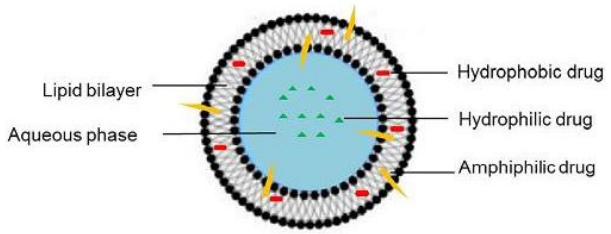

Fig. 1. Schematic representation of a liposome constituted of a lipid bilayer enclosing an aqueous phase. Hydrophobic drug (red) is entrapped in the lipid bilayer. Hydrophilic drug (green) is embedded in the aqueous phase. Amphiphilic drug (orange) is located at the water-bilayer interphase. (For interpretation of the references to colour in this figure legend, the reader is referred to the web version of this article.)

3.2. Liposomes

Liposomes are spherical self-closed structures where a lipid bilayer encloses an aqueous inner cavity. Liposomes are mainly prepared from PLs, with or without Chol. They are generally classified according to their size and number of bilayers. Small unilamellar vesicles (SUV) range between 20 and 100 nm while large unilamellar vesicles (LUV) are greater than 100 nm, and giant unilamellar vesicles (GUV) exceed 1000 nm; all these types having a single lamella. Multilamellar vesicles (MLV) are large vesicles (> 0.5 μm) possessing more than 5 concentric lamellae (Gharib et al., 2015).

Liposomes are biocompatible, biodegradable, non-immunogenic, and non-toxic structures. All these characteristics make them suitable for drug delivery. Hydrophobic and hydrophilic substances can be entrapped, respectively, within the lipid bilayer and the aqueous internal cavity, and amphiphilic molecules are located at the water-bilayer interface (Fig. 1). These properties make liposomes effective as carriers of bioactive molecules in cosmetic, pharmaceutical, food, and farming industries (Sherry et al., 2013).

4. Membrane fluidity

The fluidity of a membrane is one of its important properties; it strongly depends on the temperature and the membrane composition, in particular the presence of Chol and its content.

Depending on the temperature, a lipid bilayer can adopt distinct physical states (Fig. 2) which are characterized by different lateral organization, molecular order, and mobility of lipids constituting the bilayer (Eemen and Deleu, 2010). At low temperatures, the lamellar gel phase (also called 'solid ordered' (So) phase) is formed where the hydrocarbon chains are elongated to the maximum in all-trans configuration. Upon temperature elevation, a lipid bilayer demonstrates structural changes called 'thermotropic transitions': the pre-transition in which the lipid bilayer passes from the lamellar gel phase to the rippled gel phase, and the main transition which represents the transition from the rippled gel phase to the 'liquid disordered' (Ld) phase. Ld phase is characterized by the presence of numerous gauche conformers along the acyl chains; therefore, it shows a great increase in membrane fluidity and molecular disorder compared to the rippled gel phase (Abboud et al., 2018).

In the presence of Chol, a lipid bilayer can acquire a new phase, called 'liquid ordered' (Lo) phase. In this case, the acyl chains have intermediate properties between those of So and Ld phases. Vist and Davis (1990) presented the dynamic of DPPC membrane at various temperatures and Chol levels. The authors showed that for intermediate membrane content of Chol (7–30%), the So phase coexists with the Lo phase below the transition temperature. Above the transition temperature, the Lo phase coexists with the Ld phase. Beyond 30 mol % membrane Chol content and whatever the temperature, the Lo phase is reached.

Membrane fluidity is also influenced by the membrane PL composition. First, the nature of polar head group affects the membrane lateral organization; membrane lipids with small polar heads allow a more compact lipid assembly due to a reduced steric hindrance (Eemen and Deleu, 2010). Additionally, saturation status of acyl chains strongly affects the membrane lateral organization; namely, saturated lipids have straight tails, thus promoting their tight packing. However, the cis double bonds of unsaturated lipids prohibit their tight packing through steric hindrance resulting in a more fluid membrane. In addition, membrane fluidity depends on the length of the acyl chains; longer alkyl chains are easily held together via Van der Walls and hydrophobic interactions in comparison to those with shorter ones (Zalba and ten Hagen, 2017).

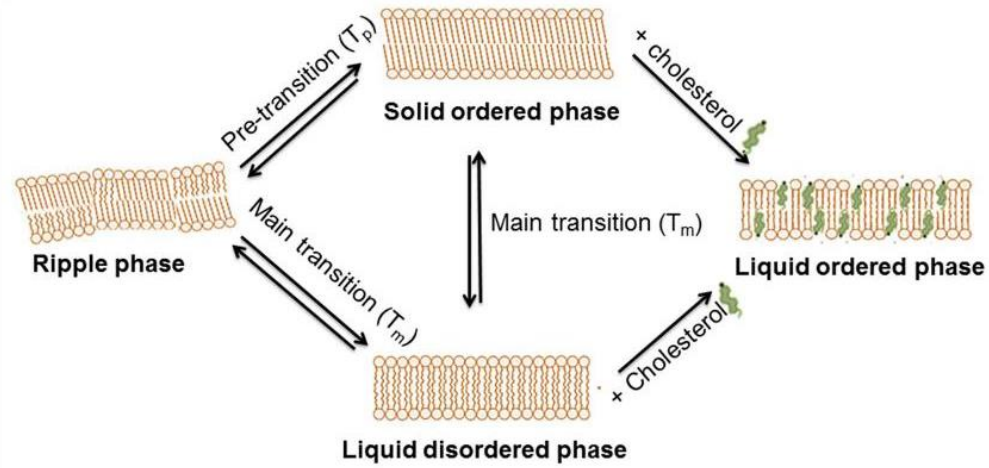

Fig. 2. The different physical states of a lipid bilayer in an aqueous environment. At low temperature, the solid ordered phase exists. At pre-transition temperature (Tp), a lipid bilayer passes from the solid ordered phase to the rippled phase (left). At main transition temperature (Tm), a lipid bilayer passes to the liquid disordered phase (down). Adding Chol (green) to a lipid bilayer induces the formation of the liquid ordered phase (right).

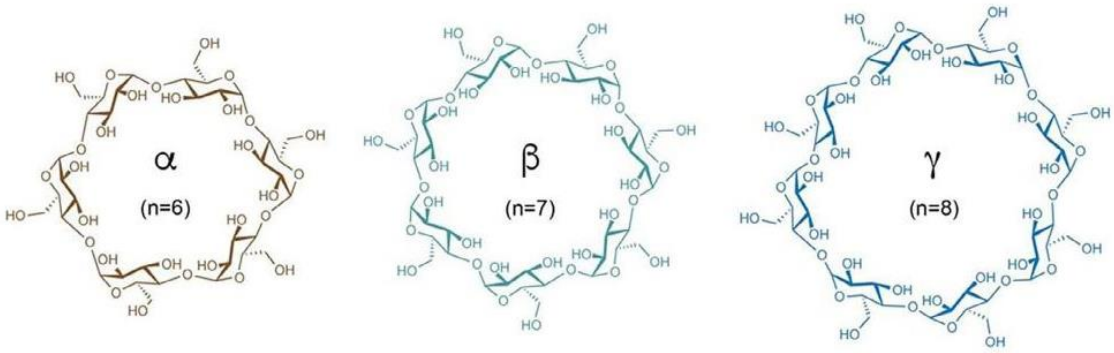

Fig. 3. The chemical structure of the most common native cyclodextrins.

5. Cyclodextrins

5.1. Structure

Cyclodextrins (CDs) are non-toxic cyclic oligosaccharides formed of α-1,4-linked D-glucopyranose units. They are obtained from starch by means of enzymatic degradation. Due to the $^4C_1$ chair conformation of glucopyranose, CDs have a bottomless bowl shape (truncated cone) of various sizes according to the number of glucose units. The most common native CDs are formed of 6 (α-CD), 7 (β-CD), or 8 (γ-CD) glucose subunits, with a respective cavity size of approximately 0.5, 0.6, and 0.8 nm (Fig. 3) (Gharib et al., 2015).

Based on X-ray studies, CDs dispose their hydroxyl functional groups to the cone exterior extending the primary hydroxyl group (C6) of glucopyranose from the narrow edge of the ring and the secondary hydroxyl groups (C2 and C3) from the wider edge as shown in Fig. 4 (Del Valle, 2004). This arrangement provides CD a hydrophilic outer surface, whereas the interior cavity is hydrophobic.

5.2. Derivatives

Natural CDs, especially β-CD, have limited solubility in water because of their relatively strong intermolecular hydrogen bonding in the crystal state. The aqueous solubility of CDs determined at 25 °C is 0.1211, 0.0163, and 0.1680 mol/L for α-CD, β-CD, and γ-CD, respectively (Connors, 1997). Chemical modifications such as amination, etherification, methylation, and esterification of the primary and secondary hydroxyl groups are applied to synthesize various hydrophobic, hydrophilic, and ionic CD derivatives with an improved aqueous solubility compared to the native CDs (Gharib et al., 2015).

In addition to the native CDs, various CD derivatives have been used to study their interaction with membranes. They include the hydroxypropyl derivatives (HP-α-CD, HP-β-CD, and HP-γ-CD), maltosylated derivatives (G_2-α-CD and G_2-β-CD), sulfobutylether-β-CD (SBE-β-CD), carboxyethylated-γ-CD (CE-γ-CD), and the methylated derivatives (Me-α-CD, DM-α-CD, Me-β-CD, dimeb, trimeb, Me-γ-CD). The latters also include the randomly methylated β-CD derivatives (rameb) and the partially methylated crystallized-β-CD (crysmeb). Recently, interest in multi-substituted-β-CDs such as hydroxypropyl-sulfobutyl-ether-β-cyclodextrin (HP_n-SBE_m-β-CD), which is substituted by hydroxypropyl and sulfobutyl groups: n-(2,3,6-O-2-hydroxypropyl)-m-(2,3,6-O-sulfobutyl)-β-CD has emerged. Two HP_n-SBE_m-β-CDs (HP_2-SBE_3-β-CD and HP_3-SBE_2-β-CD) were evaluated for their effects on biological membranes (Wang et al., 2011).

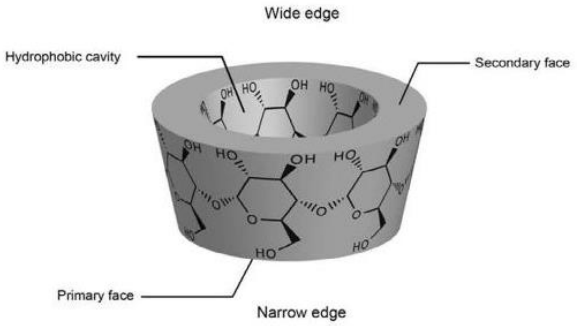

Fig. 4. The truncated cone-shaped structure of a cyclodextrin molecule with its hydroxyl groups disposed outside.

5.3. Cyclodextrins used as drug delivery enhancers

CDs are able to entrap hydrophobic drugs in their cavities forming CD/drug inclusion complexes. As a result, CDs favor drug dissolution in the aqueous phase, making them suitable to diffuse in an aqueous medium, to come in contact with membrane surface, and to permeate through membrane. Moreover, encapsulation in CD protects the drug from chemical and enzymatic degradation (Babu and Pandit, 2004; Rong et al., 2014; Rosa Teixeira et al., 2013).

6. Drug-in-cyclodextrin-in-liposome

Van der Waal forces, hydrogen bonds, and hydrophobic interactions are involved in the CD/drug inclusion complex formation (Gidwani and Vyas, 2015). Therefore, the inclusion complex will rapidly dissociate following intravenous administration where blood components may displace the encapsulated drug. As for liposomes, highly lipophilic drugs incorporated in the liposomal PL bilayer would be also rapidly released after intravenous and transdermal administration (Kirby and Gregoriadis, 1983; Maestrelli et al., 2005; Takino et al., 1994). To ensure a stable encapsulation of hydrophobic drugs, an approach has been proposed (McCormack and Gregoriadis, 1994) where the drugs are encapsulated in the aqueous phase of liposomes in the form of CD/drug inclusion complexes. This approach combines the relative advantages of both carriers in a single “drug-in-CD-in-liposome” (DCL) system. Indeed, the entrapment of a water-soluble CD/drug inclusion complex into liposomes would allow accommodation of insoluble drugs in the aqueous phase of vesicles (Fig. 5) (Gharib et al., 2017).

7. Cyclodextrin-lipid membrane interaction

The interaction of native and modified CDs with fatty acids, Chol and PLs was recently reviewed by Szente and Fenyvesi (2017). In the sections below, we will focus, in particular, on the interaction between

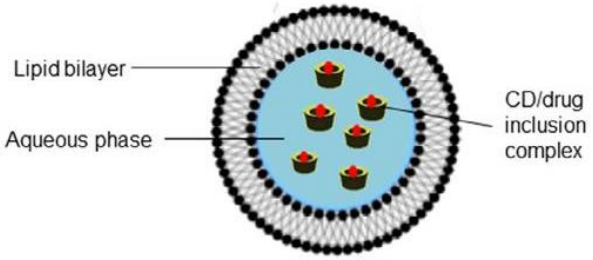

Fig. 5. Schematic representation of drug-in-cyclodextrin-in-liposome system composed of lipid bilayer and an aqueous inner cavity. The drug in the form of CD/drug inclusion complex is loaded in the aqueous phase.

CDs and both biomimetic and biological membranes, with respect to the composition of biomimetic membrane, the type of biological membrane, the lipid to CD molar ratio, as well as the CD type and concentration.

7.1. The effect of cyclodextrins on membrane fluidity

The effect of CDs on the fluidity and stability of liposome membranes and biological systems (stratum corneum and colon carcinoma cells) was evaluated using differential scanning calorimetry (DSC), fluorescence anisotropy, and electron spin resonance (ESR) techniques.

DSC is used in lipid membrane research to study the thermal behavior of lipid bilayers in the presence of active agents, i.e. CDs. The thermodynamic parameters such as pre-transition temperature (Tp), main transition temperature (Tm), main transition enthalpy (ΔH_m), and temperature width at half peak height ($\Delta T_{1/2}$) can be determined using DSC (Demetzos, 2008).

Tp is represented by a flat endothermic peak and its disappearance reflects drug interaction with the polar head groups of PLs. Tm is a sharp endotherm represented by the apex of the peak (Demetzos, 2008; Gharib et al., 2018a). ΔH_m is the heat required for the entire transition; it is calculated from the area under the main transition peak. The decrease in ΔH_m suggests an increase in the membrane fluidity and disorder (increase in the number of acyl chains in the gauche conformation) while its increase reflects an interaction of the drug with the upper glycerol head group region of the lipid bilayer. Furthermore, $\Delta T_{1/2}$ reflects the cooperativity of the transition, being inversely proportional to it. It is very sensitive to the presence of additives (Gharib et al., 2018a).

Most studies in the literature evaluated the effect of CDs on DPPC liposome membrane. The latter, in the absence of CD, displayed a pre-transition at approximately 35 °C and a main transition at around 41 °C (Gharib et al., 2018a). The interaction of CDs with liposomal membranes induced alterations in the membrane calorimetric parameters. Table 1 summarizes the literature data on the DSC results obtained with CD-loaded liposomes, showing the liposomal membrane composition, CD type and concentration as well as lipid:CD molar ratio. As can be seen from Table 1, CDs influence the membrane fluidity.

Indeed, β-CD (Castelli et al., 2006) and HP-β-CD (Gharib et al., 2018a) abolished the pre-transition peak values of DMPC and DPPC liposomes, respectively, suggesting an interaction of CDs with the polar head groups of PLs. Regarding the effect of CDs on Tm value, it was reported that dimeb, β-CD, trimeb (Puglisi et al., 1996), and HP-β-CD (Gharib et al., 2018a) increased the Tm of DPPC membranes as a function of lipid:CD molar ratio (Fig. 6). In addition, β-CD, at a concentration of 167 mM, increased the Tm of DMPC liposome membrane (Castelli et al., 2006). Thus, CDs appear to stabilize the liposome lipid bilayer by hydrogen bonding to polar lipids. In contrast, Nishijo and Mizuno (1998) showed that the Tm value of DPPC membrane was reduced in the presence of trimeb, while β-CD, γ-CD, and HP-β-CD barely influenced the Tm of this membrane model. The authors suggested that CDs exhibit a membrane fluidizing effect and may extract PLs from the membrane. On the other side, Liossi et al. (2017) showed a lowering effect of HP-β-CD towards DPPC membrane. The ΔH_m of DPPC membrane was significantly decreased in the presence of α-CD (Nishijo and Mizuno, 1998), dimeb (Nishijo and Mizuno, 1998; Puglisi et al., 1996), or HP-β-CD (Liossi et al., 2017) suggesting an increase in the membrane fluidity and disorder. Conversely, Gharib et al. (2018a) demonstrated an increase in ΔH_m of DPPC liposome at low HP-ß-CD molar fraction (1.81 and 4.54); an HP-β-CD interaction with the upper chain/glycerol/head group region of the lipid bilayer was proposed. However, at higher molar fraction (9.09 and 13.63), HP-ß-CD exerted a lowering effect on the ΔH_m; HP-β-CD was suggested to interact with the hydrophobic core of the lipid bilayer leading to perturbation of DPPC packing order. Furthermore, adding Chol appears to modulate the effect of CDs on DPPC membranes. Thus, β-CD and trimeb increased the ΔH_m of DPPC:Chol (90:10) membrane at all the studied lipid to CD molar ratios. Whereas the effect of dimeb differed depending on its molar fraction; the ΔH_m increased to its maximal value (4.94 ± 0.18 kcal/mol) at lipid:CD molar ratio of 1:7; however, a further increase in its molar fraction (1:32) led to a decrease in ΔH_m (2.88 ± 0.31 kcal/mol). According to the authors, dimeb is able to extract both DPPC and Chol at higher CD molar fraction (Puglisi et al., 1996).

Few studies have determined the effect of CD on the cooperativity of transition. The presence of dimeb, trimeb (Puglisi et al., 1996), or HP-β-CD (Gharib et al., 2018a) induced an increase in the $\Delta T_{1/2}$ of DPPC vesicles. This could be explained by the interaction between CD and the hydrophobic region of DPPC bilayer which causes membrane disruption (Gharib et al., 2018a).

Angelini et al. (2017) determined the ratio of pyrene fluorescence intensities in excimer and monomer state for palmityl-oleoyl-phosphatidylcholine (POPC) and β-CD-loaded-POPC liposomes. The results showed that β-CD increased the membrane fluidity in comparison with the control.

The anisotropy value is known to be inversely proportional to the membrane fluidity. To our knowledge, the study of Gharib et al. (2018a) is the only one using fluorescence anisotropy to evaluate the CD effect on the membrane fluidity. The authors used 1,6-diphenyl-1,3–5-hexatriene (DPH) as a probe since membranes do not exhibit a natural intrinsic fluorescence. Due to its low aqueous solubility, DPH inserts in the bilayer core; the depolarization property of DPH depends on the packing of the acyl chains. Thus, the fluorescence anisotropy of DPH in liposomes gives information about the organization of the membrane environment around the fluorescent probe (Gharib et al., 2018a). The authors determined the DPH anisotropy values of blank and HP-ß-CD-loaded DPPC liposomes prepared at different DPPC:HP-ß-CD molar ratios (100:181, 100:454, 100:909, and 100:1363) at 28, 41, and 50 °C. The results showed that HP-β-CD reduced the DPH anisotropy of DPPC membrane at all the studied temperatures in a concentration-dependent manner (Fig. 7), suggesting an increase in the membrane fluidity of DPPC liposomes in the presence of HP-β-CD (Gharib et al., 2018a).

Moreover, Gharib et al. (2018a) determined the anisotropy values of DPH inserted in liposomes composed of saturated PLs and Chol or unsaturated PLs and Chol; in addition, different PL:Chol:HP-β-CD molar ratios were used in this study. HP-β-CD was found to increase the membrane fluidity of liposome membranes composed of unsaturated PLs, while no effect was exerted on those composed of saturated lipids. Thus, the packing state of PLs can modulate the CD effect on membrane model systems.

ESR spectroscopy is another technique used to provide information about the structure and dynamic of biological membranes. The fatty acid spin-label agents, 5-doxyl stearate (5-DSA) and 16-doxyl stearate (16-DSA), are generally used as paramagnetic probes. 5-DSA is located at the lipid-aqueous interface of the membrane while 16-DSA is inserted into its hydrophobic core. The nitroxide group of the spin probes moves around the point of attachment. Hence, the ESR spectra allow the

Table 1
The effect of cyclodextrins on the thermotropic parameters of the liposome membranes determined by DSC.

Membrane composition	Lipid:CD molar ratio	CD type	[CD] (mM)	Variation in thermotropic parameters	Ref
-DPPC	1:0 1:3 1:7 1:16 1:32	- β-CD - HP-β-CD - Dimeb - Trimeb	NI	Effects of CDs on DPPC vesicles: - Dimeb, β-CD, and trimeb: Tm was increased with increasing lipid:CD molar ratio - Dimeb: ΔH_m was decreased while $\Delta T_{1/2}$ was increased - Trimeb: an increase in $\Delta T_{1/2}$ without affecting ΔH_m	Puglisi et al., 1996
-DPPC:Chol (90:100)				Effects of CDs on DPPC:Chol vesicles: - Trimeb and β-CD: ΔH_m was increased - Dimeb: an increase in ΔH_m up to DPPC:Chol molar ratio of 1:7; after that it was decreased - HP-β-CD: no effect on both vesicles.	
DPPC	8:17 8:27 8:37 8:50	- α-CD - β-CD - HP-β-CD - Dimeb - Trimeb - γ-CD	0–50	- α-CD and dimeb: ΔH_m was decreased with increasing CD concentration while Tm was not affected - Trimeb: a slight decrease in Tm without affecting ΔH_m - β-CD, γ-CD, and HP-β-CD: Tm and ΔH_m were barely affected.	Nishijo and Mizuno, 1998
DMPC	ND	β-CD	0–167	- no effect at low CD concentration - at 167 mM, the pre-transition peak was abolished and Tm was increased	Castelli et al., 2006
DPPC	80:20	HP-β-CD	NI	- both pre-transition and main transition peaks were preserved - Tm and Tp were reduced - ΔH_m was reduced.	Liossi et al., 2017
DPPC	100:181 100:454 100:909 100:1363	HP-β-CD	29–221	- the pre-transition peak was abolished - Tm was increased as a function of [CD] - an increase in ΔH_m at low molar ratios (100:181 and 100:454) but it was decreased at high ratios (100:909 and 100:1363) - $\Delta T_{1/2}$ was increased.	Gharib et al., 2018a

[CD]: Cyclodextrin concentration, Chol: cholesterol, DMPC: dimyristoyl phosphatidylcholine; DPPC: dipalmitoyl phosphatidylcholine, NI: not indicated.

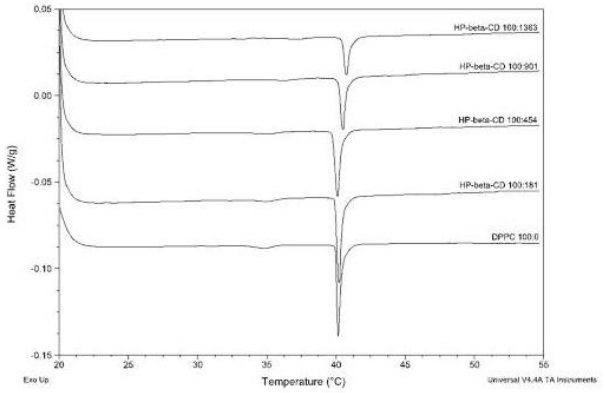

Fig. 6. DSC scans of blank and HP-ß-CD-loaded DPPC liposomes prepared at DPPC:HP-ß-CD molar ratios of 100:181; 100:454; 100:909 and 100:1363 (Gharib et al., 2018a).

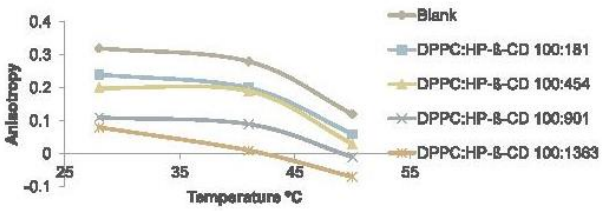

Fig. 7. DPH anisotropy values for blank and HP-ß-CD-loaded DPPC liposomes prepared at different DPPC:HP-ß-CD molar ratios at 28, 41, and 50 °C (Gharib et al., 2018a).

identification of changes in the probe rotational mobility in biological membranes and can be further correlated with membrane fluidity (Abboud et al., 2018; Grammenos et al., 2010).

ESR was applied to examine the effect of rameb (0–10 mM) on the microviscosity of human colon carcinoma cell membrane. In the absence of rameb, the microviscosity was found to be 298 cP. This value decreased with increasing CD concentration and stabilized at 265 cP for a rameb concentration of 2.5 mM. Then, the values remained constant until 10 mM (Grammenos et al., 2010).

Finally, it is worthy to note that the membrane Chol content was not considered in the above mentioned studies. Nevertheless, it is well known that Chol has a key role in maintaining the membrane fluidity; its content can modulate CD-induced membrane fluidity changes.

7.2. Extraction of lipid membrane components from biomimetic and biological membranes

Several studies evaluated the extent of lipid extraction mediated by CDs. Following the incubation of membrane with CD, the suspension is subjected to centrifugation, and the supernatant is collected to determine the amount of extracted PLs and Chol in the suspension. In general, CDs enable rapid extraction of membrane lipids. Alpha-CDs were found to extract mainly PLs; β-CDs, in particular methylated β-CDs, extract preferably Chol; γ-CDs are less lipid selective compared to the other CDs (Fig. 8).

The fluorescent analogs of PLs and Chol have been widely used to investigate the structural and dynamic properties of membranes. The interaction of CDs with fluorescent-labeled Chol (Milles et al., 2013) and PLs (Denz et al., 2016) bearing 7-nitrobenz-2-oxa-1,3-diazol-4-yl (NBD) or dipyrromethene boron difluoride (BODIPY) moieties induced a modification in Förster resonance energy transfer (FRET) signals. The latter occurred between a rhodamine moiety linked to phosphatidylethanolamine (Rh-PE) and the NBD or BODIPY moieties linked to liposomal PLs. Excitation of the BODIPY or NBD moieties induced a large FRET signal; large rhodamine fluorescence was obtained when the fluorophores came close together within the membrane. Consequently, the CD-mediated extraction of the fluorescent analogs reduced their concentration in the membrane, resulting in a decrease of FRET signals (Denz et al., 2016).

Table 2 resumes the literature data regarding CD-mediated extraction of lipid components from biomimetic and biological membranes; the studies on biomimetic membranes are presented first (liposomes

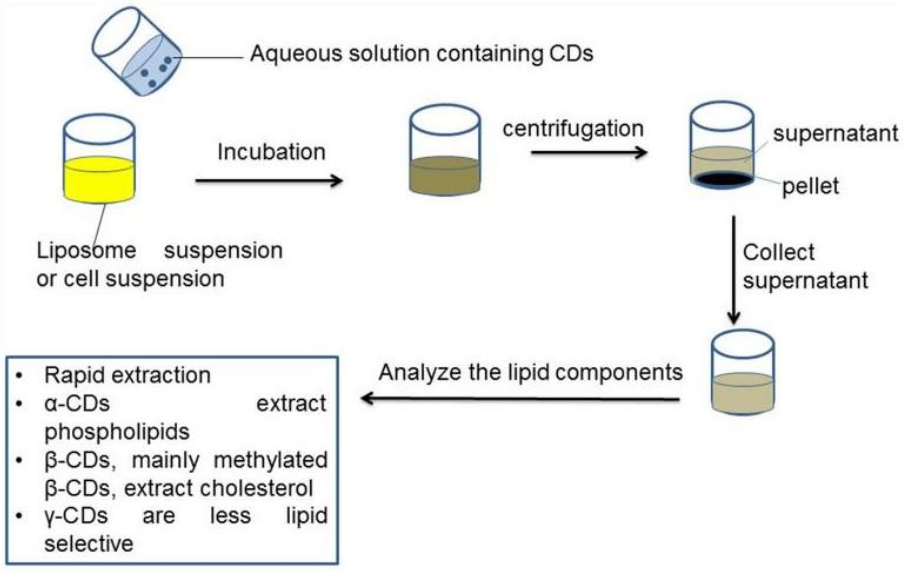

Fig. 8. A scheme presenting a general technique for evaluating the extent of cyclodextrin-mediated lipid extraction.

then monolayers) followed by those on biological membranes. Furthermore, Table 2 shows the lipid composition of liposomes and monolayers, the cell type from which membranes are extracted as well as the type and concentration of CD used in each study.

7.2.1. Kinetics of cyclodextrin-induced lipid extraction from membranes

Several studies examined the ability of CDs to induce lipid extraction from liposomal and biological membranes; the extraction kinetics was determined by monitoring the extraction as a function of time; the release rate constants or half times were evaluated.

Generally, Chol release from liposomes and biological membranes displayed a rapid exponential kinetics (Iborra et al., 2000; Milles et al., 2013). However, Yancey et al. (1996) reported that HP-β-CD-mediated Chol release from mouse L-cell fibroblasts, human fibroblasts, and rat hepatoma cells followed a bi-exponential kinetics, revealing a fast pool with half-times of 19–23 s and a slow pool with half-times ranging from 15 to 35 min. Moreover, Kilsdonk et al. (1995) demonstrated that HP-β-CD-induced a rapid Chol release from mouse L-cell fibroblasts over an initial period (up to about 2 h) until the equilibrium between Chol in the outer medium and in the membrane compartment was reached. Also, the kinetics of the PL extraction from liposomes by Me-α-CD and Me-β-CD was fitted to a bi-exponential equation (Denz et al., 2016).

7.2.2. The factors affecting lipid extraction from membranes

The data presented in Table 2 show that CDs have a potential to extract lipid components from biomimetic and biological membranes; the extent of extraction depends on CD type and concentration, PL structure, overall lipid membrane composition, and cell type.

7.2.2.1. Cyclodextrin type and concentration. The interaction of methylated CDs such as Me-α-CD, Me-β-CD, and Me-γ-CD, with liposome membrane containing NBD-labeled PLs was examined by detecting FRET between the NBD and Rh-PE as described earlier (Denz et al., 2016). Me-α-CD and Me-ß-CD were similarly efficient in inducing a high efflux of fluorescent-labeled PLs embedded in the membrane, whereas Me-γ-CD produced no effect. Also, the interaction of different CDs (α-CD, β-CD, HP-β-CD, Me-β-CD, and γ-CD) with NBD and BODIPY-labeled Chol was characterized (Milles et al., 2013). The results demonstrated that Me-β-CD induced the greatest Chol extraction while α-CD had no effect.

Moreover, many studies analyzed the effect of CDs on the erythrocyte membrane. Beta-CD induced greater Chol extraction from human erythrocytes relative to other native CDs (Irie et al., 1982; Ohtani et al., 1989). On the other hand, α-CD was more potent in inducing PL extraction (Ohtani et al., 1989). The influence of diverse CD derivatives on rabbit erythrocyte membrane was studied; α-CD and DM-α-CD were shown to extract PLs while HP-α-CD had no effect (Motoyama et al., 2006). In addition, methylated β-CD derivatives caused a greater Chol efflux from the erythrocyte membrane, as compared to β-CD (Motoyama et al., 2009b).

The presence of β-CD and its derivatives, HP-β-CD and Me-β-CD, did not modify the PL content of mouse L-cell fibroblast membrane but reduced the Chol content in the order of Me-β-CD > β-CD > HP-β-CD (Kilsdonk et al., 1995). Moreover, the impact of CD type on the lipid release was demonstrated using a blood brain barrier model. Indeed, α-CD preferentially promoted PL extraction, β-CD selectively extracted Chol, while both CD types induced SM release (Monnaert, 2004). Using various β-CD derivatives, it was shown that CDs enhanced Chol efflux from human umbilical vein endothelial cells, with rameb inducing the greatest effect (Castagne et al., 2009). In addition, β-CD derivatives (HP_2-SBE_3-β-CD, HP_3-SBE_2-β-CD, SBE-β-CD, Me-β-CD, and dimeb) caused Chol extraction from human embryonic kidney cells with dimeb exerting the strongest effect (Wang et al., 2011). The impact of the three native CDs as well as G_2-α-CD and G_2-β-CD on Caco-2 cell membrane was also investigated (Ono et al., 2001); the authors demonstrated that β-CD and G_2-β-CD did not affect the PL content while α-CD extracted most of the PLs from cell membrane, and γ-CD produced no effect. According to Szente et al. (2018), the cavity size and the substitution groups of CDs influenced their ability to extract Chol from biological membranes and to evoke cell damage. Methylated CDs (dimeb and rameb) were more potent in solubilizing Chol compared to HP-β-CD and SBE-β-CD, whereas HP-γ-CD was not found to extract Chol.

CD concentration can also influence the CD-mediated lipid extraction. All studies on this subject, both on biomimetic and biological membranes, highlight the importance of CD concentration. Indeed, increasing the CD concentration increases the extent of lipid release from membranes (Denz et al., 2016; Milles et al., 2013; Ohvo and Slotte, 1996; Ohvo-Rekilä et al., 2000; Yancey et al., 1996).

7.2.2.2. Phospholipid type. The effect of PL acyl chain length and saturation as well as PL head group type on the strength of CD-

Table 2
Extraction of lipid membrane components by cyclodextrins.

Membrane	CDs type	[CD] (mM)	Outcomes	Ref
Liposomes				
- POPC:DHE (70:30) - SM:DHE (70:30) - POPC:cholestatrienol (70:30) - SM:cholestatrienol (70:30)	HP-β-CD	0–4	- CD-mediated sterol extraction in a concentration dependent manner - Slower sterol extraction rate from SM vesicles compared to POPC vesicles - Better extraction of cholestatrienol compared to DHE.	Ohvo-Rekilä et al., 2000
- DOPC - DOPC:Chol (70:30) - DOPC:Chol (55:45) - DOPC:SM:Chol - (53:17:30) - DOPC:SM:Chol (40:40:20) - DOPC:SM:Chol (30:30:40)	Me-β-CD	0.002–8	- No DOPC extraction at all CD concentrations used - Fast Chol extraction rate - Reduced Chol extraction rate in the presence of SM.	Besenicar et al., 2008
- DOPC:Rh-PE:NBD-Chol (99:0.5:0.5) - DOPC:Rh-PE:BODIPY-Chol (99:0.5:0.5)	- α-CD - β-CD - HP-β-CD - Me-β-CD - γ-CD	0–10	- CD-mediated Chol extraction in a concentration dependent manner - Rapid exponential kinetics of Chol efflux with release rate constants ranging from 0.2 to 0.6 s^{-1} - Greater Chol extraction by Me-β-CD compared to other CDs. Slight extraction of NBD-Chol by HP-β-CD, β-CD, and γ-CD; no effect was exerted on BODIPY-Chol.	Milles et al., 2013
- POPC:Rh-PE:C6/C12 NBD-PC (99:0.5:0.5) - POPC:Rh-PE:C6/C12 NBD-PS (99:0.5:0.5) - POPC:Rh-PE:C6/C12 NBD-PE (99:0.5:0.5) - POPC:Rh-PE:C6/C12 NBD-SM (99:0.5:0.5)	- Me-α-CD - Me-β-CD - Me-γ-CD		- CD-mediated PL extraction in a concentration dependent manner - Bi-exponential kinetics of PL efflux - High extraction of PL by Me-α-CD and Me-ß-CD whereas Me-γ-CD was less effective - Better extraction of short chain PLs (C6) compared to the long ones (C12) - Better extraction of NBD-PC and NBD-SM compared to NBD-PS and NBD-PE.	Denz et al., 2016
Monolayers				
- Chol - DPPC - DDPC - SM - DPPC:Chol (0.5–1 to 9:1) - DDPC:Chol (0.5:1 to 9:1) - SM:Chol (0.5:1 to 9:1)	β-CD		- CD-mediated Chol extraction in a concentration dependent manner - Insignificant PL extraction compared to Chol extraction - β-CD-induced disappearance of Chol rich domains in DDPC:chol membranes - Reduced Chol extraction in the presence of PL and SM; SM effect > PL effect.	Ohvo and Slotte, 1996
- DHE - Cholestatrienol - Chol - POPC:DHE (70:30) - POPC:Cholestatrienol (70:30) - POPC:Chol (70:30)	HP-β-CD	1.6: pure layers 16: mixed layers	- Lipid extraction from pure sterol monolayers in the order: cholestatrienol > dehyroergosterol > Chol - Slower extraction rate from mixed monolayers compared to the pure ones.	Ohvo-Rekilä et al., 2000
- DPPC - DMPC - POPC - DMPG - SM	β-CD	0.7	- Lipid extraction in the order: SM > POPC > DPPC - No extraction of DMPG was obtained.	Grauby-Heywang and Turlet, 2008
Biological membranes				
Human erythrocytes	- α-CD - β-CD - γ-CD	0–40	CD-mediated membrane Chol extraction in the order: β-CD > γ-CD > α-CD.	Irie et al., 1982
Human erythrocytes	- α-CD - β-CD - γ-CD	0–40	- CD-mediated PLs extraction in the order: α-CD > β-CD ≫ γ-CD - CD-mediated extraction of Chol in the order: β-CD ≫ γ-CD; no effect of α-CD.	Ohtani et al., 1989
Rabbit erythrocytes	- α-CD - HP-α-CD - DM-α-CD	3	- PLs were extracted by DM-α-CD and α-CD but no effect of HP-α-CD - No Chol extraction by all CDs used.	Motoyama et al., 2006
Rabbit erythrocytes	- β-CD - Me-β-CD - Dimeb	β-CD: 3 Me-β-CD:1 Dimeb: 0.8	- Only dimeb induced PL and SM release - CD-mediated Chol extraction in the order: dimeb = Me-β-CD > β-CD.	Motoyama et al., 2009b
- Mouse L-cell fibroblast - Human fibroblast - Rat hepatoma cells	- B-CD - HP-β-CD - Me-β-CD	0–10	- CD-mediated Chol extraction in a concentration dependent manner - CD-mediated Chol extraction in the order: Me-β-CD > β-CD > HP-β-CD - HP-β-CD-induced a rapid Chol extraction (up to about 2 h) - Me-β-CD and HP-β-CD induced cellular release of desmosterol as a function of CD concentration; Me-β-CD effect > HP-β-CD effect - No significant PLs release was obtained - Extent of Chol extraction was the same for all the cell types.	Kilsdonk et al., 1995
- Mouse L-cell fibroblast	HP-β-CD	0–200		

(continued on next page)

Table 2 (*continued*)

Membrane	CDs type	[CD] (mM)	Outcomes	Ref
- Human skin fibroblast - Rat hepatoma cells			- CD-mediated Chol extraction in a concentration dependent manner till reaching saturation at high CD concentration (50 mM for rat hepatoma cells and 75 mM for L-cell fibroblasts) - Bi-exponential kinetics of Chol efflux. The range of half-times for the fast pool: 19–23 s, and that for the slow pool: 15–35 min - The Chol extraction rate from cells in the order: rat hepatoma cells > mouse L-cell fibroblasts > human skin fibroblasts.	Yancey et al., 1996
Human skin fibroblasts	HP-β-CD	5–15	- CD-mediated Chol extraction in a concentration dependent manner - Chol extraction was stimulated by SM degradation (using sphingomyelinase), while PC degradation (using PC-PLC) had no effect on Chol extraction.	Ohvo et al., 1997
Human sperm	Me-β-CD	0–10	- CD-mediated Chol extraction in a concentration dependent manner.	Cross, 1999
Goat sperm	β-CD	0–16	- CD-mediated Chol extraction in a concentration dependent manner - Rapid exponential kinetics of Chol efflux with half time of about 10 min - No PL extraction was obtained.	Iborra et al., 2000
T lymphocytes Jurkat cell lines	Me-β-CD	0.5–15	- CD-mediated Chol extraction in a concentration dependent manner - Rapid Chol efflux at a single rate; a plateau was reached after 15 min.	Mahammad and Parmryd, 2008
Rod outer segment	Me-β-CD	0–40	- CD-mediated Chol extraction in a concentration dependent manner - Significant PL extraction at CD concentration above 15 mM.	Niu et al., 2002
Rod outer segment	Me-β-CD	15	- CD-mediated membrane Chol extraction - No effect of CD on the PL membrane content.	Elliott et al., 2003
Blood brain barrier model	- α-CD - β-CD - γ-CD	γ-CD: 0–50 other: 0–5	- Selective extraction of PC by α-CD compared to other CDs - Selective Chol extraction by β-CD in a concentration dependent manner - α-CD and β-CD mediated extraction of SM - γ-CD was less lipid selective.	Monnaert, 2004
Human umbilical vein endothelial cells	- B-CD - HP-β-CD - Me-β-CD - Dimeb - Trimeb - Rameb - Crysmeb	0–10	- CD-mediated Chol extraction in a concentration dependent manner - CD extraction ability was as follows: trimeb < HP-β-CD < β-CD = crysmeb < dimeb = Me-β-CD < rameb.	Castagne et al., 2009
Human embryonic kidney-derived HEK293A cells	- HP_2-SBE_3-β-CD - HP_3-SBE_2-β-CD - SBE-β-CD - Me-β-CD - Dimeb	0–20	- CD-mediated Chol extraction in a concentration dependent manner - For the same CD concentration, the effect of CDs on Chol extraction was in the order: HP_2-SBE_3-β-CD < HP_3-SBE_2-β-CD < SBE-β-CD < Me-β-CD < dimeb.	Wang et al., 2011
Caco-2 cells	- α-CD - β-CD - γ-CD - G_2-α-CD - G_2-β-CD	β-CDs:0–15 other CDs: 0–150	- No effect of β-CD and G_2-β-CD on PLs extraction at low CD concentrations (< 15 mM) - The majority of membrane PLs were extracted by α-CD - Moderate PLs extraction was obtained at CD 37.5 mM for G_2-α-CD and G_2-β-CD - No effect of γ-CD.	Ono et al., 2001
- Human embryonic kidney derived HEK293T cells - Human cervical cancer-derived HeLa cells - T lymphocyte Jurkat cell lines	- HP-β-CD - HP-γ-CD - SBE-β-CD - Dimeb - Rameb	50	- The Chol extraction by CDs was in the order: Dimeb > Rameb ≫ HP-β-CD > SBE-β-CD - No effect of HP-γ-CD.	Szente et al., 2018

BODIPY: dipyrromethene boron difluoride; Chol: cholesterol; DDPC: didecanoyl-phosphatidylcholine; DHE: dehydroergosterol; Dimeb: dimethylated-β-cyclodextrin; DM-α-CD: dimethyl-α-cyclodextrin; DMPC: dimyristoyl-phosphatidylcholine; DMPG: dimyristoyl- phosphatidylglycerol; DOPC: dioleoyl-phosphatidylcholine; DPPC: dipalmitoyl-phosphatidylcholine; NBD: 7-nitrobenz-2-oxa-1,3-diazol-4-yl; PC: phosphatidylcholine; PE: phosphatidylethanolamine; PL: phospholipid; PLC: phospholipase C; POPC: palmitoyl-oleoyl-phosphatidylcholine; PS: phosphatidylserine; Rh: Rhodamine; SM: sphingomyelin; Trimeb: trimethylated-β-cyclodextrin.

mediated PL extraction have been discussed in the literature (Denz et al., 2016; Grauby-Heywang and Turlet, 2008). Short chain lipids are better extracted than long ones from liposome membrane when various methylated CDs were applied. In addition, PC was more effectively removed from liposome membrane in comparison with PE and PS (Denz et al., 2016). Moreover, β-CD was capable to release PC from monolayers without any effect on phosphatidylglycerol (PG) monolayers (Grauby-Heywang and Turlet, 2008).

Concerning the saturation status of acyl chains, the presence of an unsaturated acyl chain was reported to favor the β-CD-induced PLs desorption from monolayers (Grauby-Heywang and Turlet, 2008); a double bond creates a kink in the carbon chain rendering the structure less tightly packed. In addition, the lipid backbone influences its extraction; thus, SM (sphingosine backbone) was easier extracted from biomimetic membranes than PLs (glycerol backbone) (Grauby-Heywang and Turlet, 2008). This difference can be explained by the fact that SM can act as both H-bond donor and acceptor while PC is only a H-bond acceptor; H-bonds between lipids and CDs stabilize lipid-CD complex, thereby favoring lipid extraction (Boggs, 1987).

7.2.2.3. Membrane lipid composition. CD-mediated Chol desorption from pure Chol monolayer was studied and compared to those composed of Chol mixed with PLs or SM. The results showed that CDs induced minimal efflux of Chol from mixed monolayers in

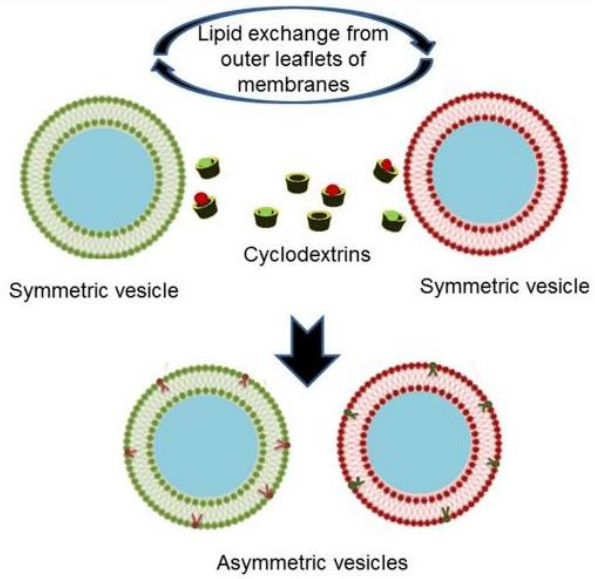

Fig. 9. A scheme for cyclodextrin-mediated formation of asymmetric vesicles: cyclodextrins can promote lipid efflux (red and green) from symmetric donor membranes, form soluble complexes in aqueous phase, and carry the lipids to acceptor membranes.

comparison with pure Chol monolayers (Ohvo and Slotte, 1996; Ohvo-Rekilä et al., 2000), and SM exerted a greater effect in lowering Chol desorption rate compared to PLs (Ohvo and Slotte, 1996). The rate of HP-β-CD-mediated sterol extraction was higher from POPC:sterol vesicles than that from SM:sterol vesicles (Ohvo-Rekilä et al., 2000). Besenicar et al. (2008) reported that the addition of SM to dioleoylphosphatidylcholine:Chol (DOPC:Chol) vesicles slowed the Me-β-CD-mediated Chol extraction. These findings are corroborated by the study of Ohvo et al. (1997). The authors stated that reducing SM content in human skin fibroblasts by about 76%, using sphingomyelinase, stimulated the HP-β-CD-induced Chol removal from the plasma membrane (23% compared to 13% from untreated cells), while reducing PC content by about 12% using PC-phospholipase C, had no effect on membrane Chol level. Hence, Chol interaction with other membrane components may retard its CD-induced extraction.

7.2.2.4. Cell type. Two studies compared the effect of CDs on the Chol extraction rate from three different cell types: mouse L-cell fibroblast, human skin fibroblast, and rat hepatoma cells (Kilsdonk et al., 1995; Yancey et al., 1996). Kilsdonk et al. (1995) used β-CD, HP-β-CD, and Me-β-CD (in the range of 0–10 mM), and Yancey et al. (1996) used HP-β-CD (0–200 mM). According to the first study, the rate of Chol release did not differ among the cell types. In contrast, Yancey et al. (1996) found that Chol release rate varied between the cells as follows: rat hepatoma cells > mouse L-cell fibroblasts > human skin fibroblasts. This difference might be due to the disparate CD concentrations tested; at high concentrations such as 200 mM, HP-β-CD might have various Chol efflux capacities towards different cell types.

7.2.3. The mechanisms of cyclodextrin-mediated lipid extraction

The mechanisms of Chol and PL extraction by CDs were discussed in several studies. Thus, Fauvelle et al. (1997) evaluated the effect of α-CD-induced PI extraction using ^{1}H NMR, ^{2}H NMR, and ^{31}P NMR spectroscopy techniques (1997). Fauvelle and coworkers showed that α-CD was attracted to membrane surface by electrostatic interaction between the positively charged primary hydroxyl side of α-CD and the negatively charged PI at the bilayer surface. This promoted the PI molecule extraction; in addition, another α-CD molecule was observed to include the PI unsaturated sn-2 acyl chain.

López et al. (2011) applied molecular dynamic (MD) simulations to study the mechanism of Chol extraction by β-CD. It is known that β-CDs in aqueous solution are associated to form dimers which are bound to the membrane surface assuming either a tilted or untilted configuration. Only the untilted configuration was appropriate to extract Chol allowing the formation of a membrane-bound CD/Chol complex. Although Chol is inserted quite deeply within the channel, the dimethyl end of its hydrophobic tail remains in contact with the monolayer surface until the CD/Chol complex tilts by 90°. Finally, the complex is desorbed where each dimer extracts one Chol molecule from membrane. It is worthy to mention that the CD monomer is able to interact with membrane but the strength of this interaction is insufficient to extract Chol. Also, Yancey et al. (1996) proposed that the CD-mediated Chol extraction occurs by its desorption from the surface directly into CD hydrophobic core (without passage through the aqueous phase). In addition, Steck et al. (2002) suggested that Chol efflux induced by CDs takes place through an activation-collision mechanism where the reversible partial projection of Chol molecules out of the erythrocyte lipid bilayer precedes their collisional capture by CD.

Furthermore, Sanchez et al. (2011) used Laurdan generalized polarization to investigate the specificity of Me-β-CD (0.25, 1, and 2 mM) in removing Chol from the coexisting macro-domains (liquid-ordered and liquid-disordered domains) of GUV membranes composed of DOPC:DMPC:Chol (1:1:1). The authors proved that Me-β-CD selectively remove Chol from the liquid disordered phase of the liposome bilayer.

7.2.4. Cyclodextrin-mediated lipid exchange between membranes

Based on the capacity of natural CDs and their derivatives to extract membrane lipid components, they had been widely used to catalyze the lipid exchange between different membrane vesicles or between a lipid vesicle membrane and a biological cell membrane. CD-mediated lipid exchange has been mainly performed to build up lipid vesicles with lipid asymmetry (Fig. 9); indeed, in natural biological membranes, the lipid composition of the inner and the outer leaflets is different (Huang and London, 2013). CDs promote the lipid molecule efflux from a donor membrane surface partially or fully forming a soluble complex with this lipid in aqueous medium and carrying it to an acceptor membrane (Tanhuanpää and Somerharju, 1999).

Various studies were carried out to investigate the transfer of PLs and Chol between donor and acceptor membranes. Donor vesicles, containing unlabeled lipids as well as labeled ones bearing a fluorescent moiety (NBD, BODIPY, pyrene, or other), a heavy isotope, or a radioactive molecule, were incubated with CDs; the unlabeled acceptor membranes are generally cells or lipid vesicles. After incubation, the acceptor membranes were separated from the donor membranes, subjected to lipid extraction, and analyzed. Besides, Huang and London (2013) studied CD-mediated lipid exchange assessing FRET between NBD-labeled lipids and rhodamine-labeled lipids embedded in donor vesicles. FRET was also used to monitor the DHE transfer from CD/DHE complex to lipid vesicles containing dansyl-PE (McCauliff et al., 2011).

Table 3 summarizes the literature regarding the CD-induced lipid exchange between membranes. The membrane lipid compositions of donor and acceptor vesicles, the type and concentration of CD used in each study are presented as well.

As it is obvious from Table 3, CDs are able to mediate efficient transfer of PLs and Chol between lipid vesicles or between a lipid vesicle and a cell; the transfer is controlled by several parameters. First, the level of CD-mediated lipid exchange between vesicles is directly proportional to the CD concentration (Huang and London, 2013; Kainu et al., 2010; Leventis and Silvius, 2001; McCauliff et al., 2011; Tanhuanpää and Somerharju, 1999). However, at high CD concentrations, it may induce membrane damage and vesicle solubilization (Huang and London, 2013). Second, the level of lipid exchange between membranes is affected by the CD type. Me-β-CD is more efficient

Table 3
CD-induced lipid exchange between membranes.

Donor membrane	Acceptor membrane	CD type	[CD] (mM)	Outcomes	Ref
Liposomes of POPC, TNP-PE, and pyrene-labelled PL with various head groups and acyl chain length	- POPC: POPA (500:20) liposomes - Human fibroblasts - Baby hamster kidney cells	CE-γ-CD	0–30	- Rate of lipid transfer was proportional to the CD concentration - Increasing acyl chain length (6–14C) decreased the PL transport rate - Transport of PI was enhanced compared to the other PLs - Rate of SM transport was 3 folds greater than that of PC.	Tanhuanpää and Somerharju, 1999
Negatively charged liposomes SOPC:SOPG (85:15) containing ^{3}H-Chol and ^{3}H-DPPC	Uncharged SOPC vesicles	- α-CD - β-CD - γ-CD - Me-β-CD	0–1	- CDs, except α-CD, induced Chol transfer. Chol transfer rate was 53, 64, 63 folds higher when treated with 1 mM Me-β-CD, γ-CD or β-CD, respectively, compared to untreated samples - Rate of Chol transfer was proportional to the CD concentration - Me-β-CD and α-CD induced DPPC transfer rather than Chol transfer - β-CD and γ-CD induced Chol transfer rather than DPPC transfer.	Leventis and Silvius, 2001
POPC:Chol: heavy isotopes labelled PL of various head group and acyl chain length liposomes	Baby hamster kidney cell	Me-β-CD	0–10	- CD induced PL transfer - Rate of PL transfer was proportional to CD concentration - Increasing acyl chain length decreased the PL transfer rate but the nature of the head group of PL had no effect.	Kainu et al., 2010
EPC:DHE (75:25) liposomes	EPC:dansyl-PE (97:3) liposomes	HP-β-CD		- CD-induced the DHE transfer - The rate of DHE transfer was proportional to the CD concentration - The DHE transfer occurred by a collisional transfer mechanism.	McCauliff et al., 2011
Liposomes with NBD labelled lipids	Liposomes with unlabelled lipids	- Me-β-CD - HP-β-CD - HP-α-CD	0–150	- Lipid exchange was observed at Me-β-CD concentration < 10 mM - CD induced vesicle solubilisation at a concentration > 50 mM - Me-β-CD induced lipid exchange more than the other CDs.	Huang and London, 2013
Liposomes containing NBD or ^{3}H labelled PLs with various head group and length of acyl chain	A549 lung carcinoma cells	Me-α-CD	0–40	- Various % of exchange was found for different lipids: ~75% for SM, 10–15% for PC and PE; there was no exchange of PS and PI - Increasing the length of acyl chain decreased the SM transport rate.	Li et al., 2016

Chol: cholesterol; DHE: dehydroergosterol; DPPC: dipalmitoyl-phosphatidylcholine; EPC: egg phosphatidylcholine; NBD: 7-nitrobenz-2-oxa-1,3-diazol-4-yl; PC: phosphatidylcholine; PE: phosphatidylethanolamine; PI: phosphatidylinositol; PL: phospholipid; POPA: palmityl-oleoyl-phosphatidic acid; POPC: palmitoyl-oleoyl-phosphatidylcholine; PS: phosphatidylserine; Rh: rhodamine; SM: sphingomyelin; SOPC: 1-stearoyl-2-oleoyl-phosphatidylcholine; SOPG: 1-stearoyl-2-oleoyl-phosphatidylglycerol; TNP-PE: N-trinitrophenyl-PE.

Table 4
Some examples of cyclodextrin-induced protein extraction.

Cell type	CD type	[CD] (mM)	Outcomes	Ref
Human erythrocytes	- α-CD - β-CD - γ-CD	0–40	- Proteins were randomly extracted, without preference to any particular ones - The CD-induced protein extraction was in the order: β-CD ≫ γ-CD > α-CD.	Ohtani et al., 1989
T lymphocytes	Me-β-CD	0–50	- Me-β-CD-induced extraction of the proteins: Thy-1 (cluster of differentiation-90), cluster of differentiation-45, cluster of differentiation-26, MHC-1, PTK-1, Lck, and Fyn.	Ilangumaran and Hoessli, 1998
Caco-2 cells	- α-CD - β-CD - γ-CD - G_2-α-CD - G_2-β-CD	β-CD: 0–15 Others: 0–150	- Proteins were randomly extracted, without preference to any particular ones - The CD-induced protein extraction was in CD concentration dependent manner - At 150 mM, the CD-induced protein extraction was in the order: γ-CD < G_2-β-CD < G_2-β-CD < < α-CD - At 15 mM, β-CD exhibited no ability for protein extraction.	Ono et al., 2001
B lymphocytes	Me-β-CD	10	- Me-β-CD induced extraction of BCR and cluster of differentiation-20.	Awasthi-Kalia et al., 2001
Rod outer segment	Me-β-CD	15	- Me-β-CD induced extraction of transducin α subunit (Tα) from detergent resistant domains.	Elliott et al., 2003
Rabbit erythrocytes	- α-CD - HP-α-CD - DM-α-CD	3	- Proteins were randomly extracted, without preference to any particular ones - DM-α-CD induced protein extraction - No extraction was detected with other CDs.	Motoyama et al., 2006
Rabbit erythrocytes	- β-CD - Me-β-CD - Dimeb	β-CD: 3 Me-β: 1 Dimeb: 0.8	- Proteins were randomly extracted, without preference to any particular ones - Me-β-CD and dimeb induced protein extraction - No extraction was obtained with β-CD.	Motoyama et al., 2009
Rod outer segment	Me-β-CD	0–20	- Me-β-CD induced extraction and purification of prenylated proteins GRK1 and PDE6.	Saito et al., 2012

BCR: B cell receptor; GRK1: rhodopsin kinase; Lck: lymphocyte-specific protein tyrosine kinase; MHC 1: major histocompatibility complex 1; PDE 6: cGMP phosphodiesterase 6; PTK: protein tyrosine kinase; Thy-1: Thymocyte antigen 1.

towards lipid exchange between liposomes compared to HP-β-CD and HP-α-CD (Huang and London, 2013). Moreover, Me-β-CD and α-CD are found to be more potent in mediating DPPC transfer between vesicles compared to that of Chol; on the contrary, β-CD and γ-CD are more efficient transfer inducers of Chol in comparison with DPPC (Leventis and Silvius, 2001). Another factor affecting the lipid exchange is the type of PL. For instance, Me-α-CD induced the transport of SM (75%), PC and PE (10–15%) but not PI and PS. Also, SM molecules with shorter acyl chains (fewer than 36C) were exchanged to a greater extent than the longer ones (Li et al., 2016). These findings are consistent with those of Kainu et al. (2010) reporting that the transport of PLs triggered by Me-β-CD depends on length of their acyl chains; at the same time, there was no consistent relation with the PLs head group. Similarly, the lipid transport rate mediated by CE-γ-CD (5 mM) decreased as the acyl chain length of PC increased from 6 to 14 C atoms (Tanhuanpää and Somerharju, 1999). Furthermore, CE-γ-CD enhanced the PI transport rate by about twice compared to PG, PE, PS, and PC; besides, the SM transport mediated by this CD was about 3 folds more rapid than that of PC. The authors concluded that the overall molecular hydrophobicity of PLs is an essential factor controlling their CE-γ-CD-mediated transport.

McCauliff et al. (2011) studied the mechanism of transfer of DHE, a fluorescent Chol analogue, from HP-β-CD/DHE complex to PL membranes. They demonstrated that the DHE transfer occurred by a collisional transfer mechanism involving a direct interaction of HP-β-CD with the membrane. HP-β-CD acts like Niemann–Pick C2 protein; the latter is involved in Chol transport and metabolism.

7.2.5. The effects of cyclodextrins on signal transduction pathways

To the best of our knowledge, CDs do not interact with specific membrane receptors. They act through a non-classical mechanism which is based on the extraction of membrane components (Chol, PL, lipid metabolites, and proteins), and/or the disruption of raft domains (Kabouridis et al., 2000; Matassoli et al., 2018). This may result in the alteration of signaling pathways; for example, Chol extraction by CDs leads to several changes including: *i)* the activation of phosphatidylinositol-3-kinase/protein kinase B/ Bcl-2-associated death promoter (PI3K/Akt/Bad) pathways (Motoyama et al., 2009); *ii)* the stimulation of ERK (extracellular signal-regulated kinase) phosphorylation and the inhibition of PI3K/Akt phosphorylation, thereby reducing the expression of the transcription factor c-Jun in colon carcinoma cells (Scheinman et al., 2013); *iii)* the suppression of resveratrol-induced activation of kinase-dependent signaling pathways (c-Jun NH_2-terminal kinase/ERK/Akt) and caspase-dependent apoptosis in colon cancer cells (Colin et al., 2011); *iv)* the activation of Wnt/β-catenin pathway which plays multiple roles at different stages of development of Xenopus laevis (Reis et al., 2016); *v)* the activation of protein kinase A and tyrosine kinase resulting in protein phosphorylation and sperm capacitation (Osheroff, 1999; Visconti et al., 1999); *vi)* the enhancement of antigen receptor-mediated intracellular calcium release in Ramos B cells (Awasthi-Kalia et al., 2001), and its inhibition in Jurkat T cells (Kabouridis et al., 2000); *vii)* the enhancement of signaling pathways associated with β1-adrenergic receptors resulting in compartmentalized cyclic adenosine monophosphate (cAMP) response in cardiac monocytes (Agarwal et al., 2011); *viii)* the suppression of cAMP-dependent protein kinase (PKA) modulation of voltage-gated potassium channel (Kv) current in rat mesenteric artery smooth muscle cells (Brignell et al., 2015); *ix)* the suppression of signaling pathways associated with chemokine receptor (CCR5), leading to the inhibition of calcium release and abrogation of inhibition of forskolin-stimulated cAMP accumulation in Chinese hamster ovary cells and human embryonic kidney cells (Cardaba et al., 2008), *x)* the suppression of insulin-stimulated Akt phosphorylation in mice hepatocytes (Key et al., 2017); *xi)* other signaling pathways may also be involved. Additionally, CD-induced extraction of other membrane components (PLs or proteins) may affect several signal transduction pathways. For instance, DM-α-CD suppressed nitric oxide and tumor necrosis factor-α (TNF-α) production as well as nuclear factor-$_K$B (NF-$_K$B) activation in stimulated macrophages due to the efflux of PLs and cluster of differentiation 14 from lipid rafts (Motoyama et al., 2005).

The signaling pathways changes would depend on the cell line (Awasthi-Kalia et al., 2001; Kabouridis et al., 2000; Motoyama et al., 2005), the CD type and concentration (Colin et al., 2011; Motoyama et al., 2005), the CD forms (free or CD/guest complex) (Key et al., 2017), etc. This illustrates the vastness of this topic and requires separate consideration in a special review.

7.3. Protein extraction

Table 4 resumes the results of several studies, as examples, on the ability of CDs to extract proteins from different cell membranes. The type and concentration of CD are also presented.

As shown in Table 4, CDs are able to solubilize membrane proteins; the CD concentration and type are modulating factors of the process (Ono et al., 2001; Ohtani et al., 1989; Motoyama et al., 2006; Motoyama et al., 2009). Thus, β-CD was more potent in inducing protein extraction from human erythrocytes compared to the other native CDs (Ohtani et al., 1989). On the other side, α-CD was more effective in inducing protein extraction from Caco-2 cell membrane, and no effect was exerted by β-CD (Ono et al., 2001). Furthermore, DM-α-CD (Motoyama et al., 2006) and the methylated derivatives of β-CD (Me-β-CD and dimeb), unlike the native α- and β-CDs (Motoyama et al., 2009b), were found to induce the extraction of proteins spanning rabbit erythrocytes membranes.

It is worthy to note that Me-β-CD was the only CD used in the literature to selectively extract membrane proteins from T lymphocytes (Ilangumaran and Hoessli, 1998) and B lymphocytes (Awasthi-Kalia et al., 2001). Also, it was observed to selectively extract prenylated proteins GRK1 and PDE6 from rod outer segment membrane. These proteins were demonstrated to have different EC50 values (effective concentration to extract 50% of total protein amount); it depends on the strength of protein-membrane association. For GRK1, EC50 was 0.17 mM while for PDE6 it was 5.1 mM (Saito et al., 2012). Moreover, Elliott et al. (2003) reported that adding Me-β-CD resulted in the extraction of the peripheral protein transducin α subunit (Tα) from the detergent resistant domains of rod outer segment membrane without any effect on caveolin-1.

7.4. The effect of cyclodextrins on the membrane permeability

Cell membrane permeability is essential for many biological processes. Therefore, liposome membrane permeability was examined in the presence of various CDs by analyzing the release of fluorescent dyes incorporated into liposomes such as carboxyfluorescein (Nishijo et al., 2000) and calcein (Besenicar et al., 2008; Hatzi et al., 2007; Piel et al., 2007). Regarding cellular membranes, permeability was evaluated by analyzing the release of intracellular components such as hemoglobin (Ohtani et al., 1989) and the enzyme lactate dehydrogenase (Wang et al., 2011). Table 5 summarizes the results of the literature search regarding the effect CDs on the membrane permeability with respect to the membrane lipid composition or cell type, CD type and concentration, and intravesicular fluorescent dye or intracellular component used to assess the membrane permeability.

The interaction of CDs with lipid membrane components increased the membrane permeability; the extent of increase in permeability is directly proportional to the CD concentration (Kilsdonk et al., 1995; Nishijo et al., 2000; Ohtani et al., 1989; Piel et al., 2007; Wang et al., 2011). On the other side, Besenicar et al. (2008) showed that Me-β-CD (0–4 mM) did not influence the membrane permeability of DOPC and DOPC:Chol liposomes. This is probably due to relatively low CD concentrations (0–4 mM) unlike other studies using higher CD concentrations up to 10 mM (Kilsdonk et al., 1995; Nishijo et al., 2000), 20 mM (Wang et al., 2011), and 100 mM (Piel et al., 2007).

Additionally, several studies stated that the CD-induced membrane permeability increase depends on the type of CD, namely its hydrophobicity and the cavity size. For instance, α-CD, dimeb, and trimeb were shown to induce carboxyfluorescein release from DPPC, distearoyl-phosphatidylcholine (DSPC), and dimyristoyl-phosphatidylcholine (DMPC) liposomes while no effect was produced by β-CD, HP-β-CD, and γ-CD (Nishijo et al., 2000). Besides, the permeability of soybean phosphatidylcholine (SPC):stearylamine (SA) liposome, assessed by studying the kinetics of calcein release, was found to increase after exposure to methylated β-CDs such as dimeb, rameb, and trimeb (Piel et al., 2007). However, other CDs used in this work, β-CD, crysmeb, HP-β-CD, SBE-β-CD, γ-CD, and HP-γ-CD, did not significantly induce calcein leakage from liposomes. As suggested by the authors, calcein molecules may escape from the liposomes as a result of the interaction of methylated CDs with membrane lipids. Moreover, the same authors showed that the methylated CDs increased the permeability of liposomes containing or not Chol; this result allowed them to conclude that Chol does not protect membranes from the effect of CDs (Piel et al., 2007). Furthermore, Hatzi et al. (2007) demonstrated that the CD-mediated membrane permeability increase was greater for Me-β-CD than for HP-β-CD or HP-γ-CD; thus, the effect of CD on the membrane permeability depends on the lipophilicity of CD rather than its cavity size.

Concerning the effect of CDs on the permeability of biological membranes, the native CDs were able to increase the permeability of human erythrocytes, with β-CD exerting the greatest effect (Ohtani et al., 1989). In addition, methylated CDs such as Me-β-CD (Kilsdonk et al., 1995; Wang et al., 2011) and dimeb (Wang et al., 2011) were demonstrated to be more potent in enhancing the membrane permeability of mouse L cell fibroblasts (Kilsdonk et al., 1995) and human embryonic kidney 293A cells (Wang et al., 2011) compared to other β-CD derivatives.

Other factors controlling the CD-induced membrane permeability are the type of PL constituting the liposomal membrane and the size of liposomal vesicles (Hatzi et al., 2007). Indeed, liposomes composed of saturated PLs (HPC) were found to be less affected by CDs in relation to the unsaturated ones. Moreover, the presence of Chol in the membrane lowered the permeability of unsaturated PC liposomes, while it increased or did not affect that of HPC or DSPC liposomes (Hatzi et al., 2007).

Moreover, for the same membrane lipid composition, the CD-induced calcein release from MLV was greater relative to SUV. The greater SUV stability is evidently due to the curvature of lipid molecules which does not allow lipids to establish an optimal contact angle to interact with CDs (Hatzi et al., 2007).

Furthermore, Monnaert (2004) measured the endothelial permeability coefficient (Pe) of [^{14}C]-sucrose across blood brain barrier at 0–5 mM for α-CD and β-CD, and at 0–50 mM for γ-CD. The sucrose permeability was determined to be dependent of CD concentration; the effect of CDs was in the order of α-CD > Me-α-CD = HP-α-CD = β-CD = Me-β-CD = HP-β-CD > γ-CD, Me-γ-CD > HP-γ-CD.

Table 5 presents the data on the kinetics of intravesicular components release from liposomes induced by different CDs. We can notice that most CDs induced an instant release of intravesicular components after CD adding to liposomes followed by a slow (Nishijo et al., 2000) or negligible (Hatzi et al., 2007) release stage. This finding can be explained by the fact that at the initial stage, the CD-induced extraction of membrane lipids results in membrane permeabilization. Following this stage, CD/lipid complexes may act as lipid donors towards membrane allowing its re-organization (Hatzi et al., 2007).

7.5. Vesicles solubilization upon cyclodextrin – membrane interaction

The particle size analysis by dynamic light scattering (Hatzi et al., 2007) and turbidity measurements (Boulmedarat et al., 2005; Hatzi et al., 2007) revealed that CDs, in particular methylated β-CDs, induced vesicle solubilization due to the CDs ability to draw PLs and Chol out of the liposome membrane (Anderson et al., 2004).

Hatzi et al. (2007) showed that Me-β-CD was more potent in solubilizing PC and PC:Chol liposomes than HP-β-CD, at a CD concentration starting from 60 mM. This result was attributed to the ability of Me-β-CD to mediate a faster extraction of Chol with respect to HP-β-CD. Also, POPC vesicles were solubilized in a concentration-dependent manner when mixed with rameb solution (15–150 mM); the increase in rameb concentration from 80 to 100 mM led to a 2-fold increase in the amount of extracted POPC (Anderson et al., 2004). In addition, rameb

Table 5
The effect of cyclodextrins on liposomal and biological membrane permeability.

Membrane	CD type	[CD] (mM)	Released substance	Outcomes	Ref
Liposome					
- DPPC - DSPC - DMPC	- α-CD - β-CD - HP-β-CD - Dimeb - Trimeb - γ-CD	0–10	CF	- Release of CF was proportional to the CD concentration - Release of CF was in the order: DPPC liposome: Dimeb > α-CD > Trimeb DSPC liposome: Dimeb > Trimeb > α-CD DMPC liposome: α-CD > Dimeb > Trimeb Other CDs had no effect - α-CD induced the CF release as function of time - Dimeb and Trimeb induced a rapid release of CF at the initial stages followed by a slow release which finally levelled off.	Nishijo et al., 2000
- SPC:SA (90:10) - SPC:Chol: SA (60:30:10)	- β-CD - Dimeb - Trimeb - Rameb - Crysmeb - HP-β-CD - SBE-β-CD - γ-CD - HP-γ-CD	β-CD: 0–7.5 Crysmeb: 0–50 others: 0–100	Calcein	- Release was proportional to the CD concentration - Release was in the order: SPC: SA liposome: Dimeb > Rameb > Trimeb SPC:Chol:SA liposome: Dimeb > Rameb > Trimeb > γ-CD Other CDs had no effect - Dimeb induced total release immediately after addition. Other CDs induced the release as a function of time.	Piel et al., 2007
- PC - PC:Chol (1:1) - HPC - HPC:Chol (1:1) - DSPC - DSPC:Chol (1:1)	- HP-β-CD - Me-β-CD - HP-γ-CD	HP-β-CD: 27 Me-β-CD: 31 HP-γ-CD: 25	Calcein	- Release of calcein was in the order: Me-β-CD > HP-β-CD = HP-γ-CD - Release of calcein was in the order: PC > HPC > DSPC - Release of calcein: MLV > SUV - The presence of Chol reduced the permeability of PC liposomes but increased or did not affect that of other liposome types - CDs induced a significant release of calcein immediately after its addition; no further effect was produced.	Hatzi et al., 2007
- DOPC - DOPC:Chol (60:40)	Me-β-CD	0–4	Calcein	- Me-β-CD did not induce the calcein release from the mentioned liposomes.	Besenicar et al., 2008
Biological cells					
Human erythrocytes	- α-CD - β-CD - γ-CD	0–40	Potassium and hemoglobin	- Release was proportional to the CD concentration - Release was in order of β-CD > α-CD > γ-CD - Higher CD concentration was needed for hemoglobin release compared to potassium release.	(Ohtani et al., 1989)
Mouse L-cell fibroblast	- B-CD - HP-β-CD - Me-β-CD	0–10	^{14}C-adenine	- Release was proportional to the CD concentration - Effect of Me-β-CD > HP-β-CD - β-CD had no effect.	(Kilsdonk et al., 1995)
Human embryonic kidney 293A cells	- HP_3-SBE_2-β-CD - HP_2-SBE_3-β-CD - SBE-β-CD - Me-β-CD - Dimeb	0–20	LD	- Release was proportional to the CD concentration - Release was in the order: Me-β-CD = Dimeb > HP_3-SBE_2-β-CD = HP_2-SBE_3-β-CD = SBE-β-CD.	(Wang et al., 2011)

CF: carboxyfluorescein; Chol: cholesterol; DMPC: dimyristoyl-phosphatidylcholine; DOPC: dioleoyl-phosphatidylcholine; DPPC: Dipalmitoyl-phosphatidylcholine; DSPC: distearoyl-phosphatidylcholine; HPC: hydrogenated phosphatidylcholine; LD: lactate dehydrogenase; PC: phosphatidylcholine; SA: stearylamine; SPC: soybean phosphatidylcholine.

(0–152 mM) caused a progressive decrease in the turbidity of SPC:Chol:SA (60:30:10) liposomes until a transparent solution was obtained (above a CD concentration of 50 mM). Furthermore, Huang and London (2013) used FRET to study CD-induced vesicle solubilization. Their results showed that, among different CDs (Me-β-CD, HP-β-CD, and HP-α-CD), a significant vesicle solubilization (abolishment of FRET signals) was achieved by Me-β-CD; the effect was depending on the acyl chain length and saturation degree as well as on the PL head group.

Based on the data discussed in this section and in the preceding sections, we can conclude that CDs are inactive at concentrations below 0.5 mM. In contrast, at moderate concentrations, they can induce lipid extraction and catalyze lipid exchange between membranes. CDs can also promote vesicles solubilization at relatively high concentrations (> 50 mM). It is worthy to mention the "shuttle-sink" model for lipid efflux described by Atger et al. (1997). According to this model, the rate of Chol exchange (influx and efflux) between cell membrane and medium compartment, as it is the case with serum lipoproteins, increases in the presence of low CD concentrations; the equilibrium is not changed and there is no clear change in the membrane and medium Chol pools. However, in the presence of lipid vesicles and CDs, the vesicles act as a sink shifting the equilibrium to favor net efflux of Chol from the cell membranes.

7.6. Cyclodextrins act as cryoprotectants during freeze-drying

Freeze-drying, also known as lyophilization, is essential to ensure the long-term storage of liposomes and biological cells. Nevertheless, it may cause membrane disruption owing to ice crystal formation, membrane phase transition, and osmotic dehydration (Chen et al., 2010; Ingvarsson et al., 2011; Wolkers, 2013). Freeze-drying appeared to be effective for storage of several cell types including erythrocytes (Arav, 2013), platelets (Crowe and Fitzpatrick, 2013), and sperms (Keskintepe and Eroglu, 2015). It was mostly applied on spermatozoa; cryopreservation may promote damage in all sperm compartments, resulting in the loss of sperm motility, viability, acrosomal integrity,

and the fertilizing capacity of the frozen-thawed sperms (Mocé et al., 2010).

Hence, maintaining the integrity of the lipid bilayer structure during freezing of liposomes and biological cells (particularly sperm cell) is highly recommended. Several papers studied the effect of CD as a cryoprotectant to preserve liposomal and biological membranes during the aforementioned process.

7.6.1. Cryopreservation of liposomes using cyclodextrins as cryoprotectants

Van den Hoven et al. (2012) demonstrated a stabilizing effect of HP-β-CD, during freeze-drying, towards PEGylated DPPC:Chol liposomes (lipid:CD w:w ratio of 1:6) loaded with prednisolone; its effect was superior to that of sucrose or trehalose, other known cryoprotectants. Sebaaly et al. (2016) compared the effect of different cryoprotectants (HP-β-CD, sucrose, trehalose, maltodextrin Glucidex6D and 19D, stearylamine, and cetyl alcohol) on phospholipon 90H-liposomes loading eugenol, an essential oil component. HP-β-CD showed the best protective effect; the mean vesicle size, pdI, Zeta potential, and eugenol encapsulation efficiency values were maintained when freeze-drying was conducted in the presence of HP-β-CD.

The effects of composition and saturation of soybean PLs on the liposome stability during freeze-drying was evaluated by Gharib et al. (2018b) using HP-β-CD as a cryoprotectant. HP-β-CD (10–100 mM) added to suspensions of conventional liposomes or present in the interior aqueous phase of CD-in-liposome system, protected hydrogenated liposomes during freeze-drying, while this effect was not observed for liposomes composed of unsaturated PLs.

HP-β-CD has a unique structure with numerous H-bond donors and acceptors. It may replace water molecules at the liposome surface during freeze-drying, thereby protecting the liposomal membrane from damage and keeping its structure intact (van den Hoven et al., 2012).

7.6.2. Cryopreservation of sperm cells using cyclodextrins as cryoprotectants

The effect of CDs on sperm cell cryopreservation was documented in a set of studies. In general, HP-β-CD and Me-β-CD, at optimal concentrations, have an ability to increase sperm cell viability after thawing, as compared to the control. However, CD-induced resistance of spermatozoa to the damage caused by freezing and thawing was shown to vary between species; the variation is due to membrane PL:Chol ratio that differs between species (Madison et al., 2013).

The study of Madison et al. (2013) on jack and stallion sperm cells demonstrated that adding HP-β-CD (60 mM) resulted in an improved cell viability and motility of both sperm cell types. In the presence of HP-β-CD, the post thaw motility was 23 ± 0.7% for jack and 17 ± 0.4% for stallion relative to control (20 ± 0.7% for jack; 15 ± 0.4% for stallion). Moreover, for both species, HP-β-CD induced the sperm post thaw acrosome reaction. Zeng and coworkers studied the effects of HP-β-CD (Zeng and Terada, 2000) and Me-β-CD (Zeng and Terada, 2001) on boar sperm cell viability, motility, and acrosomal status during freeze-drying. According to the authors, the pretreatment with HP-β-CD (up to 40 mM) and Me-β-CD (up to 20 mM) increased the number of sperm cells with intact acrosomes and enhanced the sperm motility compared to untreated cells. However, further elevation of CD concentration up to 80 mM and 40 mM for HP-β-CD and Me-β-CD, respectively, lowered the sperm viability and motility.

7.6.3. Cryopreservation of sperm cells pretreated with cyclodextrin/cholesterol complex

Chol-loaded CDs were suggested to facilitate Chol transfer into the sperm plasma membrane. The effect of Me-β-CD/Chol inclusion complex applied prior to the freeze-drying procedure, on sperm membrane integrity, sperm motility, acrosome reaction, and sperm fertility was extensively studied in the literature. Purdy and Graham (2004) showed that pretreating bull sperm with Me-β-CD/Chol can increase the number of survived sperm cells and preserve their fertilizing potential. In addition, adding treated or untreated sperm to oocytes gave similar percentages of oocytes able to cleave and develop into embryos. Similarly, Salmon et al. (2016) reported that Me-β-CD/Chol, added prior to the cryopreservation procedure, improved the goat sperm cryosurvival rate showing greater percentages of motile and live sperms with intact acrosomes relative to untreated samples. However, contradictory results were published by Pinho et al. (2016) who demonstrated that Me-β-CD/Chol application did not improve, it even decreases, the quality of Piau swine sperm.

The effect of Me-β-CD/Chol inclusion complex was concentration dependent. Pretreating boar sperm with Me-β-CD/Chol (1 mg/ 120×10^6 sperm) increased the percentages of viable (40 ± 3%) and total motile sperm (25 ± 3%) determined after 1 h, in comparison with untreated samples (viability 32 ± 3% and total motility 19 ± 3%). However, higher concentrations of Me-β-CD/Chol (above 3 mg/ 120×10^6 sperm) resulted in lower percentages of viable and motile sperm; thus, at the concentration of 6 mg/120×10^6 sperm, the cell viability and total motility were 24 ± 3% and 11 ± 3%, respectively (Blanch et al., 2012). Furthermore, freezing stallion sperm in the presence of Me-β-CD/Chol (0–7.5 mg/ 120×10^6 sperm) enhanced sperm membrane integrity, as compared to the control; the optimal Chol-Me-β-CD concentration being 1.5 mg/120×10^6 sperm (Moore et al., 2005).

One of the damaging effects during freeze-drying is osmotic stress. The use of a CD/Chol inclusion complex as a cryoprotectant was investigated by evaluating its effect on the osmotic tolerance of sperm cells incubated in both hypo-osmotic and hyper-osmotic conditions. For example, the pretreatment of ram sperm with Chol-loaded Me-β-CD protected membrane integrity after short-term (15 min) exposure to osmotic challenges and significantly increased the percentages of living and intact sperm cells (Ahmad et al., 2013). Also, Me-β-CD/Chol addition increased rabbit sperm cell viability without affecting their functional integrity during a set of osmotic challenges (Aksoy et al., 2010).

8. Recent data in DCLs development

The DCLs systems have been characterized in many publications for their morphology, size, encapsulation efficiency (EE), and rate of drug release. In this section, the focus is done on the effect of CD/drug inclusion complex on the physiochemical properties and stability (based on membrane integrity and drug retention) of liposomes by comparing the characteristics of DCLs to those of blank and drug-loaded liposomes. In 2015, a review had emerged discussing this topic (Gharib et al., 2015). Hence, only the literature data reported between 2015 and 2018 will be presented in this section.

Many studies showed that the incorporation of a drug into liposomes in the form of CD/drug inclusion complex resulted in an improvement of encapsulation efficiency (EE) and/or loading rate values, and in a delay of drug release compared to conventional liposomes. Thus, the loading rate was found to be 31.5 ± 4.2% for eugenol-loaded phospholipon90H:Chol liposomes and it doubled (63.54 ± 2.28%) when using the HP-β-CD/eugenol-loaded phospholipon90H:Chol liposomes (Sebaaly et al., 2015). Similarly, for anethole, the loading rate was 2 times higher for phospholipon90H:Chol DCLs (0.83 ± 0.15%) compared to phospholipon90H:Chol conventional liposomes (0.48 ± 0.07%). Moreover, DCLs demonstrated slower drug release behavior, retaining 38% of anethole initially present in the vesicles, with respect to 22% of anethole retained by conventional liposomes (Gharib et al., 2017). Furthermore, the EE values of flurbiprofen-loaded DCLs systems prepared with SBE-β-CD or HP-β-CD, were lower than that of flurbiprofen-loaded liposomes; on the other hand, DCLs delayed the flurbiprofen release (Zhang et al., 2015). Additionally, nerolidol was efficiently embedded into both lipoid E80 conventional liposomes and DCLs with high EE and loading rate values (> 90%), and DCLs was more effective to prolong the nerolidol release in comparison to

conventional liposomes (Azzi et al., 2018). DCLs exhibited higher estetrol EE and slower estetrol release rate in comparison with conventional liposomes; nevertheless, both formulations were characterized by a high extent of drug release (80%) after 6 h (Palazzo et al., 2019). Conversely, the EE of HP-β-CD/risperidone-loaded SPC:Chol liposomes was less than that of risperidone-loaded SPC:Chol liposomes, and risperidone was released faster from DCLs compared to conventional liposomes (Wang et al., 2016).

9. Conclusion

In this review, the interaction of CDs with biomimetic and biological membranes was analyzed. The CD effect on membranes is mediated by several factors including membrane structure and composition, in particular acyl chain length and saturation of PLs and structure of their head groups, as well as CD type and concentration. CDs can extract membrane lipids; their extraction capacity depends on CD concentration which appears to be efficient above 0.5 mM. CDs induce vesicle solubilization at concentrations near or above 50 mM. The interaction of CDs with membrane lipids promotes an increase of membrane permeability and fluidity. None of the studies evaluating CD effect on membranes considered the Chol content of lipid bilayer and few studies determined lipid:CD molar ratio. Therefore, these parameters should be analyzed in future studies. Finally, CDs and CD/Chol inclusion complexes were proven to have cryoprotective properties being able to preserve the integrity of liposomal and biological membranes during freeze-drying.

Acknowledgments

The research study was supported by the Research Funding Program at the Lebanese University and by the “Agence Universitaire de la Francophonie, Projet de Coopération Scientifique Inter-universitaire (PCSI)” 2018-2020.

Declarations of interest

None.

References

Abboud, R., Charcosset, C., Greige-Gerges, H., 2018. Biophysical methods: complementary tools to study the influence of human steroid hormones on the liposome membrane properties. Biochimie 153, 13–25. https://doi.org/10.1016/j.biochi.2018.02.005.

Agarwal, S.R., MacDougall, D.A., Tyser, R., Pugh, S.D., Calaghan, S.C., Harvey, R.D., 2011. Effects of cholesterol depletion on compartmentalized cAMP responses in adult cardiac myocytes. J. Mol. Cell. Cardiol. 50, 500–509. https://doi.org/10.1016/j.yjmcc.2010.11.015.

Ahmad, E., Aksoy, M., Serin, İ., Küçük, N., Ceylan, A., Uçan, U., 2013. Cholesterol-loaded cyclodextrin pretreatment of ram spermatozoa protects structural integrity of plasma membrane during osmotic challenge and reduces their ability to undergo acrosome reaction in vitro. Small Rumin. Res. 115, 77–81. https://doi.org/10.1016/j.smallrumres.2013.09.006.

Aksoy, M., Akman, O., Lehimcioğlu, N.C., Erdem, H., 2010. Cholesterol-loaded cyclodextrin enhances osmotic tolerance and inhibits the acrosome reaction in rabbit spermatozoa. Anim. Reprod. Sci. 120, 166–172. https://doi.org/10.1016/j.anireprosci.2010.02.014.

Anderson, T.G., Tan, A., Ganz, P., Seelig, J., 2004. Calorimetric measurement of phospholipid interaction with methyl-beta-cyclodextrin. Biochemistry 43, 2251–2261. https://doi.org/10.1021/bi0358869.

Angelini, G., Campestre, C., Boncompagni, S., Gasbarri, C., 2017. Liposomes entrapping β-cyclodextrin/ibuprofen inclusion complex: role of the host and the guest on the bilayer integrity and microviscosity. Chem. Phys. Lipids 209, 61–65. https://doi.org/10.1016/j.chemphyslip.2017.09.004.

Arav, A., 2013. 24. Freeze drying red blood cells: Development of novel technologies. Cryobiology 66, 349. https://doi.org/10.1016/j.cryobiol.2013.02.030.

Atger, V.M., de la Llera Moya, M., Stoudt, G.W., Rodrigueza, W.V., Phillips, M.C., Rothblat, G.H., 1997. Cyclodextrins as catalysts for the removal of cholesterol from macrophage foam cells. J. Clin. Invest. 99, 773–780. https://doi.org/10.1172/JCI119223.

Awasthi-Kalia, M., Schnetkamp, P.P., Deans, J.P., 2001. Differential effects of filipin and methyl-beta-cyclodextrin on B cell receptor signaling. Biochem. Biophys. Res. Commun. 287, 77–82. https://doi.org/10.1006/bbrc.2001.5536.

Azzi, J., Auezova, L., Danjou, P.-E., Fourmentin, S., Greige-Gerges, H., 2018. First evaluation of drug-in-cyclodextrin-in-liposomes as an encapsulating system for nerolidol. Food Chem. 255, 399–404. https://doi.org/10.1016/j.foodchem.2018.02.055.

Babu, R.J., Pandit, J.K., 2004. Effect of cyclodextrins on the complexation and transdermal delivery of bupranolol through rat skin. Int. J. Pharm. 271, 155–165.

Baek, J.-S., Lim, J.-H., Kang, J.-S., Shin, S.-C., Jung, S.-H., Cho, C.-W., 2013. Enhanced transdermal drug delivery of zaltoprofen using a novel formulation. Int. J. Pharm. 453, 358–362. https://doi.org/10.1016/j.ijpharm.2013.05.059.

Besenicar, M.P., Bavdek, A., Kladnik, A., Macek, P., Anderluh, G., 2008. Kinetics of cholesterol extraction from lipid membranes by methyl-beta-cyclodextrin–a surface plasmon resonance approach. Biochim. Biophys. Acta 1778, 175–184. https://doi.org/10.1016/j.bbamem.2007.09.022.

Blanch, E., Tomás, C., Graham, J., Mocé, E., 2012. Response of boar sperm to the treatment with cholesterol-loaded cyclodextrins added prior to cryopreservation: effect of cholesterol on boar sperm cryosurvival. Reprod. Domest. Anim. 47, 959–964. https://doi.org/10.1111/j.1439-0531.2012.01999.x.

Boggs, J.M., 1987. Lipid intermolecular hydrogen bonding: influence on structural organization and membrane function. Biochim. Biophys. Acta 906, 353–404.

Boulmedarat, L., Piel, G., Bochot, A., Lesieur, S., Delattre, L., Fattal, E., 2005. Cyclodextrin-mediated drug release from liposomes dispersed within a bioadhesive gel. Pharm. Res. 22, 962–971. https://doi.org/10.1007/s11095-005-4591-2.

Brignell, J.L., Perry, M.D., Nelson, C.P., Willets, J.M., Challiss, R.A.J., Davies, N.W., 2015. Steady-state modulation of voltage-gated K + channels in rat arterial smooth muscle by cyclic amp-dependent protein kinase and protein phosphatase 2B. PLOS ONE 10, e0121285. https://doi.org/10.1371/journal.pone.0121285.

Brown, D.A., London, E., 2000. Structure and function of sphingolipid- and cholesterol-rich membrane rafts. J. Biol. Chem. 275, 17221–17224. https://doi.org/10.1074/jbc.R000005200.

Brown, D.A., London, E., 1998. Functions of lipid rafts in biological membranes. Annu. Rev. Cell Dev. Biol. 14, 111–136. https://doi.org/10.1146/annurev.cellbio.14.1.111.

Burger, K., Gimpl, G., Fahrenholz, F., 2000. Regulation of receptor function by cholesterol. Cell. Mol. Life Sci. CMLS 57, 1577–1592.

Cardaba, C.M., Kerr, J.S., Mueller, A., 2008. CCR5 internalisation and signalling have different dependence on membrane lipid raft integrity. Cell. Signal. 20, 1687–1694. https://doi.org/10.1016/j.cellsig.2008.05.014.

Castagne, D., Fillet, M., Delattre, L., Evrard, B., Nusgens, B., Piel, G., 2009. Study of the cholesterol extraction capacity of β-cyclodextrin and its derivatives, relationships with their effects on endothelial cell viability and on membrane models. J. Incl. Phenom. Macrocycl. Chem. 63, 225–231. https://doi.org/10.1007/s10847-008-9510-9.

Castelli, F., Grazia Sarpietro, M., Micieli, D., Trombetta, D., Saija, A., 2006. Differential scanning calorimetry evidence of the enhancement of β-sitosterol absorption across biological membranes mediated by β-cyclodextrins. J. Agric. Food Chem. 54, 10228–10233. https://doi.org/10.1021/jf062228x.

Chen, C., Han, D., Cai, C., Tang, X., 2010. An overview of liposome lyophilization and its future potential. J. Controlled Release 142, 299–311. https://doi.org/10.1016/j.jconrel.2009.10.024.

Colin, D., Limagne, E., Jeanningros, S., Jacquel, A., Lizard, G., Athias, A., Gambert, P., Hichami, A., Latruffe, N., Solary, E., Delmas, D., 2011. Endocytosis of resveratrol via lipid rafts and activation of downstream signaling pathways in cancer cells. Cancer Prev. Res. (Phila. Pa.) 4, 1095–1106. https://doi.org/10.1158/1940-6207.CAPR-10-0274.

Connors, K.A., 1997. The stability of cyclodextrin complexes in solution. Chem. Rev. 97, 1325–1358. https://doi.org/10.1021/cr960371r.

Cooper, R.A., 1978. Influence of increased membrane cholesterol on membrane fluidity and cell function in human red blood cells. J. Supramol. Struct. 8, 413–430. https://doi.org/10.1002/jss.400080404.

Cross, N.L., 1999. Effect of methyl-beta-cyclodextrin on the acrosomal responsiveness of human sperm. Mol. Reprod. Dev. 53, 92–98. https://doi.org/10.1002/(SICI)1098-2795(199905)53:1<92::AID-MRD11>3.0.CO;2-Q.

Crowe, J.H., Fitzpatrick, M., 2013. 22. Freeze-dried platelets: moving towards clinical use. Cryobiology 66, 348. https://doi.org/10.1016/j.cryobiol.2013.02.028.

Del Valle, E.M.M., 2004. Cyclodextrins and their uses: a review. Process Biochem. 39, 1033–1046. https://doi.org/10.1016/S0032-9592(03)00258-9.

Demetzos, C., 2008. Differential scanning calorimetry (DSC): a tool to study the thermal behavior of lipid bilayers and liposomal stability. J. Liposome Res. 18, 159–173. https://doi.org/10.1080/08982100802310261.

Denz, M., Haralampiev, I., Schiller, S., Szente, L., Herrmann, A., Huster, D., Müller, P., 2016. Interaction of fluorescent phospholipids with cyclodextrins. Chem. Phys. Lipids 194, 37–48. https://doi.org/10.1016/j.chemphyslip.2015.07.017.

Drobnis, E.Z., Crowe, L.M., Berger, T., Anchordoguy, T.J., Overstreet, J.W., Crowe, J.H., 1993. Cold shock damage is due to lipid phase transitions in cell membranes: a demonstration using sperm as a model. J. Exp. Zool. 265, 432–437. https://doi.org/10.1002/jez.1402650413.

Eemen, M., Deleu, M., 2010. From biological membranes to biomimetic model membranes. Biotechnol. Agron. Soc. Environ. 14, 719–736.

Elliott, M.H., Fliesler, S.J., Ghalayini, A.J., 2003. Cholesterol-dependent association of caveolin-1 with the transducin α subunit in bovine photoreceptor rod outer segments: disruption by cyclodextrin and guanosine 5′-*O*-(3-Thiotriphosphate)[†]. Biochemistry 42, 7892–7903. https://doi.org/10.1021/bi027162n.

Fauvelle, F., Debouzy, J.C., Crouzy, S., Göschl, M., Chapron, Y., 1997. Mechanism of α-cyclodextrin-induced hemolysis. 1. The two-step extraction of phosphatidylinositol from the membrane. J. Pharm. Sci. 86, 935–943. https://doi.org/10.1021/js9602453.

Gharib, R., Auezova, L., Charcosset, C., Greige-Gerges, H., 2017. Drug-in-cyclodextrin-in-

liposomes as a carrier system for volatile essential oil components: application to anethole. Food Chem. 218, 365–371. https://doi.org/10.1016/j.foodchem.2016.09.110.

Gharib, R., Fourmentin, S., Charcosset, C., Greige-Gerges, H., 2018a. Effect of hydroxypropyl-β–cyclodextrin on lipid membrane fluidity, stability and freeze-drying of liposomes. J. Drug Deliv. Sci. Technol. 44, 101–107. https://doi.org/10.1016/j.jddst.2017.12.009.

Gharib, R., Greige-Gerges, H., Fourmentin, S., Charcosset, C., 2018b. Hydroxypropyl-ß-cyclodextrin as a membrane protectant during freeze-drying of hydrogenated and non-hydrogenated liposomes and molecule-in-cyclodextrin-in-liposomes: application to trans-anethole. Food Chem. 267, 67–74. https://doi.org/10.1016/j.foodchem.2017.10.144.

Gharib, R., Greige-Gerges, H., Fourmentin, S., Charcosset, C., Auezova, L., 2015. Liposomes incorporating cyclodextrin–drug inclusion complexes: current state of knowledge. Carbohydr. Polym. 129, 175–186. https://doi.org/10.1016/j.carbpol.2015.04.048.

Gidwani, B., Vyas, A., 2015. A comprehensive review on cyclodextrin-based carriers for delivery of chemotherapeutic cytotoxic anticancer drugs. BioMed. Res. Int. 2015, 1–15. https://doi.org/10.1155/2015/198268.

Grammenos, A., Mouithys-Mickalad, A., Guelluy, P.H., Lismont, M., Piel, G., Hoebeke, M., 2010. ESR technique for noninvasive way to quantify cyclodextrins effect on cell membranes. Biochem. Biophys. Res. Commun. 398, 350–354. https://doi.org/10.1016/j.bbrc.2010.06.050.

Grauby-Heywang, C., Turlet, J.-M., 2008. Study of the interaction of beta-cyclodextrin with phospholipid monolayers by surface pressure measurements and fluorescence microscopy. J. Colloid Interface Sci. 322, 73–78. https://doi.org/10.1016/j.jcis.2008.03.025.

Hanzal-Bayer, M.F., Hancock, J.F., 2007. Lipid rafts and membrane traffic. FEBS Lett. 581, 2098–2104. https://doi.org/10.1016/j.febslet.2007.03.019.

Hatzi, P., Mourtas, S., Klepetsanis, P.G., Antimisiaris, S.G., 2007. Integrity of liposomes in presence of cyclodextrins: effect of liposome type and lipid composition. Int. J. Pharm. 333, 167–176. https://doi.org/10.1016/j.ijpharm.2006.09.059.

Holthuis, J.C.M., Levine, T.P., 2005. Lipid traffic: floppy drives and a superhighway. Nat. Rev. Mol. Cell Biol. 6, 209–220. https://doi.org/10.1038/nrm1591.

Huang, Z., London, E., 2013. Effect of cyclodextrin and membrane lipid structure upon cyclodextrin-lipid interaction. Langmuir 29, 14631–14638. https://doi.org/10.1021/la4031427.

Iborra, A., Companyó, M., Martínez, P., Morros, A., 2000. Cholesterol efflux promotes acrosome reaction in goat spermatozoa1. Biol. Reprod. 62, 378–383. https://doi.org/10.1095/biolreprod62.2.378.

Ilangumaran, S., Hoessli, D.C., 1998. Effects of cholesterol depletion by cyclodextrin on the sphingolipid microdomains of the plasma membrane. Biochem. J. 335 (Pt 2), 433–440.

Ingvarsson, P.T., Yang, M., Nielsen, H.M., Rantanen, J., Foged, C., 2011. Stabilization of liposomes during drying. Expert Opin. Drug Deliv. 8, 375–388. https://doi.org/10.1517/17425247.2011.553219.

Irie, T., Otagiri, M., Sunada, M., Uekama, K., Ohtani, Y., Yamada, Y., Sugiyama, Y., 1982. Cyclodextrin-induced hemolysis and shape changes of human erythrocytes in vitro. J. Pharmacobiodyn. 5, 741–744.

Kabouridis, P.S., Janzen, J., Magee, A.L., Ley, S.C., 2000. Cholesterol depletion disrupts lipid rafts and modulates the activity of multiple signaling pathways in T lymphocytes. Eur. J. Immunol. 30, 954–963. https://doi.org/10.1002/1521-4141(200003)30:3<954::AID-IMMU954>3.0.CO;2-Y.

Kaddah, S., Khreich, N., Kaddah, F., Charcosset, C., Greige-Gerges, H., 2018. Cholesterol modulates the liposome membrane fluidity and permeability for a hydrophilic molecule. Food Chem. Toxicol. 113, 40–48. https://doi.org/10.1016/j.fct.2018.01.017.

Kainu, V., Hermansson, M., Somerharju, P., 2010. Introduction of phospholipids to cultured cells with cyclodextrin. J. Lipid Res. 51, 3533–3541. https://doi.org/10.1194/jlr.D009373.

Keskintepe, L., Eroglu, A., 2015. Freeze-drying of mammalian sperm. In: Wolkers, W.F., Oldenhof, H. (Eds.), Cryopreservation and Freeze-Drying Protocols. Springer New York, New York, NY, pp. 489–497. https://doi.org/10.1007/978-1-4939-2193-5_25.

Key, C.-C.C., Liu, M., Kurtz, C.L., Chung, S., Boudyguina, E., Dinh, T.A., Bashore, A., Phelan, P.E., Freedman, B.I., Osborne, T.F., Zhu, X., Ma, L., Sethupathy, P., Biddinger, S.B., Parks, J.S., 2017. Hepatocyte ABCA1 deletion impairs liver insulin signaling and lipogenesis. Cell Rep. 19, 2116–2129. https://doi.org/10.1016/j.celrep.2017.05.032.

Kilsdonk, E.P., Yancey, P.G., Stoudt, G.W., Bangerter, F.W., Johnson, W.J., Phillips, M.C., Rothblat, G.H., 1995. Cellular cholesterol efflux mediated by cyclodextrins. J. Biol. Chem. 270, 17250–17256.

Kirby, C., Gregoriadis, G., 1983. The effect of lipid composition of small unilamellar liposomes containing melphalan and vincristine on drug clearance after injection into mice. Biochem. Pharmacol. 32, 609–615. https://doi.org/10.1016/0006-2952(83)90483-5.

Leventis, R., Silvius, J.R., 2001. Use of cyclodextrins to monitor transbilayer movement and differential lipid affinities of cholesterol. Biophys. J. 81, 2257–2267. https://doi.org/10.1016/S0006-3495(01)75873-0.

Li, G., Kim, J., Huang, Z., St. Clair, J.R., Brown, D.A., London, E., 2016. Efficient replacement of plasma membrane outer leaflet phospholipids and sphingolipids in cells with exogenous lipids. Proc. Natl. Acad. Sci. 113, 14025–14030. https://doi.org/10.1073/pnas.1610705113.

Li, J., Wang, X., Zhang, T., Wang, C., Huang, Z., Luo, X., Deng, Y., 2015. A review on phospholipids and their main applications in drug delivery systems. Asian J. Pharm. Sci. 10, 81–98. https://doi.org/10.1016/j.ajps.2014.09.004.

Liossi, A.S., Ntountaniotis, D., Kellici, T.F., Chatziathanasiadou, M.V., Megariotis, G., Mania, M., Becker-Baldus, J., Kriechbaum, M., Krajnc, A., Christodoulou, E., Glaubitz, C., Rappolt, M., Amenitsch, H., Mali, G., Theodorou, D.N., Valsami, G., Pitsikalis, M., Iatrou, H., Tzakos, A.G., Mavromoustakos, T., 2017. Exploring the interactions of irbesartan and irbesartan–2-hydroxypropyl-β-cyclodextrin complex with model membranes. Biochim. Biophys. Acta BBA – Biomembr. 1859, 1089–1098. https://doi.org/10.1016/j.bbamem.2017.03.003.

Loftsson, T., Masson, M., 2001. Cyclodextrins in topical drug formulations: theory and practice. Int. J. Pharm. 225, 15–30. https://doi.org/10.1016/S0378-5173(01)00761-X.

López, C.A., de Vries, A.H., Marrink, S.J., 2011. Molecular mechanism of cyclodextrin mediated cholesterol extraction. PLoS Comput. Biol. 7, e1002020. https://doi.org/10.1371/journal.pcbi.1002020.

Madison, R.J., Evans, L.E., Youngs, C.R., 2013. The effect of 2-hydroxypropyl-β-cyclodextrin on post-thaw parameters of cryopreserved jack and stallion semen. J. Equine Vet. Sci. 33, 272–278. https://doi.org/10.1016/j.jevs.2012.07.021.

Maestrelli, F., González-Rodríguez, M.L., Rabasco, A.M., Mura, P., 2005. Preparation and characterisation of liposomes encapsulating ketoprofen–cyclodextrin complexes for transdermal drug delivery. Int. J. Pharm. 298, 55–67. https://doi.org/10.1016/j.ijpharm.2005.03.033.

Maget-Dana, R., 1999. The monolayer technique: a potent tool for studying the interfacial properties of antimicrobial and membrane-lytic peptides and their interactions with lipid membranes. Biochim. Biophys. Acta BBA – Biomembr. 1462, 109–140. https://doi.org/10.1016/S0005-2736(99)00203-5.

Mahammad, S., Parmryd, I., 2008. Cholesterol homeostasis in T cells. Methyl-beta-cyclodextrin treatment results in equal loss of cholesterol from Triton X-100 soluble and insoluble fractions. Biochim. Biophys. Acta 1778, 1251–1258. https://doi.org/10.1016/j.bbamem.2008.02.010.

Matassoli, F.L., Leão, I.C., Bezerra, B.B., Pollard, R.B., Lütjohann, D., Hildreth, J.E.K., Arruda, L.B. de, 2018. Hydroxypropyl-beta-cyclodextrin reduces inflammatory signaling from monocytes: possible implications for suppression of HIV chronic immune activation. mSphere 3. https://doi.org/10.1128/mSphere.00497-18.

McCauliff, L.A., Xu, Z., Storch, J., 2011. Sterol transfer between cyclodextrin and membranes: similar but not identical mechanism to NPC2-mediated cholesterol transfer. Biochemistry 50, 7341–7349. https://doi.org/10.1021/bi200574f.

McCormack, B., Gregoriadis, G., 1994. Drugs-in-cyclodextrins-in liposomes: a novel concept in drug delivery. Int. J. Pharm. 112, 249–258. https://doi.org/10.1016/0378-5173(94)90361-1.

McIntosh, T.J., Vidal, A., Simon, S.A., 2003. Sorting of lipids and transmembrane peptides between detergent-soluble bilayers and detergent-resistant rafts. Biophys. J. 85, 1656–1666. https://doi.org/10.1016/S0006-3495(03)74595-0.

Milles, S., Meyer, T., Scheidt, H.A., Schwarzer, R., Thomas, L., Marek, M., Szente, L., Bittman, R., Herrmann, A., Günther Pomorski, T., Huster, D., Müller, P., 2013. Organization of fluorescent cholesterol analogs in lipid bilayers – lessons from cyclodextrin extraction. Biochim. Biophys. Acta 1828, 1822–1828. https://doi.org/10.1016/j.bbamem.2013.04.002.

Mocé, E., Blanch, E., Tomás, C., Graham, J.K., 2010. Use of cholesterol in sperm cryopreservation: present moment and perspectives to future. Reprod. Domest. Anim. Zuchthyg. 45 (Suppl. 2), 57–66. https://doi.org/10.1111/j.1439-0531.2010.01635.x.

Monnaert, V., 2004. Behavior of α-, β-, and γ-cyclodextrins and their derivatives on an in vitro model of blood-brain barrier. J. Pharmacol. Exp. Ther. 310, 745–751. https://doi.org/10.1124/jpet.104.067512.

Moore, A.I., Squires, E.L., Graham, J.K., 2005. Adding cholesterol to the stallion sperm plasma membrane improves cryosurvival. Cryobiology 51, 241–249. https://doi.org/10.1016/j.cryobiol.2005.07.004.

Motoyama, K., Arima, H., Nishimoto, Y., Miyake, K., Hirayama, F., Uekama, K., 2005. Involvement of CD14 in the inhibitory effects of dimethyl-α-cyclodextrin on lipopolysaccharide signaling in macrophages. FEBS Lett. 579, 1707–1714. https://doi.org/10.1016/j.febslet.2005.01.076.

Motoyama, K., Arima, H., Toyodome, H., Irie, T., Hirayama, F., Uekama, K., 2006. Effect of 2,6-di-O-methyl-α-cyclodextrin on hemolysis and morphological change in rabbit's red blood cells. Eur. J. Pharm. Sci. 29, 111–119. https://doi.org/10.1016/j.ejps.2006.06.002.

Motoyama, K., Kameyama, K., Onodera, R., Araki, N., Hirayama, F., Uekama, K., Arima, H., 2009a. Involvement of PI3K-Akt-Bad pathway in apoptosis induced by 2,6-di-O-methyl-β-cyclodextrin, not 2,6-di-O-methyl-α-cyclodextrin, through cholesterol depletion from lipid rafts on plasma membranes in cells. Eur. J. Pharm. Sci. 38, 249–261. https://doi.org/10.1016/j.ejps.2009.07.010.

Motoyama, K., Toyodome, H., Onodera, R., Irie, T., Hirayama, F., Uekama, K., Arima, H., 2009b. Involvement of lipid rafts of rabbit red blood cells in morphological changes induced by methylated beta-cyclodextrins. Biol. Pharm. Bull. 32, 700–705.

Mura, P., Bragagni, M., Mennini, N., Cirri, M., Maestrelli, F., 2014. Development of liposomal and microemulsion formulations for transdermal delivery of clonazepam: effect of randomly methylated β-cyclodextrin. Int. J. Pharm. 475, 306–314. https://doi.org/10.1016/j.ijpharm.2014.08.066.

Nakanishi, K., Nadai, T., Masada, M., Miyajima, K., 1992. Effect of cyclodextrins on biological membrane. II. Mechanism of enhancement on the intestinal absorption of non-absorbable drug by cyclodextrins. Chem. Pharm. Bull. (Tokyo) 40, 1252–1256.

Nicolson, G.L., 2014. The fluid—mosaic model of membrane structure: still relevant to understanding the structure, function and dynamics of biological membranes after more than 40years. Biochim. Biophys. Acta BBA – Biomembr. 1838, 1451–1466. https://doi.org/10.1016/j.bbamem.2013.10.019.

Nishijo, J., Mizuno, H., 1998. Interactions of cyclodextrins with DPPC liposomes. Differential scanning calorimetry studies. Chem. Pharm. Bull. (Tokyo) 46, 120–124.

Nishijo, J., Shiota, S., Mazima, K., Inoue, Y., Mizuno, H., Yoshida, J., 2000. Interactions of cyclodextrins with dipalmitoyl, distearoyl, and dimyristoyl phosphatidyl choline liposomes. A study by leakage of carboxyfluorescein in inner aqueous phase of unilamellar liposomes. Chem. Pharm. Bull. (Tokyo) 48, 48–52.

Niu, S.-L., Mitchell, D.C., Litman, B.J., 2002. Manipulation of cholesterol levels in rod disk

membranes by methyl-beta-cyclodextrin: effects on receptor activation. J. Biol. Chem. 277, 20139–20145. https://doi.org/10.1074/jbc.M200594200.
Ohtani, Y., Irie, T., Uekama, K., Fukunaga, K., Pitha, J., 1989. Differential effects of alpha-, beta- and gamma-cyclodextrins on human erythrocytes. Eur. J. Biochem. 186, 17–22.
Ohvo, H., Olsio, C., Slotte, J.P., 1997. Effects of sphingomyelin and phosphatidylcholine degradation on cyclodextrin-mediated cholesterol efflux in cultured fibroblasts. Biochim. Biophys. Acta 1349, 131–141.
Ohvo, H., Slotte, J.P., 1996. Cyclodextrin-mediated removal of sterols from monolayers: effects of sterol structure and phospholipids on desorption rate. Biochemistry 35, 8018–8024. https://doi.org/10.1021/bi9528816.
Ohvo-Rekilä, H., Akerlund, B., Slotte, J.P., 2000. Cyclodextrin-catalyzed extraction of fluorescent sterols from monolayer membranes and small unilamellar vesicles. Chem. Phys. Lipids 105, 167–178.
Ono, N., Arima, H., Hirayama, F., Uekama, K., 2001. A moderate interaction of maltosyl-alpha-cyclodextrin with Caco-2 cells in comparison with the parent cyclodextrin. Biol. Pharm. Bull. 24, 395–402.
Osheroff, J.E., 1999. Regulation of human sperm capacitation by a cholesterol efflux-stimulated signal transduction pathway leading to protein kinase A-mediated up-regulation of protein tyrosine phosphorylation. Mol. Hum. Reprod. 5, 1017–1026. https://doi.org/10.1093/molehr/5.11.1017.
Palazzo, C., Laloy, J., Delvigne, A.-S., Nys, G., Fillet, M., Dogne, J.-M., Pequeux, C., Foidart, J.-M., Evrard, B., Piel, G., 2019. Development of injectable liposomes and drug-in-cyclodextrin-in-liposome formulations encapsulating estetrol to prevent cerebral ischemia of premature babies. Eur. J. Pharm. Sci. 127, 52–59. https://doi.org/10.1016/j.ejps.2018.10.006.
Piel, G., Piette, M., Barillaro, V., Castagne, D., Evrard, B., Delattre, L., 2007. Study of the relationship between lipid binding properties of cyclodextrins and their effect on the integrity of liposomes. Int. J. Pharm. 338, 35–42. https://doi.org/10.1016/j.ijpharm.2007.01.015.
Pinho, R.O., Lima, D.M.A., Shiomi, H.H., Siqueira, J.B., Silveira, C.O., Faria, V.R., Lopes, P.S., Guimarães, S.E.F., Guimarães, J.D., 2016. Effect of cyclodextrin-loaded cholesterol conjugates on plasma membrane viability of Piau swine breed frozen/thawed spermatozoa. Cryobiology 73, 1–6. https://doi.org/10.1016/j.cryobiol.2016.07.004.
Puglisi, G., Fresta, M., Ventura, C.A., 1996. Interaction of natural and modified β-cyclodextrins with a biological membrane model of dipalmitoylphosphatidylcholine. J. Colloid Interface Sci. 180, 542–547. https://doi.org/10.1006/jcis.1996.0335.
Purdy, P., Graham, J., 2004. Effect of cholesterol-loaded cyclodextrin on the cryosurvival of bull sperm. Cryobiology 48, 36–45. https://doi.org/10.1016/j.cryobiol.2003.12.001.
Reis, A.H., Moreno, M.M., Maia, L.A., Oliveira, F.P., Santos, A.S., Abreu, J.G., 2016. Cholesterol-rich membrane microdomains modulate Wnt/β-catenin morphogen gradient during Xenopus development. Mech. Dev. 142, 30–39. https://doi.org/10.1016/j.mod.2016.09.001.
Rong, W.-T., Lu, Y.-P., Tao, Q., Guo, M., Lu, Y., Ren, Y., Yu, S.-Q., 2014. Hydroxypropyl-sulfobutyl-β-cyclodextrin improves the oral bioavailability of edaravone by modulating drug efflux pump of enterocytes. J. Pharm. Sci. 103, 730–742. https://doi.org/10.1002/jps.23807.
Rosa Teixeira, K.I., Araújo, P.V., Almeida Neves, B.R., Bohorquez Mahecha, G.A., Sinisterra, R.D., Cortés, M.E., 2013. Ultrastructural changes in bacterial membranes induced by nano-assemblies β-cyclodextrin chlorhexidine: SEM, AFM, and TEM evaluation. Pharm. Dev. Technol. 18, 600–608. https://doi.org/10.3109/10837450.2011.649853.
Saito, N., Ishida, Y., Seno, K., Hayashi, F., 2012. Methyl-β-cyclodextrin is a useful compound for extraction and purification of prenylated enzymes from the retinal disc membrane. Protein Expr. Purif. 82, 168–173. https://doi.org/10.1016/j.pep.2011.12.007.
Salmon, V.M., Leclerc, P., Bailey, J.L., 2016. Cholesterol-loaded cyclodextrin increases the cholesterol content of goat sperm to improve cold and osmotic resistance and maintain sperm function after cryopreservation1. Biol. Reprod. 94. https://doi.org/10.1095/biolreprod.115.128553.
Sanchez, S.A., Gunther, G., Tricerri, M.A., Gratton, E., 2011. Methyl-β-cyclodextrins preferentially remove cholesterol from the liquid disordered phase in giant unilamellar vesicles. J. Membr. Biol. 241, 1–10. https://doi.org/10.1007/s00232-011-9348-8.
Scheinman, E.J., Rostoker, R., LeRoith, D., 2013. Cholesterol affects gene expression of the Jun family in colon carcinoma cells using different signaling pathways. Mol. Cell. Endocrinol. 374, 101–107. https://doi.org/10.1016/j.mce.2013.04.011.
Sebaaly, C., Greige-Gerges, H., Stainmesse, S., Fessi, H., Charcosset, C., 2016. Effect of composition, hydrogenation of phospholipids and lyophilization on the characteristics of eugenol-loaded liposomes prepared by ethanol injection method. Food Biosci. 15, 1–10. https://doi.org/10.1016/j.fbio.2016.04.005.
Sebaaly, C., Jraij, A., Fessi, H., Charcosset, C., Greige-Gerges, H., 2015. Preparation and characterization of clove essential oil-loaded liposomes. Food Chem. 178, 52–62. https://doi.org/10.1016/j.foodchem.2015.01.067.
Sherry, M., Charcosset, C., Fessi, H., Greige-Gerges, H., 2013. Essential oils encapsulated in liposomes: a review. J. Liposome Res. 23, 268–275. https://doi.org/10.3109/08982104.2013.819888.
Simons, K., Ikonen, E., 1997. Functional rafts in cell membranes. Nature 387, 569–572. https://doi.org/10.1038/42408.
Simons, K., Toomre, D., 2000. Lipid rafts and signal transduction. Nat. Rev. Mol. Cell Biol. 1, 31–39. https://doi.org/10.1038/35036052.
Singer, S.J., Nicolson, G.L., 1972. The fluid mosaic model of the structure of cell membranes Reprinted with permission from Science, Copyright AAA, 18 February 1972, Volume 175, pp. 720–731. In: Membranes and Viruses in Immunopathology. Elsevier, pp. 7–47. doi: 10.1016/B978-0-12-207250-5.50008-7. ()
Stauffer, T.P., Meyer, T., 1997. Compartmentalized IgE receptor–mediated signal transduction in living cells. J. Cell Biol. 139, 1447–1454. https://doi.org/10.1083/jcb.139.6.1447.
Steck, T.L., Ye, J., Lange, Y., 2002. Probing red cell membrane cholesterol movement with cyclodextrin. Biophys. J. 83, 2118–2125. https://doi.org/10.1016/S0006-3495(02)73972-6.
Szente, L., Fenyvesi, É., 2017. Cyclodextrin-lipid complexes: cavity size matters. Struct. Chem. 28, 479–492. https://doi.org/10.1007/s11224-016-0884-9.
Szente, L., Singhal, A., Domokos, A., Song, B., 2018. Cyclodextrins: assessing the impact of cavity size, occupancy, and substitutions on cytotoxicity and cholesterol homeostasis. Molecules 23, 1228. https://doi.org/10.3390/molecules23051228.
Takino, T., Konishi, K., Takakura, Y., Hashida, M., 1994. Long circulating emulsion carrier systems for highly lipophilic drugs. Biol. Pharm. Bull. 17, 121–125. https://doi.org/10.1248/bpb.17.121.
Tanhuanpää, K., Somerharju, P., 1999. γ-Cyclodextrins greatly enhance translocation of hydrophobic fluorescent phospholipids from vesicles to cells in culture: importance of molecular hydrophobicity in phospholipid trafficking studies. J. Biol. Chem. 274, 35359–35366. https://doi.org/10.1074/jbc.274.50.35359.
Tilloy, S., Monnaert, V., Fenart, L., Bricout, H., Cecchelli, R., Monflier, E., 2006. Methylated beta-cyclodextrin as P-gp modulators for deliverance of doxorubicin across an in vitro model of blood-brain barrier. Bioorg. Med. Chem. Lett. 16, 2154–2157. https://doi.org/10.1016/j.bmcl.2006.01.049.
van den Hoven, J.M., Metselaar, J.M., Storm, G., Beijnen, J.H., Nuijen, B., 2012. Cyclodextrin as membrane protectant in spray-drying and freeze-drying of PEGylated liposomes. Int. J. Pharm. 438, 209–216. https://doi.org/10.1016/j.ijpharm.2012.08.046.
Ventura, C.A., Fresta, M., Paolino, D., Pedotti, S., Corsaro, A., Puglisi, G., 2001. Biomembrane model interaction and percutaneous absorption of papaverine through rat skin: effects of cyclodextrins as penetration enhancers. J. Drug Target. 9, 379–393.
Vist, M.R., Davis, J.H., 1990. Phase equilibria of cholesterol/dipalmitoylphosphatidylcholine mixtures: deuterium nuclear magnetic resonance and differential scanning calorimetry. Biochemistry 29, 451–464. https://doi.org/10.1021/bi00454a021.
Visconti, P.E., Ning, X., Fornés, M.W., Alvarez, J.G., Stein, P., Connors, S.A., Kopf, G.S., 1999. Cholesterol efflux-mediated signal transduction in mammalian sperm: cholesterol release signals an increase in protein tyrosine phosphorylation during mouse sperm capacitation. Dev. Biol. 214, 429–443. https://doi.org/10.1006/dbio.1999.9428.
Wang, H., Xie, X., Zhang, F., Zhou, Q., Tao, Q., Zou, Y., Chen, C., Zhou, C., Yu, S., 2011. Evaluation of cholesterol depletion as a marker of nephrotoxicity in vitro for novel β-cyclodextrin derivatives. Food Chem. Toxicol. Int. J. Publ. Br. Ind. Biol. Res. Assoc. 49, 1387–1393. https://doi.org/10.1016/j.fct.2011.03.026.
Wang, W., Fu, Y.J., Zu, Y.G., Wu, N., Reichling, J., Efferth, T., 2009. Lipid rafts play an important role in the vesicular stomatitis virus life cycle. Arch. Virol. 154, 595–600. https://doi.org/10.1007/s00705-009-0348-2.
Wang, W.-X., Feng, S.-S., Zheng, C.-H., 2016. A comparison between conventional liposome and drug-cyclodextrin complex in liposome system. Int. J. Pharm. 513, 387–392. https://doi.org/10.1016/j.ijpharm.2016.09.043.
Wolkers, W., 2013. 085 Freeze-dried cells and tissues. Cryobiology 67, 422. https://doi.org/10.1016/j.cryobiol.2013.09.091.
Yancey, P.G., Rodrigueza, W.V., Kilsdonk, E.P., Stoudt, G.W., Johnson, W.J., Phillips, M.C., Rothblat, G.H., 1996. Cellular cholesterol efflux mediated by cyclodextrins. Demonstration Of kinetic pools and mechanism of efflux. J. Biol. Chem. 271, 16026–16034.
Zalba, S., ten Hagen, T.L.M., 2017. Cell membrane modulation as adjuvant in cancer therapy. Cancer Treat. Rev. 52, 48–57. https://doi.org/10.1016/j.ctrv.2016.10.008.
Zeng, W., Terada, T., 2000. Freezability of boar spermatozoa is improved by exposure to 2-hydroxypropyl-beta-cyclodextrin. Reprod. Fertil. Dev. 12, 223–228.
Zeng, W.X., Terada, T., 2001. Effects of methyl-beta-cyclodextrin on cryosurvival of boar spermatozoa. J. Androl. 22, 111–118.
Zhang, L., Zhang, Q., Wang, X., Zhang, W., Lin, C., Chen, F., Yang, X., Pan, W., 2015. Drug-in-cyclodextrin-in-liposomes: a novel drug delivery system for flurbiprofen. Int. J. Pharm. 492, 40–45. https://doi.org/10.1016/j.ijpharm.2015.07.011.
Zhang, L., Zhang, Z., Li, N., Wang, N., Wang, Y., Tang, S., Xu, L., Ren, Y., 2013. Synthesis and evaluation of a novel β-cyclodextrin derivative for oral insulin delivery and absorption. Int. J. Biol. Macromol. 61, 494–500. https://doi.org/10.1016/j.ijbiomac.2013.08.034.

Chapter 2

Encapsulation of natural insecticides

Introduction

Invertebrates, weeds, and pathogens, collectively termed pests, have caused significant losses in agricultural production worldwide. Synthetic organic pesticides have been extensively developed to prevent and control pests in agriculture. Nevertheless, their widespread use is associated with environmental and human health concerns. Therefore, natural-insecticides "Green pesticides" could be considered as an alternative to synthetic insecticides (Mossa, 2016). This review focuses on the use of EOs as "bio"-insecticides for insect pest management. In fact, many EOs have contact, fumigant, antifeedant, attractant, and repellent activities against a broad spectrum of insects with some selectivity (Mossa, 2016). Acting on the nervous system of insects is one of the important modes of action of EOs. The neurotoxic effects of EOs include blocking octopamine or γ-aminobutyric acid receptors, or inhibiting acetyl-cholinesterase (Enan, 2001; Priestley et al., 2003). In addition to these mechanisms of action, EOs influence the cytochrome P450-dependent monooxygenases, pheromone and hormone system of insect pests (García et al., 2005). However, EOs are volatile, poorly soluble in water and sensitive to several environmental degradation factors (light, oxygen, and temperature) (Moretti et al., 2002). Hence, there is a need to develop formulations able to improve the stability and effectiveness of these natural compounds in various applications. Formulation design is affected by numerous factors, such as the application mode, the biological, physical, and chemical properties of the pesticide, crops or food stuff to be treated, and agricultural practices.

Various types of carrier systems were used to improve the physicochemical properties of EOs, including polymer based particles, nanoemulsions and microemulsions, and solid lipid nanoparticles. Several studies in literature characterized the EO-loaded carrier systems with respect to their size, morphology, drug encapsulation efficiency (EE), drug release, and

storage stability. Variable factors were investigated to modulate these characteristics. For instance, the type of polymer used, the insecticide:polymer ratio, and the process parameters influence the characteristics of polymer based formulations. The characteristics of nanoemulsion/microemulsions depend on the type of surfactant used, the concentration of surfactant and insecticide, the addition of glycerol and its concentration, and the process parameters.

In this manuscript, which is submitted to peer-reviewed journal, the insecticidal properties and mechanisms of action of EOs are presented. Then, the various carrier systems used for the encapsulation of EOs are described. The characteristics of the EO-loaded formulations applied in agriculture pest control are considered. The literature data are resumed into conclusive tables and discussed. The last section of the review deals with the insecticidal activities of EO-loaded formulations compared to free molecules.

References

Enan, E., 2001. Insecticidal activity of essential oils: octopaminergic sites of action. Comp. Biochem. Physiol. Part C Toxicol. Pharmacol. 130, 325–337.

García, M., Donadel, O.J., Ardanaz, C.E., Tonn, C.E., Sosa, M.E., 2005. Toxic and repellent effects ofBaccharis salicifolia essential oil onTribolium castaneum. Pest Manag. Sci. 61, 612–618.

Moretti, M.D.L., Sanna-Passino, G., Demontis, S., Bazzoni, E., 2002. Essential oil formulations useful as a new tool for insect pest control. AAPS PharmSciTech 3, 64–74.

Mossa, A.T.H., 2016. Green Pesticides: Essential Oils as Biopesticides in Insect-pest Management. J. Environ. Sci. Technol. 9, 354–378.

Priestley, C.M., Williamson, E.M., Wafford, K.A., Sattelle, D.B., 2003. Thymol, a constituent of thyme essential oil, is a positive allosteric modulator of human GABA A receptors and a homo-oligomeric GABA receptor from Drosophila melanogaster: Thymol enhances ionotropic GABA receptor activity. Br. J. Pharmacol. 140, 1363–1372.

Insecticidal effects of natural products in free and encapsulated forms: an overview

Zahraa Hammoud[1,2], Maha Ben Abada[3], Hélène Greige-Gerges[1], Abdelhamid Elaissari[2], Jouda Mediouni Ben Jemâa[3]

[1]Bioactive Molecules Research Laboratory, Doctoral School of Sciences and Technologies, Faculty of Sciences, Section II, Lebanese University, Lebanon

[2]Univ Lyon, University Claude Bernard Lyon-1, CNRS, LAGEP-UMR 5007, F-69622 Lyon, France

[3]Laboratory of Biotechnology Applied to Agriculture, National Agricultural Research Institute of Tunisia (INRAT), University of Carthage, Tunisia

Contents

Abstract

In recent times, the interest in healthy foods reconsideration is rising again. Issues related to food protection and preservation for quality and safety improvements as well as longer shelf-life of products are of global concern. Additionally, the concern on hazards associated with pesticides use on human health and the environment is growing. Thus, actions targeting the investigation of potentially low-risk active substances and natural compounds for food conservation are needed. In this context, plant extracts including essential oils (EOs) have been recognized as important natural sources of pesticides with widespread range of activities. However, EOs are volatile, poorly soluble in water, and susceptible to degradation and oxidation. Therefore, EO encapsulation in delivery systems made of natural components seems to be a possible solution to overcome these restrictions. This review focuses on the insecticidal potential of EOs in free and encapsulated forms with particular emphasis on the types and characteristics of encapsulation systems loading natural insecticides.

Key words: delivery systems, essential oil, food preservation, insecticide, nanoparticles.

1. Introduction

Estimations revealed that one-third of global food is lost or wasted, entailing significant environmental, economic and social costs (Spang et al., 2019). Similarly, sobal and Nelson, (2003) reported that food waste has become recognized as a significant nutritional, environmental and social problem in recent decades. Concerns around food security have been increased in recent years, with food price spikes focusing attention on rising of food demand and how this will be met. Institutions such as the Food and Agriculture Organization of the United Nations (FAO) and the International Food Policy Research Institute (IFPRI) have published projections of an increase in global food demand out to 2050. The FAO projections indicate that world food demand may increase to 70 % by 2050 (Linehan et al., 2012). Thus, preservation of food quality and safety as well as prevention against food-borne diseases, pests, and food chemical contamination are major issues for industries worldwide.

Pests, including insects, pathogens, mites and nematodes are the main restrictive factors in profitable crop production. Traditional approaches of Integrated Pest Management (IPM) in agriculture had certain major restrictions. Indeed, in the last decade, synthetic organic pesticides have been extensively used to prevent and control pests in agriculture, showing a high toxicity against insects. Despite their benefits, chemical pesticides can be hazardous to human and animals health and to the environment (soil fertility, pollution, residue, etc.). Hence, consumers' demand for safe and natural food products free from chemical preservatives and minimally processed with a longer shelf life are notably increasing (Mossa, 2016). Accordingly, nanotechnology would provide an eco-friendly and efficient solution for pest's management without damaging the environment (Rai and Ingle, 2012).

Essential oils (EOs) are considered as promising natural alternatives of synthetic pesticides in many food industries. EOs can inhibit the growth of superficial food pathogens and modify nutritious values without affecting the sensory food qualities. Additionally, EOs, as naturally occurring functional ingredients, were widely used in active food packaging for prolonging the shelf life of food products (Ataei et al., 2020). Moreover, EOs have exhibited strong pesticide potential against insects pests, weeds and fungi (Ben Jemaa, 2014). Nevertheless, limitations related to EOs volatility, potential for oxidation and poor solubility in water presented major constraints for their industrial applications (Moretti et al., 2002). One possible solution to overcome these constraints is encapsulation (Gharib et al., 2017; Sebaaly et al., 2015).

In these regards, Martín et al., (2010) reported that encapsulation achieved controlled release of EOs, facilitated their handling and protected them against evaporation losses and

degradation. Encapsulation within nanoparticle is completed in three ways: the component could be *i)* encapsulated inside nanoporous materials, *ii)* coated with thin polymer film, or *iii)* delivered as particles or emulsions of nanoscale dimensions (Rai and Ingle, 2012).

The aim of this review is the exploration of the insecticidal effects of natural products, mainly EOs, in free and encapsulated forms. Here, the insecticidal properties and mechanisms of action of EOs are presented. Then, the encapsulation systems used in the literature to carry natural insecticides (polymer based particles and micelles, nanoemulsions and microemulsions, solid lipid nanoparticles, and cyclodextrins) were described. Moreover, the characteristics of delivery systems loading natural insecticides were discussed. The last section focused on the insecticidal effect of encapsulated EOs compared to free form of EOs.

2. Insecticidal properties and mechanism of action of essential oils on insects

During last decades, several studies have focused on the usage of EOs for insect pests' control. EOs toxicity depends on many factors including the structure and the characteristics of the various components, their ability to cross the biological membranes and their mechanism and sites of action (Mossa, 2016). The lipophilic chemicals of essential oils can enter into insects and cause biochemical dysfunction and mortality (Lee et al., 2004b). On the other hand, investigations indicated that EOs from the plants families, as Lamiaceae (Park et al., 2016), Asteraceae (Boussaada et al., 2008) Apiaceae (Ben-Khalifa et al., 2018), Myrtaceae (Ebadollahi, 2013) and Rutaceae (Zarrad et al., 2015) exhibited interesting insecticidal activities. EOs have been investigated for their attractant/ repellent (Ben Jemâa, 2014; Mediouni Ben Jemâa et al., 2012), antifeedant (Laarif et al., 2013), fumigant (Hamdi et al., 2015; Titouhi et al., 2017) and contact effects (Aouadi et al., 2020). Various activities were assessed against eggs, larvae and adults of insect species belonging to orders like Coleoptera, Lepidoptera, Diptera, Hemiptera and Isoptera (Badreddine et al., 2015; Bosly, 2013; Digilio et al., 2008; Gonçalves et al., 2005; Lima et al., 2013; Ogendo et al., 2008). On the other hand, several studies focused on site of action and toxicity mechanisms of EOs toward insect pests (Abdelaziz et al., 2014; Houghton et al., 2006; Lee et al., 2004a; Ogendo et al., 2008; Park et al., 2016). In fact, most of the essential oils are volatile; they can serve as chemical messengers for insects. Moreover, they serve as a signal of short duration, making them valuable for alarm pheromones and synomones. Also, they are toxic to animal cells, impairing respiration, decreasing cell membrane permeability and causing a severe decrease in the number of Golgi bodies and mitochondria (Lee et al., 2005; Rice and Coats, 1994; Watanabe et al., 1990). Recognitions about the mechanisms of action of EOs on insects are

recondite, but treatments with different essential oils cause symptoms that suggest their neurotoxic action (Kostyukovsky et al., 2002; Mossa, 2016; Re et al., 2000). According to Enan, (2001) and Priestley et al., (2003), the neurotoxic effects of essential oils can be presented by blocking the octopamine receptors or by acetyl-cholinesterase (AChE) inhibition and also through blocking the γ-aminobutyric acid (GABA) receptor. In addition to these modes of action, essential oils affect the cytochrome P_{450} monooxygenase, pheromone and hormone system of insect pests (García et al., 2005). Octopamine is a neurohormone, neurotransmitter and at the same time circulating neurohormone-neuromodulator. Its perturbation stops the nervous system function in insects (Enan, 2001) . According to the anti-cholinesterase, the neurotoxic action and symptoms are comparable to that provoked by carbamates and organophosphates insecticides (hyperactivity, convulsions, tremors followed by paralysis) (Enan, 2001; Isman, 2002). Several studies pointed out that monoterpenoids (1,8-cineole, carvone, fenchone and linalool) toxicity may be due to the inhibition of AChE at hydrophobic sites (Enan, 2001). Figure 1 illustrated the mechanism of essential oils-induced toxicity to insects as suggested by Mossa (2016).

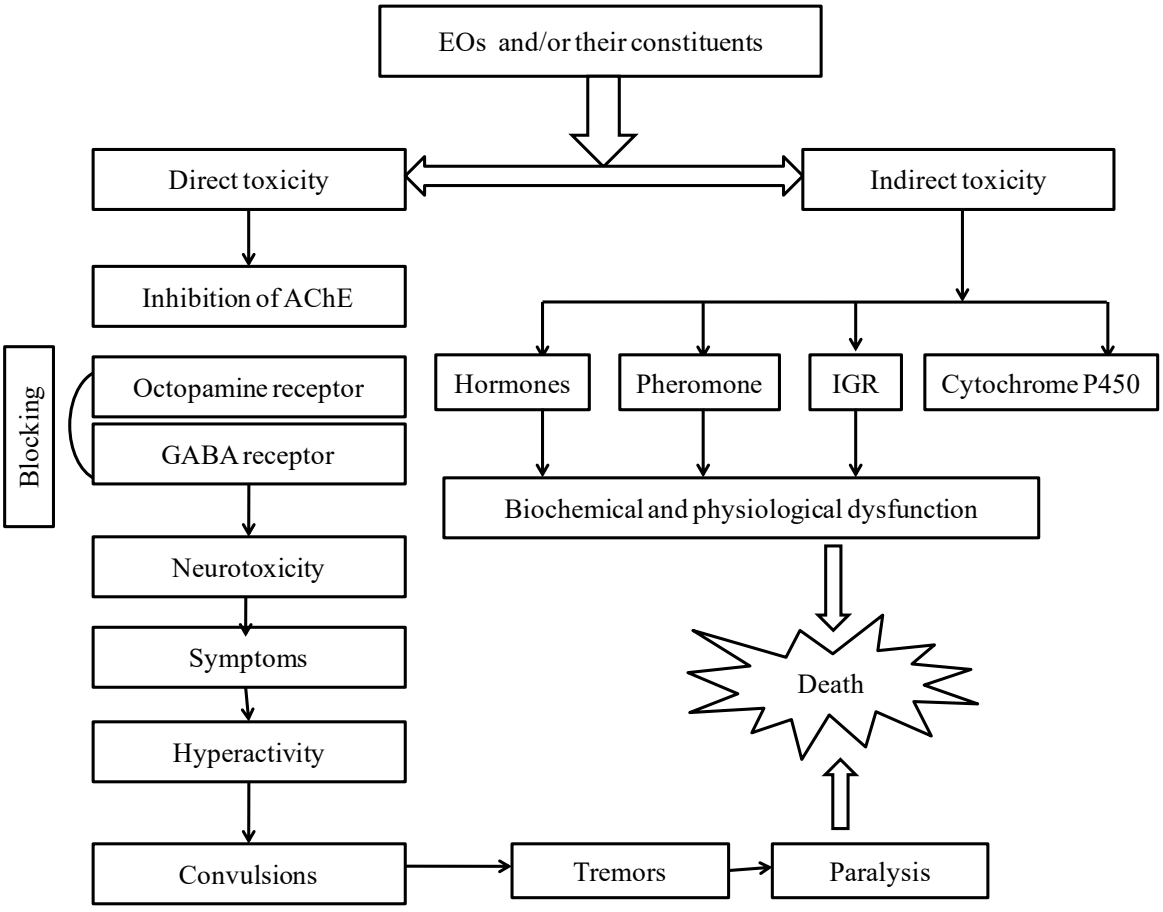

Figure 1: Proposed mechanism of essential oils toxicity against insects (Mossa, 2016) (IGR: Insect Growth Regulators).

3. Encapsulation systems

A wide variety of carrier systems have been established for delivery of natural insecticides. In this section, the traditional delivery systems are reviewed. The advantages offered by the systems are highlighted, together with the main challenges that must be resolved prior to their application for agricultural pest control. The structures of the different carrier systems used for the delivery of natural insecticides are depicted in Figure 2.

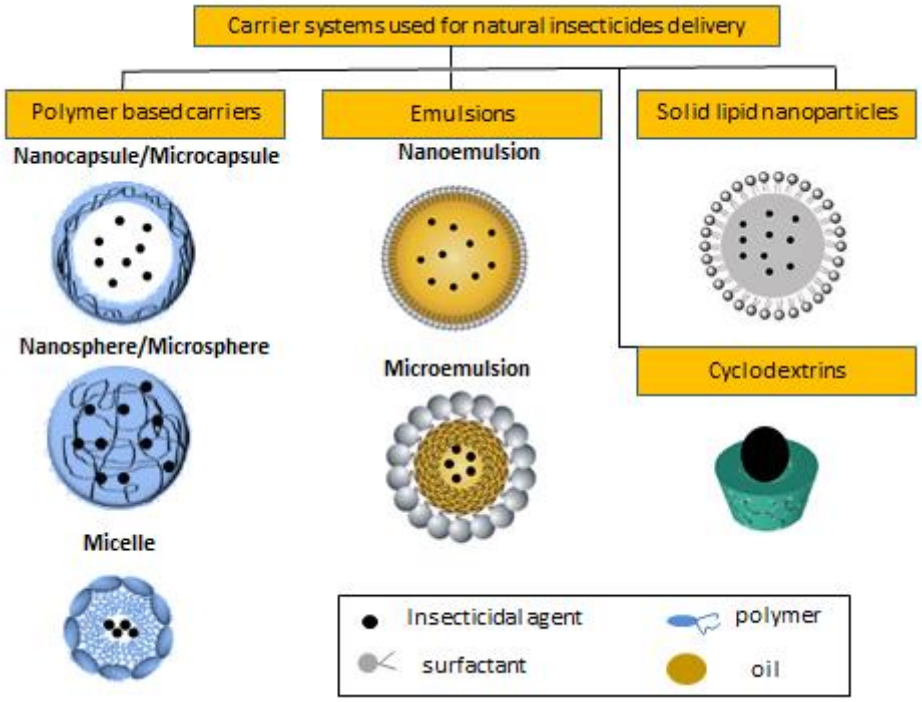

Figure 2: The structures of various delivery systems reported for delivery of natural insecticides.

3.1. Polymer based particles and micelles

Polymer based nanoparticles are solid colloidal particles of size ranging from 10 nm to 1 µm. Furthermore, polymer based microparticles are defined as structures with dimensions less than 1000 µm and greater than 1 µm. Different types of polymer based nanoparticles and microparticles could be distinguished: (1) nanospheres/microspheres, which are carriers where active molecules are dissolved, entrapped, encapsulated, chemically bound or adsorbed to the polymeric matrix; and (2) nanocapsules/microcapsules which are systems where active molecules are embedded in a cavity surrounded by a polymeric membrane (Figure 2) (Campos et al., 2013; Yadav et al., 2019). There are several methods used for the preparation of polymer based nanocapsules: nanoprecipitation, emulsion-diffusion, double emulsification, emulsion-coacervation, polymer-coating and layer-by-layer. These methods are described in Figure 3.

Polymer based particles are biocompatible, biodegradable, and nontoxic structures. All these characteristics make them suitable for delivery of natural insecticides (Campos et al., 2013; Rana and Sharma, 2019; Yadav et al., 2019). Nevertheless, polymer based nanoparticles have some drawbacks such as poor drug loading and scale up limitation (Kahraman et al., 2017). Moreover, polymeric microparticles have some disadvantages that must be taken into consideration. For instance, the high complexity and high cost of its manufacturing process and the reduced stability of the encapsulated material during processing may present a challenge (Campos et al., 2013).

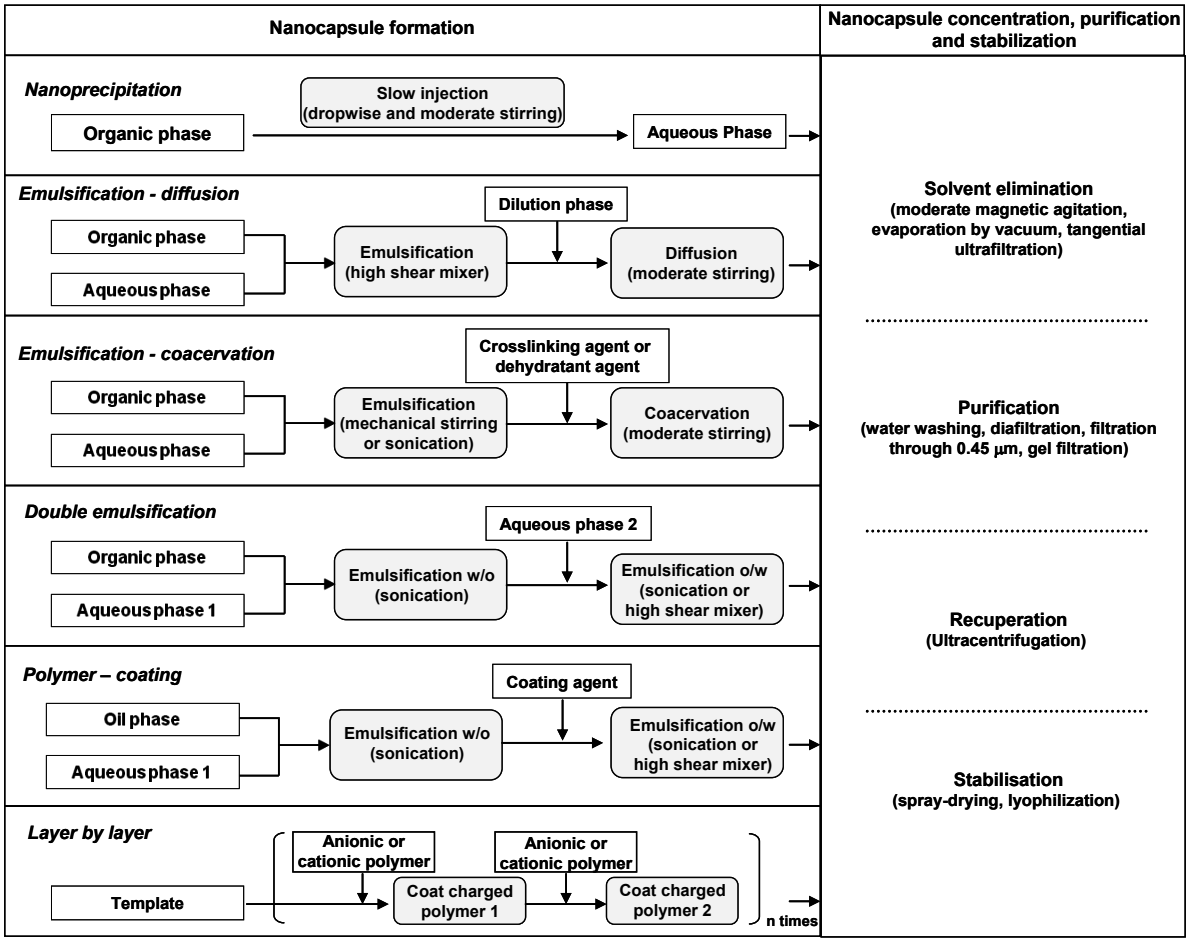

Figure 3: General procedures of the different methods developed for the preparation of nanocapsules (Mora-Huertas et al., 2010).

Polymeric micelles are nano-sized structures formed by self-assembly of amphiphilic block copolymers when added to aqueous solutions at concentration above the critical micelle concentration (Croy and Kwon, 2006). Control over the amphiphiles' shapes (by varying the critical packing factor parameter C_{pp}) gives the possibility to develop and manipulate nanostructure architectures (Figure 4) ranging from spherical micelles ($C_{pp} \leq 1/3$) to

cylindrical micelles ($1/3 \leq C_{pp} \leq 1/2$), vesicles ($1/2 \leq C_{pp} \leq 1$) and lamellar structures ($C_{pp} = 1$), while for larger values ($C_{pp} > 1$), the amphiphiles will assemble into "inverted" phases (Lombardo et al., 2019). Polymeric micelles are used in delivery of natural insecticides because of their interesting properties such as biocompatibility and low toxicity (Yadav et al., 2019). These carriers have a hydrophobic core–hydrophilic shell architecture that facilitates the entrapment of hydrophobic active molecules into the core (Figure 2) (Jones and Leroux, 1999). The major disadvantages of polymeric micelles include lack of stability and lack of suitable methods for large scale production (Lu and Park, 2013).

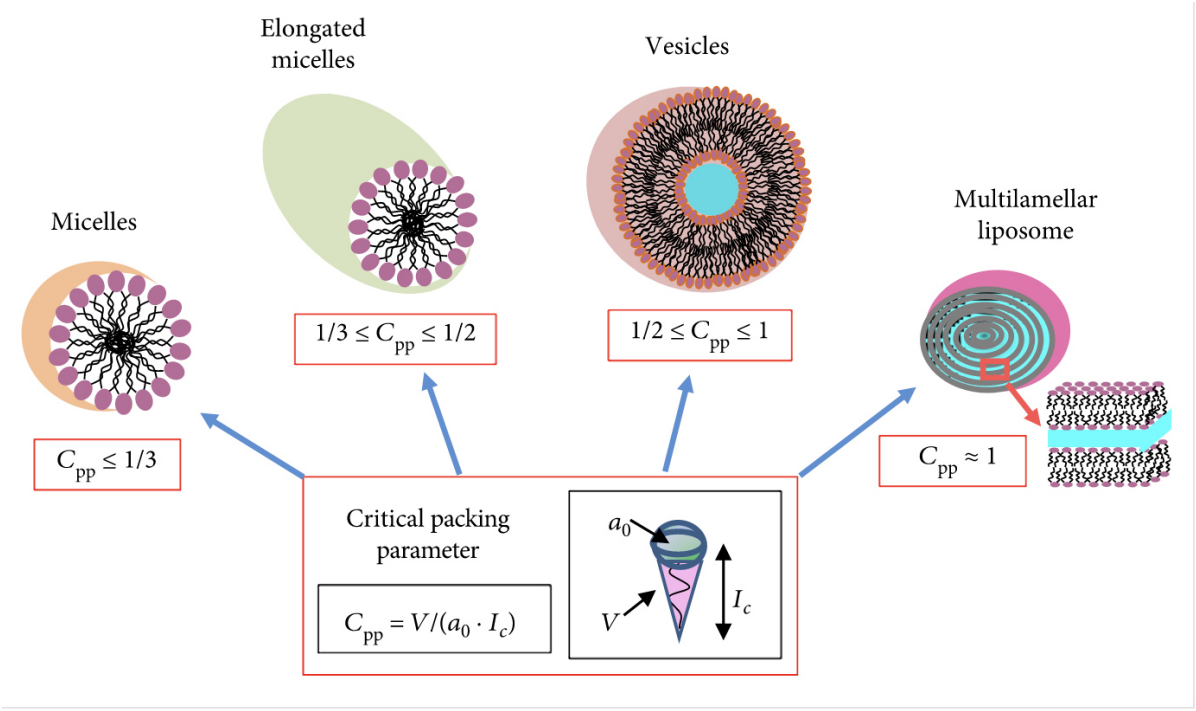

Figure 4: Analysis of the critical packing parameter C_{pp} and relevant shape factors that influence the amphiphilic nanocarrier morphology (Lombardo et al., 2019).

3.2. **Nanoemulsions and microemulsions**

Emulsions are ternary systems consisting of two immiscible liquids, generally water and oil, with one of the liquids being dispersed as small spherical droplets in the other liquid. There are two basic types of emulsions (oil-in-water and water-in-oil) depending on whether the oil is dispersed as droplets in water, or vice versa (McClements, 2012).

Emulsions applied in agricultural and food industries are classified into two categories: microemulsions and nanoemulsions which presented several similarities, but also some important differences. Figure 5 summarizes the major differences between macroemulsions, nanoemulsions and microemulsions with respect to their size, shape, stability, method of

preparation, and polydispersity. Nanoemulsions and microemulsions are usually fabricated using the same components: oil, water, surfactant and possibly a co-surfactant. For both, the nonpolar tails of the surfactant molecules protrude into the hydrophobic core (oil phase), whereas the polar head groups of the surfactant molecules protrude into the surrounding aqueous phase (Figure 2) (McClements, 2012). However, a fundamental difference is the thermodynamic stability: microemulsions are thermodynamically stable while nanoemulsions are thermodynamically unstable with spontaneous tendency to separate into the constituent phases. Consequently, an energy input is always required for the formation of nanoemulsions, and they must be prepared shortly before their use. In contrast, microemulsions can be prepared by simply mixing oil, water and surfactant together at a particular temperature without the use of any external energy (Kale and Deore, 2016).

Microemulsions are one of the best carrier systems because of their improved drug solubilization and long shelf life with ease of preparation and administration (Bagwe et al., 2001). Nevertheless, they may lose their stability if one of the constituents is chemically modified during storage or if the environmental conditions are altered into a range where the system is no longer thermodynamically stable. For example, a microemulsion may break down if the temperature is changed during fabrication and storage of the colloidal system (McClements, 2012). Regarding nanoemulsions, the lack of stability is the major disadvantage; degradation of the structure often takes place during storage due to several physicochemical mechanisms including gravitational separation (creaming/sedimentation), coalescence, flocculation, and Ostwald ripening. The rates at which these degradation processes occur depend on system composition (e.g., oil type, surfactant type, and solvent type) and environmental conditions (e.g., temperature, pH and applied forces) (Komaiko and McClements, 2016).

	macroemulsions	nanoemulsions	microemulsions
	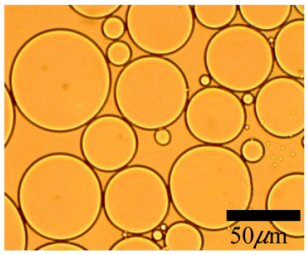	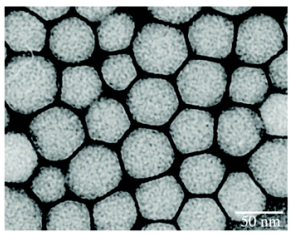	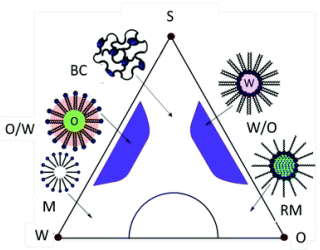
size	1-100 μm	20-500 nm	10-100 nm
shape	spherical	spherical	spherical, lamellar
stability	thermodynamically unstable, weakly kinetically stable	thermodynamically unstable, kinetically stable	thermodynamically stable
method of preparation	high & low energy methods	high & low energy methods	low energy method
polydispersity	often high (>40%)	typically low (<10-20%)	typically low (<10%)

Figure 5 : Comparison of macroemulsions, nanoemulsions, and microemulsions with respect to their size, shape, stability, method of preparation, and polydispersity (Gupta et al., 2016).

3.3. Solid lipid nanoparticles

Solid lipid nanoparticles are colloidal carrier systems developed in the last decade as an alternative system to the existing traditional carriers (emulsions, polymeric nanoparticles, etc.). Among the various carrier systems, lipid-based nanoparticles bear the advantage of being the least toxic for in vivo applications. Solid lipid nanoparticles possess a solid lipid core, which may contain triglycerides, glyceride mixtures, or waxes that are solid at room temperature. The lipid core is stabilized by surfactants (Figure 2) (Puri et al., 2009). Solid lipid nanoparticles could be prepared by mixing a lipid excipient with an aqueous emulsifier solution above the melting temperature of the lipid excipient, to produce a hot oil-in-water emulsion that is then cooled to form the solid nanoparticles as shown in Figure 6. It has been stated that solid lipid nanoparticles combine the advantages and avoid the drawbacks of other colloidal carriers. Their advantages include: (1) capability of carrying lipophilic and hydrophilic drugs, (2) possibility of controlled drug release and drug targeting, (3) biocompatibility and low toxicity, (4) ease of scaling up. Potential disadvantages such as poor

drug loading efficiency and drug release during storage have been observed (Mukherjee et al., 2009).

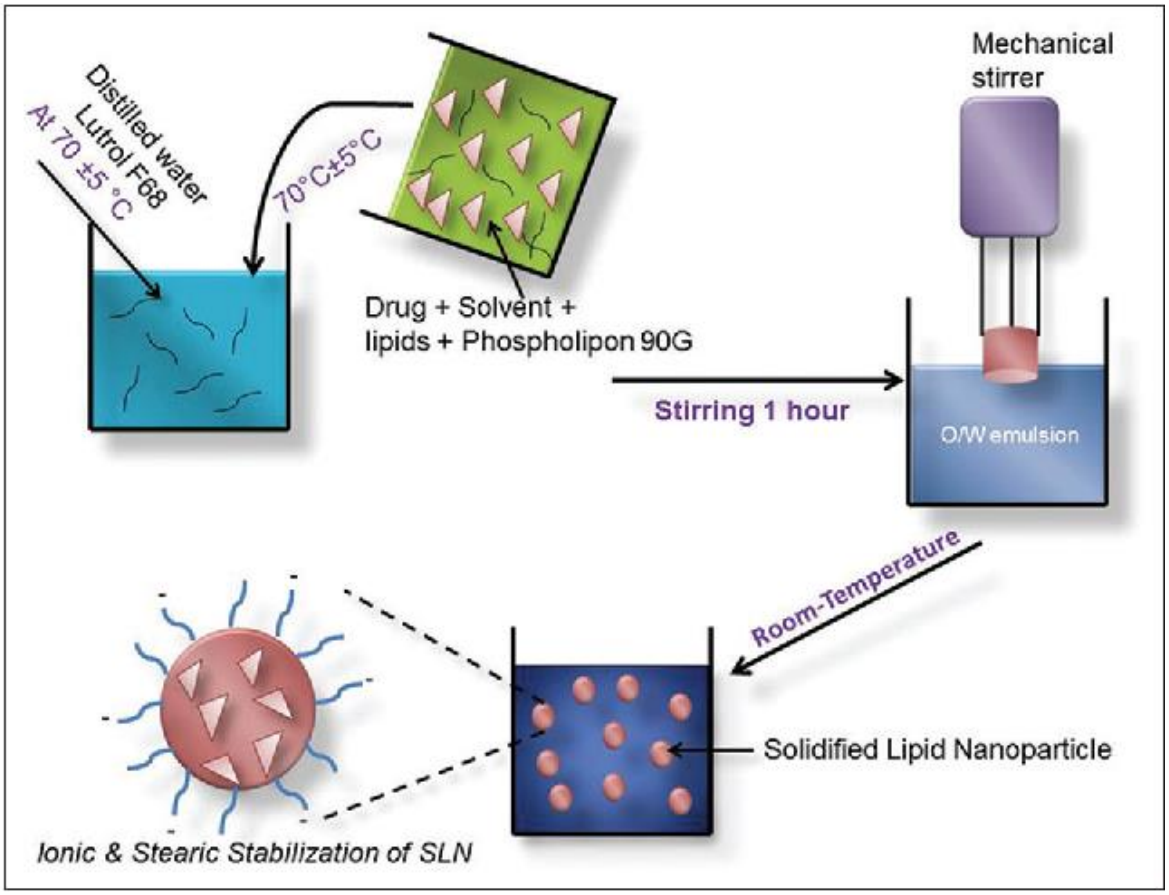

Figure 6: Preparation of nanoparticles by solvent diffusion technique (Shah et al., 2012).

3.4. Cyclodextrins (CDs)

Cyclodextrins (CDs) are non-toxic cyclic oligosaccharides formed of α-1,4-linked D-glucopyranose units. Most common native CDs are formed of 6 (α-CD), 7 (β-CD), or 8 (γ-CD) glucose subunits, with a respective cavity size of approximately 0.5, 0.6, and 0.8 nm. CDs have a form of a truncated cone with an external hydrophilic surface and an internal hydrophobic cavity (Figure 2). This particular structure offers to CDs the ability to accommodate lipophilic drugs in their cavity forming CD/drug inclusion complex. Natural CDs have limited solubility in water because of their relatively strong intermolecular hydrogen bonding in the crystal state. Chemical modifications such as amination, etherification, methylation, and esterification of the primary and secondary hydroxyl groups are applied to synthesize various hydrophobic, hydrophilic, and ionic CD derivatives with an improved aqueous solubility compared to the native CDs. However, Van der Waal forces, hydrogen bonds, and hydrophobic interactions are involved in the CD/drug inclusion complex

formation. Therefore, the inclusion complex will rapidly dissociate following intravenous administration (Piel et al., 1999; Zuo et al., 2002).

4. Characterization of delivery systems loading natural insecticides

Several characterization techniques were used to determine the properties of delivery systems loading natural insecticides. The various insecticide-loaded carriers were characterized for the mean particle size using different techniques such as photo correlation spectroscopy, transmission electron microscopy and scanning electron microscopy. Additionally, filtration and centrifugation methods were carried out to separate the particles from unloaded active molecules and the encapsulation efficiency (EE) was determined by quantifying insecticide content before and after separation. Moreover, release studies were conducted to examine the effect of encapsulation on the release of active molecules. In the sections below, we discuss the data reported in literature for the different types of insecticide-loaded formulations.

4.1. **Characteristics of polymer based particles and micelles**

In this section, we analyzed the characteristics of polymer based particles and micelles entrapping natural insecticides. Tables 1-3 resume the size, EE and active molecules release, respectively, of polymer based particles with respect to polymer type and insecticide to polymer mass ratio; the studies on capsules are presented first (nanocapsules then microcapsules) followed by those on nanospheres/microspheres (nanospheres then microspheres). The data presented in Tables 1-3 show that various parameters affect the characteristics of insecticide-loaded polymer based particles, including solubility of active molecule, insecticide:polymer ratio, type of polymer, and process parameters.

Various types of natural or synthetic polymers are used for the delivery of natural bio-insecticides. Natural polymeric materials and their derivatives are sustainable sources, which are readily available, facilitating their large-scale production. They have gained more attention than synthetic polymers in food and agriculture industries due to their non-toxicity, biodegradability, biocompatibility, and low cost (Campos et al., 2015).

The natural polymers used in the preparation of insecticide-loaded particles generally include proteins (gelatin) and polysaccharides (chitosan, starch and starch derivatives such as maltodextrins (MDX)). Gelatin is a protein-based polymer soluble in water. It is produced by the partial hydrolysis of native collagen extracted from the skin, bones, and connective tissues

of animals (Song et al., 2018). Chitosan is industrially produced by partial deacetylation of chitin, which is composed of D-glucosamine and N-acetyl-D-glucosamine monomers, linked by β-(1,4) glycosidic bonds, and is the primary component of the invertebrates' exoskeleton and of the cell walls of some bacteria and fungi (Campos et al., 2015). Chitosan is considered as one of the most promising polymeric materials for the efficient delivery of agrochemicals (Kashyap et al., 2015). A factor that limits the use of chitosan in sustained release applications is its hydrophilicity, resulting in a poor capacity to carry hydrophobic molecules. This issue can be overcome by the introduction of a cross-linker. A cross-link is formed through a chemical reaction, which links two polymers together, either through covalent/ionic bonds or weaker bonding interactions such as van der Waals forces (Ryan et al., 2017). The crosslinking agents commonly used in preparation of chitosan nanoparticles are tripolyphosphate (TTP), glutaraldehyde (GLA), and 1-ethyl-3-(3-dimethylaminopropyl) carbodiimide (EDC). Moreover, efforts have been made to improve the ability of chitosan to carry hydrophobic substances, notably by means of functionalization of the chitosan structure with CDs (Fan et al., 2012). Starch is the energy storage molecule of most green plants and is found in grains, roots, legumes and fruits. This polymeric hydrocarbon is composed of two types of polymer chains known as amylose and amylopectin. Amylose is constituted of glucose units connected by α-(1,4) bonds, forming a linear chain, while amylopectin forms branched structures between the glucose units by means of α-(1,4) and α-(1,6) bonds (Campos et al., 2015). The poor water solubility of native starch makes it difficult to process under mild conditions. Physical or chemical modifications have been adopted to improve its properties and adequacy as pesticide formulation. For example, MDX [$(C_6H_{10}O_5)_n \cdot H_2O$] are water-soluble polymers produced by the enzymatic hydrolysis of starch and consist of glucose units, primarily linked by α-1,4 glycosidic bonds (Klinjapo and Krasaekoopt, 2018).

Synthetic polymeric materials are nontoxic, or can be degraded by microbes, and their decomposition products have low hazard to non-target organisms and the environment. The most common synthetic polymers used as nanocarriers of insecticides are the polyesters poly-ε-caprolactone (PCL) and polyethylene glycol (PEG). PEG is a polyether composed of repeated ethylene glycol units [$-(CH_2CH_2O)_n$]. It is soluble in water and in most organic solvents. Because of its wide range of solubility and safety properties such as lack of toxicity, absence of antigenicity and immunotoxicity, non-interference with conformations of polypeptides and enzymatic activities as well as ease of excretion from living organisms, PEG has been FDA-approved (D'souza and Shegokar, 2016). PCL [$-(C_6H_{10}O_2)_n$] is an FDA-approved biodegradable polymer prepared by ring opening-polymerization of ε-caprolactone

using a catalyst such as stannous octanoate. PCL is insoluble in water and alcohols but soluble in almost all aromatic, polar, and chlorinated hydrocarbons (McKeen, 2013).

4.1.1. Size of particles

Table 1: Size of polymer based nanoparticles and microparticles loading natural insecticides.

Insecticide	Polymer 1. Type 2. Insecticide:polymer mass ratio	Size	Reference
Nanocapsule			
Garlic EO	1. PEG 2. 1:10	Less than 240 nm.	(Yang et al., 2009)
Geranium and bergamot EOs	1. PEG 2. 5:100, 7.5:100, 10:100, 12.5:100	Particles of 10:100 insecticide:polymer ratio were the smallest (234 ± 25 and 184 ± 18 nm for geranium and bergamot EOs, respectively).	(Werdin González et al., 2014)
PONNEEM®	1. Chitosan:TTP (1:1) Chitosan:GLA (1:1) 2. 5:50	Particles composed of TTP (122.7 nm) were smaller than those composed of GLA (243.5 nm).	(Gabriel Paulraj et al., 2017)
Geranium and Bergamot EOs	1. PEG 2. 1:10 1. Chitosan:TTP (1:1) 2. 1:1	Particles composed of PEG (253 ± 22 and 239 ± 29 nm for geranium and bergamot, respectively) were smaller than those composed of chitosan (439 ± 35 and 535 ± 42 nm for geranium and bergamot, respectively).	(Werdin González et al., 2017)
Satureja hortensis EO	1. Chitosan:TTP (2:1) 2. 25:10	EO-loaded particles (192 ± 11 nm) were slightly larger than empty ones (85 ± 5 nm).	(Ahmadi et al., 2018)
Carvacrol and linalool	1. Functionalized chitosan:TTP (3:1) 2. ND	EO-loaded particles (175.2 ± 2.9 and 245.8 ± 29.8 nm for carvacrol and linalool, respectively) were smaller than empty ones (465.7 ± 45.4 nm).	(Campos et al., 2018)
Geraniol	1. Chitosan:Arabic gum (0.15:3, 1:3, 1.5:3, 0.15:0.3, 0.15:1, and 0.15:3) 2. ND	- Decreased from 749 ± 363 (at 0.15:3 chitosan:Arabic gum ratio) to 235 ± 19 nm (at 1.5:3 chitosan:Arabic gum ratio). - Increased from 660 ± 375 (at 0.15:0.3 chitosan:Arabic gum ratio) to 749 ± 363 nm (at 0.15:3 chitosan:Arabic gum ratio).	(de Oliveira et al., 2018)
Avermectin	1. Chitosan:PGA (1:1) 2. 7.5:1	Particles prepared at pH 5.5 (56 ± 3 nm) were slightly smaller than those prepared at pH 7 (61 ± 5 nm).	(Liang et al., 2018)
Nicotine	1. Chitosan:TTP (1:1) 2. 1:0.05, 1:0.1, 1:0.15, 1:0.2	Increased from 249.9 nm (at 1:0.05 insecticide:polymer ratio) to 1376 nm (at 1:0.2 insecticide:polymer ratio).	(Yang et al., 2018)
Siparuna guianensis EO	1. Chitosan 2. 1:2	82 nm.	(P. Ferreira et al., 2019)
Peppermint and palmarosa EOs	1. PEG 2. 1:10	335 ± 38 and 167 ± 3 nm for peppermint EO- and palmarosa EO-loaded particles, respectively.	(Yeguerman et al., 2020)
Microcapsules			
Rosmarinus and *Thymus* EOs	1. Gelatin:GLA (15:3) 2. 3:1.5	58.5 and 56.7 µm for *Rosmarinus* EO- and *Thymus* EO-loaded particles.	(Moretti et al., 2002)
Citronella oil	1. Gelatin:Arabic gum (1:1) 2. 5:1	Ranges from 25 to 100 µm.	(Specos et al., 2010)
Lavandin EO	1. PEG	- Ranges from 30 to 100 µm.	(Varona et al., 2010)

	2. 2.5:10, 2.9:10, 3.2:10, 3.7:10, 3.4:10	- Influenced by process parameters.	
Schinus molle EO	1. MDX:Arabic gum (4:1, 3:2; 2:3; and 1:1) 2. 1:4	Decreased from 40 (at 4:1 MDX:Arabic gum) to 10 µm (at 1:1 MDX:Arabic gum).	(López et al., 2014)
Neem seed oil	1. - Polyvinyl alcohol - Arabic gum - whey protein isolate:MDX 2. 1:2	Significant difference between particles composed of polyvinyl alcohol (29 ± 12 µm), Arabic gum (32 ± 13 µm), and whey protein isolate:MDX (53 ± 17 µm).	(Sittipummongkol and Pechyen, 2018)
Nanosphere			
Lippia sidoides EO	1. Chitosan:angico gum (1:10) 2. 1:2, 1:4, 1:10, 1:20	Particles of 1:4 insecticide:polymer ratio were the smallest (12 ± 2 nm).	(Paula et al., 2010)
Lippia sidoides EO	1. Chitosan:cashew gum (1:1, 1:10, 10:1) 2. 1:10, 2:10	- Increased from 391 ± 55 (at 1:1 chitosan:cashew gum ratio) to 899 nm (at 10:1 chitosan:cashew gum ratio) using 1:10 insecticide:polymer ratio. - Increased from 335 ± 116 (at 1:10 insecticide:polymer ratio) to 558 ± 116 (at 2:10 insecticide:polymer ratio) using 1:10 chitosan:cashew gum ratio.	(Abreu et al., 2012)
Carum copticum EO	1. Chitosan:EDC (3:1) 2. ND	133 nm	(Ziaee et al., 2014)
Zanthoxylum rhoifolium EO	1. PCL 2. 5:15, 10:15, 25:15	No difference between blank (452± 0.2 nm) and EO-loaded particles for all insecticide:polymer ratios used.	(Christofoli et al., 2015)
Microsphere			
Spinosad:emamectin benzoate (4:1)	1. PLA:PCL (5:1, 4:2, 3:3, 2:4, 1:5) 2. ND	Around 7 µm for all formulations.	(Huang et al., 2017)

EDC: 1-ethyl-3-(3-dimethylaminopropyl) carbodiimide; EO: essential oil; GLA: glutaraldehyde; MDX : maltodextrin, PCL: polycaprolactone; PEG: polyethylene glycol; PGA: poly-γ-glutamic acid; PLA: polylactic acid; TTP: tripolyphosphate

Several papers characterized insecticide-loaded polymer based particles with respect to their size. For example, Yang et al., 2009 developed PEG nanocapsules carrying garlic EO; the mean size of the resulting particles was less than 240 nm. The sizes of PEG nanocapsules containing peppermint and palmarosa EOs were 335 ± 38 and 167 ± 3 nm, respectively (Yeguerman et al., 2020). The size of *Siparuna guianensis* EO-loaded chitosan nanocapsule was 82 nm (Ferreira et al., 2019). Citronella oil was encapsulated into gelatin:Arabic gum microcapsules; the size of the obtained batches ranges between 25 and 100 µm (Specos et al., 2010). The mean size of chitosan:EDC nanosphere retaining *Carum copticum* EO was 133 nm (Ziaee et al., 2014). The size of polylactic acid:PLC (PLA:PCL) microsphere entrapping spinosad and emamectin benzoate were around 7 µm (Huang et al., 2017).

Ahmadi et al., 2018 prepared and characterized empty and *Satureja hortensis* EO-loaded chitosan:TTP nanocapsules. Size analysis showed that EO-loaded particles were larger than empty ones. Campos et al., 2018 prepared and characterized functionalized chitosan:TTP nanocapsules containing carvacrol and linalool. The size of blank particles was 465.7 ± 45.4 nm, and the addition of active agents led to a significant reduction of the mean size to 175.2 ± 2.9 and 245.8 ± 29.8 nm for carvacrol and linalool, respectively. Moreover, geranium and bergamot EOs were encapsulated into PEG nanocapsules. No important difference in size was observed between both formulations; the particle size ranges from 230 to 620 nm for geranium EO and from 240 to 580 nm for bergamot EO (Werdin González et al., 2014). Similarly, *Rosmarinus* EO- (58.5 μm) and *Thymus* EO-loaded (56.7 μm) gelatin:GLA microcapsules were of similar size (Moretti et al., 2002).

The effect of active molecule concentration on nanoparticle size was previously examined. Empty and *Zanthoxylum rhoifolium* EO-loaded PCL nanospheres were prepared using different insecticide:polymer ratios (5:15, 10:15, 25:15). For all ratios, no significant difference was found between the sizes of empty and EO-loaded particles (Christofoli et al., 2015). However, the effect of *Lippia sidoides* EO on nanoparticle size was concentration dependent; the increase in *Lippia sidoides* EO:polymer mass ratio from 1:10 to 2:10 led to an increase in chitosan:cashew gum nanosphere size from 335 ± 116 nm to 558 ± 116 nm (Abreu et al., 2012).

Additionally, the type of polymer used and its concentration influence the size of nanoparticles and microparticles. Nanocapsules containing geranium EO and bergamot EO were fabricated using PEG and chitosan. The size of PEG nanocapsules (253 ± 22 and 239 ± 29 nm for geranium and bergamot, respectively) was significantly smaller than that of chitosan nanocapsules (439 ± 35 and 535 ± 42 for geranium and bergamot, respectively) (Werdin González et al., 2017). Also, the size of PONNEEM®-loaded chitosan:TTP nanocapsule (122.7 nm) was noticeably smaller than that of chitosan:GLA nanocapsule (243.5 nm) (Gabriel Paulraj et al., 2017). Sittipummongkol and Pechyen, 2018 synthesized and characterized neem seed oil-loaded microcapsules using three different polymeric shells: polyvinyl alcohol, Arabic gum, and whey protein isolate in combination with MDX. The results showed that all formulations have a broad size distribution, and the average size was 29 ± 12, 32 ± 13, and 53± 17 μm for microcapsules containing polyvinyl alcohol, Arabic gum, and whey protein isolate:MDX, respectively. According to the authors, the large particle size of whey protein isolate:MDX microcapsule compared to that of polyvinyl alcohol and Arabic gum microcapsules may result from weak core-shell interactions, as neem seed oil is

hydrophobic while the whey protein isolate:MDX shell surface is hydrophilic due to the presence of polar protein and carbohydrate moieties. Regarding polymer concentration, Paula et al., 2010 reported that a slight increase in chitosan:angico gum nanosphere size was observed after the addition of *Lippia sidoides* EO but the increase is independent of polymer concentration. On the contrary, chitosan:TTP nanocapsule size increased from 249.9 to 1376 nm with increasing nicotine:polymer mass ratio from 1:0.05 to 1:0.2 (Yang et al., 2018). *Schinus molle* EO was incorporated into MDX:Arabic gum microcapsules using different MDX:Arabic gum ratios (4:1, 3:2; 2:3; and 1:1). The size of microcapsule was 40 μm at 4:1 MDX:Arabic gum ratio and 10 μm at 1:1 ratio (López et al., 2014). Moreover, de Oliveira et al., 2018 determined the size of geraniol-loaded nanocapsules composed of chitosan and Arabic gum, and different chitosan:Arabic gum ratios (0.15:3, 1:3, 1.5:3, 0.15:0.3, 0.15:1, and 0.15:3) were used. The researchers found that chitosan had a negative effect on the mean particle size while Arabic gum showed a positive effect. Opposite results were reported by Abreu et al., 2012 study which investigated that increasing chitosan content in the polymer matrix induced an increase in chitosan:cashew gum nanosphere size. According to the authors, the increase of chitosan proportion in the polymer matrix reduces gum-chitosan interactions, and consequently favors the formation of hydrogen bonds between chitosan chains. The positive amino group of chitosan causes repulsion between the chains, leading to large nanoparticle size.

Liang et al., 2018 examined the effect of pH on the mean size of avermectin-loaded chitosan:PGA nanocapsule by suspending freeze-dried particles in 20% ethanol phosphate buffer (pH 5.5, pH 7.0 or pH 8.5). The nanocapsules showed a slightly smaller size at pH 5.5 (56 ± 3 nm) compared to pH 7 (61 ± 5 nm). Under mildly alkaline conditions (pH 8.5), nanoparticles lost their integrity and formed heterogeneously-sized aggregates.

Lavandin EO was incorporated into PEG microcapsules through a high pressure precipitation technique (particle precipitation from gas saturated solutions) using various gas to product ratios (0.50 and 1.3) and pre-expansion pressures (5-9 MPa). The influence of the process parameters on the particle size was investigated. The results demonstrated that particle size decreased as the pre-expansion pressure or gas to product ratio increased. Higher pre-expansion pressures and higher gas to product ratios induce Joule-Thomson effect, and therefore promote faster PEG solidification, leading to the formation of smaller particles (Varona et al., 2010).

4.1.2. Morphology

Morphological characterization revealed spherical shapes for *Lippia sidoides* EO- (Abreu et al., 2012), Lavandin EO- (Varona et al., 2010), *Satureja hortensis* EO- (Ahmadi et al., 2018), *Zanthoxylum riedelianum* EO- (Pereira et al., 2018) and geraniol-loaded (de Oliveira et al., 2018) polymer based particles with smooth surfaces for *Carum copticum* EO- (Ziaee et al., 2014) and *Siparuna guianensis* EO-loaded (Ferreira et al., 2019) particles. Garlic EO-loaded PEG nanocapsule has a round shape with an external surface presenting no apparent cracks (Yang et al., 2009). Microcapsules loading *Rosmarinus* EO, *Thymus* EO (Moretti et al., 2002) and citronella oil (Specos et al., 2010) self-assemble into spherical "blackberry"-like structures.

4.1.3. Encapsulation efficiency

Table 2: The encapsulation efficiency of natural insecticides into polymer based nanoparticles and microparticles

Insecticide	Polymer 1. Type 2. Insecticide:polymer mass ratio	Encapsulation efficiency	Reference
Nanocapsule			
Geranium and bergamot EOs	1. PEG 2. 5:100, 7.5:100, 10:100, 12.5:100	- EE of geranium increased from 75 ± 5% at 7.5:100 insecticide:polymer ratio to 84 ± 3% at 12.5:100 ratio. - EE of bergamot increased from 71 ± 3% at 7.5:100 insecticide:polymer ratio to 89 ± 6% at 12.5:100 ratio.	(Werdin González et al., 2014)
PONNEEM ®	1. Chitosan:TTP (1:1) Chitosan:GLA (1:1) 2. 5:50	EE was 59.3 and 65.0% using TPP and GLA, respectively.	(Gabriel Paulraj et al., 2017)
Geranium and bergamot EOs	1. PEG 2. 1:10 1. Chitosan:TTP (1:1) 2. 1:1	- EE was 77 ± 7 and 68 ± 5% for PEG nanoparticles containing geranium and bergamot, respectively. - EE was 38 ± 4 and 22 ± 3% for chitosan nanoparticles containing geranium and bergamot, respectively.	(Werdin González et al., 2017)
Satureja hortensis EO	1. Chitosan:TTP (2:1) 2. 5:10, 10:10, 25:10, 40:10, 50:10	EE decreased from 97.7% at 5:10 insecticide:polymer ratio to 46.2% at 50:10 ratio.	(Ahmadi et al., 2018)
Carvacrol and linalool	1. Functionalized chitosan:TTP (3:1) 2. ND	EE was 95.3 ± 0.8 and 93.1 ± 1.2% for carvacrol and linalool, respectively.	(Campos et al., 2018)
Geraniol	1. Chitosan:Arabic gum (0.15:3, 1:3, 1.5:3, 0.15:0.3, 0.15:1, and 0.15:3) 2. ND	- EE was more than 90% for all formulations. - EE was not influenced by chitosan and Arabic gum content.	(de Oliveira et al., 2018)
Avermectin	1. Chitosan:PGA (1:1) 2. 7.5:1	EE was around 34.7%.	(Liang et al., 2018)
Nicotine	1. Chitosan:TTP (1:1) 2. 1:0.05, 1:0.1, 1:0.15, 1:0.2	EE increased from 42.1% at insecticide:polymer ratio of 1:0.05 to 59.7% at 1:0.2 ratio	(Yang et al., 2018)

Peppermint and palmarosa EO	1. PEG 2. 1:10	EE was 93.8 and 94.5% for peppermint and palmarosa EOs, respectively.	(Yeguerman et al., 2020)
Microcapsules			
Rosmarinus and Thymus EOs	1. Gelatin:GLA (15:3) 2. 30:15	EE was 99.2 and 98.6% for *Rosmarinus* and *Thymus* EOs, respectively.	(Moretti et al., 2002)
Zanthoxylum limonella EO	1. Gelatin:GLA (2:5, 3:1, 3:2, 3:5, 3:10) 2. 7:2, 5:3, 7:3, 10:3, 13:3, 15:3, 7:5	- EE increased from 78.4 ± 0.9% at 7:2 insecticide:polymer ratio to 97.5 ± 1.0% at 7:3 ratio. - EE decreased from 98.2 ± 1.1% at 5:3 insecticide:polymer ratio to 78.0 ± 1.7% at 15:3 ratio	(Maji et al., 2007)
Lavandin EO	1. PEG 2. 2.5:10, 2.9:10, 3.2:10, 3.7:10, 3.4:10	- EE ranges between 14 and 66%. - EE was influenced by the process parameters.	(Varona et al., 2010)
Citronella oil	1. Gelatin 2. 1:1, 2:1	- EE increased with increasing oil concentration. - EE was influenced by the process parameters.	(Solomon et al., 2012)
Schinus molle EO	1. MDX:Arabic gum (4:1, 3:2; 2:3; and 1:1) 2. 1:4	EE was about 100% in all the formulations.	(López et al., 2014)
Neem seed oil	1. Polyvinyl alcohol Arabic gum whey protein isolate:MDX 2. 1:2	EE was 92.9 ± 3.8, 89.6 ± 1.5, and 60.7 ± 2.7% for particles composed of polyvinyl alcohol, Arabic gum, and whey protein isolate:MDX, respectively.	(Sittipummongkol and Pechyen, 2018)
Nanosphere			
Lippia sidoides EO	1. Chitosan:angico gum (1:10) 2. 1:2, 1:4, 1:10, 1:20	EE increased from 16.0% at 1:2 insecticide:polymer ratio to 69.3% at 1:20 ratio	(Paula et al., 2010)
Carum copticum EO	1. Chitosan:EDC (3:1) 2. ND	EE was 83.6 ± 1.0%.	(Ziaee et al., 2014)
Zanthoxylum rhoifolium EO	1. PCL 2. 5:15, 10:15, 25:15	EE was not influenced by insecticide:polymer ratio (> 96% for all formulations).	(Christofoli et al., 2015)

EDC: 1-ethyl-3-(3-dimethylaminopropyl) carbodiimide; EO: essential oil; GLA: glutaraldehyde; MDX : maltodextrin, PCL: polycaprolactone; PEG: polyethylene glycol; PGA: poly-γ-glutamic acid; PLA: polylactic acid; TTP: tripolyphosphate

Many studies evaluated the EE of several natural insecticides into polymer based particles. Ziaee et al., 2014 reported that *Carum copticum* EO was encapsulated into chitosan:EDC nanospheres with EE value of 83.6 ± 1.0%. The EE of avermectin into chitosan:PGA nanocapsules was around 34.7% (Liang et al., 2018). *Schinus molle* EO-loaded MDX:Arabic gum microcapsules showed high EE value (about 100%) (López et al., 2014). Besides, *Rosmarinus* EO- and *Thymus* EO-loaded gelatin:GLA microcapsules (Moretti et al., 2002) as

well as peppermint EO- and palmarosa EO-loaded PEG nanocapsules (Yeguerman et al., 2020) presented high EE values (more than 93%). Also, a high EE value of 95.3 ± 0.8% and 93.1 ± 1.2% was obtained for carvacrol- and linalool-loaded functionalized chitosan:TTP nanocapsules, respectively (Campos et al., 2018).

Variable factors modulate the incorporation of natural insecticides into polymer based particles. The effect of polymer type on the EE of natural insecticides was studied in literature. The EE of PONNEEM® into chitosan : GLA nanocapsules was higher (65%) than that of chitosan:TTP (59.3%) nanocapsules (Gabriel Paulraj et al., 2017). Geranium and bergamot EOs were entrapped more effectively in PEG nanocapsules (more than 65%) in comparison to chitosan nanocapsules (less than 40%) (Werdin González et al., 2017). The EE of neem seed oil-loaded microcapsules composed of whey protein isolate and MDX (60.7 ± 2.7%) was smaller than that of microcapsules composed of polyvinyl alcohol (92.9 ± 3.8%) and Arabic gum (89.6 ± 1.5%) (Sittipummongkol and Pechyen, 2018). Namely, polymeric particles exhibiting stronger interactions between the shell components and the core constituents showed a higher EE of insecticides (Porras-Saavedra et al., 2015; Sittipummongkol and Pechyen, 2018). Moreover, the EE of natural insecticides into polymer based particles relies on the insecticide to polymer ratio. The encapsulation of *Zanthoxylum rhoifolium* EO into PCL nanospheres was characterized using various insecticide:polymer ratios (5:15, 10:15, and 25:15). There was no significant EE variation between all formulations (Christofoli et al., 2015). For geranium EO, bergamot EO (Werdin González et al., 2014) and citronella oil (Solomon et al., 2012), the EE values increased with increasing the concentration of EO. In contrast, the EE of *Satureja hortensis* EO (Ahmadi et al., 2018) and *Zanthoxylum limonella* EO (Maji et al., 2007) into chitosan:TTP and gelatin:GLA particles, respectively, decreased with increasing the concentration of EOs. Besides, it was demonstrated that the extent of insecticide incorporation (insecticide EE) into polymer based particles depends on the initial concentration of polymer utilized to fabricate the particles (Maji et al., 2007; Paula et al., 2010; Yang et al., 2018). However, no correlation was found between the EE of geraniol into chitosan:Arabic gum nanocapsules and the initial concentration of chitosan and Arabic gum used to prepare the formulations (de Oliveira et al., 2018). The dependency of EE on oil and polymer concentrations was explained by Maji et al., (2007), who postulated that upon increasing the initial concentration of polymer, a higher polymer amount will be available to encapsulate the insecticide, and thereby EE would increase. Also, according to Maji and coauthors, EE decreased with increasing the initial concentration of EO due to the higher percentage of EO loss during separation of loaded and

unloaded EO. At high EO concentration, the amount of polymer present in the system might not be sufficient to encapsulate the whole EO amount. The unloaded EO content might get lost during separation.

Other factors controlling the incorporation of natural insecticides into polymeric particles are the process parameters. For instance, increasing the stirring rate from 500 to 750 rpm induced an increase in the EE of citronella oil into gelatin microcapsules (Solomon et al., 2012). The EE of lavandin EO into PEG microcapsules fabricated using a high-pressure precipitation technique decreased when pre-expansion pressure and gas to product ratios increased (Varona et al., 2010).

4.1.4. Active molecule release

Table 3: Release of natural insecticides from polymer based nanoparticles and microparticles

Insecticide	Polymer 1. Type 2. Insecticide:polymer mass ratio	Active molecule release	Reference
Nanocapsules			
Satureja hortensis EO	1. Chitosan:TTP (2:1) 2. 25:10	Rapid release at the initial stages followed by a slow release.	(Ahmadi et al., 2018)
Geraniol	1. Chitosan:Arabic gum (1.5:0.3) 2. ND	- Rapid release at the initial stages followed by a slow release which finally leveled off. - The release rate increased with increasing temperature from 20 (72 ± 1% at 5 h) to 30 ºC (81 ±1% at 5 h). - Fickian diffusion mechanism	(de Oliveira et al., 2018)
Avermectin	1. Chitosan:PGA (1:1) 2. 7.5:1	- Rapid release at the initial stages followed by slow release which finally leveled off. - The release at pH 5.5 was slower (57.6% at 72 h) compared to pH 8.5 (69.1% at 72 h).	(Liang et al., 2018)
Microcapsules			
Rosmarinus and *Thymus* EOs	1. Gelatin:GLA (15:3) 2. 30:15	Rapid release at the initial stages followed by a slow release.	(Moretti et al., 2002)
Zanthoxylum limonella EO	1. Gelatin:GLA (2:5, 3:5, 5:5) 2. 7:2, 5:3, 7:3, 10:3, 13:3, 15:3, 7:5	- Rapid release at the initial stages followed by slow release which finally leveled off. - The release at 7:2 insecticide:polymer ratio (65% at 70 h) was faster compared to 7:5 ratio (45% at 70 h). - The release at 5:3 insecticide:polymer ratio (60% at 70 h) was slower compared to 15:3 ratio (100% at 70 h).	(Maji et al., 2007)
Citronella oil	1. Gelatin 2. 2:1	Rapid release at the initial stages followed by a slow release.	(Solomon et al., 2012)
Schinus molle EO	1. MDX:Arabic gum (1:1) 2. 1:4	The release was prolonged when loaded in nanoparticles: 85% of free EO was released after 24 h compared to less than 15% for	(López et al., 2014)

		encapsulated EO.	
Neem seed oil	1. Polyvinyl alcohol Arabic gum whey protein isolate:MDX 2. 1:2	- Rapid release at the initial stages followed by a slow release - The release from whey protein isolate:MDX particles was greater (79% at 72 h) compared to polyvinyl alcohol (50% at 72 h) and Arabic gum (65% at 72 h) particles. - Fickian diffusion mechanism	(Sittipummongkol and Pechyen, 2018)
Nanospheres			
Lippia sidoides EO	1. Chitosan:angico gum (1:10) 2. 1:10, 1:20	- Rapid release at the initial stages followed by a slow release. - The release at 1:10 insecticide:polymer ratio was slower (26.7% at 24 h) compared to 1:20 ratio (52.6% at 24 h). - Non-Fickian diffusion mechanism	(Paula et al., 2010)
Lippia sidoides EO	1. Chitosan: cashew gum (1:1, 1:10, 10:1) 2. 2:10	- Rapid release at the initial stages followed by a slow release. - The release was slower at 10:1 chitosan:cashew gum ratio (30% at 3h) compared to 1:10 chitosan:cashew gum ratio (65% at 3 h). - Fickian diffusion mechanism	(Abreu et al., 2012)
Nicotine	1. Chitosan:TTP 2. 1:0.1	The release was prolonged when loaded in nanoparticles: 90% of free nicotine was released after 24 h compared to less than 20% for encapsulated nicotine.	(Yang et al., 2018)
Zanthoxylum rhoifolium EO	1. PCL 2. 5:15, 10:15, 25:15	Rapid release at the initial stages followed by a slow release.	(Christofoli et al., 2015)
Microspheres			
Spinosad:emamectin benzoate (4:1)	1. PLA:PCL (5:1, 4:2, 3:3, 2:4, 1:5) 2. ND	- Rapid release at the initial stages followed by a slow release - The release at 5:1 PLA:PCL ratio (75% at 15 h) was slower compared to 1:5 ratio (98% at 15 h).	(Huang et al., 2017)

EO: essential oil; GLA: glutaraldehyde; MDX: maltodextrin, PCL: polycaprolactone; PGA: poly-γ-glutamic acid; PLA: polylactic acid; TTP: tripolyphosphate.

The in-vitro release profile of natural insecticidal agents from polymeric based particles is characterized by a burst release followed by a sustained release which finally leveled off (Abreu et al., 2012; Ahmadi et al., 2018; Christofoli et al., 2015; de Oliveira et al., 2018; Huang et al., 2017; Liang et al., 2018; Maji et al., 2007; Moretti et al., 2002; Paula et al., 2010; Sittipummongkol and Pechyen, 2018; Solomon et al., 2012). The initial fast release may be related to the amount of active principle adsorbed at the surface of the particles. The slower release can be assigned to the active molecule diffusion from the interior of particles. Encapsulation of nicotine (Yang et al., 2018) and *Schinus molle* EO (López et al., 2014) into

chitosan:TTP nanosphere and MDX:Arabic gum microcapsules, respectively, prolonged their release compared to free molecules.

The mechanisms of insecticides release from polymeric based particles were discussed in several studies. The release of geraniol (de Oliveira et al., 2018), *Lippia sidoides* EO (Abreu et al., 2012), and neem seed oil (Sittipummongkol and Pechyen, 2018) from polymeric based particles occurred via Fickian diffusion. Sittipummongkol and Pechyen, (2018) demonstrated that the loss of structural integrity over time promotes the egress of insecticide from the particles via diffusion under the influence of a chemical potential gradient. However, Paula et al., (2010) showed that the release of *Lippia sidoides* EO from chitosan:angico gum nanospheres followed a non-Fickian diffusion.

Upon temperature elevation from 20 to 30 °C, the release rate of geraniol from chitosan:Arabic gum nanocapsules increased; 72 ± 1 and 81 ± 1% were released after 5 h at 20 and 30 °C, respectively. Changes in temperature can directly affect the diffusion of the active compound and the interactions between the nanoparticle components, thereby affecting the release of the active agent (de Oliveira et al., 2018).

Insecticides release from polymer based particles depends on the pH of the medium. The release of avermectin from chitosan:PGA nanocapsule was evaluated at various pH values (5.5, 7.0 or 8.5). After 72 h, the lowest amount of released avermectin (57.6%) was obtained at pH 5.5 and the highest amount (69.1%) at pH 8.5 (Liang et al., 2018). According to the authors, the slower release at pH 5.5 was attributed to the high stability of the nanoparticles in an acidic environment resulting from the strong electrostatic interaction between the constituents of the particles, while the release was facilitated at the alkaline pH due to the disintegration of the particles.

The impact of insecticide to polymer ratio on insecticide release was demonstrated in some studies. *Lippia sidoides* EO-loaded nanocapsule of 10:1 insecticide:polymer ratio showed a slower release profile (26.7% after 24 h) than that of 20:1 ratio (52.6% after 24 h) (Paula et al., 2010). Besides, the increase of cashew gum concentration in the polymer matrix of cashew gum:chitosan nanospheres loading *Lippia sidoides* EO seemed to favor the release of EO from the formulations: 30, 50 and 65% of EO were released after 3 h at cashew gum:chitosan ratio of 1:10, 1:1 and 10:1, respectively (Abreu et al., 2012). The release rate of *Zanthoxylum limonella* EO from gelatin:GLA microcapsules was found to increase with increasing the initial concentration of EO: after 70 h, 60% of EO was released at 5:3 insecticide:polymer ratio compared to 100% at 15:3 insecticide:polymer ratio (Maji et al., 2007). Moreover, the same authors showed that the release rate of *Zanthoxylum limonella* EO

decreased with increasing the initial concentration of gelatin; 65% of EO was released at 7:2 insecticide:polymer ratio compared to 45% at 7:5 ratio. As suggested by the authors, the increase in wall thickness of microcapsules with increasing gelatin concentration or decreasing oil concentration might be responsible for delaying EO release; the increase in wall thickness elongates the diffusional path for the active molecule release (Madan, 1981).

The insecticide release rate from polymer based particles can also differ according to the type of polymer constituting the particle membrane. Microcapsules composed of whey protein isolate and MDX were found to exhibit the lowest retention capacity toward neem seed oil relative to those composed of polyvinyl alcohol or Arabic gum. The percentage of released neem seed oil after 72 h was 79, 50, and 65% from whey protein isolate:MDX, polyvinyl alcohol, and Arabic gum microcapsules, respectively (Sittipummongkol and Pechyen, 2018). The authors concluded that the degree of affinity between the active molecule and the polymer modulates the active molecule retention level into particles. Furthermore, spinosad and emamectin benzoate were encapsulated into microspheres using various concentrations of wall constituents (PLA and PLC), and the active molecule release from the various formulations was studied. The results showed that increasing the hydrophilic PCL content in the PLA:PCL mixture accelerated the release of active molecules (Huang et al., 2017).

In addition, it was demonstrated that smooth surfaces prevent oil loss, while the presence of pores and cracks on the particle surfaces may facilitate the solvent diffusion into the particles, thereby enhancing the EO release rates (Sittipummongkol and Pechyen, 2018).

4.1.5. Stability studies

Chitosan:TTP microcapsules loading nicotine were stable after 45 days of storage at 25 ºC; neither nicotine leakage nor vesicle size alteration occurred during this period (Yang et al., 2018). Similarly, the sizes of geranium EO- and bergamot EO-loaded PEG nanocapsules were not altered after 6 months of storage at 25 ºC. However, the EE decreased from 83 to 60% and from 78 to 52% for geranium and bergamot nanoparticles, respectively (Werdin González et al., 2014).

The entrapment of avermectin (Liang et al., 2018), geraniol (de Oliveira et al., 2018) and *Zanthoxylum riedelianum* EO (Pereira et al., 2018) into polymeric nanoparticles protected them from degradation induced by ultraviolet (UV) irradiation. Heat stability measurements of free and microencapsulated *Schinus molle* EO indicated that MDX:Arabic gum microcapsules enhanced the stability of the EO. Less than 15% of free EO was retained after 24 h of storage at 45 ºC while 71% of encapsulated EO was retained after 366 h of storage (López et al., 2014). On the other hand, Zhang et al., (2019) characterized the encapsulation

of natural pyrethrins into mixed micelles using three amphiphilic copolymers including a temperature-responsive copolymer (poly[2-(2-Methoxyethoxy) ethyl methacrylate-co-Octadecyl methacrylate]) and two block polymers: monomethoxy (polyethylene glycol)13-poly(D, L-Lactide-co-glycolide) and monomethoxy (polyethylene glycol)45-poly(D, L-Lactide). Zhang and coworkers demonstrated that the mixed micelles loaded with natural pyrethrins represented a spherical shape with particle diameter ranging from 60 to 120 nm. Also, the formulations showed a controlled pyrethrin release in response to temperature changes; the amount of released pyrethrin increased with the increase of temperature. Finally, this system protected the encapsulated pyrethrin from UV degradation at 26 ºC.

4.2. Characteristics of nanoemulsions and microemulsions:

The nanoemulsions and microemulsions loading natural insecticides have been characterized in many publications for their size, morphology, EE, stability, and rate of insecticide release. The main findings of these studies are discussed below. In general, we can conclude that the properties of insecticide-loaded nanoemulsions and microemulsions depend not only on the composition variables (initial amounts of insecticide and surfactant, the presence of a co-solvent such as glycerol) but also on preparation variables (emulsifying energy and time), and environmental conditions (temperature, pH, etc.).

4.2.1. Size of particles

In Table 4, we summarized the literature regarding the size of the various insecticide-loaded nanoemulsions and microemulsions, showing the insecticide used in each study, the type of surfactant molecules and the insecticide:surfactant mass ratio. The studies on nanoemulsions are presented first followed by those on microemulsions. In general, the polydispersity index (PdI) values of the various formulations were inferior to 0.5; thus the formulations were largely homogeneous.

Table 4: The size of nanoemulsions and microemulsions loading natural insecticides.

Insecticide	Surfactant 1. Type 2. Insecticide:surfactant mass ratio	Size of droplets	Reference
Nanoemulsion			
Citronella oil	1. Montanov 82 with/without glycerol (0-100%) 2. 20:2.5, 20:5, 20:10	- At 25% glycerol concentration, the size decreased from 178 nm (at 20:2.5 insecticide:surfactant ratio) to 135 nm (at 20:10 ratio). - At 75% glycerol concentration, the size increased from 175 nm (at 20:2.5 insecticide:surfactant ratio) to 334 nm (at 20:10 ratio).	(Sakulku et al., 2009)
Lavandin EO	1. OSA-modified starches Tween 20:span 20 2. 18:1, 3:1, 1:1, 1:3	- No difference between emulsions composed of span 20:tween 20 and OSA-modified starches. - The size decreased from 1020 nm (at 18:1 insecticide:surfactant ratio) to 503 nm (at 1:3 ratio). - The size decreased with increasing of the amount of energy input provided for formation of emulsions.	(Varona et al., 2009)
Neem oil	1. Tween 20 2. 1:0.30, 1:0.50, 1:0.62, 1:0.66, 1:0.77, 1:1, 1:1.5, 1:2, 1:2.33, 1:3, 1:4, 1:5	The size decreased from 251 (at 1:0.3 imsecticide:surfactant ratio) to 31 nm (at 1:5 ratio).	(Anjali et al., 2012)
Mentha×piperita oil	1. CABS-70:NP-20 2. 40:12	The size decreased with increasing the amount of energy input provided for formation of emulsions.	(Kumar et al., 2013)
Rosmarinus officinalis EO	1. Tween 20 2. 5:5	50 nm.	(Duarte et al., 2015)
Pulegone	1. Tween 80 2. 1:1, 5:1, 10:1	The size increased from 62 ± 7 (at 1:1 insecticide:surfactant ratio) to 220 ± 10 nm (at 10:1 ratio).	(Golden et al., 2018)
Citral	1. Tween 80 2. 1:2	- Three populations were obtained with the largest population being the major one. - The mean droplet size was 59, 712, and 2670 nm for populations 1, 2 and 3, respectively.	(Pascual-Villalobos et al., 2017)
Ocimum basilicum L. EO	1. Tween 80 2. 1:1	The particles size was less than 200 nm.	(Sundararajan et al., 2018)
Avermectin	1. CO-PU 2. 1:18.9, 1.5:18.9, 2:18.8, 2.5:18.9	Insecticide loaded batches were slightly larger than empty ones (39 nm).	(Zhang et al., 2018)
Microemulsion			
T. ammi EO and C. maritimum EO	1. Tween 80 with glycerol (30%) 2. 0.25:13, 0.5:13, 0.75:13, 1.5:13	- Two populations were obtained with the smaller population being the major one. - The mean droplet size of the two populations was 58 and 700 nm for T. ammi EO as well as 50 and 500 nm for C. maritimum EO.	(Pavela et al., 2019)

CABS: calcium salt of alkyl benzene sulfonate, *C. maritimum*: *Crithmum maritimum*, CO-PU: castor oil-based polyurethane, EO: essential oil, NP: nonylphenol, OSA: n-octenyl succinic anhydride, Span: sorbitan monolaurate, T.ammi: Trachyspermum ammi

It can be seen from Table 4, that the various insecticide-loaded nanoemulsions studied in the literature exhibited a small mean droplet size (Anjali et al., 2012; Duarte et al., 2015; Golden et al., 2018; Kumar et al., 2013; Pavela et al., 2019; Sakulku et al., 2009; Sundararajan et al., 2018; Zhang et al., 2018). However, Pascual-Villalobos et al., 2017 reported that citral-loaded nanoemulsions, composed of the surfactant tween 80, presented a large particle size in which three populations, centered at 59 nm, 712 nm and 2670 nm, were obtained. The fraction of the population with the largest droplet size was predominant. Also, from Table 4, we conclude that the size of droplet might be affected by the concentration of surfactant and insecticide used, the addition of glycerol and its concentration, and the amount of energy input applied for the fabrication of the nanoemulsion.

Blank and avermectin-loaded nanoemulsions were prepared by Zhang et al., 2018. The size of blank formulations was around 39 nm, and it increased slightly after the addition of avermectin. The size of avermectin-loaded particles was less than 50 nm. In addition, Golden et al., 2018 fabricated pulegone-loaded nanoemulsions using various pulegone:tween 80 ratios (1:1, 5:1 and 10:1). The authors investigated that increasing pulegone:tween 80 ratio from 1:1 to 10:1 led to an increase in nanoemulsion particles size from 62 ± 7 to 220 ± 10 nm.

Lavandin EO-loaded nanoemulsions were prepared using n-octenyl succinic anhydride (OSA)-modified starches as well as with tween 20 in combination with span 20. The various formulations were characterized and compared in terms of their droplet size. The size of the nanoemulsions prepared with OSA-modified starches was very similar to that obtained with the non-ionic surfactants (combination of tween 20 and span 20) (Varona et al., 2009). Additionally, several studies demonstrated that increasing the surfactant concentration used for nanoemulsion preparation resulted in a decrease in the droplet size of nanoemulsion (Anjali et al., 2012; Sakulku et al., 2009; Varona et al., 2009) (Table 4). According to Reiss, 1975, the reduction of particle size with increasing the concentration of surfactant might be ascribed to the fact that surfactants can freely move and absorb around oil droplets, thus increasing the surface to volume ratio of the particles. Furthermore, the surfactant minimizes the interfacial free energy and provides a mechanical barrier to coalescence. However, the addition of glycerol at high concentration cancelled this pronounced impact of surfactants. At low glycerol concentration (less than 50%), a decrease in the mean particle diameter of citronella oil-loaded nanoemulsions was found (eg. from 178 to 135 nm at glycerol

concentration of 25%) upon increasing the concentration of the surfactant Montanov 82 from 2.5 to 10%. At high glycerol concentration (75%), an increase in the droplet size from 175 to 334 nm was obtained upon increasing the surfactant concentration. According to the authors, glycerol behaves as co-solvent and possesses a high viscous property. The highly viscous environment obtained in the presence of a high amount of glycerol may complicate the ability of surfactants to prevent coalescence (Sakulku et al., 2009).

As mentioned earlier, mechanical energy must be applied for the fabrication of nanoemulsions. Some studies evaluated the effect of the emulsifying energy level on the size of nanoemulsions. For example, Varona et al., 2009 produced Lavandin EO-loaded nanoemulsions using a rotor stator machine at three different homogenization velocities (quantified with the frequency of rotation of the rotor, set to 50, 60 and 70 Hz). The authors published that a noticeable reduction in the size of droplet was observed when the velocity of the rotor stator machine was increased. Similarly, Kumar et al., 2013 prepared *Mentha×piperita* oil-loaded nanoemulsions, subjected the samples to three cycles of homogenization (each cycle of 5000 rpm for 30 min) as further preparative steps, and evaluated the droplet size after each cycle. A slight decrease in the average particle size was obtained after each homogenization cycle. It might be that particle coalescence is counteracted upon increasing the amount of energy input applied for nanoemulsion production (Chen and Tao, 2005).

4.2.2. Morphology

A few studies, which characterized the encapsulation of an insecticide into nanoemulsions, determined the morphology of the particles. However, all of these studies agreed that the insecticide-loaded nanoemulsions demonstrated a spherical shape (Anjali et al., 2012; Golden et al., 2018; Sundararajan et al., 2018) and a homogeneous aspect (Sundararajan et al., 2018; Zhang et al., 2018).

4.2.3. Amount of natural insecticide loaded into the formulations

A few studies evaluated the EE values of natural insecticides into nanoemulsions. For instance, the EE was 28.7 ± 2.2% and 10.2 ± 1.3% for basil and coriander oils, respectively (Pascual-Villalobos et al., 2015). Furthermore, Zhang et al., 2018 calculated the EE of avermectin into nanoemulsions using various concentrations of avermectin (20, 30, 40 and 50%). The authors demonstrated that the EE values of avermectin were more than 85% for all the formulations. Hence, a small loss of avermectin occurred during the preparation of nanoemulsions, and most of the insecticide amount could be effectively loaded into the samples.

4.2.4. Active molecules release

Some papers in the literature examined the release of insecticides from nanoemulsions. The insecticides avermectin (Zhang et al., 2018) and pulegone (Golden et al., 2018) manifested biphasic release patterns in which the release was fast at the first phase, followed by a slow release over the second phase. The initial rapid release of insecticides is related to the non-uniform distribution of insecticides in the batches; some of active molecules including those adsorbed on the particle surface and close to the surface inside the particles would be released quickly with respect to the active molecules incorporated more deeply inside the particles. The release rate of insecticides from nanoemulsions is influenced by the concentrations of surfactant, insecticide, and glycerol used, and the environmental conditions (temperature, pH).

With respect to the insecticide content, Zhang et al., 2018 reported that the release rate of avermectin from nanoemulsions was slightly increased with the increase of avermectin concentration from 20 to 50%. However, Golden et al., 2018 published contradictory results regarding the impact of insecticide content on its release. The authors stated that increasing the concentration of pulegone from 1 to 10% induced a decrease in pulegone release rate from nanoemulsions.

On the other hand, the release rate of avermectin (Zhang et al., 2018) and pulegone (Golden et al., 2018) significantly increased as the temperature rose from 25 to 40 ºC and from 10 to 32 ºC, respectively. With respect to Zhang et al., 2018, the increase in release rate with increasing temperature may be attributed to the accelerated molecular thermal motion and increased insecticide solubility at higher temperature. In addition, Zhang et al., 2018 evaluated the effect of the pH of the medium (4, 6.8, 7.2, 9, 10) on the release behavior of avermectin from nanoemulsions constituted of castor oil-based polyurethane as a building material. The authors demonstrated that the release rate of avermectin was moderate at pH 7.2 compared to the other pH values. The release was accelerated at both acidic and alkali conditions but the acceleration was faster in acidic medium: After 120 h, the release rate reached 99.6 and 94.1% at pH 4.0 and 10.0, respectively, but this value was only 71.7% at pH 7.2. The authors explained their results by the break of the electrical equilibrium of particles when the pH changes. This induces a decrease in the electrical double layer of the particles, and as a consequence a decrease in their stability.

The effect of Montanov 82 and glycerol concentrations on the release of citronella oil from nanoemulsions was studied by Sakulku et al., 2009. A slow release of citronella oil from the formulations was obtained at high surfactant concentration (10%) compared to lower

concentrations (2.5 and 5%) at glycerol concentration of 50%. According to the authors, it is possible that the nanoemulsions are abundantly covered by the surfactant molecules at high surfactant concentration. Also, it might be possible that there is an excess amount of surfactants capable of inhibiting the diffusion of citronella oil to the carrier solution. Furthermore, the authors investigated that the concentration of glycerol greatly affected the release of citronella oil from the emulsion: the avermectin release was slower at high glycerol concentration (75 and 100%) compared to its lower concentrations (0, 50%). These findings were related to the high viscosity of nanoemulsions at high glycerol concentration, resulting in a less diffusion of insecticides into the carrier solution.

4.2.5. Stability studies

The stability of nanoemulsions loading natural insecticidal agents was assessed by simply monitoring the droplet size or evaluating the kinetics of creaming during a storage period. Most of the formulations revealed an increment in droplet size after storage. For instance, the mean droplet size of nanoemulsions incorporating *Rosmarinus officinalis* EO (Duarte et al., 2015), *Ocimum basilicum* EO (Sundararajan et al., 2018), and citronella oil (Sakulku et al., 2009) significantly increased after a storage period of 1 month, 1 month, and 2 months, respectively. Moreover, Golden et al., 2018 examined the change in droplet size of pulegone-loaded nanoemulsion over a period of a month. The results showed that the droplet size increased at the beginning, whereas after 7 days, the size remained with no significant alterations during the measurement period. For the nanoemulsions encapsulating Lavandin EO (Varona et al., 2009) and *Mentha* × *piperita* oil (Kumar et al., 2013), the droplet size and the creaming volume significantly increased after a period of storage of 50 days and 2 months, respectively.

4.3. Characteristics of solid lipid nanoparticles

Solid lipid nanoparticles containing pyrethrum were prepared and characterized by Oliveira et al., (2019) using tripalmitin (glyceryl tripalmitate) as a solid lipid and polyvinyl alcohol as a surfactant. The pyrethrum-loaded samples had a mean diameter of 261 ± 3 nm, and they remained physically stable after 2 months. Pyrethrum was efficiently encapsulated in the formulations; the EE of pyrethrum into this carrier system was 99%. Moreover, the incorporation of *Artemisia arborescens* L EO into solid lipid nanoparticles was previously studied. Two different formulations were prepared using Compritol 888 ATO as lipid and Poloxamer 188 or Miranol Ultra C32 (sodium cocoamphoacetate) as surfactants (Lai et al., 2006). The size was 199 and 207 nm for nanoparticles composed of Poloxamer 188 and Miranol Ultra C32, respectively. Both formulations presented a high capability of entrapping

the EO. In particular, the EE of EO was 87% and 92% into Poloxamer 188 and Miranol Ultra C32 nanoparticles, respectively. Additionally, the authors analyzed the release of EO from both formulations. During the first 24 h, both formulations showed a higher release rate than that in the subsequent hours. Also, the release of EO from Miranol Ultra C32 particles (45.5% of EO was released after 48 h) was faster compared to Poloxamer 188 particles (37.1% of EO was released after 48 h). Similar to pyrethrum-loaded nanoparticles, the *Artemisia arborescens* L EO-loaded solid lipid nanoparticles were physically stable after 2 months.

5. Insecticidal toxicity of encapsulated EOs

Recently, several studies have focused on essential oils' applications as alternative methods for insect pests and microorganisms' control due to their protective effects on human health and environment as opposed to synthetic pesticides (Pillmoor et al., 1993). Table 5 illustrates some insecticidal uses of encapsulated essential oils.

Among Coleoptera, Kaushik et al., (2013) studied the insecticidal activity of alginate formulation of *Curcuma longa* (Zingiberaceae) essential oil against *Callosobruchus maculatus* (Chrysomelidae). This study showed that this formulation is an appropriate tool to protect pulses grains from the attack of this pest. According to the same authors, low mortality of *C. maculatus* in high alginate concentration beads could be attributed to the low diffusion rate through the pores of alginate beads. Furthermore, better performance of *Artemisia sieberi* (Asteraceae) essential oil was attended when encapsulated under urea formaldehyde. The fumigant toxicity of encapsulated essential oil (LC_{50}= 11.24 ppm) against *Tribolium castaneum* (Tenebrionidae) was significantly higher than that of pure essential oil (LC_{50}= 15.68 ppm) (Negahban et al., 2012). Also, Sankar and Abideen (2015), showed that from the 4^{th} day after application, the toxicity of free *Avicennia marina* (Acanthaceae) essential oils against *Sitophilus oryzae* (Curculionidae) was very low compared to silver and lead nanoparticles.

Several researchers indicated the efficacy of encapsulated essential oils as tools to control infestation with Lepidoptera species. In this context, Chung et al., (2013) pointed out that thyme (Lamiaceae) essential oil encapsulated using melamine–formaldehyde prepolymer expressed high repellent efficacy (over 90% after 4 weeks) against larvae of *Plodia interpunctella* (Pyralidae). Additionally, Jesser et al., (2020) demonstrated the potential of encapsulation to enhance the toxicity of geranium (Geraniaceae) essential oil against larvae of *Culex pipiens* (Culicidae) (Crude essential oil LC_{50}=80.97 ppm, encapsulated essential oil

LC_{50}=48.27 ppm) and *P. interpunctella* (Crude essential oil LD_{50}=0.16 µg $larvae^{-1}$, encapsulated essential oil LD_{50}=0.07 µg $larvae^{-1}$). This study pointed out that nanoemulsions can increase by twofold the insecticidal efficacy of *Geranium maculatum* essential oil. Similarly, Werdin González et al., (2017) investigated the larvicidal toxicity of *G. maculatum* and *Citrus bergamia* (Rutaceae) essential oils polymeric nanoparticle and chitosan as the polymeric matrix/coating) against *Culex pipiens* (Diptera). The toxicological test showed that chitosan nanoparticles produced higher acute and residual activity than PEG particles. This study illustrated also that chitosan nanoparticles and PEG nanoparticles (LC_{50}=38.52 ppm and LC_{50}=22.63 ppm, respectively) containing *G. maculatum* were more toxic than crude essential oil (CL_{50}=57.28 ppm). According to the authors, high efficacy of the encapsulated essential oil compared with crude one might be due to their nanometric size which amplified surface area, allowed a better penetration into the larval body and an effective distribution of the active ingredient, enhancing the larvicidal toxicity. In addition, many studies showed that the encapsulation of EOs can be successfully exploited to furnish prolonged security from insect infestation. In this context, Negahban et al., (2012) demonstrated that encapsulation allowed the essential oil to be entrapped without any changes in its composition and control release. Also, the half-life time of the encapsulated essential oil (LT_{50}= 28.73 days) was significantly much longer than that of the crude essential oil (LT_{50}= 4.27 days). On the other hand, the study of López et al., (2014) illustrated that over a period of 366 h, a very slow liberation profile of the encapsulated essential oil was observed as well as a slower time-dependent insecticide effect (32 and 73% of dead flies at 2 and 4 h of exposure time) compared to the free EO (96% of dead flies at 2 h of exposure).

Table 5: Insecticidal activities of some encapsulated essential oils.

Order	Insect species	Essential oil/ Botanical family	Encapsulation system	Reference
Coleoptera	*Callosobruchus maculatus*	*Curcuma longa* / Zingiberaceae	Calcium alginate	(Kaushik et al., 2013)
	Tribolium casteneum	*Artemisia sieberi* / Asteraceae/	Urea and formaldehyde	(Negahban et al., 2012)
	Tribolium castaneum	*Rosmarinus officinalis* / Lamiaceae	Polycaprolactone	(Khoobdel et al., 2017)
	Zabrotes subfasciatus	*Azadirachta indica* / Meliaceae	Polymer nanoparticles	(da Costa et al., 2014)
	Tribolium castaneum	*Allium sativum*/ Liliaceae	Polyethylene glycol (PEG)	(Yang et al., 2009)
	Sitophilus oryzae	*Euphorbia prostrate* / Euphorbiaceae	Silver nanoparticles	(Zahir et al., 2012)
	Sitophilus oryzae	*Avicennia marina*/ Acanthaceae	Silver and lead nanoparticles	(Sankar and Abideen, 2015)
Lepidoptera	*Plodia interpunctella*	*Thymus herbabarona* / Lamiaceae	Melamine and formaldehyde	(Chung et al., 2013)
	Limantria dispar	*Rosmarinus officinalis Thymus herbabarona* / Lamiaceae	Gelatin and glutaraldehyde solution	(Côté et al., 2005)
	Plutella xylostella	*Azadirachta indica* / Meliaceae	Polycaprolactone	(Forim et al., 2013)
	Tuta absoluta	Lemon Mandarin sweet orange / Rutaceae	Polyethylene glycol (PEG)	(Campolo et al., 2018)
	Culex pipiens pipiens	*Geranium maculatum* / Geraniaceae	Nanoemulsions with Tween 80 as surfactant.	(Jesser et al., 2020)
	Plodia interpunctella			
	Lymantria dispar	*Thymus herba-barona Rosmarinus officinalis Salvia officinalis* / Lamiaceae	Gelatin	(Moretti et al., 2002)
	Plodia interpunctella			
		Myrtus communis Eucalyptus globules / Myrtaceae		
		Helichrysum italicum / Asteraceae		
		Disterigma microphyllum /		

		Ericaceae		
Hemiptera	*Haematobia irritans*	*Schinus molle* / Anacardiaceae	Maltodextrin (MDX) and gum Arabic as carrier (wall material)	(Pereira et al., 2018)
Blattoptera	*Bemisia tabaci*	*Zanthoxylum rhoifolium/* Rutaceae	Polycaprolactone	(Christofoli et al., 2015)
Diptera	*Culex pipiens*	*Geranium maculatum /* Geraniaceae	Polyethylene glycol (PEG 6000) and chitosan	(Werdin González et al., 2017)
		Citrus bergamia / Rutaceae		

6. Conclusions and perspectives

Diverse opportunities exist for nanotechnologies applications in food preservation against insect pests, diseases and microorganisms. Many studies reported that encapsulation displays the benefit of more effective and targeted usage of herbicides, pesticides and insecticides in eco-friendly greener manner. On the other hand, in recent years, plant extracts including essential oil (EOs) have been recognized as important natural sources of pesticides with widespread range of activities. Numerous researches indicated the great prospects for essential oils as bioactive ingredients in botanical pesticides production. However, EOs are sensitive to several environmental degradation factors (light, oxygen availability, temperature). Therefore, conventional formulating procedure will diminish their efficiency and limit their uses in practice. Thus, loading them in protective nanostructures will offer controlled release and delay their fast evaporation and degradation. Many EOs and their bioactive components were encapsulated in different systems including nanodispersions, nanoemulsions and polymer based formulations. Various studies highlighted the applications potentials of nanotechnologies in crop protection comprising pathogen and pest control with metallic and biopolymer nanoparticles and post-harvest management of diseases and insect pests. The key issues which remain to be considered consist of the demonstration of the clear cut effectiveness of the formulations compared to conventional ones under industrial conditions (mills, silos, etc.). Furthermore, other key future challenges, including the development of nanomaterials (microencapsulation stabilization processes), the limitations and current issues of nanomaterials applications in food industry (safety, eco-toxicity, costs of commercial nanoparticles production, commercial prices,…), the optimization of aromatic and medicinal plant cropping conditions and extraction procedures permitting homogeneous composition of EOs, should be also addressed. In addition, biopesticides authorization requirements should be a priority when these biopesticides will be applied to food conservation.

Acknowledgements

We thank the “Agence Universitaire de la Francophonie, Projet de Coopération Scientifique Inter-Universitaire 2018-2020” for supporting the project.

References

Ben Abdelaziz, N.F., Salem, H.A., Sammour, E.A., 2014. Insecticidal effect of certain ecofriendly compounds on some scale insects and mealybugs and their side effects on antioxidant enzymes of mango nurslings. Arch. Phytopathol. Plant Prot. 47, 1–14. https://doi.org/10.1080/03235408.2013.800693

Abreu, F.O.M.S., Oliveira, E.F., Paula, H.C.B., de Paula, R.C.M., 2012. Chitosan/cashew gum nanogels for essential oil encapsulation. Carbohydr. Polym. 89, 1277–1282. https://doi.org/10.1016/j.carbpol.2012.04.048

Ahmadi, Z., Saber, M., Akbari, A., Mahdavinia, G.R., 2018. Encapsulation of Satureja hortensis L. (Lamiaceae) in chitosan/TPP nanoparticles with enhanced acaricide activity against Tetranychus urticae Koch (Acari: Tetranychidae). Ecotoxicol. Environ. Saf. 161, 111–119. https://doi.org/10.1016/j.ecoenv.2018.05.051

Anjali, C., Sharma, Y., Mukherjee, A., Chandrasekaran, N., 2012. Neem oil (Azadirachta indica) nanoemulsion-a potent larvicidal agent against Culex quinquefasciatus. Pest Manag. Sci. 68, 158–163. https://doi.org/10.1002/ps.2233

Aouadi, G., Haouel, S., Soltani, A., Ben Abada, M., Boushih, E., Elkahoui, S., Taibi, F., Mediouni Ben Jemâa, J., Bennadja, S., 2020. Screening for insecticidal efficacy of two Algerian essential oils with special concern to their impact on biological parameters of Ephestia kuehniella (Zeller) (Lepidoptera: Pyralidae). J. Plant Dis. Prot. 127, 471–482. https://doi.org/10.1007/s41348-020-00340-y

Ataei, S., Azari, P., Hassan, A., Pingguan-Murphy, B., Yahya, R., Muhamad, F., 2020. Essential Oils-Loaded Electrospun Biopolymers: A Future Perspective for Active Food Packaging. Adv. Polym. Technol. 2020, 1–21. https://doi.org/10.1155/2020/9040535

Badreddine, B.S., Olfa, E., Samir, D., Hnia, C., Lahbib, B.J.M., 2015. Chemical composition of Rosmarinus and Lavandula essential oils and their insecticidal effects on Orgyia trigotephras (Lepidoptera, Lymantriidae). Asian Pac. J. Trop. Med. 8, 98–103. https://doi.org/10.1016/S1995-7645(14)60298-4

Bagwe, R.P., Kanicky, J.R., Palla, B.J., Patanjali, P.K., Shah, D.O., 2001. Improved drug delivery using microemulsions: rationale, recent progress, and new horizons. Crit. Rev. Ther. Drug Carrier Syst. 18, 77–140.

Ben Jemaa, J.M., 2014. Essential Oil as a Source of Bioactive Constituents for the Control of Insect Pests of Economic Importance in Tunisia. Med. Aromat. Plants 03. https://doi.org/10.4172/2167-0412.1000158

Ben-Khalifa, N., Chaieb, I., Laarif, A., Haouala, R., 2018. Insecticidal activity of six Apiaceae essential oils against Spodoptera littoralis Biosduval (Lepidoptera: Noctuidae). Journal of New Sciences 55, 3603–3609.

Bosly, B., 2013. Evaluation of insecticidal activities of Mentha piperita and Lavandula angustifolia essential oils against house fly, Musca domestica L. (Diptera: Muscidae). J. Entomol. Nematol. 5, 50–54. https://doi.org/10.5897/JEN2013.0073

Boussaada, O., Ben Halima, M., Ammar, S., Haouas, D., Gannoun, S., Helal, A.N., 2008. Insecticidal activity of some Asteraceae plant extracts against Tribolium confusum. Bull. Insectology 61, 283–289.

Campolo, O., Giunti, G., Russo, A., Palmeri, V., Zappalà, L., 2018. Essential Oils in Stored Product Insect Pest Control. J. Food Qual. 2018, 1–18. https://doi.org/10.1155/2018/6906105

Campos, E., Branquinho, J., Carreira, A.S., Carvalho, A., Coimbra, P., Ferreira, P., Gil, M.H., 2013. Designing polymeric microparticles for biomedical and industrial applications. Eur. Polym. J. 49, 2005–2021. https://doi.org/10.1016/j.eurpolymj.2013.04.033

Campos, E.V.R., de Oliveira, J.L., Fraceto, L.F., Singh, B., 2015. Polysaccharides as safer release systems for agrochemicals. Agron. Sustain. Dev. 35, 47–66. https://doi.org/10.1007/s13593-014-0263-0

Campos, E.V.R., Proença, P.L.F., Oliveira, J.L., Melville, C.C., Della Vechia, J.F., de Andrade, D.J., Fraceto, L.F., 2018. Chitosan nanoparticles functionalized with β-cyclodextrin: a promising carrier for botanical pesticides. Sci. Rep. 8, 2067. https://doi.org/10.1038/s41598-018-20602-y

Chen, G., Tao, D., 2005. An experimental study of stability of oil–water emulsion. Fuel Process. Technol. 86, 499–508. https://doi.org/10.1016/j.fuproc.2004.03.010

Christofoli, M., Costa, E.C.C., Bicalho, K.U., de Cássia Domingues, V., Peixoto, M.F., Alves, C.C.F., Araújo, W.L., de Melo Cazal, C., 2015. Insecticidal effect of nanoencapsulated essential oils from Zanthoxylum rhoifolium (Rutaceae) in Bemisia tabaci populations. Ind. Crops Prod. 70, 301–308. https://doi.org/10.1016/j.indcrop.2015.03.025

Chung, S.K., Seo, J.Y., Lim, J.H., Park, H.H., Yea, M.J., Park, H.J., 2013. Microencapsulation of Essential Oil for Insect Repellent in Food Packaging System: Microencapsulation of essential oil…. J. Food Sci. 78, E709–E714. https://doi.org/10.1111/1750-3841.12111

Côté, J.-C., Vincent, C., Son, K.-H., Bok, S.H., 2005. Persistence of insecticidal activity of novel bio-encapsulated formulations of Bacillus thuringiensis var. kurstaki against Choristoneura rosaceana [Lepidoptera: Tortricidae]. Phytoprotection 82, 73–82. https://doi.org/10.7202/706218ar

Croy, S., Kwon, G., 2006. Polymeric Micelles for Drug Delivery. Curr. Pharm. Des. 12, 4669–4684. https://doi.org/10.2174/138161206779026245

da Costa, J.T., Forim, M.R., Costa, E.S., De Souza, J.R., Mondego, J.M., Boiça Junior, A.L., 2014. Effects of different formulations of neem oil-based products on control Zabrotes subfasciatus (Boheman, 1833) (Coleoptera: Bruchidae) on beans. J. Stored Prod. Res. 56, 49–53. https://doi.org/10.1016/j.jspr.2013.10.004

de Oliveira, J.L., Campos, E.V.R., Pereira, A.E.S., Nunes, L.E.S., da Silva, C.C.L., Pasquoto, T., Lima, R., Smaniotto, G., Polanczyk, R.A., Fraceto, L.F., 2018. Geraniol Encapsulated in Chitosan/Gum Arabic Nanoparticles: A Promising System for Pest Management in Sustainable Agriculture. J. Agric. Food Chem. 66, 5325–5334. https://doi.org/10.1021/acs.jafc.8b00331

Digilio, M.C., Mancini, E., Voto, E., De Feo, V., 2008. Insecticide activity of Mediterranean essential oils. J. Plant Interact. 3, 17–23. https://doi.org/10.1080/17429140701843741

D'souza, A.A., Shegokar, R., 2016. Polyethylene glycol (PEG): a versatile polymer for pharmaceutical applications. Expert Opin. Drug Deliv. 13, 1257–1275. https://doi.org/10.1080/17425247.2016.1182485

Duarte, J.L., Amado, J.R.R., Oliveira, A.E.M.F.M., Cruz, R.A.S., Ferreira, A.M., Souto, R.N.P., Falcão, D.Q., Carvalho, J.C.T., Fernandes, C.P., 2015. Evaluation of larvicidal activity of a nanoemulsion of Rosmarinus officinalis essential oil. Rev. Bras. Farmacogn. 25, 189–192. https://doi.org/10.1016/j.bjp.2015.02.010

Ebadollahi, A., 2013. Essential oils isolated from Myrtaceae family as natural insecticides. Annu. Res. Rev. Biol. 3, 148–175.

Enan, E., 2001. Insecticidal activity of essential oils: octopaminergic sites of action. Comp. Biochem. Physiol. Part C Toxicol. Pharmacol. 130, 325–337. https://doi.org/10.1016/S1532-0456(01)00255-1

Fan, L., Li, M., Lv, Z., Sun, M., Luo, C., Lu, F., Qiu, H., 2012. Fabrication of magnetic chitosan nanoparticles grafted with β-cyclodextrin as effective adsorbents toward hydroquinol. Colloids Surf. B Biointerfaces 95, 42–49. https://doi.org/10.1016/j.colsurfb.2012.02.007

Forim, M.R., Costa, E.S., da Silva, M.F. das G.F., Fernandes, J.B., Mondego, J.M., Boiça Junior, A.L., 2013. Development of a New Method To Prepare Nano-/microparticles Loaded with Extracts of

Azadirachta indica, Their Characterization and Use in Controlling Plutella xylostella. J. Agric. Food Chem. 61, 9131–9139. https://doi.org/10.1021/jf403187y

Gabriel Paulraj, M., Ignacimuthu, S., Gandhi, M.R., Shajahan, A., Ganesan, P., Packiam, S.M., Al-Dhabi, N.A., 2017. Comparative studies of tripolyphosphate and glutaraldehyde cross-linked chitosan-botanical pesticide nanoparticles and their agricultural applications. Int. J. Biol. Macromol. 104, 1813–1819. https://doi.org/10.1016/j.ijbiomac.2017.06.043

García, M., Donadel, O.J., Ardanaz, C.E., Tonn, C.E., Sosa, M.E., 2005. Toxic and repellent effects ofBaccharis salicifolia essential oil onTribolium castaneum. Pest Manag. Sci. 61, 612–618. https://doi.org/10.1002/ps.1028

Gharib, R., Auezova, L., Charcosset, C., Greige-Gerges, H., 2017. Drug-in-cyclodextrin-in-liposomes as a carrier system for volatile essential oil components: Application to anethole. Food Chem. 218, 365–371. https://doi.org/10.1016/j.foodchem.2016.09.110

Golden, G., Quinn, E., Shaaya, E., Kostyukovsky, M., Poverenov, E., 2018. Coarse and nano emulsions for effective delivery of the natural pest control agent pulegone for stored grain protection: Coarse and nano emulsions of pulegone for insecticide use. Pest Manag. Sci. 74, 820–827. https://doi.org/10.1002/ps.4787

Gonçalves, V.L., Laranjeira, M.C.M., Fávere, V.T., Pedrosa, R.C., 2005. Effect of crosslinking agents on chitosan microspheres in controlled release of diclofenac sodium. Polímeros 15, 6–12. https://doi.org/10.1590/S0104-14282005000100005

Gupta, A., Eral, H.B., Hatton, T.A., Doyle, P.S., 2016. Nanoemulsions: formation, properties and applications. Soft Matter 12, 2826–2841. https://doi.org/10.1039/C5SM02958A

Hamdi, S.H., Hedjal-Chebheb, M., Kellouche, A., Khouja, M.L., Boudabous, A., Ben Jemâa, J.M., 2015. Management of three pests' population strains from Tunisia and Algeria using Eucalyptus essential oils. Ind. Crops Prod. 74, 551–556. https://doi.org/10.1016/j.indcrop.2015.05.072

Houghton, P.J., Ren, Y., Howes, M.-J., 2006. Acetylcholinesterase inhibitors from plants and fungi. Nat. Prod. Rep. 23, 181. https://doi.org/10.1039/b508966m

Huang, B.B., Zhang, S.F., Chen, P.H., Wu, G., 2017. Release and Degradation of Microencapsulated Spinosad and Emamectin Benzoate. Sci. Rep. 7, 10864. https://doi.org/10.1038/s41598-017-11419-2

Isman, M., 2002. Insect antifeedants. Pestic. Outlook 13, 152–157. https://doi.org/10.1039/b206507j

Jesser, E., Lorenzetti, A.S., Yeguerman, C., Murray, A.P., Domini, C., Werdin-González, J.O., 2020. Ultrasound assisted formation of essential oil nanoemulsions: Emerging alternative for Culex pipiens pipiens Say (Diptera: Culicidae) and Plodia interpunctella Hübner (Lepidoptera: Pyralidae) management. Ultrason. Sonochem. 61, 104832. https://doi.org/10.1016/j.ultsonch.2019.104832

Jones, M.-C., Leroux, J.-C., 1999. Polymeric micelles – a new generation of colloidal drug carriers. Eur. J. Pharm. Biopharm. 48, 101–111. https://doi.org/10.1016/S0939-6411(99)00039-9

Kahraman, E., Güngör, S., Özsoy, Y., 2017. Potential enhancement and targeting strategies of polymeric and lipid-based nanocarriers in dermal drug delivery. Ther. Deliv. 8, 967–985. https://doi.org/10.4155/tde-2017-0075

Kale, S.N., Deore, S.L., 2016. Emulsion Micro Emulsion and Nano Emulsion: A Review. Syst. Rev. Pharm. 8, 39–47. https://doi.org/10.5530/srp.2017.1.8

Kashyap, P.L., Xiang, X., Heiden, P., 2015. Chitosan nanoparticle based delivery systems for sustainable agriculture. Int. J. Biol. Macromol. 77, 36–51. https://doi.org/10.1016/j.ijbiomac.2015.02.039

Kaushik, P., Shakil, N.A., Kumar, J., Singh, Mukesh Kumar, Singh, Manish Kumar, Yadav, S.K., 2013. Development of controlled release formulations of thiram employing amphiphilic polymers and their bioefficacy evaluation in seed quality enhancement studies. J. Environ. Sci. Health Part B 48, 677–685. https://doi.org/10.1080/03601234.2013.778614

Khoobdel, M., Ahsaei, S.M., Farzaneh, M., 2017. Insecticidal activity of polycaprolactone nanocapsules loaded with *Rosmarinus officinalis* essential oil in *Tribolium castaneum* (Herbst): Insecticidal activity of nanocapsules. Entomol. Res. 47, 175–184. https://doi.org/10.1111/1748-5967.12212

Klinjapo, R., Krasaekoopt, W., 2018. Microencapsulation of Color and Flavor in Confectionery Products, in: Natural and Artificial Flavoring Agents and Food Dyes. Elsevier, pp. 457–494. https://doi.org/10.1016/B978-0-12-811518-3.00014-4

Komaiko, J.S., McClements, D.J., 2016. Formation of Food-Grade Nanoemulsions Using Low-Energy Preparation Methods: A Review of Available Methods: Formation of food-grade nanoemulsions…. Compr. Rev. Food Sci. Food Saf. 15, 331–352. https://doi.org/10.1111/1541-4337.12189

Kostyukovsky, M., Rafaeli, A., Gileadi, C., Demchenko, N., Shaaya, E., 2002. Activation of octopaminergic receptors by essential oil constituents isolated from aromatic plants: possible mode of action against insect pests. Pest Manag. Sci. 58, 1101–1106. https://doi.org/10.1002/ps.548

Kumar, P., Mishra, S., Malik, A., Satya, S., 2013. Preparation and characterization of Mentha×piperita oil emulsion for housefly (Musca domestica L.) control. Ind. Crops Prod. 44, 611–617. https://doi.org/10.1016/j.indcrop.2012.09.013

Laarif, A., Zarrad, K., Tayeb, W., Ayed, A., Souguirs, S., Chaieb, I., 2013. Chemical composition and Insecticidal activity of essential oils from Citrus aurantium (Rutaceae) Fruits Peels against two greenhouse insects; Spodoptera littoralis (Noctuidae) and Tuta absoluta (Gelechiidae). Adv. Agric. Sci. Eng. Res. 3, 825–30.

Lai, F., Wissing, S.A., Müller, R.H., Fadda, A.M., 2006. Artemisia arborescens L essential oil-loaded solid lipid nanoparticles for potential agricultural application: Preparation and characterization. AAPS PharmSciTech 7. https://doi.org/10.1208/pt070102

Lee, A., Schade, G.W., Holzinger, R., Goldstein, A.H., 2005. A comparison of new measurements of total monoterpene flux with improved measurements of speciated monoterpene flux. Atmospheric Chem. Phys. 5, 505–513. https://doi.org/10.5194/acp-5-505-2005

Lee, B.-H., Annis, P.C., Tumaalii, F., Choi, W.-S., 2004a. Fumigant toxicity of essential oils from the Myrtaceae family and 1,8-cineole against 3 major stored-grain insects. J. Stored Prod. Res. 40, 553–564. https://doi.org/10.1016/j.jspr.2003.09.001

Lee, B.-H., Annis, P.C., Tumaalii, F., Lee, S.-E., 2004b. Fumigant toxicity ofEucalyptus blakelyi andMelaleuca fulgens essential oils and 1,8-cineole against different development stages of the rice weevilSitophilus oryzae. Phytoparasitica 32, 498–506. https://doi.org/10.1007/BF02980444

Liang, W., Yu, A., Wang, G., Zheng, F., Jia, J., Xu, H., 2018. Chitosan-based nanoparticles of avermectin to control pine wood nematodes. Int. J. Biol. Macromol. 112, 258–263. https://doi.org/10.1016/j.ijbiomac.2018.01.174

Lima, J.K.A., Albuquerque, E.L.D., Santos, A.C.C., Oliveira, A.P., Araújo, A.P.A., Blank, A.F., Arrigoni-Blank, M. de F., Alves, P.B., Santos, D. de A., Bacci, L., 2013. Biotoxicity of some plant essential oils against the termite Nasutitermes corniger (Isoptera: Termitidae). Ind. Crops Prod. 47, 246–251. https://doi.org/10.1016/j.indcrop.2013.03.018

Linehan, V., Thorpe, S., Andrews, N., Kim, Y., Beaini, F., 2012. Food demand to 2050: opportunities for Australian agriculture, algebraic description of agrifood model. ABARES.

Lombardo, D., Kiselev, M.A., Caccamo, M.T., 2019. Smart Nanoparticles for Drug Delivery Application: Development of Versatile Nanocarrier Platforms in Biotechnology and Nanomedicine. J. Nanomater. 2019, 1–26. https://doi.org/10.1155/2019/3702518

López, A., Castro, S., Andina, M.J., Ures, X., Munguía, B., Llabot, J.M., Elder, H., Dellacassa, E., Palma, S., Domínguez, L., 2014. Insecticidal activity of microencapsulated Schinus molle essential oil. Ind. Crops Prod. 53, 209–216. https://doi.org/10.1016/j.indcrop.2013.12.038

Lu, Y., Park, K., 2013. Polymeric micelles and alternative nanonized delivery vehicles for poorly soluble drugs. Int. J. Pharm. 453, 198–214. https://doi.org/10.1016/j.ijpharm.2012.08.042

Madan, P.L., 1981. Clofibrate Microcapsules II: Effect of Wall Thickness on Release Characteristics. J. Pharm. Sci. 70, 430–433. https://doi.org/10.1002/jps.2600700422

Maji, T., Baruah, I., Dube, S., Hussain, M., 2007. Microencapsulation of Zanthoxylum limonella oil (ZLO) in glutaraldehyde crosslinked gelatin for mosquito repellent application. Bioresour. Technol. 98, 840–844. https://doi.org/10.1016/j.biortech.2006.03.005

Martín, Á., Varona, S., Navarrete, A., Cocero, M.J., 2010. Encapsulation and Co-Precipitation Processes with Supercritical Fluids:Applications with Essential Oils. Open Chem. Eng. J. 4, 31–41. https://doi.org/10.2174/1874123101004010031

McClements, D.J., 2012. Nanoemulsions versus microemulsions: terminology, differences, and similarities. Soft Matter 8, 1719–1729. https://doi.org/10.1039/C2SM06903B

McKeen, L.W., 2013. Introduction to Use of Plastics in Food Packaging, in: Plastic Films in Food Packaging. Elsevier, pp. 1–15. https://doi.org/10.1016/B978-1-4557-3112-1.00001-6

Mediouni Ben Jemâa, J., Tersim, N., Toudert, K.T., Khouja, M.L., 2012. Insecticidal activities of essential oils from leaves of Laurus nobilis L. from Tunisia, Algeria and Morocco, and comparative chemical composition. J. Stored Prod. Res. 48, 97–104. https://doi.org/10.1016/j.jspr.2011.10.003

Mora-Huertas, C.E., Fessi, H., Elaissari, A., 2010. Polymer-based nanocapsules for drug delivery. Int. J. Pharm. 385, 113–142. https://doi.org/10.1016/j.ijpharm.2009.10.018

Moretti, M.D.L., Sanna-Passino, G., Demontis, S., Bazzoni, E., 2002. Essential oil formulations useful as a new tool for insect pest control. AAPS PharmSciTech 3, 64–74. https://doi.org/10.1208/pt030213

Mossa, A.-T.H., 2016. Green Pesticides: Essential Oils as Biopesticides in Insect-pest Management. J. Environ. Sci. Technol. 9, 354–378. https://doi.org/10.3923/jest.2016.354.378

Mukherjee, S., Ray, S., Thakur, R., 2009. Solid lipid nanoparticles: A modern formulation approach in drug delivery system. Indian J. Pharm. Sci. 71, 349. https://doi.org/10.4103/0250-474X.57282

Negahban, M., Moharramipour, S., Zandi, M., Hashemi, S., 2012. Fumigant properties of nano-encapsulated essential oil from Artemisia sieberi on Tribolium castaneum. Proc 15–19.

Ogendo, J.O., Kostyukovsky, M., Ravid, U., Matasyoh, J.C., Deng, A.L., Omolo, E.O., Kariuki, S.T., Shaaya, E., 2008. Bioactivity of Ocimum gratissimum L. oil and two of its constituents against five insect pests attacking stored food products. J. Stored Prod. Res. 44, 328–334. https://doi.org/10.1016/j.jspr.2008.02.009

Oliveira, C.R., Domingues, C.E.C., de Melo, N.F.S., Roat, T.C., Malaspina, O., Jones-Costa, M., Silva-Zacarin, E.C.M., Fraceto, L.F., 2019. Nanopesticide based on botanical insecticide pyrethrum and its potential effects on honeybees. Chemosphere 236, 124282. https://doi.org/10.1016/j.chemosphere.2019.07.013

P. Ferreira, T., Haddi, K., F. T. Corrêa, R., Zapata, V.L.B., Piau, T.B., Souza, L.F.N., Santos, S.-M.G., Oliveira, E.E., Jumbo, L.O.V., Ribeiro, B.M., Grisolia, C.K., Fidelis, R.R., Maia, A.M.S., S. Aguiar, R.W., 2019. Prolonged mosquitocidal activity of Siparuna guianensis essential oil encapsulated in chitosan nanoparticles. PLoS Negl. Trop. Dis. 13, e0007624. https://doi.org/10.1371/journal.pntd.0007624

Park, C.G., Jang, M., Yoon, K.A., Kim, J., 2016. Insecticidal and acetylcholinesterase inhibitory activities of Lamiaceae plant essential oils and their major components against Drosophila suzukii (Diptera: Drosophilidae). Ind. Crops Prod. 89, 507–513. https://doi.org/10.1016/j.indcrop.2016.06.008

Pascual-Villalobos, M.J., Cantó-Tejero, M., Vallejo, R., Guirao, P., Rodríguez-Rojo, S., Cocero, M.J., 2017. Use of nanoemulsions of plant essential oils as aphid repellents. Ind. Crops Prod. 110, 45–57. https://doi.org/10.1016/j.indcrop.2017.05.019

Pascual-Villalobos, M.J., López, M.D., Castañé, C., Soler, A., Riudavets, J., 2015. Encapsulated Essential Oils as an Alternative to Insecticides in Funnel Traps. J. Econ. Entomol. 108, 2117–2120. https://doi.org/10.1093/jee/tov127

Paula, H.C.B., Sombra, F.M., Abreu, F.O.M.S., Paul, R.C.M. de, 2010. Lippia sidoides essential oil encapsulation by angico gum/chitosan nanoparticles. J. Braz. Chem. Soc. 21, 2359–2366. https://doi.org/10.1590/S0103-50532010001200025

Pavela, R., Benelli, G., Pavoni, L., Bonacucina, G., Cespi, M., Cianfaglione, K., Bajalan, I., Morshedloo, M.R., Lupidi, G., Romano, D., Canale, A., Maggi, F., 2019. Microemulsions for delivery of Apiaceae essential oils—Towards highly effective and eco-friendly mosquito larvicides? Ind. Crops Prod. 129, 631–640. https://doi.org/10.1016/j.indcrop.2018.11.073

Pereira, K., Quintela, E., da Silva, D., do Nascimento, V., da Rocha, D., Silva, J., Forim, M., Silva, F., Cazal, C., 2018. Characterization of Nanospheres Containing Zanthoxylum riedelianum Fruit Essential Oil and Their Insecticidal and Deterrent Activities against Bemisia tabaci (Hemiptera: Aleyrodidae). Molecules 23, 2052. https://doi.org/10.3390/molecules23082052

Piel, G., Evrard, B., Van Hees, T., Delattre, L., 1999. Comparison of the IV pharmacokinetics in sheep of miconazole–cyclodextrin solutions and a micellar solution. Int. J. Pharm. 180, 41–45. https://doi.org/10.1016/S0378-5173(98)00403-7

Pillmoor, J.B., Wright, K., Terry, A.S., 1993. Natural products as a source of agrochemicals and leads for chemical synthesis. Pestic. Sci. 39, 131–140. https://doi.org/10.1002/ps.2780390206

Porras-Saavedra, J., Palacios-González, E., Lartundo-Rojas, L., Garibay-Febles, V., Yáñez-Fernández, J., Hernández-Sánchez, H., Gutiérrez-López, G., Alamilla-Beltrán, L., 2015. Microstructural properties and distribution of components in microparticles obtained by spray-drying. J. Food Eng. 152, 105–112. https://doi.org/10.1016/j.jfoodeng.2014.11.014

Priestley, C.M., Williamson, E.M., Wafford, K.A., Sattelle, D.B., 2003. Thymol, a constituent of thyme essential oil, is a positive allosteric modulator of human GABA $_A$ receptors and a homo-oligomeric GABA receptor from *Drosophila melanogaster*: Thymol enhances ionotropic GABA receptor activity. Br. J. Pharmacol. 140, 1363–1372. https://doi.org/10.1038/sj.bjp.0705542

Puri, A., Loomis, K., Smith, B., Lee, J.-H., Yavlovich, A., Heldman, E., Blumenthal, R., 2009. Lipid-based nanoparticles as pharmaceutical drug carriers: from concepts to clinic. Crit. Rev. Ther. Drug Carrier Syst. 26, 523–580. https://doi.org/10.1615/critrevtherdrugcarriersyst.v26.i6.10

Rai, M., Ingle, A., 2012. Role of nanotechnology in agriculture with special reference to management of insect pests. Appl. Microbiol. Biotechnol. 94, 287–293. https://doi.org/10.1007/s00253-012-3969-4

Rana, V., Sharma, R., 2019. Recent Advances in Development of Nano Drug Delivery, in: Applications of Targeted Nano Drugs and Delivery Systems. Elsevier, pp. 93–131. https://doi.org/10.1016/B978-0-12-814029-1.00005-3

Re, L., Barocci, S., Sonnino, S., Mencarelli, A., Vivani, C., Paolucci, G., Scarpantonio, A., Rinaldi, L., Mosca, E., 2000. Linalool modifies the nicotinic receptor–ion channel kinetics at the mouse neuromuscular junction. Pharmacol. Res. 42, 177–181. https://doi.org/10.1006/phrs.2000.0671

Reiss, H., 1975. Entropy-induced dispersion of bulk liquids. J. Colloid Interface Sci. 53, 61–70. https://doi.org/10.1016/0021-9797(75)90035-1

Rice, P.J., Coats, J.R., 1994. Insecticidal Properties of Several Monoterpenoids to the House Fly (Diptera: Muscidae), Red Flour Beetle (Coleoptera: Tenebrionidae), and Southern Corn Rootworm (Coleoptera: Chrysomelidae). J. Econ. Entomol. 87, 1172–1179. https://doi.org/10.1093/jee/87.5.1172

Ryan, C., Alcock, E., Buttimer, F., Schmidt, M., Clarke, D., Pemble, M., Bardosova, M., 2017. Synthesis and characterisation of cross-linked chitosan composites functionalised with silver and gold

nanoparticles for antimicrobial applications. Sci. Technol. Adv. Mater. 18, 528–540. https://doi.org/10.1080/14686996.2017.1344929

Sakulku, U., Nuchuchua, O., Uawongyart, N., Puttipipatkhachorn, S., Soottitantawat, A., Ruktanonchai, U., 2009. Characterization and mosquito repellent activity of citronella oil nanoemulsion. Int. J. Pharm. 372, 105–111. https://doi.org/10.1016/j.ijpharm.2008.12.029

Sankar, M., Abideen, S., 2015. Pesticidal effect of Green synthesized silver and lead nanoparticles using Avicennia marina against grain storage pest Sitophilus oryzae. International Journal of Nanomaterials and Biostructures 5, 32–39.

Sebaaly, C., Jraij, A., Fessi, H., Charcosset, C., Greige-Gerges, H., 2015. Preparation and characterization of clove essential oil-loaded liposomes. Food Chem. 178, 52–62. https://doi.org/10.1016/j.foodchem.2015.01.067

Shah, M., Agrawal, Y., Garala, K., Ramkishan, A., 2012. Solid lipid nanoparticles of a water soluble drug, ciprofloxacin hydrochloride. Indian J. Pharm. Sci. 74, 434. https://doi.org/10.4103/0250-474X.108419

Sittipummongkol, K., Pechyen, C., 2018. Production, characterization and controlled release studies of biodegradable polymer microcapsules incorporating neem seed oil by spray drying. Food Packag. Shelf Life 18, 131–139. https://doi.org/10.1016/j.fpsl.2018.09.001

sobal, J., Nelson, M., 2003. Food waste. In S. H. Katz (ed.). Encyclopedia of Food and Culture, New york.

Solomon, B., Sahle, F.F., Gebre-Mariam, T., Asres, K., Neubert, R.H.H., 2012. Microencapsulation of citronella oil for mosquito-repellent application: Formulation and in vitro permeation studies. Eur. J. Pharm. Biopharm. 80, 61–66. https://doi.org/10.1016/j.ejpb.2011.08.003

Song, R., Murphy, M., Li, C., Ting, K., Soo, C., Zheng, Z., 2018. Current development of biodegradable polymeric materials for biomedical applications. Drug Des. Devel. Ther. Volume 12, 3117–3145. https://doi.org/10.2147/DDDT.S165440

Spang, E.S., Moreno, L.C., Pace, S.A., Achmon, Y., Donis-Gonzalez, I., Gosliner, W.A., Jablonski-Sheffield, M.P., Momin, M.A., Quested, T.E., Winans, K.S., Tomich, T.P., 2019. Food Loss and Waste: Measurement, Drivers, and Solutions. Annu. Rev. Environ. Resour. 44, 117–156. https://doi.org/10.1146/annurev-environ-101718-033228

Specos, M.M.M., García, J.J., Tornesello, J., Marino, P., Vecchia, M.D., Tesoriero, M.V.D., Hermida, L.G., 2010. Microencapsulated citronella oil for mosquito repellent finishing of cotton textiles. Trans. R. Soc. Trop. Med. Hyg. 104, 653–658. https://doi.org/10.1016/j.trstmh.2010.06.004

Sundararajan, B., Moola, A.K., Vivek, K., Kumari, B.D.R., 2018. Formulation of nanoemulsion from leaves essential oil of Ocimum basilicum L. and its antibacterial, antioxidant and larvicidal activities (Culex quinquefasciatus). Microb. Pathog. 125, 475–485. https://doi.org/10.1016/j.micpath.2018.10.017

Titouhi, F., Amri, M., Messaoud, C., Haouel, S., Youssfi, S., Cherif, A., Mediouni Ben Jemâa, J., 2017. Protective effects of three Artemisia essential oils against Callosobruchus maculatus and Bruchus rufimanus (Coleoptera: Chrysomelidae) and the extended side-effects on their natural enemies. J. Stored Prod. Res. 72, 11–20. https://doi.org/10.1016/j.jspr.2017.02.007

Varona, S., Kareth, S., Martín, Á., Cocero, M.J., 2010. Formulation of lavandin essential oil with biopolymers by PGSS for application as biocide in ecological agriculture. J. Supercrit. Fluids 54, 369–377. https://doi.org/10.1016/j.supflu.2010.05.019

Varona, S., Martín, Á., Cocero, M.J., 2009. Formulation of a natural biocide based on lavandin essential oil by emulsification using modified starches. Chem. Eng. Process. Process Intensif. 48, 1121–1128. https://doi.org/10.1016/j.cep.2009.03.002

Watanabe, K., Umeda, K., Kurita, Y., Takayama, C., Miyakado, M., 1990. Two insecticidal monoterpenes, telfairine and aplysiaterpenoid A, from the red alga Plocamium telfairiae: Structure elucidation, biological activity, and molecular topographical consideration by a semiempirical molecular

orbital study. Pestic. Biochem. Physiol. 37, 275–286. https://doi.org/10.1016/0048-3575(90)90134-N

Werdin González, J.O., Gutiérrez, M.M., Ferrero, A.A., Fernández Band, B., 2014. Essential oils nanoformulations for stored-product pest control – Characterization and biological properties. Chemosphere 100, 130–138. https://doi.org/10.1016/j.chemosphere.2013.11.056

Werdin González, J.O., Jesser, E.N., Yeguerman, C.A., Ferrero, A.A., Fernández Band, B., 2017. Polymer nanoparticles containing essential oils: new options for mosquito control. Environ. Sci. Pollut. Res. 24, 17006–17015. https://doi.org/10.1007/s11356-017-9327-4

Yadav, H.K.S., Almokdad, A.A., shaluf, S.I.M., Debe, M.S., 2019. Polymer-Based Nanomaterials for Drug-Delivery Carriers, in: Nanocarriers for Drug Delivery. Elsevier, pp. 531–556. https://doi.org/10.1016/B978-0-12-814033-8.00017-5

Yang, F.-L., Li, X.-G., Zhu, F., Lei, C.-L., 2009. Structural Characterization of Nanoparticles Loaded with Garlic Essential Oil and Their Insecticidal Activity against *Tribolium castaneum* (Herbst) (Coleoptera: Tenebrionidae). J. Agric. Food Chem. 57, 10156–10162. https://doi.org/10.1021/jf9023118

Yang, Y., Cheng, J., Garamus, V.M., Li, N., Zou, A., 2018. Preparation of an Environmentally Friendly Formulation of the Insecticide Nicotine Hydrochloride through Encapsulation in Chitosan/Tripolyphosphate Nanoparticles. J. Agric. Food Chem. 66, 1067–1074. https://doi.org/10.1021/acs.jafc.7b04147

Yeguerman, C., Jesser, E., Massiris, M., Delrieux, C., Murray, A.P., Werdin González, J.O., 2020. Insecticidal application of essential oils loaded polymeric nanoparticles to control German cockroach: Design, characterization and lethal/sublethal effects. Ecotoxicol. Environ. Saf. 189, 110047. https://doi.org/10.1016/j.ecoenv.2019.110047

Zahir, A., Bagavan, A., Kamaraj, C., Elango, G., Rahuman, A., 2012. Efficacy of plant-mediated synthesized silver nanoparticles against Sitophilus oryzae. Journal of Biopesticides 5, 95–102.

Zarrad, K., Hamouda, A.B., Chaieb, I., Laarif, A., Jemâa, J.M.-B., 2015. Chemical composition, fumigant and anti-acetylcholinesterase activity of the Tunisian Citrus aurantium L. essential oils. Ind. Crops Prod. 76, 121–127. https://doi.org/10.1016/j.indcrop.2015.06.039

Zhang, H., Qin, H., Li, L., Zhou, X., Wang, W., Kan, C., 2018. Preparation and Characterization of Controlled-Release Avermectin/Castor Oil-Based Polyurethane Nanoemulsions. J. Agric. Food Chem. 66, 6552–6560. https://doi.org/10.1021/acs.jafc.7b01401

Zhang, Y., Chen, W., Jing, M., Liu, S., Feng, J., Wu, H., Zhou, Y., Zhang, X., Ma, Z., 2019. Self-assembled mixed micelle loaded with natural pyrethrins as an intelligent nano-insecticide with a novel temperature-responsive release mode. Chem. Eng. J. 361, 1381–1391. https://doi.org/10.1016/j.cej.2018.10.132

Ziaee, M., Moharramipour, S., Mohsenifar, A., 2014. Toxicity of *Carum copticum* essential oil-loaded nanogel against *Sitophilus granarius* and *Tribolium confusum*. J. Appl. Entomol. 138, 763–771. https://doi.org/10.1111/jen.12133

Zuo, Z., Tam, Y.K., Diakur, J., Wiebe, L.I., 2002. Hydroxypropyl-beta-cyclodextrin-flutamide inclusion complex. II. Oral and intravenous pharmacokinetics of flutamide in the rat. J. Pharm. Pharm. Sci. Publ. Can. Soc. Pharm. Sci. Soc. Can. Sci. Pharm. 5, 292–298.

Experimental studies

Chapter 3

The effect of the chemical structure and the physicochemical properties of essential oil components on the characteristics of the selected delivery systems

Introduction

Liposomes and DCLs were recognized as effective drug delivery systems applied to preserve EO components, thereby enlarging their applications. In this chapter, we evaluated the effect of the chemical structure and the physicochemical parameters of an EO component on its incorporation and release from CLs and DCLs. This chapter is presented in the form of two articles that are published in the International Journal of Pharmaceutics. The first article focuses on the factors influencing the characteristics of EO-loaded liposomes. The second article concerns the identification of the parameters that affect the DCL encapsulation of EOs.

EOs are complex compounds formed by aromatic plants as secondary metabolites. They are a mixture of volatile components which can be classified into four groups: (i) terpenes; (ii) PPs; (iii) hydrocarbons; (iv) miscellaneous components such as sulfur- or nitrogen-containing compounds. According to the number of isoprene units, terpenes are classified into: hemiterpenes (C5), MTs (C10), sesquiterpenes (C15) and diterpenes (C20). The terpenes present in EOs are mainly sesquiterpenes and MTs (Morsy, 2017).

Several previous studies prepared and characterized EO-loaded liposomes and DCLs. However, these studies used different experimental conditions to prepare the liposome and DCL formulations (liposome preparation method, process parameters, type and concentration of PL used, presence of CHOL and its concentration, etc.). Particularly, using the ethanol injection method, trans-anethole and eugenol were loaded into CLs and DCLs composed of Lipoid S100 or Phospholipon 90H in combination with CHOL (Gharib et al., 2017; Sebaaly et al., 2015, 2016a) and nerolidol was loaded into CLs and DCLs composed of Lipoid E80 (Azzi et al., 2018). Using the thin film hydration method: Zanthoxylum tinguassuiba EO was entrapped into

DPPC liposomes (Detoni et al., 2009), Artemisia arborescens L. EO was loaded into liposomes composed of hydrogenated (Phospholipon 90H) and non-hydrogenated (Phospholipon 90) PLs (Sinico et al., 2005), carvacrol and THY were encapsulated in liposomes composed of egg phosphatidylcholine and CHOL (Liolios et al., 2009). Moreover, a few studies investigated the effect of the experimental conditions on the liposomes characteristics (Sebaaly et al., 2016b; Shaker et al., 2017). Hence, the effect of the chemical structure and the physicochemical properties of EO components on their incorporation and release from liposomes and DCLs cannot be extracted from the literature data. For that, this work was conducted to encapsulate a series of EO components (EST, EUC, ISOEUG, PUL, TER and THY) in liposomes and DCLs under the same experimental conditions. The selected EO components differ by their aqueous solubility, volatility, and hydrophobicity.

The EO-loaded liposomes and DCLs were prepared by the ethanol injection method using Lipoid S100 and CHOL as liposome membrane constituents. The size of vesicles, their morphology, the PL and CHOL incorporation rates (IR), the drug encapsulation efficiency (EE), the drug loading rate (LR), the release kinetics, and the storage stability of liposome and DCL vesicles were assessed. Their H_c values are also experimentally determined.

It was shown that several parameters control the incorporation and release of EOs from CLs and DCLs. The features of EO components promoting their incorporation in CLs were the presence of a hydroxyl group in their structure and exhibiting a low H_c as well as a low aqueous solubility value. Also, the drug release from liposomes was controlled by the liposome size and composition. Regarding DCLs, the EO components manifesting a high log P value were better loaded in the vesicles. Furthermore, the presence of a propenyl tail or a hydroxyl group in the structure of the EO component may improve its loading into DCLs. Moreover, the EE of EO

components into DCLs was shown to decrease with increasing the CHOL membrane content of vesicles. DCLs exhibiting a high EE value presented delayed drug release compared to the corresponding inclusion complex. The results obtained in these studies may allow predicting the ability of Lipoid S100-liposomes and DCLs to encapsulate an EO component based on its physicochemical properties.

The successful investigation of the parameters that control the encapsulation of EO components into CLs and DCLs allowed us to proceed further. According to the results obtained in this chapter, we predicted the degree of encapsulation of the MTs α-PIN and CAM into Lipoid S100:CHOL liposomes and DCLs based on their physicochemical properties (log P and aqueous solubility) before performing the experiments to confirm our prediction. CL and DCL vesicles may highly entrap α-PIN since it exhibits a very low aqueous solubility value and a high log P value compared to the other studied EO components. On the other hand, CAM possesses higher solubility in water and lower log P value compared to the other components. Accordingly, we supposed that it may show lower encapsulation in both CLs and DCLs.

References

Azzi, J., Auezova, L., Danjou, P.-E., Fourmentin, S., Greige-Gerges, H., 2018. First evaluation of drug-in-cyclodextrin-in-liposomes as an encapsulating system for nerolidol. Food Chem. 255, 399–404.

Detoni, C.B., Cabral-Albuquerque, E.C.M., Hohlemweger, S.V.A., Sampaio, C., Barros, T.F., Velozo, E.S., 2009. Essential oil from Zanthoxylum tingoassuiba loaded into multilamellar liposomes useful as antimicrobial agents. J. Microencapsul. 1–8.

Gharib, R., Auezova, L., Charcosset, C., Greige-Gerges, H., 2017. Drug-in-cyclodextrin-in-liposomes as a carrier system for volatile essential oil components: Application to anethole.

Liolios, C.C., Gortzi, O., Lalas, S., Tsaknis, J., Chinou, I., 2009. Liposomal incorporation of carvacrol and thymol isolated from the essential oil of Origanum dictamnus L. and in vitro antimicrobial activity. Food Chem. 112, 77–83.

Morsy, N.F.S., 2017. Chemical Structure, Quality Indices and Bioactivity of Essential Oil Constituents, in: El-Shemy, H.A. (Ed.), Active Ingredients from Aromatic and Medicinal Plants. InTech.

Sebaaly, C., Charcosset, C., Stainmesse, S., Fessi, H., Greige-Gerges, H., 2016a. Clove essential oil-in-cyclodextrin-in-liposomes in the aqueous and lyophilized states: From laboratory to large scale using a membrane contactor. Carbohydr. Polym. 138, 75–85.

Sebaaly, C., Greige-Gerges, H., Stainmesse, S., Fessi, H., Charcosset, C., 2016b. Effect of composition, hydrogenation of phospholipids and lyophilization on the characteristics of eugenol-loaded liposomes prepared by ethanol injection method. Food Biosci. 15, 1–10.

Sebaaly, C., Jraij, A., Fessi, H., Charcosset, C., Greige-Gerges, H., 2015. Preparation and characterization of clove essential oil-loaded liposomes. Food Chem. 178, 52–62.

Shaker, S., Gardouh, A., Ghorab, M., 2017. Factors affecting liposomes particle size prepared by ethanol injection method. Res. Pharm. Sci. 12, 346.

Sinico, C., De Logu, A., Lai, F., Valenti, D., Manconi, M., Loy, G., Bonsignore, L., Fadda, A.M., 2005. Liposomal incorporation of Artemisia arborescens L. essential oil and in vitro antiviral activity. Eur. J. Pharm. Biopharm. 59, 161–168.

Article 1

New findings on the incorporation of essential oil components into liposomes composed of lipoid S100 and cholesterol

Zahraa Hammoud[1,3], Riham Gharib[1], Sophie Fourmentin[2], Abdelhamid Elaissari[3], Hélène Greige-Gerges[1*]

[1]Bioactive Molecules Research Laboratory, Doctoral School of Sciences and Technologies, Faculty of Sciences, Section II, Lebanese University, Lebanon

[2]Unité de Chimie Environnementale et Interactions sur le Vivant (UCEIV, EA 4492), SFR Condorcet FR CNRS 3417, ULCO, F-59140 Dunkerque, France

[3]University Claude Bernard Lyon-1, CNRS, LAGEP-UMR 5007, F-69622 Lyon, France

International Journal of Pharmaceutics 561 (2019) 161–170

Contents lists available at ScienceDirect

International Journal of Pharmaceutics

journal homepage: www.elsevier.com/locate/ijpharm

New findings on the incorporation of essential oil components into liposomes composed of lipoid S100 and cholesterol

Zahraa Hammoud[a,c], Riham Gharib[a], Sophie Fourmentin[b], Abdelhamid Elaissari[c], Hélène Greige-Gerges[a,*]

[a] Bioactive Molecules Research Laboratory, Doctoral School of Sciences and Technologies, Faculty of Sciences, Section II, Lebanese University, Lebanon
[b] Unité de Chimie Environnementale et Interactions sur le Vivant (UCEIV, EA 4492), SFR Condorcet FR CNRS 3417, ULCO, F-59140 Dunkerque, France
[c] University Claude Bernard Lyon-1, CNRS, LAGEP-UMR 5007, F-69622 Lyon, France

ARTICLE INFO

Keywords:
Aqueous solubility
Encapsulation
Essential oil components
Henry's law constant
Liposomes
Release

ABSTRACT

The encapsulation of essential oil components into liposomes was demonstrated to improve their solubility and chemical stability. In this study, we investigated the effect of chemical structure, Henry's law constant (H_c), and aqueous solubility of essential oil components on their liposomal encapsulation. Estragole, eucalyptol, isoeugenol, pulegone, terpineol, and thymol were encapsulated in lipoid S100-liposomes using the ethanol injection method. The H_c values were determined. The incorporation in liposomes was more efficient (encapsulation efficiency > 90%) for the essential oil components exhibiting low aqueous solubility (estragole, isoeugenol, and pulegone). Moreover, efficient entrapment into vesicles (loading rate > 18%) was obtained for isoeugenol, terpineol, and thymol. This result suggests that the presence of a hydroxyl group in the structure and a low Hc value enhance the entrapment of essential oil components into liposomes. Furthermore, drug release rate from liposomes was controlled by the loading rate of essential oil components into liposomes, the size of particles, the location of essential oil components within the lipid bilayer, and the cholesterol incorporation rate of liposomes. Finally, considerable concentrations of isoeugenol, pulegone, terpineol, and thymol were retained in liposomes after 10 months with respect to the initial concentration.

1. Introduction

Essential oils are complex mixtures composed mainly of monoterpenes and phenylpropenes biosynthesized in nature by aromatic plants for their protection against various pathogens (Bakkali et al., 2008). Recently, essential oils have received remarkable attention in the food, cosmetics, and pharmaceutical industries. For instance, they are widely used as flavouring agents and food preservatives, as well as in several dosage forms including suppositories, capsules, soap, perfumes, and others (Asbahani et al., 2015). In the present study, the phenylpropenes estragole and isoeugenol, and the monoterpenes eucalyptol, pulegone, terpineol, and thymol, are chosen as models of essential oil components. These components exhibit considerable biological effects including antimicrobial, antifungal, antinociceptive, and anti-inflammatory (de Oliveira et al., 2012; de Sousa et al., 2011; Dogan et al., 2017; Kfoury et al., 2016; Melo Júnior et al., 2017; Riella et al., 2012; Wattanasatcha et al., 2012), antioxidant (Kfoury et al., 2014b), and anaesthetic (Reiner et al., 2013) activities.

The selected essential oil components differ with respect to their aqueous solubility, octanol/water partition coefficient (Log P) and Henry's law constant (H_c) values. According to the literature, log P values vary between 2.6 (Pubchem, n.d.) and 3.4 (Pubchem, n.d.) for isoeugenol and estragole, respectively (Table 1). Their aqueous solubility ranges between 178 for estragole (Yalkowsky and Dannenfelser, 1992) and 7100 mg/L for terpineol (Li and Perdue, 1995) (Table 1). In the literature, H_c values of the chosen essential oil components were estimated from the vapour pressure and aqueous solubility values at 25 °C using the vapour pressure/aqueous solubility method (US EPA, 2012). However, to the best of our knowledge, no experimental H_c values have been reported for these essential oil components.

The use of essential oil components is limited by their volatility, poor water solubility, and instability in the presence of heat, light, and oxygen (Turek and Stintzing, 2012). It was demonstrated that their encapsulation into different carrier systems including liposomes, cyclodextrins, solid lipid nanoparticles, micelles, polymer-based nanocarriers, and others could overcome these drawbacks and preserve their activities (Cristani et al., 2007; Gomes et al., 2011; Hosseini et al., 2013; Kfoury et al., 2014a,b; Lai et al., 2006; Moghimipour et al., 2013;

* Corresponding author.
E-mail addresses: greigegeorges@yahoo.com, hgreige@ul.edu.lb (H. Greige-Gerges).

https://doi.org/10.1016/j.ijpharm.2019.02.022
Received 31 October 2018; Received in revised form 13 February 2019; Accepted 13 February 2019
Available online 02 March 2019
0378-5173/ © 2019 Elsevier B.V. All rights reserved.

Table 1
The structure, log P, and aqueous solubility of the studied essential oil components.

Essential oil component	Structure	Log P	Aqueous solubility (mg/L)
Estragole	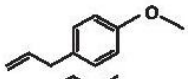	3.4 (Pubchem, n.d.)	178 (Yalkowsky and Dannenfelser, 1992)
Eucalyptol	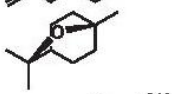	2.74 (Griffin et al., 1999)	3500 (Yalkowsky, He, and Jain, 2010)
Isoeugenol	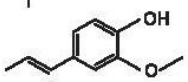	2.6 (Pubchem, n.d.)	665; 810 (HERA, 2012; Kfoury et al., 2014b)
Pulegone	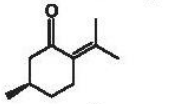	3.08 (Griffin et al., 1999)	276 (US EPA, 2012)
Terpineol	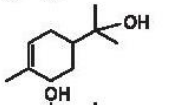	2.98 (Li and Perdue, 1995)	7100 (Li and Perdue, 1995)
Thymol	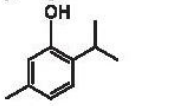	3.3 (Pubchem, n.d.)	900 (Yalkowsky and Dannenfelser, 1992)

Sebaaly et al., 2015).

Liposomes are spherical microscopic vesicles comprising a central aqueous compartment surrounded by a membrane constituted mainly of phospholipids that may contain cholesterol. They are biocompatible, biodegradable, non-immunogenic, and non-toxic (Gharib et al., 2015). Thus, liposomes are suitable for the delivery of bioactive compounds. In liposomes, hydrophobic substances can be entrapped within the lipid bilayer, hydrophilic molecules within the aqueous internal cavity, and amphiphilic structures at the water-bilayer interface (Laouini et al., 2012). It has been reported that the liposomal incorporation of essential oil components results in improving their solubility and chemical stability (Detoni et al., 2012).

The interaction of the selected essential oil components with dipalmitoylphosphatidylcholine (DPPC) membrane was studied by Raman spectroscopy, differential scanning calorimetry, and fluorescence anisotropy (Gharib et al., 2017b, 2018). The results demonstrated that the oil components exhibit a membrane fluidizing effect. Additionally, their incorporation, except in the case of eucalyptol, decreased the transition enthalpy (ΔH_m) value and increased the gauche conformers, leading to an increase in lipid bilayer disorder.

Several studies prepared essential oil component loaded liposomes and characterized them in terms of size, drug encapsulation efficiency (EE) and loading rate (LR), release kinetics, storage stability, and biological activities (Gharib et al., 2017a; Detoni et al., 2009; Coimbra et al., 2011; Sinico et al., 2005; Liolios et al., 2009; Sebaaly et al., 2015). However, few studies discussed the effect of drug properties on liposome characteristics. Zhigaltsev et al. compared the characteristics of egg sphingomyelin/cholesterol liposomes containing three structurally related vinca alkaloids (vincristine, vinorelbine and vinblastine) and demonstrated that the lipophilicity of a drug, determined by its log P value, influenced its loading and release kinetics from liposomes (Zhigaltsev et al., 2005).

Several methods have been employed for liposome preparation. The ethanol injection method offers several advantages compared to other methods. It is simple, a one step process, inexpensive, rapid, and avoids the use of harmful solvents as well as strong forces that may disrupt the liposomes and the entrapped molecules (Justo and Moraes, 2010). In addition, this method is reproducible and allows for the possibility to prepare small-sized vesicles (Batzri and Korn, 1973). Previous studies were conducted in our laboratory to incorporate essential oil components into liposomes (Gharib et al., 2017a; Sebaaly et al., 2015) in which several parameters, such as phospholipid concentration, cholesterol concentration, and ethanol to water ratio of the aforementioned process, were optimized (Sebaaly et al., 2016).

In the present study, liposomal formulations containing estragole, eucalyptol, isoeugenol, pulegone, terpineol, and thymol were prepared by the ethanol injection method using lipoid S100 and cholesterol as liposome constituents. The liposomal batches were characterized with respect to their size, drug encapsulation efficiency (EE), loading rate (LR), and drug release from liposomes. Phospholipids and cholesterol incorporation rates were also determined. Finally, the stability of liposomal suspensions was evaluated after 10 months of storage at 4 °C. The effects of the physiochemical properties of essential oil components, including their H_c and aqueous solubility values, the presence of hydroxyl groups in the structure and the final liposomal compositions (phospholipid: cholesterol: drug molar ratio) on liposome characteristics were discussed. This is the first study that includes a series of components and estimates the factors that modulate their liposomal encapsulation and release.

2. Materials and methods

2.1. Materials

Non-hydrogenated soybean phosphatidylcholine lipoid S100 (94% soybean phosphatidylcholine, 3% lysophosphatidylcholine, 0.5% N-acyl-phosphatidylethanolamine, 0.1% phosphatidylethanolamine, 0.1% phosphatidylinositol, 2% water, 0.2% ethanol) was supplied by lipoid GmBh, Germany. 4-Amino-3-hydroxy-1-naphthalenesulfonic acid was purchased from Fluka, India and hydrogen peroxide from Fisher Scientific, UK. Cholesterol (94%) was purchased from Sigma-Aldrich, Japan; ammonium molybdate, eugenol, isoeugenol, potassium dihydrogenophosphate and thymol from Sigma-Aldrich, Germany; pulegone and terpineol from Sigma- Aldrich, Switzerland; estragole from Sigma-Aldrich, China; eucalyptol and triton X-100 from Sigma–Aldrich, USA; and methanol HPLC grade from Sigma-Aldrich, France. Absolute ethanol and sulfuric acid were purchased from VWR Pro-labo chemicals, France. Cholesterol assay kit was purchased from Spin react Company, Spain.

2.2. Preparation of liposomes

Ethanol injection method was applied to prepare the liposomal formulations. The required amounts of lipoid S100 (10 mg/ml) and cholesterol (5 mg/ml) were dissolved in absolute ethanol. 10 ml of the obtained organic phase was later injected using a syringe pump (Fortuna optima, GmbH-Germany) into 20 ml aqueous phase at a flow rate of 1 ml/min, under magnetic stirring at 400 rpm at room temperature. As soon as the organic phase was in contact with the aqueous phase, spontaneous liposomes formation occurred. The liposomal suspensions were then kept for 15 min under stirring (400 rpm) at room temperature. Finally, ethanol was removed by rotary evaporation (Heidolph instruments GmbH and co., Germany) at 41 °C and 60 rpm under reduced pressure. Both blank liposomes and drug loaded liposomes were formed in which the essential oil component (estragole, eucalyptol, isoeugenol, pulegone, terpineol or thymol) was added to the organic phase at a concentration of 2.5 mg/mL. Each of the batches was prepared in triplicate. The liposomal formulations were stored at 4 °C prior to analysis.

2.3. Characterization of liposomal formulations

2.3.1. Measurement of liposome particle size

The particle size of liposomes was determined by a laser

granulometer (Partica Laser scattering, LA-950V2 particle size distribution analyser; HORIBA, Japan) designed for measuring particle sizes between 0.01 and 3000 µm. The liposomal particle size and the percentage of each population in the suspension were measured, and data were expressed as the mean ± standard deviation.

2.3.2. Morphological characterization by scanning electron microscopy

The liposomal suspensions were subjected to centrifugation at 15,000 rpm and 4 °C for 1 h. The pellets were collected and dried at room temperature. The powders were sputtered with gold, in a Cressington 108 auto sputter coater (Watford, UK), for 20 s using a current of 25 mA/mbar. The samples were imaged using a scanning electron microscope (SEM, AIS2100C, Seron Technology, Korea).

2.3.3. Determination of phospholipid: cholesterol: drug molar ratio in the formulations

The liposomal suspension was centrifuged at 15,000 rpm and 4 °C for 1 h using a Vivaspin 500 centrifugal concentrator (Sartorius Stedim Biotech, Germany, MW cut off = 10,000 Da) to separate the un-retained components from the retained ones. Aliquots were removed from liposomal suspensions, then sonicated for 10 min in ice to determine the total concentration of liposomal constituents (phospholipids, cholesterol, and drugs). Aliquots were also removed from the filtrate to determine the free concentration of liposomal constituents. For each formulation, the phospholipids: cholesterol: drug molar ratio was later calculated.

2.3.3.1. Assay of phospholipids. The phospholipids concentration in the liposomal suspension and the liposomal filtrate was quantified through Bartlett's method. The organic phosphates in the samples (500 µL from filtrate, liposomal suspension, and standard solution of phosphorus) were digested by the addition of 400 µL sulfuric acid (5 M) at 200 °C for 1 h. Then, the organic phosphates were oxidized to inorganic phosphates by incubating the samples in the presence of 100 µL H_2O_2 (30%) for 30 min at 200 °C. The phosphomolybdic complex was formed through interaction with ammonium molybdite (4.6 ml). The complex was reduced to a blue product upon interaction with 4-amino-3-hydroxy-1-naphthalenesulfonic acid (200 µL) at 100 °C for 15 min and the absorbance of this blue compound was later measured at 815 nm using a UV–vis spectrophotometer (U-2900, Hitachi High-Tech Science Corporation, Japan). Stock solution of potassium dihydrogenophosphate was prepared in ultrapure water at a concentration of 3.2 mM and diluted to obtain final concentrations of phosphorus ranging from 0.016 to 0.416 mM. The corresponding absorbance against the concentration of phosphorus was plotted. The phospholipids incorporation rate (IR %) was calculated as follows

$$IR_{PO_4^{3-}}(\%) = \frac{m_{PO_4^{3-}\_T} - m_{PO_4^{3-}\_F}}{m_{PO_4^{3-}\ \text{organic phase}}} \times 100 \quad (1)$$

in which $m_{PO_4^{3-}\_T}$ is the mass of phospholipids in the liposomal suspension, $m_{PO_4^{3-}\_F}$ is the mass of phospholipids in the liposomal filtrate and $m_{PO_4^{3-}\_organicphase}$ is the initial mass of phospholipids added to the organic phase during liposomes preparation.

2.3.3.2. Dosage of cholesterol. For quantifying the total and free concentrations of cholesterol in a suspension, the enzymatic colorimetric method was utilized. 1 ml of the cholesterol assay kit containing cholesterol esterase, cholesterol oxidase, peroxidase, and 4-aminophenazone, was added to the samples (10 µL of cholesterol standards, filtrate and liposomal suspension). Cholesterol in the samples was oxidized by cholesterol oxidase into 4-cholestenona and hydrogen peroxide. The latter reacts with 4-aminophenazone in the presence of peroxidase to form a coloured complex, quinonimine, having a colour intensity proportional to cholesterol concentration in the sample. The absorbance of the compound was measured at 505 nm using a UV–vis spectrophotometer (U-2900, Hitachi High-Tech Science Corporation, Japan). Cholesterol stock solution was prepared in triton X-100 at a concentration of 2 mg/ml then diluted to obtain concentrations ranging between 0.05 and 2 mg/ml. The cholesterol incorporation rate IR (%) was determined based on the following equation:

$$IR_{CHO}(\%) = \frac{m_{CHO_T} - m_{CHO_F}}{m_{CHO_{organic\ phase}}} \times 100 \quad (2)$$

where m_{CHO_T} is the cholesterol mass in the liposomal suspension, m_{CHO_F} is the mass of cholesterol in the filtrate and $m_{CHO_{organicphase}}$ is the initial mass of cholesterol added to the organic phase during liposomal preparation.

2.3.3.3. Determination of drug encapsulation efficiency and loading rate. The EE (%) and LR (%) values of the selected essential oil components were calculated after HPLC analysis of the samples. The analysis was performed using an analytic column (C 18: 15 cm × 4.6 mm (Agilent)) at 204 nm. Methanol and water mixture (70:30) was used as mobile phase for all samples except for pulegone (65:35). The flow rate was set at 1 ml/min. The injection volume was 20 µL.

The drugs stock solutions were prepared in methanol at a concentration of 1 mg/ml and then diluted to desired concentrations. Linearity was proved between 1 and 250 µg/mL for estragole, 50–1000 µg/mL for eucalyptol, 0.2–100 µg/mL for isoeugenol and thymol, 2.5–100 µg/mL for pulegone, and 1–100 µg/mL for terpineol. Besides, stock solutions (1 mg/ml) of the internal standards were prepared in methanol and diluted to desired concentrations. Thymol (100 µg/ml) was used as an internal standard for the dosage of estragole and isoeugenol. Eugenol was used at a concentration of 1 µg/ml for eucalyptol dosage and at a concentration of 2 µg/ml for the dosages of pulegone, terpineol, and thymol.

100 µL of each solution (standard solution, liposomal suspension, or liposomal filtrate) was added to a solution of internal standard (100 µL) and methanol (200 µL). The EE (%) value of each formulation was calculated as follows:

$$EE(\%) = \frac{[Drug]_{total} - [Drug]_{free}}{[Drug]_{total}} \times 100 \quad (3)$$

where $[Drug]_{total}$ and $[Drug]_{free}$ correspond to the total and free drug concentrations in liposomal suspension, respectively.

Besides, the LR (%) values were calculated according to the following equation:

$$LR(\%) = \frac{m_{liposomal\ suspension} - m_{filtrate}}{m_{organic\ phase}} \times 100 \quad (4)$$

where $m_{liposomalsuspension}$ and $m_{filtrate}$ correspond to the mass of drug in the liposomal suspension (total) and the liposomal filtrate (free), respectively. $m_{organicphase}$ is the initial mass of drug added to the organic phase during liposome preparation.

2.3.4. Determination of drug loading capacity

The drug loading capacity (LC) values were calculated based on the final liposomal composition (phospholipid:cholesterol:drug molar ratio) determined as described above. They are expressed as µg of drug/mg of total organic components of liposomes:

$$LC = \frac{m_{drug}}{m_{PL} + m_{CHO} + m_{drug}} \quad (5)$$

where m_{PL}, m_{CHO}, and m_{drug} correspond to the masses of phospholipids, cholesterol, and drug loaded in liposomes, respectively.

2.3.5. In vitro drug release kinetics

The dynamic release of drugs from liposomes was studied by multiple headspace extraction (MHE) coupled to gas chromatography. 1 ml

of each drug loaded liposome sample was added to 9 ml of water in 22 ml sealed vials; the corresponding free drug (estragole and thymol at 1 ppm, isoeugenol at 200 ppm, terpineol at 5 ppm, pulegone at 2 ppm, and eucalyptol at 0.5 ppm) was also introduced in 22 ml sealed vials. After equilibrium, vials were submitted to 30 successive gas extractions at constant time interval (8 min). The oven temperature of headspace was set at 60 °C, transfer line temperature at 250 °C and nitrogen was used as carrier gas. 1 ml of the vapour present in the gaseous phase was then transferred to gas chromatography (GC) for analysis. All measurements were conducted using an Agilent G1888 headspace sampler coupled to a Perkin Elmer Autosystem XL gas chromatography equipped with a flame ionization detector and a DB624 column. GC conditions were set as follows: GC cycle of 8 min and column temperature of 160 °C for estragole, eucalyptol, terpineol, pulegone, and thymol and of 180 °C for isoeugenol. The percentage of essential oil component remaining at time t was calculated as follows:

$$\textit{Percentage of remaining essential oil component} = \frac{A_t}{A_1} \times 100 \quad (6)$$

where A_t and A_1 correspond to the area of the chromatographic peak of studied essential oil component at time t and at the first extraction, respectively.

2.3.6. Study of liposome storage stability

After 10 months of storage at 4 °C, the hydrodynamic particle sizes of the liposomal formulations were measured by laser granulometry technique. The free and encapsulated concentration of each essential oil component in liposomal suspension was assessed after 10 months by HPLC analysis and compared to those obtained immediately after preparation.

2.4. Determination of Henry's law constant

Henry's law constant (H_c) is the vapor-liquid partition coefficient of a volatile compound. H_c could be determined by static headspace–gas chromatography (SH-GC). The dimensionless H_c is expressed as follows (Kolb and Ettre, 2006):

$$H_C = \frac{C_G}{C_L} \quad (7)$$

where C_G and C_L correspond to the concentration of drug in the vapour and aqueous phases, respectively.

For the determination of H_c in water, several headspace vials were prepared containing different amounts of water (0.5, 0.6, 1, 2, 3, and 5 ml for estragole, pulegone, eucalyptol and 0.1, 0.2, 0.3, 0.4, 0.5, and 0.6 ml for thymol, isoeugenol, and terpineol). Then, the same amount of drug was added to these vials (10 µL from a standard solution of 10,000 ppm). The headspace settings were as follows: an oven temperature of 30 or 60 °C and an equilibrium time of 30 min. The transfer line temperature was set at 250 °C. The GC settings were the same as described above.

Using the phase ratio variation (PRV) method described by Kolb and Ettre (2006), the values of H_C were determined by the relationship between the reciprocal chromatographic peak areas and the vapor–liquid volumetric ratio (V_G/V_L, with V_G and V_L being the vapor volume and the liquid volume, respectively):

$$\frac{1}{AV_L} = \frac{1}{\alpha}\frac{V_G}{V_L} + \frac{1}{\alpha H_C} \quad (8)$$

where A is the peak area, α is a constant incorporating several parameters and H_C is the vapor-liquid partition coefficient, directly calculated from the ratio of the slope and intercept of the fit of the experimental data.

Table 2
Estimated and experimental Henry's law constants (dimensionless) of the selected essential oil components at 30 and 60 °C.

Drug	Henry's law constant (25 °C)	Henry's law constant (30 °C)	Henry's law constant (60 °C)
Estragole	0.019[a]	0.03	0.07
Eucalyptol	0.004[a]	0.01	0.05
Isoeugenol	0.0001[b]	0.005	0.008
Pulegone	0.002[a]	0.005	0.009
Terpineol	0.0001[c]	0.001	0.003
Thymol	0.0001[a]	0.003	0.009

[a] (US EPA, 2012).
[b] (US EPA, 2011).
[c] (Copolovici and Niinemets, 2005).

2.5. Statistical analysis

Statistical analysis was carried out using the two samples student's *t*-test. All assays were performed in triplicate, and the results are expressed as the mean value ± standard deviation. P values equal to or less than 0.05 were considered significant.

3. Results and discussion

3.1. Henry's law constants of the studied essential oil components

H_c values of the selected essential oil components were determined by the PRV method, and the results are listed in Table 2. We can observe that H_c values increase upon increasing temperature from 30 to 60 °C. Thus, increasing temperature led to more essential oil components in the gaseous phase. This is in agreement with the Copolovici study, which demonstrated a strong influence of temperature on the H_c value of each of the ten plant monoterpenes studied, including terpineol, within the temperature range from 25 to 50 °C (Copolovici and Niinemets, 2005). Furthermore, the H_c values of estragole and eucalyptol were approximately 10 times greater than those of isoeugenol, pulegone, terpineol, and thymol at 30 and 60 °C. Finally, we could notice that the experimental H_c values determined in our study at 30 °C are in good agreement with the predicted H_c values found in the literature: an R^2 coefficient of 0.98 was obtained when plotting the experimental H_c values versus the predicted H_c values (Fig. S1).

3.2. Determination of phospholipid: cholesterol: drug molar ratio

3.2.1. Phospholipids

The total and free phospholipid concentrations in liposomal suspension were assessed through Bartlett's method, and the incorporation rate (IR) values were calculated according to Eq. (1). The results are summarized in Table 3. A standard curve was constructed by plotting the corresponding absorbance against the concentration of phosphorus in mM. The linear relationships were evaluated by regression analysis with the least squares method, and the correlation coefficient was found to be 0.99.

For blank liposomes, the phospholipid IR value was high (94.2 ± 6.45%), indicating that a small loss of phospholipids occurred during liposome preparation. The studied components exert different effects on the incorporation of phospholipids in the liposome membrane. Compared to the initial phospholipid: cholesterol: drug molar ratio, it is obvious that the additions of estragole, eucalyptol, and terpineol did not greatly influence the loading of phospholipids into liposomes. However, the presence of isoeugenol, pulegone, and thymol significantly reduced phospholipid retention in liposomes, and their effect decreased in the order of pulegone > thymol > isoeugenol. Hence, isoeugenol, pulegone, and thymol replaced phospholipid molecules in the lipid bilayer.

Table 3
Phospholipid and cholesterol incorporation rates (IR), drug encapsulation efficiency (EE), drug loading rate (LR), phospholipid:cholesterol:drug molar ratio and loading capacity for the various essential oil component-loaded liposomes.

Liposomal formulation	Liposomal components				Pho:CHO:drug molar ratio	Loading capacity (μg of drug /mg of total organic components)
	IR (%) of Phospholipids (pho)	IR (%) of Cholesterol (CHO)	EE (%) of essential oil components	LR (%) of essential oil components		
Blank liposome	94.2 ± 6.45	77.6 ± 1.18	–	–	125:129:0 **118:95:0**	–
Drug loaded liposomes						
Estragole	98.1 ± 0.85	84.8 ± 2.78*	90.9 ± 0.74	1.12 ± 0.28	125:129:168 **113:110:2**	2.2
Eucalyptol	88.3 ± 0.63	44.4 ± 1.69*	61.9 ± 7.05	4.99 ± 0.07	125:129:162 **111:57:8**	11.1
Isoeugenol	68.5 ± 8.85*	50.4 ± 3.39*	96.4 ± 3.25	19.86 ± 2.16	125:129:152 **96:73:30**	44.6
Pulegone	72.2 ± 5.52*	39.6 ± 5.09*	90.5 ± 0.32	2.91 ± 0.32	125:129:164 **90:51:5**	8.3
Terpineol	85.4 ± 4.36	95.2 ± 4.41*	73.7 ± 4.13	18.67 ± 0.62	125:129:162 **107:116:30**	34.5
Thymol	81.3 ± 2.55*	68.4 ± 5.09*	79.1 ± 3.86	20.54 ± 1.89	125:129:166 **94:78:34**	46.1

For the Pho:CHO:drug ratio, normal font is based on the initial moles of the liposomal component used for liposome preparation, while bold is based on the liposomal components embedded in liposomes.
* $P < 0.05$ in comparison to blank liposomes.

Upon interaction with the phospholipid bilayer, some molecules cause variation of both transition temperature Tm and enthalpy difference (ΔH), acting thus as "substitution impurities" of the membrane and taking the place of lipid molecules. However, other molecules cause only Tm variation, acting thus as "interstitial impurities" by insertion among the flexible acyl chains of lipids (Cristani et al., 2007). In particular, Gharib et al. studied the interaction of several phenylpropenes and monoterpenes, including the ones selected in this study, with DPPC liposomes (Gharib et al., 2017b, 2018). As a result, it was demonstrated that the essential oil components, except eucalyptol, act as substitution impurities, taking place of lipid molecules, while eucalyptol acts as an interstitial impurity and intercalates in the bilayer. Thus, it does not affect the incorporation of phospholipids in the membrane. Moreover, it was proven that the presence of estragole induces smaller decrease in Tm and ΔH_m compared to other phenylpropenes. ΔH_m decreases significantly in the presence of estragole from the DPPC: estragole molar ratio of 100:5 in a concentration-dependent manner. As revealed by the phospholipid: cholesterol: estragole molar ratio (113:110:2) determined in our study (Table 3), the minimal incorporation of estragole could provide a logical reasoning for its weak effect on the phospholipid incorporation rate compared to the other studied components.

3.2.2. Cholesterol

Cholesterol concentration in the liposomal suspension and filtrate was determined using the enzymatic colorimetric method, and cholesterol IR values were calculated according to Eq. (2). Results are shown in Table 3. For blank liposomes, the IR of cholesterol was 77.6 ± 1.18%. Compared to empty vesicles, a significant increase in the cholesterol IR was only obtained upon the addition of estragole and terpineol to liposomes. Gharib et al. demonstrated that the selected essential oil components are able to fluidize the membrane by decreasing the phase transition temperature of DPPC vesicles (Gharib et al., 2017b, 2018). Hence, we may propose an increase in cholesterol incorporation into estragole and terpineol-loaded liposomes, with an increased membrane fluidity induced by the presence of estragole and terpineol. On the other hand, the loading of eucalyptol, isoeugenol, pulegone, and thymol into liposomes reduced cholesterol incorporation in the formulations. Hence, eucalyptol, isoeugenol, pulegone, and thymol replaced cholesterol in the lipid bilayer. Fang et al. reported that certain lipid soluble drugs compete with cholesterol molecules for the hydrophobic space in the liposomal membrane (Fang et al., 2001), thereby decreasing cholesterol incorporation in liposomes.

3.2.3. Drugs

The retention times determined by HPLC methods were 8.4 ± 0.04, 6.9 ± 0.09, 3.5 ± 0.00, 7.8 ± 0.06, 6.3 ± 0.01, and 5.6 ± 0.01 min for estragole, eucalyptol, isoeugenol, pulegone, terpineol, and thymol, respectively. The retention time of eugenol was 3.4 ± 0.00 min with all drugs, except in the case of pulegone, where it was 4.3 ± 0.00 min. This difference is due to the use of two different eluent compositions: methanol: water (65:35, v:v) for pulegone analysis and methanol: water (70:30, v:v) for other molecules. The calibration curves were constructed by plotting $\frac{AUC_{drug}}{AUC_{internal\ standard}}$ against the drug concentrations in μg/ml. The linear relationships were evaluated by regression analysis with the least squares method, and the correlation coefficient (R^2) ranged between 0.989 and 0.999. After HPLC analysis, the EE and LR values of the drugs into lipoid S100-liposomes were calculated according to Eqs. (3) and (4), respectively.

The entrapment of drugs in liposomes, determined by their LR values, varied depending on the studied essential oil components. The LR values of essential oil components bearing a hydroxyl group in their structure (isoeugenol, terpineol, and thymol) were high (> 18%), with $LR_{thymol} > LR_{isoeugenol} > LR_{terpineol}$, while the other essential oil components (estragole, eucalyptol, and pulegone) presented lower LR values (< 5%) with $LR_{eucalyptol} > LR_{pulegone} > LR_{estragole}$.

The better incorporation of hydroxylated drugs into liposomes might be explained by the interaction of hydroxyl groups of drugs with the membrane components of liposomes (phospholipids, cholesterol). For instance, hydrogen bonds between the hydroxyl groups of drugs and the phosphate head groups of phospholipids have been proposed in many studies; the hydroxyl group serves as a hydrogen bond donor, and the phosphate head group of phospholipids acts as a hydrogen bond acceptor (Cristani et al., 2007; Phan et al., 2014). This interaction has also been described as a key factor modulating the effect of essential oil components on the lipid bilayer fluidity; essential oil components presenting a hydroxyl group in their structures more greatly fluidized the membranes than those without a hydroxyl group (Gharib et al., 2018; Reiner et al., 2013). Moreover, increasing the fluidity of the membrane promotes the incorporation of essential oil components.

On the other hand, the lower LR values of estragole and eucalyptol

into liposomes may be attributed to the greater loss of these components, which results from their higher H_c compared to the other studied components. Regarding the experimental H_c values determined at 30 °C, estragole and eucalyptol exhibited higher H_c values compared to the other selected components. However, pulegone exhibited a low Hc(0.005 at 30 °C) with a low LR value (2.91 ± 0.32%). Hence, exhibiting a high H_c value could be a factor that reduces the liposomal incorporation of essential oil components, although other factors could also affect this retention.

Concerning drug EE in liposomes, the results differed. Incorporation in liposomes was better for essential oil components exhibiting lower aqueous solubility. Very high EE values (> 90%) into liposomes were obtained for estragole, isoeugenol, and pulegone (Table 3), with aqueous solubility of 178, 665 and 276 mg/L, respectively. However, eucalyptol, terpineol, and thymol, with aqueous solubility of 3500, 7100, and 900 mg/L, respectively, exhibited lower EE (< 80%) values. Therefore, eucalyptol, terpineol, and thymol are better able to partition between aqueous and lipid compartments of liposomes. The correlation coefficient (R^2) between EE into liposomes and the aqueous solubility were determined equal to 0.85, with the exception of terpineol (Fig. S2). Hydrophobicity is another factor that may influence drug encapsulation in liposomes (Zhigaltsev et al., 2005). Indeed, the hydrophobicity of essential oil components, determined by their log P values, increased in the order of isoeugenol (2.376, 2.6) < eucalyptol (2.74) < terpineol (2.98) < pulegone (3.08) < estragole (3.13, 3.4) ~ thymol (3.34). Thus, our results demonstrated that the hydrophobicity of essential oil components did not influence their encapsulation into liposomes.

From the above results, bearing a hydroxyl group in the chemical structure of essential oil components, exhibiting low aqueous solubility and low H_c value are the main parameters that improve the liposomal encapsulation of essential oil components, as evidenced by the high EE and LR values.

3.3. Loading capacity of drugs

The LC values of the essential oil components were calculated based on the final liposomal compositions (phospholipid: cholesterol: drug molar ratio) presented in Table 3. They are expressed as µg of drug/mg of total organic components of liposomes (Table 3). The LC values differ among the selected drugs. Isoeugenol, terpineol, and thymol exhibited high LC values into liposomes (> 30 µg of drug/mg of total organic components) in the order $LC_{thymol} > LC_{isoeugenol} > LC_{terpineol}$. However, estragole, eucalyptol, and pulegone presented lower LC values (< 15 µg of drug /mg of total organic components); their LC values decreased in the order $LC_{eucalyptol} > LC_{pulegone} > LC_{estragole}$. As expected, the drugs follow the same order for LC values and LR values.

3.4. Liposomal particle size measurement

The particle size distributions of the liposomal batches were measured using laser granulometry for the various batches. Table 4 represents the number, percentage distribution, and the mean particle size of the populations obtained in each formulation. For blank liposomes, a single micrometric sized (6.16 ± 0.51 µm) population appeared. Thus, larger vesicles were obtained in comparison to the literature. This difference can be ascribed to the mechanism by which vesicles are formed during the selected method (Lasic, 1988). During ethanol diffusion into the water phase, phospholipids dissolved in the organic phase precipitate at the water/organic boundary phase, forming bi-layered phospholipid fragments (BPFs). BPFs seal off to form vesicles, and the short distance between them enhances the possibility of forming larger vesicles by facilitating their coalescence probability (Yang et al., 2012). Moreover, the difference in blank liposome particle size compared to the literature could be related to the different methods used for size characterization. Indeed, some are determined using a dynamic light scattering (DLS) apparatus which allows measurement of only submicron size range populations (Storti and Balsamo, 2010). However, the laser granulometry technique used in this study is designed for measuring particle sizes between 0.01 and 3000 µm.

Eucalyptol- and pulegone-loaded liposomes were the most similar to blank liposomes, in which one micrometric sized population appeared. However, the presence of the other essential oil components induced an increase in the population number. For isoeugenol and thymol-loaded liposomes, two micrometric sized populations appeared. For estragole and terpineol-loaded liposomes, three populations arose; one of nanometric and two of micrometric sizes (Table 4).

Various effects on particle size were observed upon adding the selected essential oil components (Table 4). In comparison to blank formulations, the additions of estragole and terpineol promoted the production of nanometric batches. On the other hand, the incorporation of estragole, isoeugenol, terpineol, and thymol boosted the formation of larger vesicles (and accordingly reduced the percentage of smaller micrometric vesicles) compared to blank liposomes. This result might be because the accumulation of lipophilic drugs in the hydrophobic part of the membrane affects the interactions between the acyl chains of phospholipids and induces swelling of the membrane, leading to the formation of larger vesicles (Sikkema et al., 1995). Moreover, large particles could result from aggregation/fusion of smaller particles (Domazou and Luigi Luisi, 2002).

In addition, the mean particle sizes of estragole, eucalyptol, pulegone, and terpineol-loaded liposomes did not significantly differ from that of blank batches; the sizes of the major populations obtained were close to the size of blank liposomes. However, the encapsulation of the phenolic components, isoeugenol and thymol, in liposomes increased liposome particle size: the sizes of the major populations (70.76 ± 5.65 and 27.7 ± 5.89 µm for isoeugenol and thymol, respectively) were significantly greater than that of blank liposome (6.16 ± 0.51 µm). To explain whether the large vesicles were aggregates of smaller particles, SEM imaging was performed on dried suspensions.

3.5. Morphological study

Dried liposome vesicles were imaged by SEM. Fig. 1(A–F) presents examples of SEM images for estragole-, eucalyptol-, isoeugenol-, pulegone-, terpineol-, and thymol-loaded liposomes, respectively.

The SEM images demonstrated that the dried vesicles had a smooth surface and a spherical shape with a micrometric size. Estragole-, eucalyptol- and pulegone-loaded liposomes did not demonstrate aggregation. However, isoeugenol-, terpineol-, and thymol-loaded liposomes showed aggregates or fused structures. The SEM results explained the different size distributions determined by granulometry and did not deny the aggregation process, in particular for the compounds bearing a hydroxyl group.

3.6. Drug release study

The drug release experiments were conducted at 60 °C using the MHE method. Fig. 2 depicts, at each extraction step, the remaining percentage of essential oil components as free molecules or when encapsulated in liposomes.

Several studies demonstrated that high temperatures decrease the stability of liposomes and, consequently, drug incorporation (Roy et al., 2016; Ullrich et al., 2013). Furthermore, at high temperatures, unsaturated phospholipids are prone to oxidation through various pathways (Shahidi and Zhong, 2010). However, different release patterns were obtained for the free essential oil components and the essential oil component-loaded liposomes (Fig. 2); therefore, drug encapsulation seems not to be greatly attenuated at 60 °C. In the presence of cholesterol and above the main transition temperature, the lipid bilayers acquire the liquid-ordered (Lo) phase. The presence of cholesterol exerts a

Table 4
Percentage distribution and mean particle size of populations for blank liposomes and drug loaded liposomes on the day of preparation and after 10 months of storage at 4 °C.

Liposomal formulations	Population 1		Population 2		Population 3	
	(%)	Mean size (μm)	(%)	Mean size (μm)	(%)	Mean size (μm)
Blank liposomes	–	–	100.0 ± 0	6.16 ± 0.51	–	–
			100.0 ± 0	*7.13 ± 1.51*		
Estragole loaded liposomes	19.3 ± 5.5	0.23 ± 0.02	64.6 ± 6.42	7.74 ± 1.04	16.0 ± 4.35	65.4 ± 13.05
	14.6 ± 3.78	*0.23 ± 0.02*	*64.0 ± 14.79*	*11.14 ± 1.81*	*21.3 ± 16.28*	*68.8 ± 17.13*
Eucalyptol loaded liposomes	–	–	100 ± 0.00	6.43 ± 0.49	–	–
			100 ± 0.00	*9.45 ± 0.64*		
Isoeugenol loaded liposomes	–	–	22.6 ± 12.42	12.12 ± 0.96	77.3 ± 12.42	70.76 ± 5.65
			13.4 ± 5.77	*16.10 ± 3.42*	*86.6 ± 5.77*	*81.08 ± 6.49*
Pulegone loaded liposomes	–	–	100 ± 0.00	6.43 ± 0.49	–	–
			17.7 ± 6.35	*16.82 ± 0.95*	*82.3 ± 6.35*	*81.08 ± 6.49*
Terpineol loaded liposomes	26.7 ± 7.09	0.24 ± 0.01	64.3 ± 9.01	7.04 ± 0.56	9.00 ± 2.64	49.23 ± 3.75
	25.5 ± 9.19	*0.23 ± 0.04*	*59.0 ± 2.82*	*7.67 ± 0.00*	*15.5 ± 12.02*	*68.14 ± 13.0*
Thymol loaded liposomes	–	–	74.0 ± 6.00	27.7 ± 5.89	26.0 ± 6.00	184 ± 27.7
			82.0 ± 7.81	*23.9 ± 1.91*	*18.0 ± 7.81*	*175 ± 23.8*

Italic: after 10 months of storage at 4 °C.

profound influence on the properties of the lipid bilayers. Cholesterol addition to a fluid phase bilayer decreases its permeability and favours encapsulation. Cholesterol molecules fill the free space that was formed due to the kink in the chain of the unsaturated lipid, leading to a decrease in the flexibility of the surrounding lipid chains (Monteiro et al., 2014). Several publications demonstrated that cholesterol incorporation within liposomes reduces the temperature effect on the membranes (Vist and Davis, 1990). Moreover, it was demonstrated that the increase of cholesterol content in membranes promotes the integrity of unsaturated liposomes (Holzschuh et al., 2018). In our study, cholesterol constitutes more than half of the final liposome membrane composition (Table 3), explaining the retention of volatile drugs at 60 °C.

In their free form, the studied essential oil components exhibited different release patterns, and the remaining percentage at the last extraction differed among the various essential oil components (Fig. 2). The latter increased in the order of estragole (74.8%) < eucalyptol (85.6%) < isoeugenol (85.9%) < thymol (91.1%) < pulegone (94.1%) < terpineol (96.8%). This order correlates with the order of H_c determined at 60 °C; the correlation coefficient R^2 was 0.89 (Fig. S3).

Moreover, when loaded in liposomes, the essential oil components displayed different release profiles. Isoeugenol and thymol manifested biphasic release patterns in which they remain unreleased for a period of time (first phase), followed by a slow release over the second phase. The other essential oil components exhibited one phase release pattern with different release rates. Terpineol and pulegone showed slow release rates, while estragole and eucalyptol showed rapid release rates. In addition, the remaining percentage at the last extraction increased in the order of estragole (78.9%) < eucalyptol (85.6%) < pulegone (94.9%) < terpineol (95.6%) < isoeugenol (96.5%) < thymol (96.4%).

Based on the above results, we could observe that the EE of essential oil components into liposomes, chemical structures of components, their aqueous solubility values, and their log P values did not seem to influence their release rates from liposomes as poor/no correlations were found between the release rate and each of the mentioned parameters. Moreover, the release of components from liposomes was not affected by their H_c, so liposomes efficiently retained them, thereby reducing their volatility.

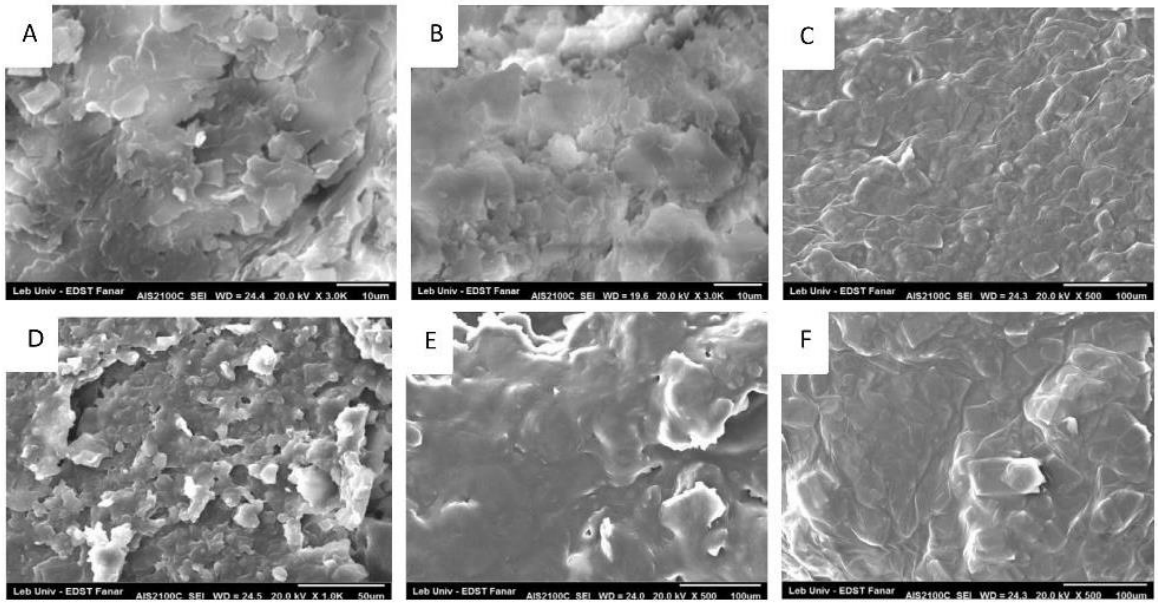

Fig. 1. SEM micrographs of liposomes containing estragole (A), eucalyptol (B), isoeugenol (C), pulegone (D), terpineol (E), and thymol (F).

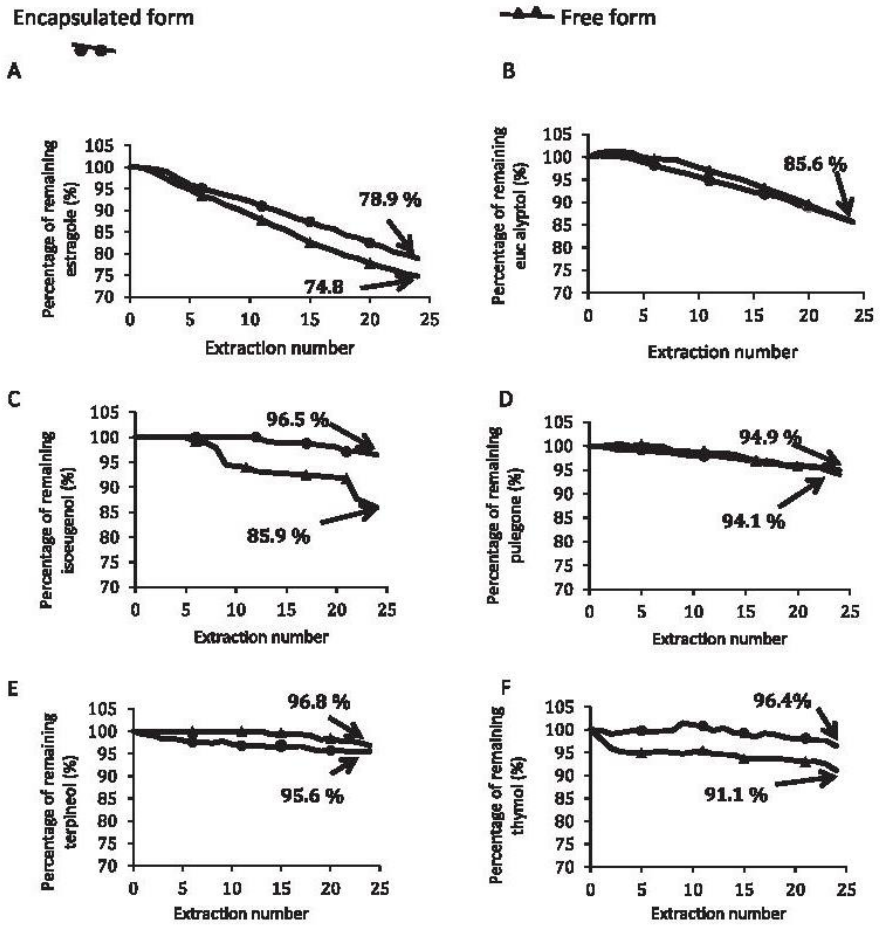

Fig. 2. The remaining percentage of various free and liposome encapsulated essential oil components after different extractions. (A) estragole; (B) eucalyptol; (C) isoeugenol; (D) pulegone; (E) terpineol; (F) thymol.

However, the LR of essential oil components into liposomes may control their release rate. A linear relationship was found between the percentage of essential oil components determined at the last extraction step and the LR of essential oil components into liposomes, except for pulegone; the R^2 value was 0.54 with pulegone, but 0.95 without pulegone (Fig. S4).

In addition, release rate results from liposomes may be attributed to the size of formulations and the location of essential oil components within the lipid bilayer (Juliano et al., 1978). Based on the results of particle size measurement (batches are of size greater than 0.5 μm) and the method of liposome preparation, it can be stated that the formulations are multi-lamellar vesicles (Jaafar-Maalej et al., 2010; Rongen et al., 1997). Additionally, the sizes of isoeugenol and thymol loaded liposomes were significantly greater than those of the other formulations. Therefore, isoeugenol and thymol may be encapsulated within the internal lamellae of liposomes and must pass several barriers before being released to the outer environment. This explains the biphasic release pattern of isoeugenol and thymol when loaded into liposomes. Moreover, regarding the location of essential oil components within the lipid bilayer, Gharib et al. studied the interactions of the selected essential oil components with DPPC liposomes and specified their locations within the bilayer (Gharib et al., 2017b, 2018). As a result, it was proven that the position of the double bond in the propenyl group of phenylpropenes controlled its incorporation into liposomes. Isoeugenol, possessing the double bond at position C7–C8 in the propenyl side chain, was inserted deeply within the bilayer in comparison to estragole. Additionally, the presence of a hydroxyl group allowed a deep bilayer incorporation of terpineol and thymol in comparison to pulegone and eucalyptol.

Pulegone exhibited a low LR value (2.91 ± 0.32%), and a previous study reported that it did not deeply incorporate into the DPPC bilayer (Gharib et al., 2018). Nevertheless, it exhibited a slow release rate (94.9% remained at the final extraction step). This could be ascribed to the lower cholesterol incorporation rate (39.6 ± 5.09%) for pulegone loaded liposomes in comparison to the other prepared vesicles. It was confirmed that the liposomal retention of floxuridine was enhanced by decreasing cholesterol content in the formulation (Tardi et al., 2007) and that idarubicin was more effectively retained in cholesterol free vesicles in comparison to those containing cholesterol (Dos Santos et al., 2002).

Hence, the size of liposomal batches, IR of cholesterol into liposomes, LR of essential oil components, and the location of components within the lipid bilayer are the primary factors that affect the release rate of essential oil components from lipoid S-100 liposomes.

3.7. Storage stability

The stability of the formulations was examined after 10 months of storage at 4 °C. All of the prepared batches, except thymol loaded liposomes, showed a significant increase in liposome particle size (Table 4). These results were similar to those obtained by Sebaaly et al., which reported that the particle size of eugenol loaded lipoid-S100

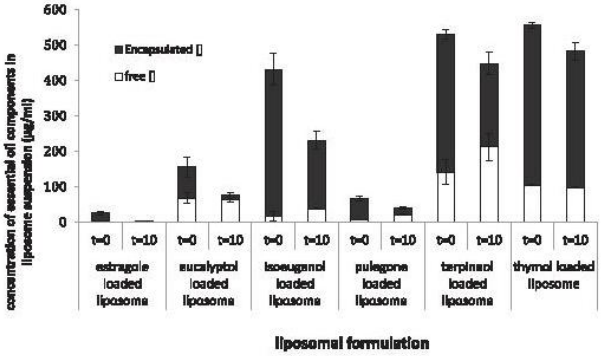

Fig. 3. Storage stability of the various prepared liposomal batches: remaining concentrations of free and encapsulated drugs in liposome suspension.

liposomes increased after 2 months of storage at 4 °C (Sebaaly et al., 2015).

For each formulation, the total and free concentrations of essential oil components in liposomal suspensions were determined on the day of preparation and after 10 months. Fig. 3 summarizes the obtained results. In general, a considerable amount of essential oil components remained in liposomal suspension in comparison to the initial amount (> 50%), except in the case of estragole loaded liposomes. In addition, with respect to the initial concentration of essential oil components incorporated into liposomes, a noticeable concentration of isoeugenol, pulegone, terpineol, and thymol remained in liposomes after 10 months. Those findings, combined with the release study in which isoeugenol, pulegone, terpineol, and thymol exhibited a delayed release, showed that these compounds were still satisfactorily incorporated into liposomes after 10 months. Thus, the encapsulation of isoeugenol, pulegone, terpineol, and thymol in lipoid S-100 liposomes is efficient for protecting them against degradation and rapid release.

4. Conclusion

Drug loaded lipoid S-100 liposomes were prepared by ethanol injection method and characterized via several techniques. The parameters affecting liposomal particle size, EE and LR, release kinetics, and liposome storage stability were discussed. The addition of the phenolic essential oil components, isoeugenol and thymol, induced an enlargement of vesicles in comparison to blank liposomes. In addition, EE values into liposomes were greater for the essential oil components exhibiting lower aqueous solubility. Regarding the LR values, the results differed. Hydroxylated essential oil components were better entrapped in liposomes than were non-hydroxylated components and the liposomal incorporation was higher for essential oil components with low Henry's law constants. Furthermore, the release profiles were variable among the various formulations. Liposome particle size, LR of essential oil components into liposomes, location of components within liposome bilayer, and IR of cholesterol into liposomes were the key parameters affecting the release of essential oil components from liposomes. Finally, liposomes loaded with isoeugenol, pulegone, terpineol, and thymol were stable after long term storage at 4 °C. Hence, liposomes could be useful for the encapsulation of essential oil components, extending their various applications. However, the factors that control their incorporation into liposomes must be considered in future studies.

Declaration of interest

None.

Acknowledgements

This research study was supported by the Research Funding Program at the Lebanese University and the "Agence Universitaire de la Francophonie, Projet de Coopération Scientifique Inter-Universitaire 2018-2021."

Appendix A. Supplementary data

Supplementary data to this article can be found online at https://doi.org/10.1016/j.ijpharm.2019.02.022.

References

Asbahani, A.E., Miladi, K., Badri, W., Sala, M., Addi, E.H.A., Casabianca, H., Mousadik, A.E., Hartmann, D., Jilale, A., Renaud, F.N.R., Elaissari, A., 2015. Essential oils: from extraction to encapsulation. Int. J. Pharm. 483, 220–243. https://doi.org/10.1016/j.ijpharm.2014.12.069.

Bakkali, F., Averbeck, S., Averbeck, D., Idaomar, M., 2008. Biological effects of essential oils–a review. Food Chem. Toxicol. 46, 446–475. https://doi.org/10.1016/j.fct.2007.09.106.

Batzri, S., Korn, E.D., 1973. Single bilayer liposomes prepared without sonication. Biochim. Biophys. Acta BBA, Biomembr. 298, 1015–1019. https://doi.org/10.1016/0005-2736(73)90408-2.

Coimbra, M., Isacchi, B., van Bloois, L., Torano, J.S., Ket, A., Wu, X., Broere, F., Metselaar, J.M., Rijcken, C.J.F., Storm, G., Bilia, R., Schiffelers, R.M., 2011. Improving solubility and chemical stability of natural compounds for medicinal use by incorporation into liposomes. Int. J. Pharm. 416, 433–442. https://doi.org/10.1016/j.ijpharm.2011.01.056.

Copolovici, L.O., Niinemets, Ü., 2005. Temperature dependencies of Henry's law constants and octanol/water partition coefficients for key plant volatile monoterpenoids. Chemosphere 61, 1390–1400. https://doi.org/10.1016/j.chemosphere.2005.05.003.

Cristani, M., D'Arrigo, M., Mandalari, G., Castelli, F., Sarpietro, M.G., Micieli, D., Venuti, V., Bisignano, G., Saija, A., Trombetta, D., 2007. Interaction of four monoterpenes contained in essential oils with model membranes: implications for their antibacterial activity. J. Agric. Food Chem. 55, 6300–6308. https://doi.org/10.1021/jf070094x.

de Oliveira, M.G.B., Marques, R.B., de Santana, M.F., Santos, A.B.D., Brito, F.A., Barreto, E.O., De Sousa, D.P., Almeida, F.R.C., Badauê-Passos, D., Antoniolli, A.R., Quintans-Júnior, L.J., 2012. α-terpineol reduces mechanical hypernociception and inflammatory response. Basic Clin. Pharmacol. Toxicol. 111, 120–125. https://doi.org/10.1111/j.1742-7843.2012.00875.x.

de Sousa, D.P., Nóbrega, F.F.F., de Lima, M.R.V., de Almeida, R.N., 2011. Pharmacological activity of (R)-(+)-pulegone, a chemical constituent of essential oils. Z. Naturforsch., C: J. Biosci. 66, 353–359.

Detoni, C.B., Cabral-Albuquerque, E.C.M., Hohlemweger, S.V.A., Sampaio, C., Barros, T.F., Velozo, E.S., 2009. Essential oil from *Zanthoxylum tingoassuiba* loaded into multilamellar liposomes useful as antimicrobial agents. J. Microencapsul. 1–8. https://doi.org/10.1080/02652040802661887.

Detoni, C.B., de Oliveira, D.M., Santo, I.E., Pedro, A.S., El-Bacha, R., da Silva Velozo, E., Ferreira, D., Sarmento, B., de Magalhães Cabral-Albuquerque, E.C., 2012. Evaluation of thermal-oxidative stability and antiglioma activity of *Zanthoxylum tingoassuiba* essential oil entrapped into multi- and unilamellar liposomes. J. Liposome Res. 22, 1–7. https://doi.org/10.3109/08982104.2011.573793.

Dogan, G., Kara, N., Bagci, E., Gur, S., 2017. Chemical composition and biological activities of leaf and fruit essential oils from *Eucalyptus camaldulensis*. Z. Naturforsch., C 72. https://doi.org/10.1515/znc-2016-0033.

Domazou, A.S., Luigi Luisi, P., 2002. Size distribution of spontaneously formed liposomes by the alcohol injection method. J. Liposome Res. 12, 205–220. https://doi.org/10.1081/LPR-120014758.

Dos Santos, N., Mayer, L.D., Abraham, S.A., Gallagher, R.C., Cox, K.A.K., Tardi, P.G., Bally, M.B., 2002. Improved retention of idarubicin after intravenous injection obtained for cholesterol-free liposomes. Biochim. Biophys. Acta BBA, Biomembr. 1561, 188–201. https://doi.org/10.1016/S0005-2736(02)00345-0.

Fang, J.Y., Hong, C.T., Chiu, W.T., Wang, Y.Y., 2001. Effect of liposomes and niosomes on skin permeation of enoxacin. Int. J. Pharm. 219, 61–72.

Gharib, R., Auezova, L., Charcosset, C., Greige-Gerges, H., 2018. Effect of a series of essential oil molecules on DPPC membrane fluidity: a biophysical study. J. Iran. Chem. Soc. 15, 75–84. https://doi.org/10.1007/s13738-017-1210-1.

Gharib, R., Auezova, L., Charcosset, C., Greige-Gerges, H., 2017a. Drug-in-cyclodextrin-in-liposomes as a carrier system for volatile essential oil components: application to anethole. Food Chem. 218, 365–371. https://doi.org/10.1016/j.foodchem.2016.09.110.

Gharib, R., Greige-Gerges, H., Fourmentin, S., Charcosset, C., Auezova, L., 2015. Liposomes incorporating cyclodextrin–drug inclusion complexes: current state of knowledge. Carbohydr. Polym. 129, 175–186. https://doi.org/10.1016/j.carbpol.2015.04.048.

Gharib, R., Najjar, A., Auezova, L., Charcosset, C., Greige-Gerges, H., 2017b. Interaction of selected phenylpropenes with dipalmitoylphosphatidylcholine membrane and their relevance to antibacterial activity. J. Membr. Biol. 250, 259–271. https://doi.org/10.1007/s00232-017-9957-y.

Gomes, C., Moreira, R.G., Castell-Perez, E., 2011. Poly (DL-lactide-co-glycolide) (PLGA)

nanoparticles with entrapped trans-cinnamaldehyde and eugenol for antimicrobial delivery applications. J. Food Sci. 76, N16–N24. https://doi.org/10.1111/j.1750-3841.2010.01985.x.
Griffin, S., Wyllie, S.G., Markham, J., 1999. Determination of octanol-water partition coefficient for terpenoids using reversed-phase high-performance liquid chromatography. J. Chromatogr. A 864, 221–228.
HERA, 2012. HERA Risk Assessment of Isoeugenol (Draft) human and environmental risk assessment on ingredients of household cleaning products. Isoeugenol (CAS 97-54-1).
Holzschuh, S., Kaeß, K., Bossa, G.V., Decker, C., Fahr, A., May, S., 2018. Investigations of the influence of liposome composition on vesicle stability and drug transfer in human plasma: a transfer study. J. Liposome Res. 28, 22–34. https://doi.org/10.1080/08982104.2016.1247101.
Hosseini, S.F., Zandi, M., Rezaei, M., Farahmandghavi, F., 2013. Two-step method for encapsulation of oregano essential oil in chitosan nanoparticles: preparation, characterization and in vitro release study. Carbohydr. Polym. 95, 50–56. https://doi.org/10.1016/j.carbpol.2013.02.031.
Jaafar-Maalej, C., Diab, R., Andrieu, V., Elaissari, A., Fessi, H., 2010. Ethanol injection method for hydrophilic and lipophilic drug-loaded liposome preparation. J. Liposome Res. 20, 228–243. https://doi.org/10.3109/08982100903347923.
Juliano, R.L., Stamp, D., McCullough, N., 1978. Pharmacokinetics of liposome-encapsulated antitumor drugs and implications for therapy. Ann. N. Y. Acad. Sci. 308, 411–425. https://doi.org/10.1111/j.1749-6632.1978.tb22038.x.
Justo, O.R., Moraes, Ã.M., 2010. Economical feasibility evaluation of an ethanol injection liposome production plant. Chem. Eng. Technol. 33, 15–20. https://doi.org/10.1002/ceat.200800502.
Kfoury, M., Auezova, L., Fourmentin, S., Greige-Gerges, H., 2014a. Investigation of monoterpenes complexation with hydroxypropyl-β-cyclodextrin. J. Incl. Phenom. Macrocycl. Chem. 80, 51–60. https://doi.org/10.1007/s10847-014-0385-7.
Kfoury, M., Landy, D., Auezova, L., Greige-Gerges, H., Fourmentin, S., 2014b. Effect of cyclodextrin complexation on phenylpropanoids' solubility and antioxidant activity. Beilstein J. Org. Chem. 10, 2322–2331. https://doi.org/10.3762/bjoc.10.241.
Kfoury, M., Lounès-Hadj Sahraoui, A., Bourdon, N., Laruelle, F., Fontaine, J., Auezova, L., Greige-Gerges, H., Fourmentin, S., 2016. Solubility, photostability and antifungal activity of phenylpropanoids encapsulated in cyclodextrins. Food Chem. 196, 518–525. https://doi.org/10.1016/j.foodchem.2015.09.078.
Kolb, B., Ettre, L.S., 2006. Static Headspace-gas Chromatography: Theory and Practice, second ed. Wiley, Hoboken, N.J.
Lai, F., Wissing, S.A., Müller, R.H., Fadda, A.M., 2006. *Artemisia arborescens* L. essential oil-loaded solid lipid nanoparticles for potential agricultural application: preparation and characterization. AAPS PharmSciTech 7. https://doi.org/10.1208/pt070102.
Laouini, A., Jaafar-Maalej, C., Limayem-Blouza, I., Sfar, S., Charcosset, C., Fessi, H., 2012. Preparation, characterization and applications of liposomes: state of the art. J. Colloid Sci. Biotechnol. 1, 147–168. https://doi.org/10.1166/jcsb.2012.1020.
Lasic, D.D., 1988. The mechanism of vesicle formation. Biochem. J. 256, 1–11. https://doi.org/10.1042/bj2560001.
Li, J., Perdue, E.M., 1995. Preprints of Papers Presented at the 209th ACS National Meeting, Anaheim, CA. pp. 134–137.
Liolios, C.C., Gortzi, O., Lalas, S., Tsaknis, J., Chinou, I., 2009. Liposomal incorporation of carvacrol and thymol isolated from the essential oil of *Origanum dictamnus* L. and in vitro antimicrobial activity. Food Chem. 112, 77–83. https://doi.org/10.1016/j.foodchem.2008.05.060.
Melo Júnior, J.de M.de A.de, Damasceno, M.de B.M.V., Santos, S.A.A.R., Barbosa, T.M., Araújo, J.R.C., Vieira-Neto, A.E., Wong, D.V.T., Lima-Júnior, R.C.P., Campos, A.R., 2017. Acute and neuropathic orofacial antinociceptive effect of eucalyptol. Inflammopharmacology 25, 247–254. https://doi.org/10.1007/s10787-017-0324-5.
Moghimipour, E., Ramezani, Z., Handali, S., 2013. Solid lipid nanoparticles as a delivery system for *Zataria multiflora* essential oil: formulation and characterization. Curr. Drug Deliv. 10, 151–157.
Monteiro, N., Martins, A., Reis, R.L., Neves, N.M., 2014. Liposomes in tissue engineering and regenerative medicine. J. R. Soc. Interface 11https://doi.org/10.1098/rsif.2014.0459. 20140459–20140459.
Phan, H.T.T., Yoda, T., Chahal, B., Morita, M., Takagi, M., Vestergaard, M.C., 2014. Structure-dependent interactions of polyphenols with a biomimetic membrane system. Biochim. Biophys. Acta BBA, Biomembr. 1838, 2670–2677. https://doi.org/10.1016/j.bbamem.2014.07.001.
Pubchem, n.d. Isoeugenol [WWW Document]. https://pubchem.ncbi.nlm.nih.gov/compound/853433 (accessed 6.22.18a).
Pubchem, n.d. Estragole [WWW Document]. https://pubchem.ncbi.nlm.nih.gov/compound/8815 (accessed 6.22.18b).
Pubchem, n.d. Thymol [WWW Document]. https://pubchem.ncbi.nlm.nih.gov/compound/6989 (accessed 6.22.18c).
Reiner, G.N., Perillo, M.A., García, D.A., 2013. Effects of propofol and other GABAergic phenols on membrane molecular organization. Colloids Surf., B 101, 61–67. https://doi.org/10.1016/j.colsurfb.2012.06.004.
Riella, K.R., Marinho, R.R., Santos, J.S., Pereira-Filho, R.N., Cardoso, J.C., Albuquerque-Junior, R.L.C., Thomazzi, S.M., 2012. Anti-inflammatory and cicatrizing activities of thymol, a monoterpene of the essential oil from *Lippia gracilis*, in rodents. J. Ethnopharmacol. 143, 656–663. https://doi.org/10.1016/j.jep.2012.07.028.
Rongen, H.A., Bult, A., van Bennekom, W., 1997. Liposomes and immunoassays. J. Immunol. Methods 204, 105–133. https://doi.org/10.1016/S0022-1759(97)00041-0.
Roy, B., Guha, P., Bhattarai, R., Nahak, P., Karmakar, G., Chettri, P., Panda, A.K., 2016. Influence of lipid composition, pH, and temperature on physicochemical properties of liposomes with curcumin as model drug. J. Oleo Sci. 65, 399–411. https://doi.org/10.5650/jos.ess15229.
Sebaaly, C., Greige-Gerges, H., Stainmesse, S., Fessi, H., Charcosset, C., 2016. Effect of composition, hydrogenation of phospholipids and lyophilization on the characteristics of eugenol-loaded liposomes prepared by ethanol injection method. Food Biosci. 15, 1–10. https://doi.org/10.1016/j.fbio.2016.04.005.
Sebaaly, C., Jraij, A., Fessi, H., Charcosset, C., Greige-Gerges, H., 2015. Preparation and characterization of clove essential oil-loaded liposomes. Food Chem. 178, 52–62. https://doi.org/10.1016/j.foodchem.2015.01.067.
Shahidi, F., Zhong, Y., 2010. Lipid oxidation and improving the oxidative stability. Chem. Soc. Rev. 39, 4067. https://doi.org/10.1039/b922183m.
Sikkema, J., de Bont, J.A., Poolman, B., 1995. Mechanisms of membrane toxicity of hydrocarbons. Microbiol. Rev. 59, 201–222.
Sinico, C., De Logu, A., Lai, F., Valenti, D., Manconi, M., Loy, G., Bonsignore, L., Fadda, A.M., 2005. Liposomal incorporation of *Artemisia arborescens* L. essential oil and in vitro antiviral activity. Eur. J. Pharm. Biopharm. 59, 161–168. https://doi.org/10.1016/j.ejpb.2004.06.005.
Storti, F., Balsamo, F., 2010. Particle size distributions by laser diffraction: sensitivity of granular matter strength to analytical operating procedures. Solid Earth 1, 25–48. https://doi.org/10.5194/se-1-25-2010.
Tardi, P.G., Gallagher, R.C., Johnstone, S., Harasym, N., Webb, M., Bally, M.B., Mayer, L.D., 2007. Coencapsulation of irinotecan and floxuridine into low cholesterol-containing liposomes that coordinate drug release in vivo. Biochim. Biophys. Acta BBA, Biomembr. 1768, 678–687. https://doi.org/10.1016/j.bbamem.2006.11.014.
Turek, C., Stintzing, F.C., 2012. Impact of different storage conditions on the quality of selected essential oils. Food Res. Int. 46, 341–353. https://doi.org/10.1016/j.foodres.2011.12.028.
Ullrich, M., Hanuš, J., Dohnal, J., Štěpánek, F., 2013. Encapsulation stability and temperature-dependent release kinetics from hydrogel-immobilised liposomes. J. Colloid Interface Sci. 394, 380–385. https://doi.org/10.1016/j.jcis.2012.11.016.
US EPA, 2012. Estimation Program Interface (EPI) Suite. Ver. 4.1.
US EPA, 2011. Estimation Program Interface (EPI) Suite. Ver. 4.1.
Vist, M.R., Davis, J.H., 1990. Phase equilibria of cholesterol/dipalmitoylphosphatidylcholine mixtures: deuterium nuclear magnetic resonance and differential scanning calorimetry. Biochemistry 29, 451–464. https://doi.org/10.1021/bi00454a021.
Wattanasatcha, A., Rengpipat, S., Wanichwecharungruang, S., 2012. Thymol nanospheres as an effective anti-bacterial agent. Int. J. Pharm. 434, 360–365. https://doi.org/10.1016/j.ijpharm.2012.06.017.
Yalkowsky, S., He, Y., Jain, P., 2010. Handbook of Aqueous Solubility Data, second ed. CRC Press 10.1201/EBK1439802458.
Yalkowsky, S.H., Dannenfelser, R.M., 1992. Aquasol Database of Aqueous Solubility. Coll. Pharm. Univ. Ariz, Tucson AZ.
Yang, K., Delaney, J.T., Schubert, U.S., Fahr, A., 2012. Fast high-throughput screening of temoporfin-loaded liposomal formulations prepared by ethanol injection method. J. Liposome Res. 22, 31–41. https://doi.org/10.3109/08982104.2011.584319.
Zhigaltsev, I.V., Maurer, N., Akhong, Q.-F., Leone, R., Leng, E., Wang, J., Semple, S.C., Cullis, P.R., 2005. Liposome-encapsulated vincristine, vinblastine and vinorelbine: a comparative study of drug loading and retention. J. Controlled Release 104, 103–111. https://doi.org/10.1016/j.jconrel.2005.01.010.

Supplementary materials

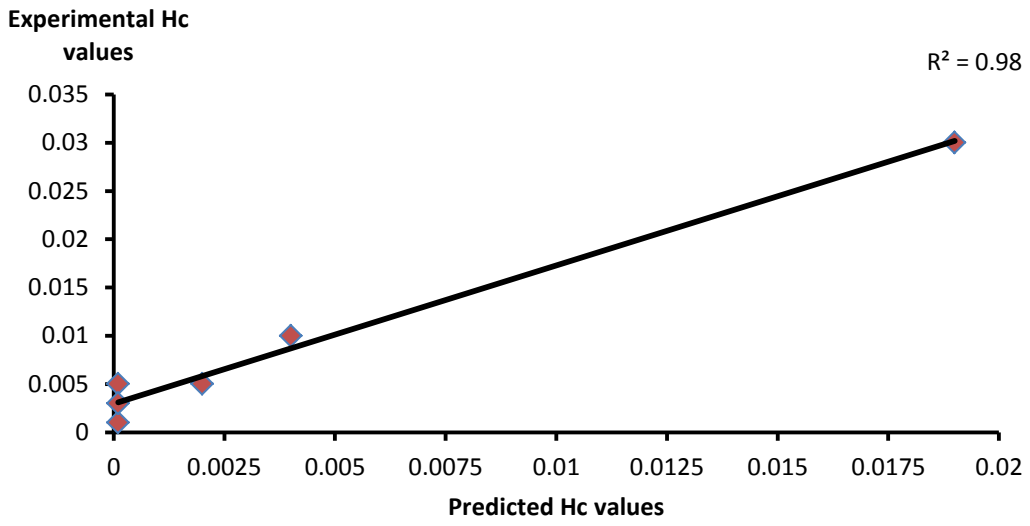

Figure S1: Experimental henry's law constant values determined at 30 ºC versus predicted henry's law constant values determined in literature

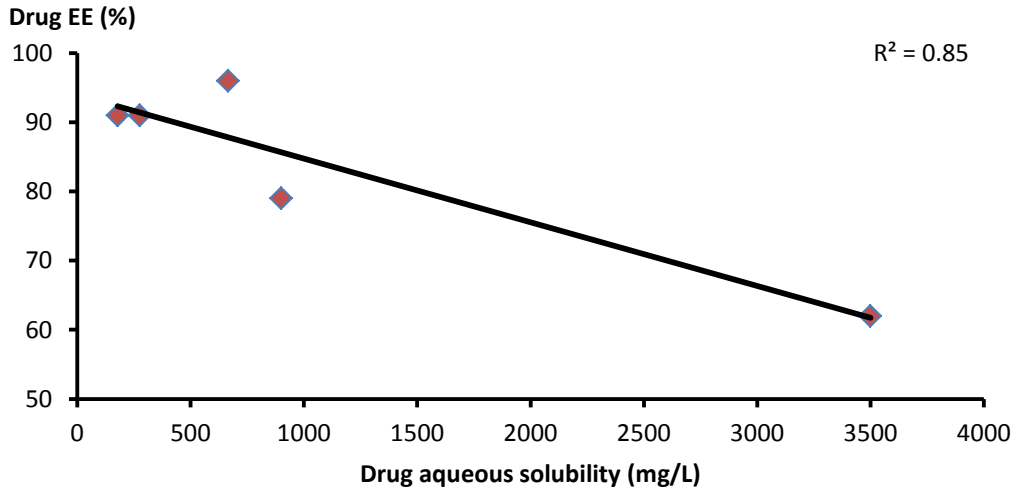

Figure S2: Drug encapsulation efficiency (EE %) versus drug aqueous solubility

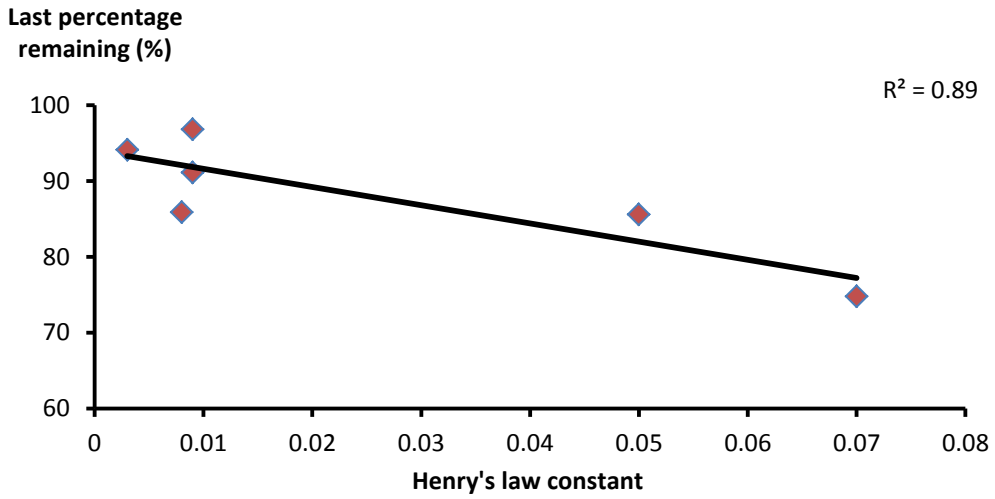

Figure S3: The remaining percentage at the last extraction for free drug versus experimental henry's law constant determined at 60 ºC

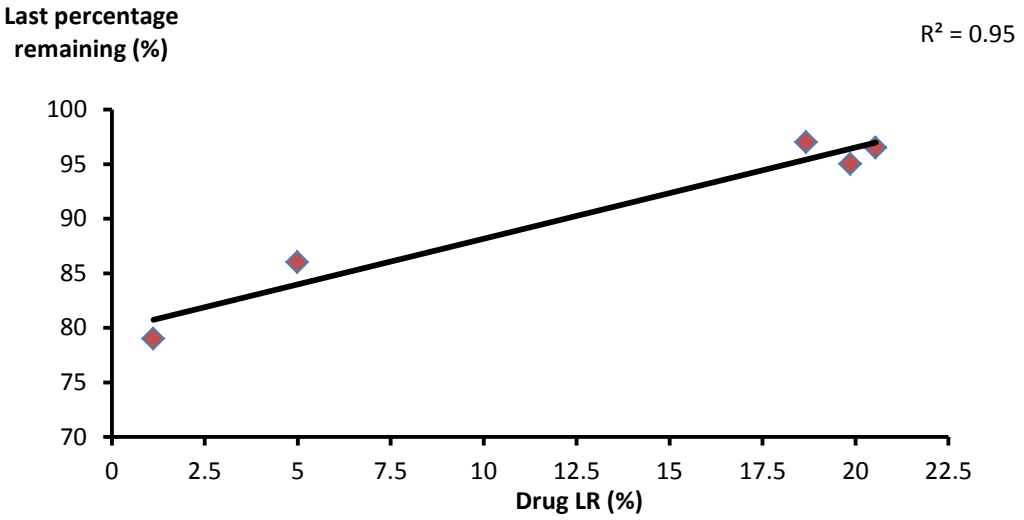

Figure S4: Percentage determined at the last extraction step for drug in liposome versus loading rate (LR) of drug into liposomes

Article 2

Drug-in-hydroxypropyl-β-cyclodextrin-in-lipoid S100/cholesterol liposomes: Effect of the characteristics of essential oil components on their encapsulation and release

Zahraa Hammoud[a,b], Riham Gharib[a], Sophie Fourmentin[c], Abdelhamid Elaissari[b], Hélène Greige-Gerges[a*]

[a]Bioactive Molecules Research Laboratory, Doctoral School of Sciences and Technologies, Faculty of Sciences, Section II, Lebanese University, Lebanon

[b]Univ Lyon, University Claude Bernard Lyon-1, CNRS, LAGEP-UMR 5007, F-69622 Lyon, France

[c]Unité de Chimie Environnementale et Interactions sur le Vivant (UCEIV, EA 4492), SFR Condorcet FR CNRS 3417, ULCO, F-59140 Dunkerque, France

International Journal of Pharmaceutics 579 (2020) 119151

Contents lists available at ScienceDirect

International Journal of Pharmaceutics

journal homepage: www.elsevier.com/locate/ijpharm

Drug-in-hydroxypropyl-β-cyclodextrin-in-lipoid S100/cholesterol liposomes: Effect of the characteristics of essential oil components on their encapsulation and release

Zahraa Hammoud[a,b], Riham Gharib[a], Sophie Fourmentin[c], Abdelhamid Elaissari[b], Hélène Greige-Gerges[a,*]

[a] Bioactive Molecules Research Laboratory, Doctoral School of Sciences and Technologies, Faculty of Sciences, Section II, Lebanese University, Lebanon
[b] Univ Lyon, University Claude Bernard Lyon-1, CNRS, LAGEP-UMR 5007, F-69622 Lyon, France
[c] Unité de Chimie Environnementale et Interactions sur le Vivant (UCEIV, EA 4492), SFR Condorcet FR CNRS 3417, ULCO, F-59140 Dunkerque, France

ARTICLE INFO

Keywords:
Drug-in-cyclodextrin-in-liposome
Encapsulation
Monoterpene
Phenylpropene
Release

ABSTRACT

Drug-in-cyclodextrin-in-liposome (DCL) represents a very promising approach for preserving essential oil (EO) components, thereby extending their shelf life and activity. In this study, we examined the effect of chemical structure, octanol/water partition coefficient (log P), and Henry's law constant (H_c) on the encapsulation and the release of monoterpenes (eucalyptol, pulegone, terpineol, and thymol) and phenylpropenes (estragole and isoeugenol) from DCLs. Hydroxypropyl-β-cyclodextrin/EO component (HP-β-CD/EO component) inclusion complexes were prepared in aqueous solution and loaded into liposomes by the ethanol injection method. The phospholipid:cholesterol:EO component molar ratio determined for DCL structures was affected by characteristics of EO components. The presence of a propenyl tail or a hydroxyl group in the structure of EO component may improve its loading into DCLs. Furthermore, low encapsulation efficiency (EE) was obtained for DCLs exhibiting high cholesterol membrane content. In addition, a positive linear relationship was found between the loading ratio of monoterpenes into DCLs and their hydrophobic character expressed as log P. The release of components from DCLs was influenced by their EE into the formulations. Finally, DCL formulations retain considerable amounts of EO components after 10 months.

1. Introduction

Essential oils (EO) are volatile and natural compounds synthesized by aromatic plants as secondary metabolites. They represent a complex mixture of primarily monoterpenes and phenylpropenes (Bakkali et al., 2008). In this study, the phenylpropenes, estragole and isoeugenol, and the monoterpenes, eucalyptol, pulegone, terpineol, and thymol, are used as models of EO components. The selected components exhibit a wide range of important biological functions including antifungal (Dogan et al., 2017; Kfoury et al., 2016b), antibacterial (Dogan et al., 2017; Wattanasatcha et al., 2012), anti-inflammatory (de Oliveira et al., 2012; Riella et al., 2012), antinociceptive (de Oliveira et al., 2012; de Sousa et al., 2011; Melo Júnior et al., 2017), antioxidant (Kfoury et al., 2014b), and anaesthetic (Reiner et al., 2013) activities.

The selected EO components have different octanol/water partition coefficient (Log P), aqueous solubility, and Henry's law constant (Hc) values. Table 1 represents both the structure and the aforementioned properties of the selected EO components. The aqueous solubility varies between 178 (Yalkowsky and Dannenfelser, 1992) and 7100 mg/L (Li and Perdue, 1995) for estragole and terpineol, respectively. Also, log P values range between 2.6 for isoeugenol (Pubchem; CID 853433, n.d.) and 3.4 for estragole (Pubchem; CID 8815, n.d.). Furthermore, the H_c values of estragole and eucalyptol were approximately 10 times greater than those of isoeugenol, pulegone, terpineol, and thymol (Hammoud et al., 2019a).

Despite their remarkable properties, the use of EO components is limited by their volatility, poor water solubility, and instability in the presence of heat, light, and oxygen (Turek and Stintzing, 2013). The encapsulation of EO components in carrier systems like cyclodextrins (CDs), liposomes, and drug-in-cyclodextrin-in-liposomes (DCLs) is under development as being a promising tool for overcoming the drawbacks of components, thereby extending their shelf life and activity (Azzi et al., 2018; Gharib et al., 2017a; Kfoury et al., 2014a, 2014b; Moghimipour et al., 2012; Sebaaly et al., 2015, 2016a; Wang et al., 2011).

DCLs are drug carriers comprising one or more phospholipid

* Corresponding author.

https://doi.org/10.1016/j.ijpharm.2020.119151
Received 23 October 2019; Received in revised form 13 February 2020; Accepted 14 February 2020
Available online 15 February 2020
0378-5173/ © 2020 Published by Elsevier B.V.

Table 1
The structure, log P, aqueous solubility, and Henry's law constant of the studied EO components, and the formation constant (K_f) of HP-β-CD/EO component inclusion complexes.

EO component	Structure	Log P	Aqueous solubility (mg/L)	H_c		K_f (M^{-1})
				30 °C	60 °C	
Estragole	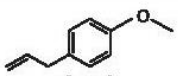	3.4[a]	178[f]	0.03[k]	0.07[k]	1581[l]
Eucalyptol	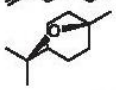	2.74[b]	3500[g]	0.01[k]	0.05[k]	334[l]; 1200[m];1112[m]
Isoeugenol	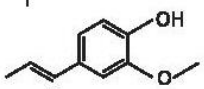	2.6[c]	665[h]; 810[i]	0.005[k]	0.008[k]	441[l]
Pulegone	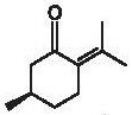	3.08[b]	276[j]	0.005[k]	0.009[k]	676[l]; 867[m]; 798[m]
α-Terpineol	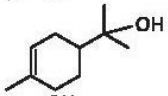	2.98[d]	7100[d]	0.001[k]	0.003[k]	761[l]
Thymol	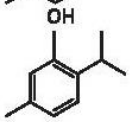	3.3[e]	900[f]	0.003[k]	0.009[k]	806[l]; 1400[m]; 1313[m]

ND: not determined.
[a] Pubchem CID 8815, n.d..
[b] Griffin et al., 1999.
[c] Pubchem CID: 853433, n.d.
[d] Li and Perdue, 1995.
[e] Pubchem; CID 6989, n.d..
[f] Yalkowsky and Dannenfelser, 1992.
[g] Yalkowsky, He, and Jain, 2010.
[h] Kfoury et al., 2014b.
[i] HERA, 2012.
[j] US EPA, 2012.
[k] Hammoud et al., 2019a.
[l] Kfoury et al., 2016a.
[m] Kfoury et al., 2014a.

bilayers and an aqueous internal cavity where a CD/drug inclusion complex is loaded (McCormack and Gregoriadis, 1994). DCLs were used to preserve volatile and hydrophobic EO components, thereby extending their various applications in the food, cosmetics, and pharmaceutical industries. Namely, they were used to encapsulate a variety of monoterpenes and phenylpropenes including eugenol (Sebaaly et al., 2016a), trans-anethole (Gharib et al., 2017a), and estragole (Gharib et al., 2019).

Cyclodextrins (CDs) represent a family of non-toxic cyclic oligosaccharides characterized by a hydrophilic outer surface and a hydrophobic cavity. Thus, in an aqueous environment, these carbohydrates can accommodate lipophilic EO components in their cavity forming CD/EO component inclusion complex; the interaction of a EO component with CD is not permanent, but rather a dynamic process in which the guest continuously associates and dissociates with CD host. The native CDs consist of six, seven, or eight subunits of α-1,4-linked D-glucopyranose forming α-, β-, and γ-CDs, respectively. Besides, functional groups could be added to native CDs, leading to a modification in their solubility and stability (Gharib et al. 2015; Szejtli 1998). We specifically selected, herein, hydroxypropyl-β-CD (HP-β-CD) due to its high aqueous solubility (> 500 mg/mL) and strong complexing ability with EO components (Kfoury et al., 2014a, 2014b; Malanga et al., 2016; Miranda et al., 2011). Previous studies investigated the formation of inclusion complexes between HP-β-CD and the selected phenylpropenes and monoterpenes. The formation constant (K_f) values of HP-β-CD/EO component inclusion complexes were determined in the literature using different techniques such as fluorescence spectrophotometry and static headspace gas chromatography. The results are shown in Table 1. It should be noted that applying different methods may provide different K_f values for the same guest molecule (Ciobanu et al., 2013). Furthermore, a linear relationship was demonstrated between K_f of HP-β-CD/monoterpene inclusion complex and log P of a monoterpene (Kfoury et al., 2014a). In addition, a strong negative correlation was found between the solubilizing potential of HP-β-CD and the intrinsic aqueous solubility of phenylpropenes and monoterpenes (Kfoury et al., 2014b).

Liposomes are viewed as attractive materials by the food and pharmaceutical industries. They are spherical vesicles capable of entrapping hydrophilic and hydrophobic drugs in their aqueous core and lipid bilayer, respectively (Gharib et al., 2015). However, the loading of hydrophobic drugs into liposomes may affect the lipid membrane properties, causing a rapid release of drug from the bilayer (Kirby and Gregoriadis, 1983; Takino et al., 1994). Additionally, Gharib et al. demonstrated that the selected EO components interact with dipalmitoyl phosphatidylcholine (DPPC) liposomal membrane, leading to an increase in the lipid bilayer fluidity and disorder (Gharib et al., 2017b, 2018a). In an older study, Cristani et al. (2007) proved that the

incorporation of a series of EO components, including thymol, into liposomes causes perturbation in the lipid bilayer and influences the membrane properties such as fluidity and permeability.

The DCL system was proposed by McCormack B and Gregoriadis G in 1994. After that, DCL characteristics were determined and compared to those of conventional liposomes in several studies. It has been proved that DCLs improve drug encapsulation efficiency (EE) and loading ratio (LR) and delay drug release compared to conventional liposomes (Azzi et al., 2018; Chen et al., 2007; Gharib et al., 2017a; Sebaaly et al., 2016a; Zhang et al., 2013). Added to that, compared to conventional liposomes, DCLs showed a prolonged biological effect due to the slower drug release (Bragagni et al., 2010; Maestrelli et al., 2010; Zhu et al., 2013). For example, Zhu et al., 2013 evaluated the intestinal mucous membrane penetration capacity of liposomes and DCLs carrying tacrolimus after their administration to rats by oral route. Compared to tacrolimus loaded liposomes, β-CD/tacrolimus loaded liposomes ameliorate the penetration capability of the drug to the epithelial surfaces through the mucus, allowing the drug to reach the underlying mucous membrane.

In addition, regarding DCL formulations, it is crucial to consider the effect of CDs on liposome membrane. We have recently published a review concerning the interaction of CDs with biomimetic and biological membranes (Hammoud et al., 2019b). In brief, CDs are able to extract lipid components from membranes; the effect depends on: the length of the fatty acid acyl chains, their saturation, the nature of the head groups of phospholipids, the CD type and concentration, the presence of cholesterol, and the percentage of cholesterol in the formulation (Denz et al., 2016; Milles et al., 2013; Ohvo-Rekilä et al., 2000). Moreover, CDs can impact the membrane properties, mainly fluidity, stability, and permeability (Hatzi et al., 2007; Puglisi et al., 1996). Furthermore, it was demonstrated that HP-β-CD does not influence, or exerts a smaller effect on, the liposome membrane integrity in comparison to other CDs (Nishijo et al., 2000; Piel et al., 2007). Nevertheless, HP-β-CD interacts with the choline head groups and the alkyl chains of DPPC lipid bilayer, leading to an increase in its fluidity and disorder. Also, it increases the disorder of lipoid S100: cholesterol liposomal membrane (Gharib et al., 2018b).

In the present study, a series of EO components including estragole, eucalyptol, isoeugenol, pulegone, terpineol, and thymol were encapsulated into DCLs using the ethanol injection method for vesicle preparation. The size of vesicles, their morphology, the EE, the LR, the release kinetics, and the storage stability of DCL suspensions were evaluated. The final composition of DCL (phospholipid: cholesterol: EO component molar ratio) was determined. In DCL structure, the DCL constituents (phospholipid, cholesterol, and EO component) could be present in free form (not complexed with CD) and CD/constituent form; they could also partition between the lipid membrane and the aqueous core of vesicles. The impact of chemical structure, log P and H_c of EO components on DCL characteristics was also analyzed.

2. Materials and methods

2.1. Materials

Non-hydrogenated soybean phosphatidylcholine lipoid S100 (94% soybean phosphatidylcholine, 3% lysophosphatidylcholine, 0.5% N-acyl-phosphatidylethanolamine, 0.1% phosphatidylethanolamine, 0.1% phosphatidylinositol, 2% water, 0.2% ethanol) was supplied by Lipoid GmbH, Germany. HP-ß-CD (DS = 5.6) was obtained from Roquette (Lestrem, France). Cholesterol (94%) was purchased from Sigma-Aldrich, Japan; ammonium molybdate, eugenol, isoeugenol, potassium dihydrogen phosphate and thymol from Sigma-Aldrich, Germany; pulegone and terpineol from Sigma- Aldrich, Switzerland; estragole from Sigma-Aldrich, China; eucalyptol and triton X-100 from Sigma–Aldrich, USA; and methanol HPLC grade from Sigma-Aldrich, France. Cholesterol CHOD-POD kit was provided by Spin react Company, Spain. Absolute ethanol and sulfuric acid were purchased from VWR Pro-labo chemicals, France; hydrogen peroxide from Fisher Scientific, UK; and 4-amino-3-hydroxy-1-naphthalenesulfonic acid from Fluka, India.

2.2. HPLC analysis

The concentration of EO components in the formulations was determined by reversed phase HPLC method as previously described (Hammoud et al., 2019a). Briefly, HPLC analysis was accomplished using an analytic column (C 18: 15 cm × 4.6 mm (Agilent)) at a wavelength of 204 nm. Methanol and water mixture (70:30) was used as a mobile phase for all samples, except in the case of pulegone (65:35). The injection volume was 20 µl. The flow rate was set at 1 mL/min.

2.3. Optimization of HP-β-CD:EO component molar ratio for inclusion complex preparation

HP-β-CD/EO component inclusion complexes were prepared in aqueous solutions. Estragole (7.44 mg), eucalyptol (7.71 mg), isoeugenol (8.21 mg), pulegone (7.61 mg), terpineol (7.71 mg), and thymol (7.51 mg) were added to 5 mL of HP-β-CD solutions of different concentrations (0, 10, 25, 50, 75, 100 mM). The mixtures were agitated at a stirring rate of 125 rpm for 24 h at 26 °C, and then filtered through a 0.45 µm pore size cellulose acetate filter to eliminate the un-dissolved compounds. Based on HPLC analysis, the concentration of EO component present in the filtrate was determined. The complexation efficiency (CE) was calculated using the following equation:

$$CE(\%) = \frac{m_{exp}}{m_{the}} \times 100 \quad (1)$$

in which m_{exp} stands for the experimental mass of EO component determined in the filtrate. m_{the} is the theoretical mass of EO component initially used to prepare the inclusion complex.

2.4. Preparation of HP-β-CD/EO component inclusion complex for DCL preparations

HP-β-CD was dissolved in ultrapure water, and the required amount of EO component was added to obtain HP-β-CD/EO component molar ratio of 2.5:1 for eucalyptol, isoeugenol, pulegone, and terpineol, respectively as well as 7.5:1 for estragole and thymol. The mixtures were shaken at 125 rpm for 24 h at 26 °C then filtered through a 0.45 µm membrane filter. The filtrate was used as the aqueous phase in DCL preparation as described below. Additionally, free HP-β-CD (25 and 75 mM) was dissolved in water for preparing blank DCLs.

2.5. Preparation of EO component-in-HP-β-CD-in-liposome

The DCL formulations were prepared by the ethanol injection method as previously described (Gharib et al., 2017a) (Fig. S1). Lipoid S100 (10 mg/mL) and cholesterol (5 mg/mL) were dissolved in absolute ethanol. Then, 10 mL of the organic phase was injected, using a syringe pump (Fortuna optima, GmbH, Germany) at an injection flow rate of 1 mL/min, into 20 mL aqueous phase (containing either free HP-β-CD or HP-β-CD/EO component inclusion complex) under magnetic stirring (400 rpm) at room temperature. Spontaneous formation of liposomes occurred as soon as the organic phase was in contact with the aqueous phase. DCL suspensions were kept for 15 min under stirring (400 rpm) at room temperature. Finally, ethanol was removed by rotary evaporation (Heidolph instruments GmbH and co, Germany) at 41 °C and 60 rpm under reduced pressure. Each of the batches was prepared in triplicate. The DCL formulations were stored at 4 °C prior to analysis.

2.6. Characterization of DCL formulations

2.6.1. Determination of DCL particle size

In this study, a laser granulometer (Partica Laser scattering, LA-950V2 particle size distribution analyzer, HORIBA, Japan) designed for measuring particle sizes between 0.01 and 3000 μm was used to determine the mean sizes of the prepared batches. The particle size of DCL and the percentage of each population in the suspension were evaluated; data were expressed as the means ± standard deviation.

2.6.2. Morphological characterization by scanning electron microscopy

Aliquots were removed from the suspensions and submitted to centrifugation at 21,382*g* and 4 °C for 1 h. The pellets were collected and dried at room temperature. The powders were sputtered with gold, in a Cressington 108 auto sputter coater (Watford, UK), for 20 s using a current of 25 mA/mbar. A scanning electron microscope (SEM, AIS2100C, Seron Technology, Korea) was used to image the samples.

2.6.3. Determination of phospholipid: cholesterol: EO component molar ratio in DCL structures

The DCL suspensions were subjected to centrifugation at 21,382*g* and 4 °C for 1 h using a Vivaspin 500 centrifugal concentrator (Sartorius Stedim Biotech, Germany, MW cut off = 10,000 Da) to separate the unloaded liposome components from the loaded ones (Fig. S1). Aliquots were removed from the filtrates to determine the concentration of unloaded constituents (phospholipids, cholesterol, EO component un-included in CDs, and CD/EO component complex). Also, aliquots were removed from the DCL suspensions, then sonicated for 10 min in ice to determine the total concentration of the DCL constituents. For each formulation, the phospholipid: cholesterol: EO component molar ratio was later calculated.

2.6.3.1. Determination of phospholipid incorporation ratio. The concentration of phospholipids in the DCL suspension and the DCL filtrate was quantified by Bartlett's method as described in our previous studies (Hammoud et al., 2019a; Sebaaly et al., 2016b). Briefly, the organic phosphate in the samples (DCL suspension, filtrate) was digested by sulfuric acid, then the samples were incubated in the presence of H_2O_2 to allow the oxidation of organic phosphates to inorganic phosphates. Upon interaction with ammonium molybdate, the phosphomolybdic complex was formed. This was followed by its reduction to a blue product through interaction with 4-amino-3-hydroxy-1-naphthalenesulfonic acid. The absorbance of the blue compound was measured at 815 nm. The incorporation ratio (IR) of phospholipids was calculated based on the following equation:

$$IR_{PO_4^{3-}}(\%) = \frac{m_{PL_{total}} - m_{PL_{unloaded}}}{m_{PL_{organicphase}}} \times 100 \quad (2)$$

in which $m_{PL_{total}}$ is the mass of phospholipids in the DCL suspension, $m_{PL_{unloaded}}$ is the mass of phospholipids in the DCL filtrate (unloaded in vesicles), and $m_{PL_{organicphase}}$ is the initial mass of phospholipids added to the organic phase during DCL preparation.

2.6.3.2. Determination of cholesterol incorporation ratio. The enzymatic colorimetric method was utilized to determine the total and the unloaded concentrations of cholesterol in a suspension (Hammoud et al., 2019a). In brief, 1 mL of a cholesterol CHOD-POD kit was added to the samples (cholesterol standards prepared in triton X-100, filtrate, and DCL suspension). The absorbance of the colored complex was measured at 505 nm. The IR of cholesterol was determined according to the following equation:

$$IR_{CHO}(\%) = \frac{m_{CHO_{total}} - m_{CHO_{unloaded}}}{m_{CHO_{organicphase}}} \times 100 \quad (3)$$

in which $m_{CHO_{total}}$ is the cholesterol mass in the DCL suspension, $m_{CHO_{unloaded}}$ is the mass of cholesterol in the filtrate, and $m_{CHO_{organicphase}}$ is the initial mass of cholesterol added to the organic phase during DCL preparation.

2.6.3.3. Determination of the encapsulation efficiency and loading ratio of EO components. The concentration of EO component in the DCL suspension and the DCL filtrate was determined by HPLC analysis. The EE and LR of EO component into DCL were calculated as follows:

$$EE_{DCL}(\%) = \frac{[EOcomponent]_{total} - [EOcomponent]_{unloaded}}{[EOcomponent]_{total}} \times 100 \quad (4)$$

in which $[EOcomponent]_{total}$ and $[EOcomponent]_{unloaded}$ correspond to the total and unloaded concentrations of EO component in the DCL suspension, respectively.

$$LR(\%) = \frac{m_{EOcomponents_{total}} - m_{EOcomponents_{unloaded}}}{m_{initial}} \times 100 \quad (5)$$

in which $m_{EOcomponents_{total}}$ and $m_{EOcomponents_{unloaded}}$ correspond to the mass of EO component in the DCL suspension and the DCL filtrate, respectively. $m_{initial}$ is the mass of EO component initially used to prepare the HP-β-CD/EO component inclusion complex.

2.6.4. In vitro release kinetics

The release studies were conducted using the multiple headspace extraction (MHE) method coupled to gas chromatography (GC). Aliquots (1 mL) were removed from the DCL formulations and added to 9 mL of water in 22 mL sealed vials. In parallel, the corresponding free EO component (estragole and thymol at 1 ppm, isoeugenol at 200 ppm, terpineol at 5 ppm, pulegone at 2 ppm, and eucalyptol at 0.5 ppm) was inserted in 22 mL sealed vials. Following equilibrium, vials were subjected to 30 successive gas extractions at a constant time interval (8 min), using nitrogen as a carrier vector, oven temperature of 60 °C, and transfer line temperature of 250 °C. 1 mL of the vapor present in the gaseous phase was later analyzed by GC. All measurements were carried out using an Agilent G1888 headspace sampler coupled to a Perkin Elmer Autosystem XL gas chromatography equipped with a flame ionization detector and a DB624 column. GC conditions were set as follows: GC cycle of 8 min, column temperature of 160 °C for estragole, eucalyptol, pulegone, terpineol, and thymol, and of 180 °C for isoeugenol. For each EO constituent, the percentage remaining at time t was calculated based on the following equation:

$$Percentage\ of\ remaining\ EO\ component = \frac{A_t}{A_1} \times 100 \quad (6)$$

in which A_t and A_1 correspond to the area of the chromatographic peak of EO component at time t and at the first extraction, respectively.

2.6.5. DCLs storage stability

The particle sizes of the DCL batches were measured by laser granulometry after 10 months of storage at 4 °C. After the same period of time, aliquots were removed from the formulations and analyzed by HPLC to determine the total and the unloaded concentrations of EO component in the suspension; the deduced values were compared to those obtained on the day of preparation.

2.7. Statistical analysis

Statistical analysis was carried out using the two samples student's *t*-test. All assays were performed in triplicate, and the results are expressed as the mean values ± standard deviation. Significance was reported when the *P* values were equal to or less than 0.05.

Table 2
The solubilized EO component concentration (μg/mL) and CE of the selected EO components in the presence of different HP-β-CD concentrations.

		HP-β-CD concentration (mM)					
		0	10	25	50	75	100
Estragole	μg/mL	17.7 ± 2.3	507.7 ± 65.7	1112.2 ± 3.6	1097.3 ± 39.4	1362.3 ± 96.8	1455.2 ± 40.7
	CE (%)	–	34.1 ± 5.4	74.8 ± 0.3	73.8 ± 1.4	91.6 ± 6.9	97.8 ± 2.7
Eucalyptol	μg/mL	1122.2 ± 93.1	1044.1 ± 72.9	1431.3 ± 67.6	1521.3 ± 78.2	1239.2 ± 26.9	1538.4 ± 27.8
	CE (%)	–	55.9 ± 4.7	92.8 ± 5.4	95.7 ± 5.2	80.3 ± 2.1	99.1 ± 2.2
Isoeugenol	μg/mL	536.8 ± 55.3	886.9 ± 40.1	1557.3 ± 24.5	1481.3 ± 14.9	1522.6 ± 35.8	1317.6 ± 57.9
	CE (%)	–	54.0 ± 2.4	94.8 ± 1.8	90.2 ± 1.1	92.7 ± 2.2	88.3 ± 1.3
Pulegone	μg/mL	924.5 ± 62.6	1304.1 ± 64.2	1497.5 ± 28.3	1484.7 ± 13.7	1407.4 ± 116.6	1374.3 ± 50.9
	CE (%)	–	85.8 ± 5.2	98.4 ± 2.3	97.5 ± 0.9	91.5 ± 7.5	90.3 ± 3.3
Terpineol	μg/mL	642.3 ± 85.6	685.9 ± 2.7	1121.3 ± 86.3	1036.5 ± 62.3	1067.2 ± 106.9	919.4 ± 107.4
	CE (%)	–	44.5 ± 0.2	72.7 ± 6.8	67.2 ± 4.9	69.2 ± 6.9	60.0 ± 8.4
Thymol	μg/mL	834.8 ± 73.4	1068.1 ± 9.2	1176.1 ± 101.1	1295.5 ± 19.2	1465.2 ± 51.3	1292.1 ± 11.1
	CE (%)	–	71.1 ± 0.6	78.3 ± 6.7	86.2 ± 1.2	97.6 ± 4.1	86.0 ± 0.9

Table 3
Percentage distribution and mean particle size of populations 1, 2, and 3 for HP-β-CD-loaded liposomes and DCL formulations determined on the day of preparation and after 10 months of storage at 4 °C.

DCL formulations	Population 1		Population 2		Population 3	
	(%)	Mean size (μm)	(%)	Mean size (μm)	(%)	Mean size (μm)
Blank liposomes	–	–	**100.0 ± 0.1**	**6.2 ± 0.5**	–	–
			100.0 ± 0.1	*7.1 ± 1.5*		
DCLs (HP-β-CD 25 mM)						
Blank DCL	–	–	**75.5 ± 6.4**	**12.1 ± 0.9**	**24.5 ± 6.4**	**63.2 ± 6.1**
			38.0 ± 2.8	*15.2 ± 0.1*	*62.0 ± 2.8*	*58.9 ± 0.1*
Eucalyptol	–	–	**60.0 ± 5.6**	**12.1 ± 0.9**	**40.0 ± 5.6**	**67.9 ± 9.2**
			32.5 ± 4.9	*15.3 ± 2.9*	*67.5 ± 4.9*	*51.5 ± 0.1*
Isoeugenol	**5.5 ± 0.7**	**0.3 ± 0.1**	**94.5 ± 0.7**	**10.8 ± 1.0**	–	–
	7.3 ± 2.5	*0.3 ± 0.1*	*92.7 ± 2.5*	*12.1 ± 0.9*	–	–
Pulegone	–	–	**100.0 ± 0.1**	**13.2 ± 0.1**	–	–
			27.0 ± 18.3	*28.3 ± 15.4*	*73.0 ± 18.4*	*262 ± 0.1*
Terpineol	**7.0 ± 9.9**	**0.3 ± 0.1**	**65.5 ± 9.2**	**11.6 ± 0.1**	**27.5 ± 0.7**	**82.9 ± 7.9**
	17.0 ± 1.4	*0.2 ± 0.1*	*66.5 ± 9.2*	*11.6 ± 0.1*	*16.5 ± 7.8*	*101.0 ± 0.1*
DCLs (HP-β-CD 75 mM)						
Blank DCL	–	–	**67.5 ± 4.9**	**7.7 ± 0.1**	**32.5 ± 4.9**	**78.0 ± 14.9**
			25.5 ± 9.2	*11.7 ± 2.2*	*74.5 ± 9.2*	*72.4 ± 14.9*
Estragole	–	–	–	–	**100.0 ± 0.1**	**28.0 ± 2.7**
					100.0 ± 0.1	*34.6 ± 6.6*
Thymol	–	–	**100.0 ± 0.1**	**13.5 ± 2.9**	–	–
	14.5 ± 6.4	*0.3 ± 0.1*	*85.5 ± 6.4*	*15.3 ± 2.9*	–	–

Bold: immediately after preparation; *italic*: after 10 months of storage at 4 °C.

3. Results and discussion

3.1. Determination of the optimal HP-β-CD concentration for inclusion complex preparation

The incorporation of free CDs at high concentration inside the aqueous compartments of liposomes may perturb the lipid membrane organization (Hammoud et al., 2019b). Hence, for DCL preparation, the CD concentration is chosen in such a way to produce an efficient solubilization of EO component while keeping the membrane intact. The concentration of EO component solubilized in the presence of different HP-β-CD concentrations (0–100 mM) is presented in Table 2. In the absence of HP-β-CD, the concentrations of EO components were 17.7 ± 2.3, 1122 ± 93.1, 536.8 ± 55.3, 924.5 ± 62.6, 642.3 ± 85.6, and 834.8 ± 73.4 μg/mL for estragole, eucalyptol, isoeugenol, pulegone, terpineol, and thymol, respectively. These values are not consistent with the aqueous solubility values presented in Table 1. The latter are not experimentally measured but they are predicted using computational models. Moreover, it is complicated to obtain accurate intrinsic aqueous solubility values for poorly-soluble drugs. Self-association of lipophilic drug molecules in aqueous media can lead to erroneous results (Saokham et al., 2018). The addition of HP-β-CD enhanced the solubility of the selected EO components in accordance with the literature (Azzi et al., 2018; Kfoury et al., 2014b; Wang et al., 2011; Zhang et al., 2009). Optimal solubilization of eucalyptol, isoeugenol, pulegone, and terpineol occurred at HP-β-CD concentration of 25 mM, while HP-β-CD concentration of 75 mM was required to ensure efficient solubilization of estragole and thymol.

The CE of EO component into HP-β-CD was calculated as described in Eq. (1), and the results are summarized in Table 2. The optimal CE value was 91.6 ± 6.9, 92.8 ± 5.4, 94.8 ± 1.8, 98.4 ± 2.3, 72.7 ± 6.8, and 97.6 ± 4.1% for estragole, eucalyptol, isoeugenol, pulegone, terpineol, and thymol, respectively. The lower entrapment of terpineol into HP-β-CD cavity compared to the other EO components could be explained by its high aqueous solubility which causes a reduction in the ability of HP-β-CD to solubilize EO components (Kfoury et al., 2014b). During DCL preparation, the HP-β-CD/EO component inclusion complex was prepared at the respective optimal HP-β-CD concentration.

Table 4
Phospholipid (Pho) and cholesterol (CHO) incorporation ratio (IR), EO component encapsulation efficiency (EE), EO component loading ratio (LR), and Pho:CHO:EO component molar ratio for the various DCL formulations. The initial Pho:CHO:EO component molar ratio was 125:129:0 and 125:129:200 for blank batches and EO component-loaded batches, respectively.

	Liposomal components				Final Pho:CHO: EO component molar ratio
	Phospholipid IR (%)	Cholesterol IR (%)	EO component		
			EE (%)	LR (%)	
Blank liposomes	94.2 ± 6.4	77.6 ± 1.1	–	–	118:95:0
DCLs (HP-β-CD 25 mM)					
Blank DCLs	82.7 ± 0.7	77.3 ± 1.0	–	–	100:102:0
Eucalyptol	80.6 ± 6.8	32.4 ± 5.0*	49.4 ± 8.4	2.18 ± 0.3	101:42:4
Isoeugenol	86.6 ± 4.3	15.2 ± 1.3*	88.7 ± 0.9	13.0 ± 1.0	102:20:26
Pulegone	65.5 ± 2.9*	24.8 ± 2.7*	61.8 ± 6.7	9.33 ± 1.1	82:32:19
Terpineol	78.8 ± 2.0	78.4 ± 1.6	25.3 ± 1.8	13.3 ± 1.6	99:104:27
DCLs (HP-β-CD 75 mM)					
Blank DCLs	81.1 ± 4.4	76.8 ± 4.8	–	–	102:99:0
Estragole	67.2 ± 6.9*	24.0 ± 2.4*	89.7 ± 3.8	10.9 ± 3.1	76:31:22
Thymol	85.6 ± 4.8	57.6 ± 8.6*	49.5 ± 4.0	23.1 ± 1.0	107:74:46

* $P < 0.05$ in comparison to blank DCLs.

3.2. Particle size measurement

The particle size distributions of the lipid vesicles were assessed by a laser granulometer on the day of preparation and after 10 months of storage at 4 °C. The number of populations, their percentage, and the mean particle size of each population in blank- and EO component-loaded DCL batches are shown in Table 3.

3.2.1. The effect of HP-β-CD on liposome particle size

For blank liposomes, one population of micrometric size (6.2 ± 0.5 μm) was observed. For HP-β-CD loaded liposomes of 25 and 75 mM HP-β-CD concentrations, two populations of micrometric sizes appeared (Table 3). The difference in blank DCL particle size compared to the literature studies (Bragagni et al., 2010; Cavalcanti et al., 2011; Gharib et al., 2017a; Maestrelli et al., 2010, 2005; Sebaaly et al., 2016a) could be related to the different methods used for size characterization. Indeed, most studies in literature used dynamic light scattering for size characterization where the detection could be limited to submicron size range populations (Storti and Balsamo, 2010). In this study, the laser granulometry apparatus allows determining particle sizes between 0.01 and 3000 μm.

HP-β-CD promoted the formation of larger vesicles compared to blank liposomes. Giant particles could be clusters or aggregates of smaller liposomes (Domazou and Luigi Luisi, 2002). In addition, HP-β-CD interacts with the acyl chains of lipoid S100 constituting DCL membrane. Consequently, the packing of the acyl chains is reduced; thus, leading to membrane swelling and particle size enlargement. Actually, HP-β-CD did not influence the size of saturated liposomes (Gharib et al., 2017a; Sebaaly et al., 2016a). Nevertheless, a previous study determined the anisotropy value of the probe 1,6-diphenyl-1,3–5-hexatriene inserted in liposomes composed of either saturated phospholipids and cholesterol or unsaturated phospholipids and cholesterol. The results showed that HP-β-CD increased the membrane fluidity of liposomes composed of unsaturated phospholipids and cholesterol (Lipoid S100:cholesterol liposomes) while no effect was exerted on liposomes composed of saturated phospholipid and cholesterol (Phospholipon 80H:cholesterol and Phospholipon 90H: cholesterol liposomes) (Gharib et al., 2018b). The particle size of the blank DCL formulations significantly increased after 10 months of storage at 4 °C. It is probable that the blank DCL particles aggregate into large particles during storage.

3.2.2. The effect of HP-β-CD/EO component inclusion complex on the liposome particle size

The selected HP-β-CD/EO component inclusion complexes exerted different effects on the liposome particle size (Table 3). The entrapment of HP-β-CD/estragole, HP-β-CD/eucalyptol, and HP-β-CD/terpineol inclusion complexes into the aqueous phase of liposomes boosted the production of larger vesicles compared to the respective blank DCLs. However, HP-β-CD/isoeugenol, HP-β-CD/pulegone, and HP-β-CD/thymol complexes abolished the formation of large vesicles compared to their respective blank DCLs; the percentage of smaller micrometric sized liposomes increased. Also, a small percentage of nanometric sized vesicles appeared in isoeugenol- and terpineol-loaded DCLs.

It was previously investigated that the presence of phenolic hydroxyl groups in the structure of an EO component (such as in the case of isoeugenol and thymol) promoted an increase in lipoid S-100 liposome particle size (Hammoud et al., 2019a). This finding implies that the aromatic rings of isoeugenol and thymol are completely incorporated within the hydrophobic cavity of HP-β-CD, thereby hindering the interaction of isoeugenol and thymol with the acyl chains of lipid bilayer. Hence, the effects of isoeugenol and thymol on liposome membrane and particle size are lowered. The results of our study agree with those demonstrated for eugenol; eugenol-loaded liposomes exhibit a larger particle size compared to eugenol-loaded DCLs (Sebaaly et al., 2016a). Furthermore, the various EO component-loaded DCL formulations showed a significant increase in their particle size after long term storage. Dried DCL suspensions were imaged by SEM after 10 months of storage to explain whether the large vesicles result from aggregation/fusion of smaller particles.

3.3. Morphological study

Dried DCL batches were imaged by SEM. The SEM images (Fig. S2) showed that the dried vesicles are of a micrometric size. The obtained images confirm the broad size distributions of blank DCLs and EO component-loaded DCLs determined by laser granulometry. Also, these images prove that aggregation/fusion of DCLs during drying or storage cannot be excluded.

3.4. The effect of HP-β-CD on phospholipid and cholesterol incorporation into liposomes

The IR values of phospholipids and cholesterol into blank DCLs were calculated according to Eqs. (2) and (3), respectively, and the results are summarized in Table 4.

For blank liposomes, the phospholipid IR value was high (94.2 ± 6.4%), indicating that a small loss of phospholipids occurred during the preparation of liposomes. HP-β-CD, at a concentration of 25 and 75 mM, reduced the incorporation of phospholipids into the liposome membrane. CDs have a potential to extract lipid components from biomimetic and biological membranes. The extent of this extraction depends on CD type, CD concentration, phospholipid type (head group and acyl chains), lipid membrane composition, and cell type (Hammoud et al., 2019b). To our knowledge, the literature lacks noticeable data on HP-β-CD interaction with lipoid S-100 liposome membrane. Nevertheless, it was demonstrated that β-CD and its derivative, HP-β-CD, did not modify the membrane phospholipid content of mouse L-cell fibroblasts (Kilsdonk et al., 1995) and Caco-2 cells (Ono et al., 2001). Furthermore, HP-β-CD scarcely interacted with saturated DPPC liposome membrane (Nishijo and Mizuno, 1998). However, the presence of a double bond in the acyl chain was reported to favor the β-CD-induced phospholipid extraction from membranes where the double bond produces strong disorder and induces kink of chain; the unsaturated phospholipid palmityl oleoyl phosphatidylcholine was more effectively desorbed from monolayer by β-CD compared to DPPC (Grauby-Heywang and Turlet, 2008).

The cholesterol IR value of blank liposome was 77.6 ± 1.1%. The addition of HP-β-CD at a concentration of 25 and 75 mM did not markedly impact the incorporation of cholesterol into liposomes in accordance with Szente et al. (2018) who demonstrated that HP-β-CD (50 mM) induced less extraction of cholesterol from human embryo kidney-derived HEK293T cells, human cervical cancer-derived HeLa and TZM-bl cells, and human T-lymphocyte-derived Jurkat cells compared to the methylated CDs, dimethylated β-CD and randomly methylated β-CD. Namely, HP-β-CD may interact with liposome membrane, and the formation of HP-β-CD/phospholipid and HP-β-CD/cholesterol inclusion complexes cannot be excluded.

3.5. Determination of phospholipid: cholesterol: EO component molar ratio in EO component-loaded DCLs

The IR values of phospholipids and cholesterol as well as the EE and LR values of EO components in the various EO component-loaded DCLs were determined as previously described. The results are shown in Table 4.

3.5.1. Phospholipid incorporation in EO component-loaded DCL

In comparison to blank DCLs, HP-β-CD/estragole and HP-β-CD/pulegone inclusion complexes lowered the incorporation of phospholipids into liposomes whereas the other complexes did not greatly affect the retention of phospholipids in the lipid vesicles. Previous studies in the literature showed that the selected EO components, except eucalyptol, may act as substitution impurities of the membrane and replace lipid molecules (Gharib et al., 2018a, 2017b) whereas eucalyptol acts as an interstitial impurity and intercalates in the bilayer (Gharib et al., 2018a). Hence, it is probable that some inclusion complexes are dissociated during DCL preparation leading to release the EO component from HP-β-CD cavity; the released EO component may then replace phospholipid molecules in the liposome membrane.

3.5.1.1. Cholesterol incorporation in EO component-loaded DCL. All the HP-β-CD/EO component inclusion complexes, except HP-β-CD/terpineol complex, considerably lowered cholesterol incorporation into liposomes compared to blank DCLs (Table 4). The prepared inclusion complexes might have dissociated leading to the release of EO components. The released EO components may interact with the liposome lipid bilayer, and, thus, minimize the incorporation of cholesterol into the vesicles. We have previously demonstrated that eucalyptol, isoeugenol, pulegone, and thymol reduced cholesterol incorporation into lipoid S-100 liposome membrane. On the contrary, the decrease in cholesterol IR value was not observed for estragole- and terpineol-loaded conventional liposomes compared to the blank formulations (Hammoud et al., 2019a). The difference could be related to the concentration of estragole embedded in liposomes; estragole LR value was 1.1 ± 0.2% into conventional liposomes (Hammoud et al., 2019a) and 10.9 ± 3.1% into DCLs (Table 4).

3.5.1.2. Incorporation of EO components into DCLs. If we assume that lipophilic EO components are retained in the hydrophobic structures of DCLs (liposome membrane and CD cavity), the factors that control EO component encapsulation into DCLs are those related to EO component -lipid membrane interaction and CD- EO component interaction. The EE and LR values of EO components into DCLs were determined, and the results are presented in Table 4. A noticeable difference in the EE values was observed between the phenylpropenes, estragole and isoeugenol (EE > 85%), and the monoterpenes eucalyptol, pulegone, terpineol, and thymol (EE < 62%). Thereby, the presence of a propenyl tail in the structure of an EO component could enhance its retention in DCL vesicles. This finding could be explained by the greater increase in liposome membrane fluidity and disorder demonstrated in the presence of phenylpropenes compared to monoterpenes. The interaction of phenylpropenes (Gharib et al., 2017b) and monoterpenes (Gharib et al., 2018a) with DPPC liposomal membrane was previously studied. Raman spectroscopy showed that the presence of phenylpropenes (particularly isoeugenol) caused a greater increment in the rotational disorder of DPPC membrane compared to monoterpenes. Also, the results of differential scanning calorimetry revealed that the presence of the studied components decreased the transition temperature (T_m) of DPPC membrane, thereby raised its fluidity. Additionally, the effect of the studied monoterpenes on the membrane fluidity was less noticeable compared to isoeugenol which abolished the main transition peak at a high DPPC:isoeugenol molar ratio (100:25). The increase in fluidity of the membrane may promote the loading of the CD/EO component complexes into liposomes. Also, Gharib et al., 2017b investigated that phenylpropenes interact with the choline head groups and the alkyl chains of DPPC membrane, and the presence of a double bond in the propenyl group seems to control the incorporation of EO components. Considering CD-EO components interaction, it might be that the allyl chain of phenylpropenes remains outside the cavity of HP-β-CD and interacts with the hydroxypropyl moieties present on CD ring. This contributes to an increase in the stability of the inclusion complex (Jug et al., 2010).

Furthermore, Fig. 1 shows a decreasing trend of incorporation into DCLs with increasing the cholesterol content of lipid vesicles; the correlation coefficient (R^2) between the EE of EO components and the IR of cholesterol into DCLs was equal to 0.77 (Fig. 1). Cholesterol molecules accommodate within the free space that was formed due to the kink in the chain of unsaturated lipid, causing a decrease in the flexibility of the surrounding lipid chains (Monteiro et al., 2014); therefore, the loading

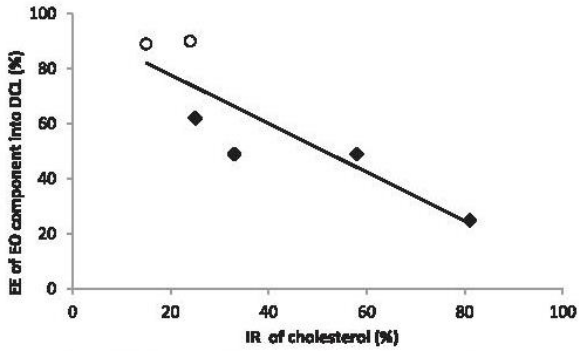

Fig. 1. Relationship between the encapsulation efficiency of EO components and the incorporation ratio of cholesterol into DCLs. (○: phenylpropenes, ◆: monoterpenes).

of the inclusion complexes into liposomal aqueous phase is lowered.

The EO components have variable LR values into DCLs. Isoeugenol, terpineol, and thymol exhibited higher LR values (13.0 ± 1.0%, 13.3 ± 1.6%, 23.1 ± 1.0% for isoeugenol, terpineol, and thymol, respectively) compared to those determined for estragole (10.9 ± 3.1%), eucalyptol (2.2 ± 0.3%), and pulegone (9.3 ± 1.1%). In addition, the non-hydroxylated phenylpropene, anethole, exhibited a low LR value (5.1 ± 0.2%) into lipoid S-100 DCLs (Gharib et al., 2017a). Thus, bearing a hydroxyl group in the chemical structure of EO component may improve its incorporation into DCLs. The hydroxyl groups of EO components boost their lipid membrane-fluidizing effect (Gharib et al., 2018a). The formation of hydrogen bonds between the hydroxyl groups of EO components and the phosphate head groups of phospholipids has been proposed in many studies; the hydroxyl group serves as a hydrogen bond donor, and the phosphate head group of phospholipids acts as a hydrogen bond acceptor (Cristani et al., 2007; Phan et al., 2014). On the other hand, inclusion complexes mostly originate from non-covalent interactions such as hydrophobic interaction as well as van der Waals and hydrogen bonding. As HP-β-CD contains 25- and 39- hydrogen bond donor and acceptor groups, respectively (Saokham et al., 2018), the formation of hydrogen bonds between the hydroxyl group of EO component and CD would take place.

Also, a linear relationship (the correlation coefficient was 0.87) was established between the LR of monoterpenes into DCLs and their hydrophobicity character expressed as log P value. This result could be evidently ascribed to the strong positive correlation between log P of monoterpenes and the K_f value of HP-β-CD/monoterpene inclusion complex (Kfoury et al., 2014a). The plots of the LR value of monoterpenes into DCLs and the K_f value of CD/monoterpene complex (Kfoury et al., 2014a) against log P are shown in Fig. 2A. The entrapment of EO components into DCLs strongly depends on the stability of the inclusion complexes (determined by K_f value). The plot of the LR value of monoterpenes into DCL against the K_f of HP-β-CD/monoterpene inclusion complex is shown in Fig. 2B. The HP-β-CD/monoterpene inclusion complex with a greater K_f value (complex entrapping monoterpene with greater log P) presented an improved retention of monoterpenes into HP-β-CD cavity; thus, the LR of EO components into DCLs would further increase. Based on the results illustrated in Fig. 2, we may propose that during DCL preparation, ethanol did not greatly influence the solubilizing effect and the stability of the inclusion complexes.

3.6. Release kinetics

The release experiment was carried out at 60 °C using the MHE method. Fig. 3 depicts the in vitro release profile of EO components from HP-β-CD/ EO component inclusion complex and DCLs. The results are expressed as the percentage of EO component remaining in the suspension as a function of extraction number.

In their free form, the selected EO components manifested different release profiles. The remaining percentage at the last extraction (Fig. 3) increased in the order of estragole (74.8%) < eucalyptol (85.6%) < isoeugenol (85.9%) < thymol (91.1%) < pulegone (94.1%) < terpineol (96.8%).

Notably, the inclusion of EO components into the cavity of HP-β-CD reduced their volatility and allowed their sustained release; the percentage remaining at the last extraction step for all the HP-β-CD/EO component inclusion complexes was higher compared to that of the corresponding free EO component. The HP-β-CD/EO component inclusion complexes displayed different release patterns. Estragole and eucalyptol showed rapid release rates from HP-β-CD cavity compared to those of the other EO components; the remaining percentage at the last extraction was 80.4% for estragole, 85% and eucalyptol, and > 95% for the other EO components. The remaining percentage of EO component in the solution of HP-β-CD/EO component inclusion complex at the last extraction step was plotted as a function of the H_c value of EO components determined at 60 °C (Fig. S3); a good linearity was observed between the two parameters. H_c is a key factor that influences the release of free- and HP-β-CD-encapsulated EO components. This relation was not found for EO component-loaded DCLs, indicating that the release mechanism of EO components from DCLs is more complex compared to HP-β-CD as additional factors control their release from DCLs.

In general, all the selected EO components showed a slow release pattern from DCLs, indicating that they efficiently retained EO components and consequently, reduced their volatility. DCLs delayed the release of estragole, eucalyptol, and isoeugenol compared to their respective inclusion complexes. For DCLs, EO components are incorporated in the aqueous compartment of liposomes as HP-β-CD/EO component inclusion complex and they must overcome several barriers before being released from the system (Chen et al., 2014). On the other hand, the release rates of pulegone, terpineol, and thymol from DCLs were similar to their respective inclusion complexes. The low EE values of pulegone, terpineol, and thymol into DCLs could explain this difference. Namely, the inclusion complexes are highly present in the outer aqueous phase rather than the inner aqueous compartment. Consequently, the release of EO components from DCL suspension will not greatly differ from that of the inclusion complex. Hence, the EE of EO components into DCLs influences their release from the formulations. Similarly, Piel et al. (2006) evaluated the release of betamethasone from DCLs using different CD types (HP-β-CD, randomly

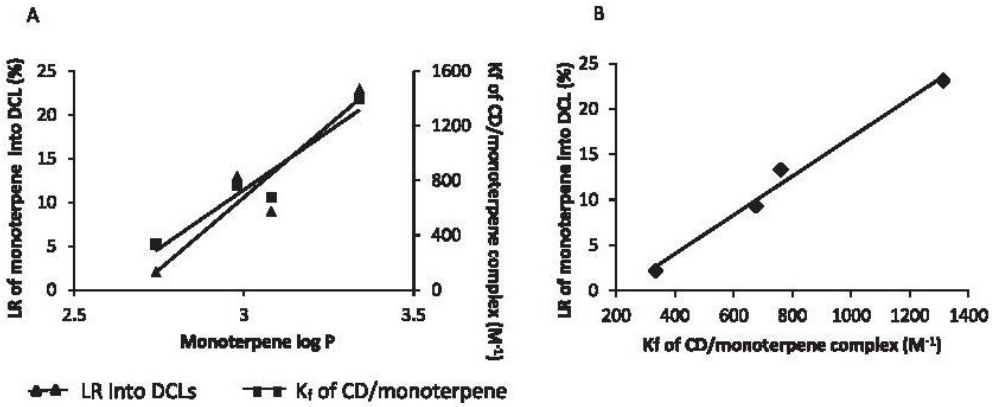

Fig. 2. (A) Relationship between the loading ratio of monoterpenes into DCLs, their formation constants with HP-β-CD (Kfoury et al., 2014a) and their log P values; (B) Relationship between the loading ratio of monoterpenes into DCLs and the formation constants of HP-β-CD/monoterpene complexes.

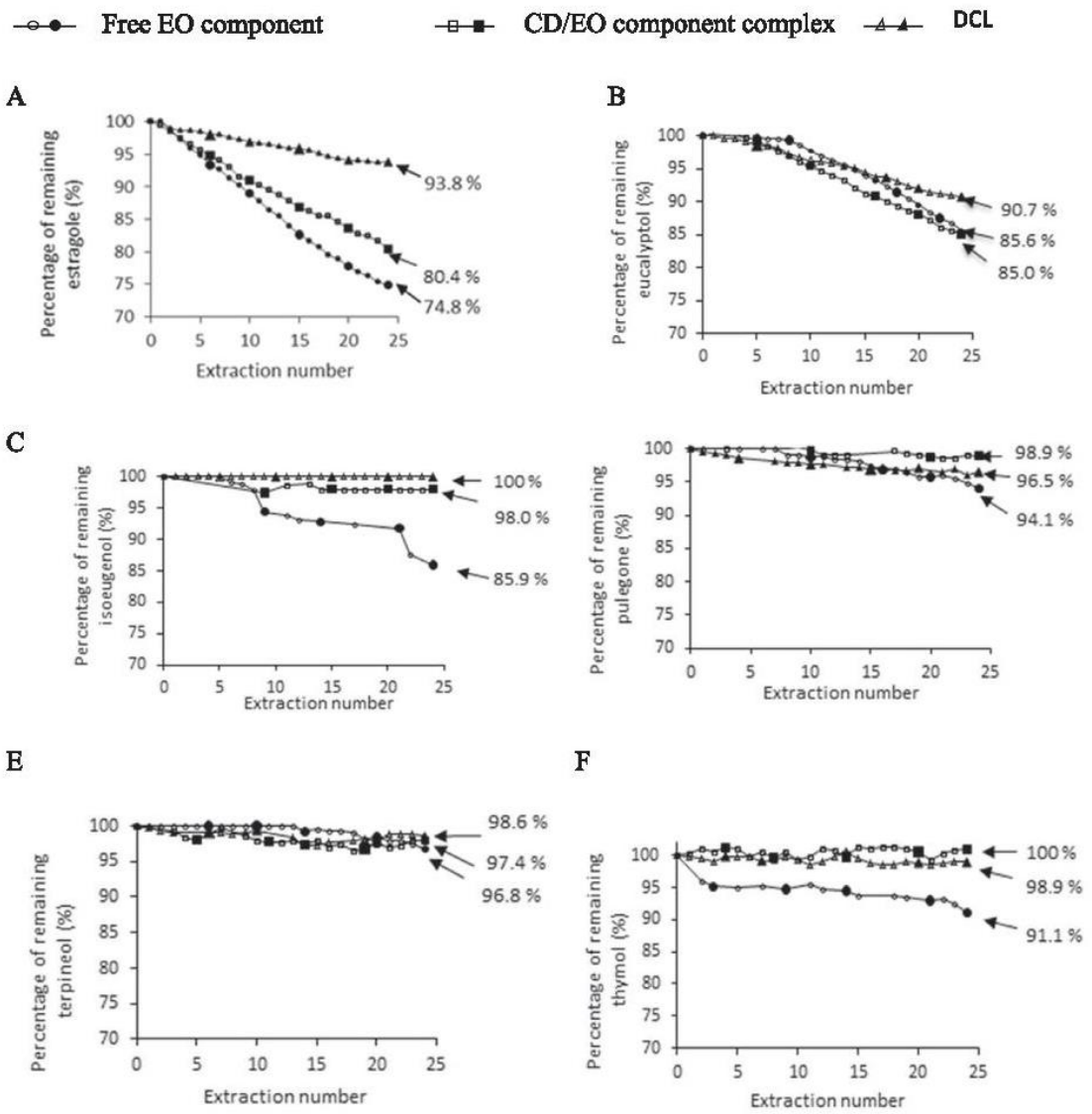

Fig. 3. The remaining percentage of EO components in aqueous solution of an EO component, HP-β-CD/EO component inclusion complex, and EO component-loaded DCL after different extractions. (A) estragole, (B) eucalyptol, (C) isoeugenol, (D) pulegone, (E) terpineol, (F) thymol.

methylated β-CD, partially methylated crystallized-β-CD, HP-γ-CD) and CD concentrations (10, 40 mM). The authors demonstrated a direct correlation between the release rate of betamethasone from the various DCL formulations and its EE value into vesicles.

3.7. Storage stability

During DCL storage, an amount of EO component could be lost from DCL suspension. Thus, the storage stability was examined by assessing the total (in suspensions), unloaded (outside vesicles) and loaded (inside vesicles) EO component amount after long term storage. Fig. 4 illustrates the unloaded and the DCL-loaded concentrations of EO component determined on the day of preparation and after 10 months of storage at 4 °C. The ratio of DCL-loaded EO component concentration to the unloaded EO component concentration was calculated, and the values are presented in Fig. 4. In comparison to the initial concentration, a noticeable concentration of EO components remained in DCL suspensions after long term storage. However, a considerable decrease in the DCL-loaded concentration was obtained. By comparing the ratios of DCL-loaded EO component concentration to the unloaded EO component concentration calculated on the day of preparation and after 10 months, we could observe that the selected EO components manifested different retention capabilities in DCLs after long term storage with estragole and terpineol showing the highest retention.

3.8. The advantages of EO component incorporation into DCLs with respect to that into conventional liposomes

In our previous study (Hammoud et al., 2019a) we characterized the encapsulation and the release of the selected EO components from lipoid S100:cholesterol liposomes. By comparing the characteristics of HP-β-CD/EO component-loaded liposomes presented in this study to those of conventional liposomes we found that the DCL carrier system significantly improved the loading ratio of estragole, pulegone, and thymol. These results are in agreement with other studies in literature (Gharib et al., 2017a; Sebaaly et al., 2016a). Also, as expected, DCLs

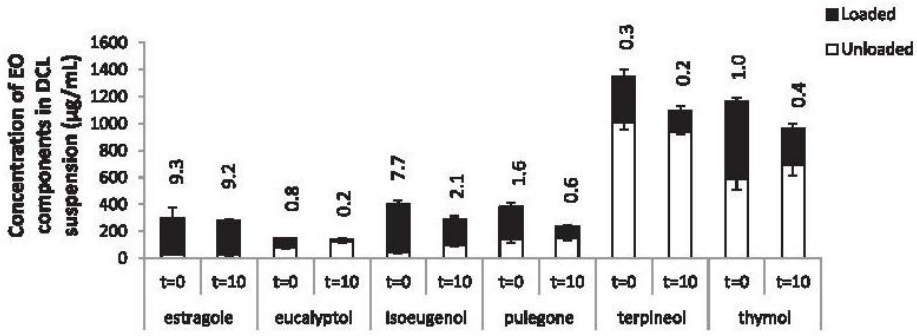

Fig. 4. Storage stability of DCLs: unloaded and DCL-loaded concentrations of EO components determined on the day of preparation and after 10 months of storage at 4 °C. Values above diagrams correspond to the ratio of DCL-loaded EO component concentration to the unloaded EO component concentration.

prolonged the release of all EO components compared to conventional liposomes. Compounds must overcome more barriers to be released from the system (Chen et al., 2014).

4. Conclusion

DCL batches encapsulating several monoterpenes and phenylpropenes were prepared by the ethanol injection method and characterized with respect to their particle size, morphology, EE, LR, release kinetics, and storage stability. The factors that influence DCL characteristics were discussed. The optimal complexation efficiency of EO components into HP-β-CD was high (> 90%) for all EO components, except in the case of terpineol whose complexation efficiency was 72.7 ± 6.8%. Hydroxylated EO components displayed a higher LR into DCLs compared to the non-hydroxylated ones. Also, phenylpropenes were better incorporated into DCLs compared to monoterpenes. In addition, we found a strong positive correlation between the LR of monoterpenes into DCLs and their log P. The release study showed that all the EO components exhibited a slow release from DCLs, and the latter is influenced by the EE of EO component into the formulation. Finally, DCLs were stable after long term storage at 4 °C. The results obtained in this work may allow predicting the ability of lipoid S100-DCL to encapsulate a phenylpropene or a monoterpene compound based on its physiochemical properties. The developed DCL formulations carrying several antimicrobial and antioxidant agents may be suitable for preventing microbial spoilage of the food, cosmetics and pharmaceutical products during storage.

Authors contributions

Z. H. and R. G. performed most of the experiments. Z. H. wrote the manuscript and analyzed the data under the supervision of H. G-G., S. F., and A. ElA. H. G-G. conceived the idea of the paper and supervised the work. All authors have contributed to the writing of the paper and approved its final version.

Declaration of Competing Interest

The authors declare that they have no known competing financial interests or personal relationships that could have appeared to influence the work reported in this paper.

Acknowledgements

This research study was supported by the Research Funding Program at the Lebanese University and the "Agence Universitaire de la Francophonie, Projet de Coopération Scientifique Inter-Universitaire 2018-2020."

Appendix A. Supplementary material

Supplementary data to this article can be found online at https://doi.org/10.1016/j.ijpharm.2020.119151.

References

Azzi, J., Auezova, L., Danjou, P.-E., Fourmentin, S., Greige-Gerges, H., 2018. First evaluation of drug-in-cyclodextrin-in-liposomes as an encapsulating system for nerolidol. Food Chem. 255, 399–404. https://doi.org/10.1016/j.foodchem.2018.02.055.

Bakkali, F., Averbeck, S., Averbeck, D., Idaomar, M., 2008. Biological effects of essential oils–a review. Food Chem. Toxicol. Int. J. Publ. Br. Ind. Biol. Res. Assoc. 46, 446–475. https://doi.org/10.1016/j.fct.2007.09.106.

Bragagni, M., Maestrelli, F., Mennini, N., Ghelardini, C., Mura, P., 2010. Liposomal formulations of prilocaine: effect of complexation with hydroxypropyl-ß-cyclodextrin on drug anesthetic efficacy. J. Liposome Res. 20, 315–322. https://doi.org/10.3109/08982100903544169.

Cavalcanti, I.M.F., Mendonça, E.A.M., Lira, M.C.B., Honrato, S.B., Camara, C.A., Amorim, R.V.S., Filho, J.M., Rabello, M.M., Hernandes, M.Z., Ayala, A.P., Santos-Magalhães, N.S., 2011. The encapsulation of β-lapachone in 2-hydroxypropyl-β-cyclodextrin inclusion complex into liposomes: A physicochemical evaluation and molecular modeling approach. Eur. J. Pharm. Sci. 44, 332–340. https://doi.org/10.1016/j.ejps.2011.08.011.

Chen, H., Gao, J., Wang, F., Liang, W., 2007. Preparation, characterization and pharmacokinetics of liposomes-encapsulated cyclodextrins inclusion complexes for hydrophobic drugs. Drug Deliv. 14, 201–208. https://doi.org/10.1080/10717540601036880.

Chen, J., Lu, W.-L., Gu, W., Lu, S.-S., Chen, Z.-P., Cai, B.-C., Yang, X.-X., 2014. Drug-in-cyclodextrin-in-liposomes: a promising delivery system for hydrophobic drugs. Expert Opin. Drug Deliv. 11, 565–577. https://doi.org/10.1517/17425247.2014.884557.

Ciobanu, A., Landy, D., Fourmentin, S., 2013. Complexation efficiency of cyclodextrins for volatile flavor compounds. Food Res. Int. 53, 110–114. https://doi.org/10.1016/j.foodres.2013.03.048.

Cristani, M., D'Arrigo, M., Mandalari, G., Castelli, F., Sarpietro, M.G., Micieli, D., Venuti, V., Bisignano, G., Saija, A., Trombetta, D., 2007. Interaction of four monoterpenes contained in essential oils with model membranes: implications for their antibacterial activity. J. Agric. Food Chem. 55, 6300–6308. https://doi.org/10.1021/jf070094x.

de Oliveira, M.G.B., Marques, R.B., de Santana, M.F., Santos, A.B.D., Brito, F.A., Barreto, E.O., De Sousa, D.P., Almeida, F.R.C., Badauê-Passos, D., Antoniolli, A.R., Quintans-Júnior, L.J., 2012. α-terpineol reduces mechanical hypernociception and inflammatory response. Basic Clin. Pharmacol. Toxicol. 111, 120–125. https://doi.org/10.1111/j.1742-7843.2012.00875.x.

de Sousa, D.P., Nóbrega, F.F.F., de Lima, M.R.V., de Almeida, R.N., 2011. Pharmacological activity of (R)-(+)-pulegone, a chemical constituent of essential oils. Z. Naturforschung C J. Biosci. 66, 353–359.

Denz, M., Haralampiev, I., Schiller, S., Szente, L., Herrmann, A., Huster, D., Müller, P., 2016. Interaction of fluorescent phospholipids with cyclodextrins. Chem. Phys. Lipids 194, 37–48. https://doi.org/10.1016/j.chemphyslip.2015.07.017.

Dogan, G., Kara, N., Bagci, E., Gur, S., 2017. Chemical composition and biological activities of leaf and fruit essential oils from Eucalyptus camaldulensis. Z. Für Naturforschung C 72. https://doi.org/10.1515/znc-2016-0033.

Domazou, A.S., Luigi Luisi, P., 2002. Size distribution of spontaneously formed liposomes by the alcohol injection method. J. Liposome Res. 12, 205–220. https://doi.org/10.1081/LPR-120014758.

Gharib, R., Auezova, L., Charcosset, C., Greige-Gerges, H., 2018a. Effect of a series of essential oil molecules on DPPC membrane fluidity: a biophysical study. J. Iran. Chem. Soc. 15, 75–84. https://doi.org/10.1007/s13738-017-1210-1.

Gharib, R., Auezova, L., Charcosset, C., Greige-Gerges, H., 2017a. Drug-in-cyclodextrin-in-liposomes as a carrier system for volatile essential oil components: Application to anethole. Food Chem. 218, 365–371. https://doi.org/10.1016/j.foodchem.2016.09.110.

Gharib, R., Fourmentin, S., Charcosset, C., Greige-Gerges, H., 2018b. Effect of hydroxypropyl-β-cyclodextrin on lipid membrane fluidity, stability and freeze-drying of liposomes. J. Drug Deliv. Sci. Technol. 44, 101–107. https://doi.org/10.1016/j.jddst.2017.12.009.

Gharib, R., Greige-Gerges, H., Fourmentin, S., Charcosset, C., Auezova, L., 2015. Liposomes incorporating cyclodextrin–drug inclusion complexes: Current state of knowledge. Carbohydr. Polym. 129, 175–186. https://doi.org/10.1016/j.carbpol.2015.04.048.

Gharib, R., Haydar, S., Charcosset, C., Fourmentin, S., Greige-Gerges, H., 2019. First study on the release of a natural antimicrobial agent, estragole, from freeze-dried delivery systems based on cyclodextrins and liposomes. J. Drug Deliv. Sci. Technol. 52, 794–802. https://doi.org/10.1016/j.jddst.2019.05.032.

Gharib, R., Najjar, A., Auezova, L., Charcosset, C., Greige-Gerges, H., 2017b. Interaction of selected phenylpropenes with dipalmitoylphosphatidylcholine membrane and their relevance to antibacterial activity. J. Membr. Biol. 250, 259–271. https://doi.org/10.1007/s00232-017-9957-y.

Grauby-Heywang, C., Turlet, J.-M., 2008. Study of the interaction of beta-cyclodextrin with phospholipid monolayers by surface pressure measurements and fluorescence microscopy. J. Colloid Interface Sci. 322, 73–78. https://doi.org/10.1016/j.jcis.2008.03.025.

Griffin, S., Wyllie, S.G., Markham, J., 1999. Determination of octanol-water partition coefficient for terpenoids using reversed-phase high-performance liquid chromatography. J. Chromatogr. A 864, 221–228.

Hammoud, Z., Gharib, R., Fourmentin, S., Elaissari, A., Greige-Gerges, H., 2019a. New findings on the incorporation of essential oil components into liposomes composed of lipoid S100 and cholesterol. Int. J. Pharm. 561, 161–170. https://doi.org/10.1016/j.ijpharm.2019.02.022.

Hammoud, Z., Khreich, N., Auezova, L., Fourmentin, S., Elaissari, A., Greige-Gerges, H., 2019b. Cyclodextrin-membrane interaction in drug delivery and membrane structure maintenance. Int. J. Pharm. 564, 59–76. https://doi.org/10.1016/j.ijpharm.2019.03.063.

Hatzi, P., Mourtas, S.G., Klepetsanis, P., Antimisiaris, S.G., 2007. Integrity of liposomes in presence of cyclodextrins: Effect of liposome type and lipid composition. Int. J. Pharm. 333, 167–176. https://doi.org/10.1016/j.ijpharm.2006.09.059.

HERA, 2012. HERA Risk Assessment of Isoeugenol (Draft) human and environmental risk assessment on ingredients of household cleaning products. Isoeugenol (2012). (CAS 97-54-1).

Jug, M., Mennini, N., Melani, F., Maestrelli, F., Mura, P., 2010. Phase solubility, 1H NMR and molecular modelling studies of bupivacaine hydrochloride complexation with different cyclodextrin derivates. Chem. Phys. Lett. 500, 347–354. https://doi.org/10.1016/j.cplett.2010.10.046.

Kfoury, M., Auezova, L., Fourmentin, S., Greige-Gerges, H., 2014a. Investigation of monoterpenes complexation with hydroxypropyl-β-cyclodextrin. J. Incl. Phenom. Macrocycl. Chem. 80, 51–60. https://doi.org/10.1007/s10847-014-0385-7.

Kfoury, M., Hădărugă, N.G., Hădărugă, D.I., Fourmentin, S., 2016a. Cyclodextrins as encapsulation material for flavors and aroma. In: Encapsulations. Elsevier, pp. 127–192. 10.1016/B978-0-12-804307-3.00004-1.

Kfoury, M., Landy, D., Auezova, L., Greige-Gerges, H., Fourmentin, S., 2014b. Effect of cyclodextrin complexation on phenylpropanoids' solubility and antioxidant activity. Beilstein J. Org. Chem. 10, 2322–2331. https://doi.org/10.3762/bjoc.10.241.

Kfoury, M., Lounès-Hadj Sahraoui, A., Bourdon, N., Laruelle, F., Fontaine, J., Auezova, L., Greige-Gerges, H., Fourmentin, S., 2016b. Solubility, photostability and antifungal activity of phenylpropanoids encapsulated in cyclodextrins. Food Chem. 196, 518–525. https://doi.org/10.1016/j.foodchem.2015.09.078.

Kilsdonk, E.P., Yancey, P.G., Stoudt, G.W., Bangerter, F.W., Johnson, W.J., Phillips, M.C., Rothblat, G.H., 1995. Cellular cholesterol efflux mediated by cyclodextrins. J. Biol. Chem. 270, 17250–17256.

Kirby, C., Gregoriadis, G., 1983. The effect of lipid composition of small unilamellar liposomes containing melphalan and vincristine on drug clearance after injection into mice. Biochem. Pharmacol. 32, 609–615. https://doi.org/10.1016/0006-2952(83)90483-5.

Li, J., Perdue, E.M., 1995. Preprints of Papers Presented at the 209th ACS National Meeting. Anaheim, CA, pp. 134–137.

Maestrelli, F., González-Rodríguez, M.L., Rabasco, A.M., Ghelardini, C., Mura, P., 2010. New "drug-in cyclodextrin-in deformable liposomes" formulations to improve the therapeutic efficacy of local anaesthetics. Int. J. Pharm. 395, 222–231. https://doi.org/10.1016/j.ijpharm.2010.05.046.

Maestrelli, F., González-Rodríguez, M.L., Rabasco, A.M., Mura, P., 2005. Preparation and characterisation of liposomes encapsulating ketoprofen–cyclodextrin complexes for transdermal drug delivery. Int. J. Pharm. 298, 55–67. https://doi.org/10.1016/j.ijpharm.2005.03.033.

Malanga, M., Szemán, J., Fenyvesi, É., Puskás, I., Csabai, K., Gyémánt, G., Fenyvesi, F., Szente, L., 2016. "Back to the Future": A New Look at Hydroxypropyl Beta-Cyclodextrins. J. Pharm. Sci. 105, 2921–2931. https://doi.org/10.1016/j.xphs.2016.04.034.

McCormack, B., Gregoriadis, G., 1994. Drugs-in-cyclodextrins-in liposomes: a novel concept in drug delivery. Int. J. Pharm. 112, 249–258. https://doi.org/10.1016/0378-5173(94)90361-1.

Melo Júnior, J. de M. de A. de, Damasceno, M. de B.M.V., Santos, S.A.A.R., Barbosa, T.M., Araújo, J.R.C., Vieira-Neto, A.E., Wong, D.V.T., Lima-Júnior, R.C.P., Campos, A.R., 2017. Acute and neuropathic orofacial antinociceptive effect of eucalyptol. Inflammopharmacology 25, 247–254. 10.1007/s10787-017-0324-5.

Milles, S., Meyer, T., Scheidt, H.A., Schwarzer, R., Thomas, L., Marek, M., Szente, L., Bittman, R., Herrmann, A., Günther Pomorski, T., Huster, D., Müller, P., 2013. Organization of fluorescent cholesterol analogs in lipid bilayers - lessons from cyclodextrin extraction. Biochim. Biophys. Acta 1828, 1822–1828. https://doi.org/10.1016/j.bbamem.2013.04.002.

de Miranda, J.C., Martins, T.E.A., Veiga, F., Ferraz, H.G., 2011. Cyclodextrins and ternary complexes: technology to improve solubility of poorly soluble drugs. Braz. J. Pharm. Sci. 47, 665–681. https://doi.org/10.1590/S1984-82502011000400003.

Moghimipour, E., Aghel, N., Zarei Mahmoudabadi, A., Ramezani, Z., Handali, S., 2012. Preparation and characterization of liposomes containing Essential oil of eucalyptus camaldulensis leaf. Jundishapur J. Nat. Pharm. Prod. 7, 117–122.

Monteiro, N., Martins, A., Reis, R.L., Neves, N.M., 2014. Liposomes in tissue engineering and regenerative medicine. 20140459–20140459. J. R. Soc. Interface 11. https://doi.org/10.1098/rsif.2014.0459.

Nishijo, J., Mizuno, H., 1998. Interactions of cyclodextrins with DPPC liposomes. Differential scanning calorimetry studies. Chem. Pharm. Bull. (Tokyo) 46, 120–124.

Nishijo, J., Shiota, S., Mazima, K., Inoue, Y., Mizuno, H., Yoshida, J., 2000. Interactions of cyclodextrins with dipalmitoyl, distearoyl, and dimyristoyl phosphatidyl choline liposomes. A study by leakage of carboxyfluorescein in inner aqueous phase of unilamellar liposomes. Chem. Pharm. Bull. (Tokyo) 48, 48–52.

Ohvo-Rekilä, H., Akerlund, B., Slotte, J.P., 2000. Cyclodextrin-catalyzed extraction of fluorescent sterols from monolayer membranes and small unilamellar vesicles. Chem. Phys. Lipids 105, 167–178.

Ono, N., Arima, H., Hirayama, F., Uekama, K., 2001. A moderate interaction of maltosyl-alpha-cyclodextrin with Caco-2 cells in comparison with the parent cyclodextrin. Biol. Pharm. Bull. 24, 395–402.

Phan, H.T.T., Yoda, T., Chahal, B., Morita, M., Takagi, M., Vestergaard, M.C., 2014. Structure-dependent interactions of polyphenols with a biomimetic membrane system. Biochim. Biophys. Acta BBA - Biomembr. 1838, 2670–2677. https://doi.org/10.1016/j.bbamem.2014.07.001.

Piel, G., Piette, M., Barillaro, V., Castagne, D., Evrard, B., Delattre, L., 2007. Study of the relationship between lipid binding properties of cyclodextrins and their effect on the integrity of liposomes. Int. J. Pharm. 338, 35–42. https://doi.org/10.1016/j.ijpharm.2007.01.015.

Piel, G., Piette, M., Barillaro, V., Castagne, D., Evrard, B., Delattre, L., 2006. Betamethasone-in-cyclodextrin-in-liposome: The effect of cyclodextrins on encapsulation efficiency and release kinetics. Int. J. Pharm. 312, 75–82. https://doi.org/10.1016/j.ijpharm.2005.12.044.

Pubchem; CID 6989 [WWW Document], n.d. URL https://pubchem.ncbi.nlm.nih.gov/compound/6989 (accessed 3.10.19).

Pubchem; CID 8815 [WWW Document], n.d. URL https://pubchem.ncbi.nlm.nih.gov/compound/8815 (accessed 3.10.19).

Pubchem; CID 853433 [WWW Document], n.d. URL https://pubchem.ncbi.nlm.nih.gov/compound/853433 (accessed 3.10.19).

Pubchem CID:853433, n.d.

Puglisi, G., Fresta, M., Ventura, C.A., 1996. Interaction of Natural and Modified β-Cyclodextrins with a Biological Membrane Model of Dipalmitoylphosphatidylcholine. J. Colloid Interface Sci. 180, 542–547. https://doi.org/10.1006/jcis.1996.0335.

Reiner, G.N., Perillo, M.A., García, D.A., 2013. Effects of propofol and other GABAergic phenols on membrane molecular organization. Colloids Surf. B Biointerfaces 101, 61–67. https://doi.org/10.1016/j.colsurfb.2012.06.004.

Riella, K.R., Marinho, R.R., Santos, J.S., Pereira-Filho, R.N., Cardoso, J.C., Albuquerque-Junior, R.L.C., Thomazzi, S.M., 2012. Anti-inflammatory and cicatrizing activities of thymol, a monoterpene of the essential oil from Lippia gracilis, in rodents. J. Ethnopharmacol. 143, 656–663. https://doi.org/10.1016/j.jep.2012.07.028.

Saokham, P., Muankaew, C., Jansook, P., Loftsson, T., 2018. Solubility of cyclodextrins and drug/cyclodextrin complexes. Molecules 23, 1161. https://doi.org/10.3390/molecules23051161.

Sebaaly, C., Charcosset, C., Stainmesse, S., Fessi, H., Greige-Gerges, H., 2016a. Clove essential oil-in-cyclodextrin-in-liposomes in the aqueous and lyophilized states: From laboratory to large scale using a membrane contactor. Carbohydr. Polym. 138, 75–85. https://doi.org/10.1016/j.carbpol.2015.11.053.

Sebaaly, C., Greige-Gerges, H., Stainmesse, S., Fessi, H., Charcosset, C., 2016b. Effect of composition, hydrogenation of phospholipids and lyophilization on the characteristics of eugenol-loaded liposomes prepared by ethanol injection method. Food Biosci. 15, 1–10. https://doi.org/10.1016/j.fbio.2016.04.005.

Sebaaly, C., Jraij, A., Fessi, H., Charcosset, C., Greige-Gerges, H., 2015. Preparation and characterization of clove essential oil-loaded liposomes. Food Chem. 178, 52–62. https://doi.org/10.1016/j.foodchem.2015.01.067.

Storti, F., Balsamo, F., 2010. Particle size distributions by laser diffraction: sensitivity of granular matter strength to analytical operating procedures. Solid Earth 1, 25–48. https://doi.org/10.5194/se-1-25-2010.

Szejtli, J., 1998. Introduction and general overview of cyclodextrin chemistry. Chem. Rev. 98, 1743–1754. https://doi.org/10.1021/cr970022c.

Szente, L., Singhal, A., Domokos, A., Song, B., 2018. Cyclodextrins: assessing the impact of cavity size, occupancy, and substitutions on cytotoxicity and cholesterol homeostasis. Molecules 23, 1228. https://doi.org/10.3390/molecules23051228.

Takino, T., Konishi, K., Takakura, Y., Hashida, M., 1994. Long circulating emulsion carrier systems for highly lipophilic drugs. Biol. Pharm. Bull. 17, 121–125. https://doi.org/10.1248/bpb.17.121.

Turek, C., Stintzing, F.C., 2013. Stability of Essential Oils: A Review: Stability of essential oils.... Compr. Rev. Food Sci. Food Saf. 12, 40–53. https://doi.org/10.1111/1541-4337.12006.

US EPA, 2012. Estimation Program Interface (EPI) Suite. Ver. 4.1.

Wang, J., Cao, Y., Sun, B., Wang, C., 2011. Characterisation of inclusion complex of transferulic acid and hydroxypropyl-β-cyclodextrin. Food Chem. 124, 1069–1075. https://doi.org/10.1016/j.foodchem.2010.07.080.

Wattanasatcha, A., Rengpipat, S., Wanichwecharungruang, S., 2012. Thymol nanospheres as an effective anti-bacterial agent. Int. J. Pharm. 434, 360–365. https://doi.org/10.1016/j.ijpharm.2012.06.017.

Yalkowsky, S.H., Dannenfelser, R.M, 1992. Arizona Database of Aqueous Solubilites. Univ. of AZ, College of Pharmacy.
Yalkowsky, S., He, Y., Jain, P., 2010. Handbook of Aqueous Solubility Data, Second Edition. CRC Press. 10.1201/EBK1439802458.
Zhang, L., Zhang, Z., Li, N., Wang, N., Wang, Y., Tang, S., Xu, L., Ren, Y., 2013. Synthesis and evaluation of a novel β-cyclodextrin derivative for oral insulin delivery and absorption. Int. J. Biol. Macromol. 61, 494–500. https://doi.org/10.1016/j.ijbiomac.2013.08.034.
Zhang, M., Li, J., Jia, W., Chao, J., Zhang, L., 2009. Theoretical and experimental study of the inclusion complexes of ferulic acid with cyclodextrins. Supramol. Chem. 21, 597–602. https://doi.org/10.1080/10610270802596403.
Zhu, Q., Guo, T., Xia, D., Li, X., Zhu, C., Li, H., Ouyang, D., Zhang, J., Gan, Y., 2013. Pluronic F127-modified liposome-containing tacrolimus-cyclodextrin inclusion complexes: improved solubility, cellular uptake and intestinal penetration: Liposome-containing CD inclusion complex. J. Pharm. Pharmacol. 65, 1107–1117. https://doi.org/10.1111/jphp.12074.

Supplementary materials

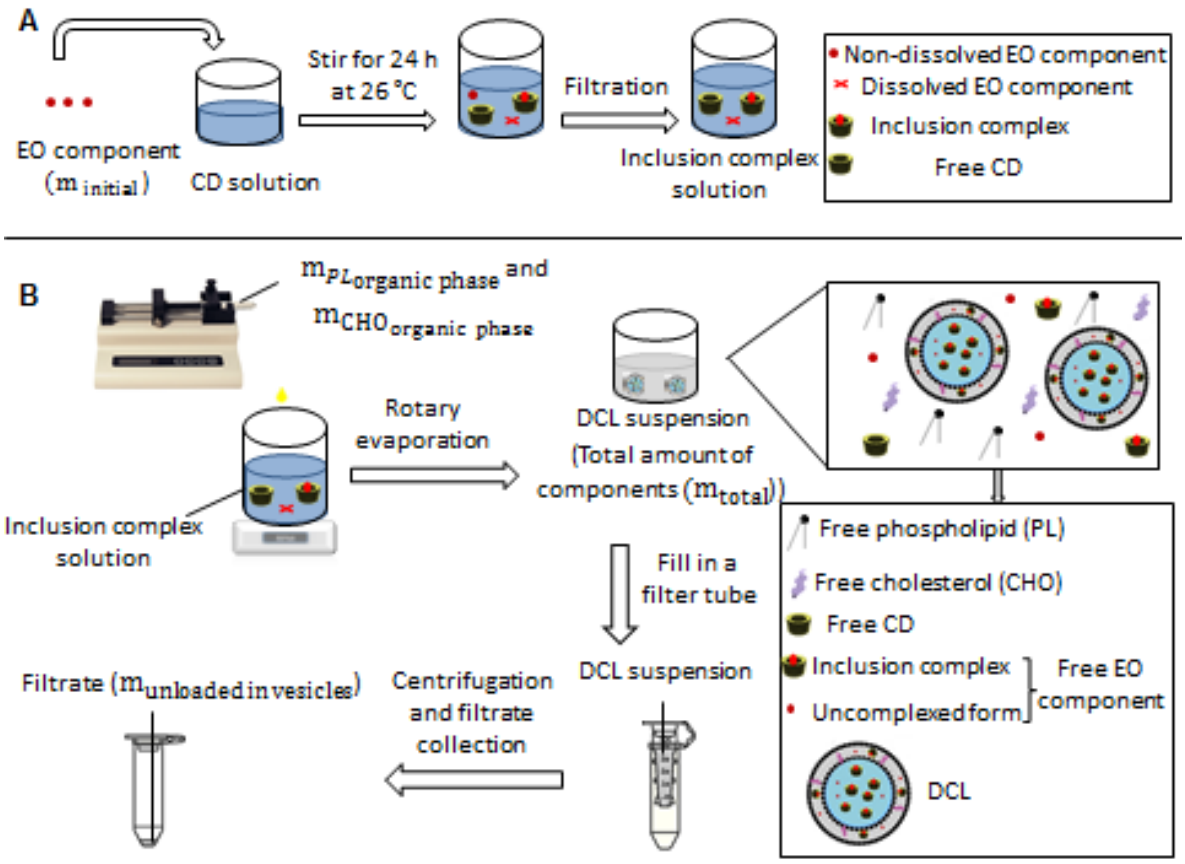

Determination of:

- Phospholipid incorporation ratio: $IR_{PL}\ (\%) = \frac{m_{PL_{total}} - m_{PL_{unloaded}}}{m_{PL_{organic\ phase}}} \times 100$
- Cholesterol incorporation ratio: $IR_{CHO}\ (\%) = \frac{m_{CHO\ total} - m_{CHO\ unloaded}}{m_{CHO\ organic\ phase}} \times 100$
- EO component Loading ratio: $LR\ (\%) = \frac{m_{EO\ component\ total} - m_{EO\ component\ unloaded}}{m_{initial}} \times 100$
- EO component EE: $EE\ (\%) = \frac{[EO\ component]_{total} - [EO\ component]_{unloaded}}{[EO\ component]_{total}} \times 100$

Figure S1: A: Preparation of cyclodextrin/EO component inclusion complex; B: Preparation of drug-in-cyclodextrin-in-liposomes and determination of phospholipid and cholesterol incorporation ratio, EO component encapsulation efficiency and EO component loading ratio.

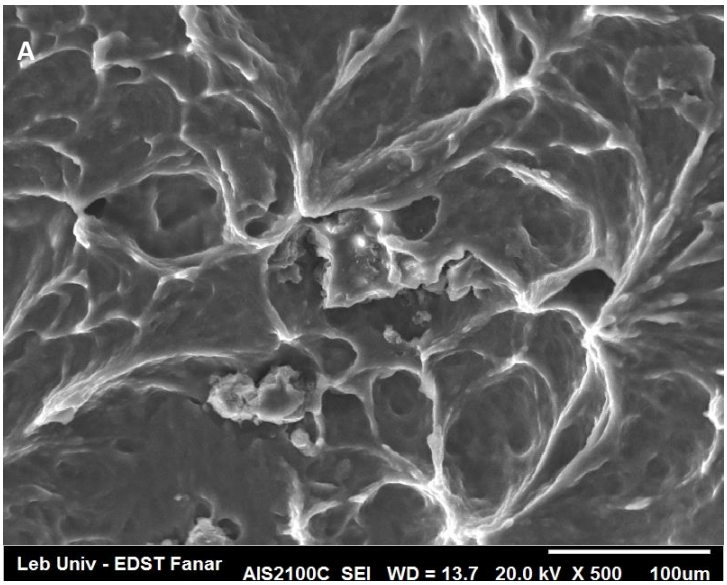
A
Leb Univ - EDST Fanar
AIS2100C SEI WD = 13.7 20.0 kV X 500 100um

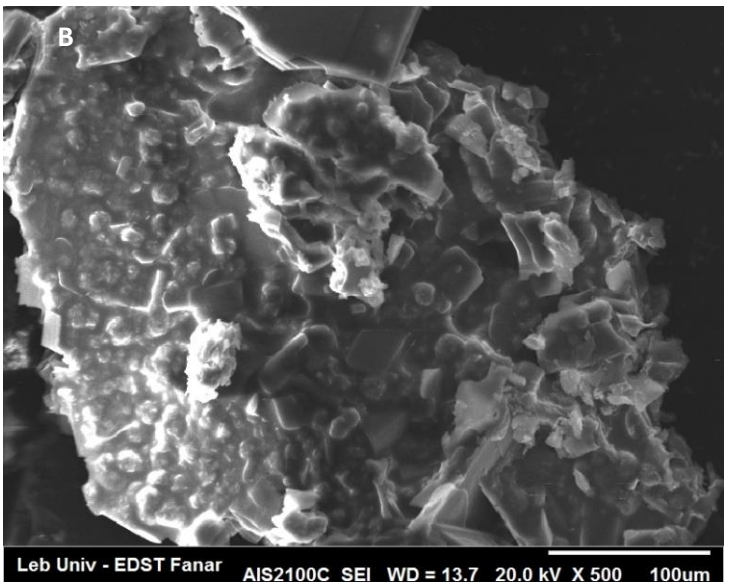
B
Leb Univ - EDST Fanar
AIS2100C SEI WD = 13.7 20.0 kV X 500 100um

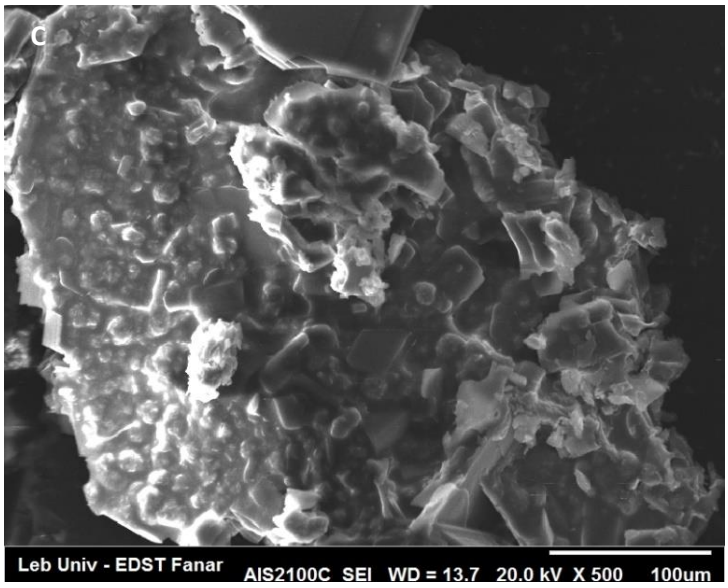
C
Leb Univ - EDST Fanar
AIS2100C SEI WD = 13.7 20.0 kV X 500 100um

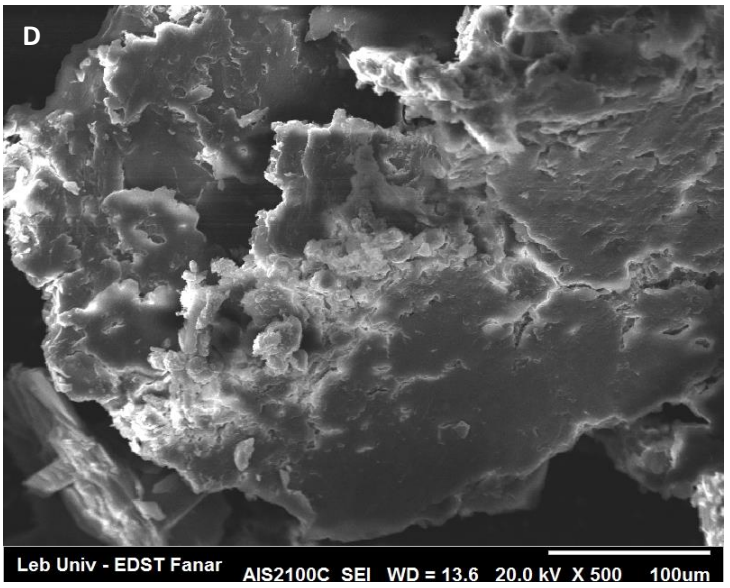
D
Leb Univ - EDST Fanar
AIS2100C SEI WD = 13.6 20.0 kV X 500 100um

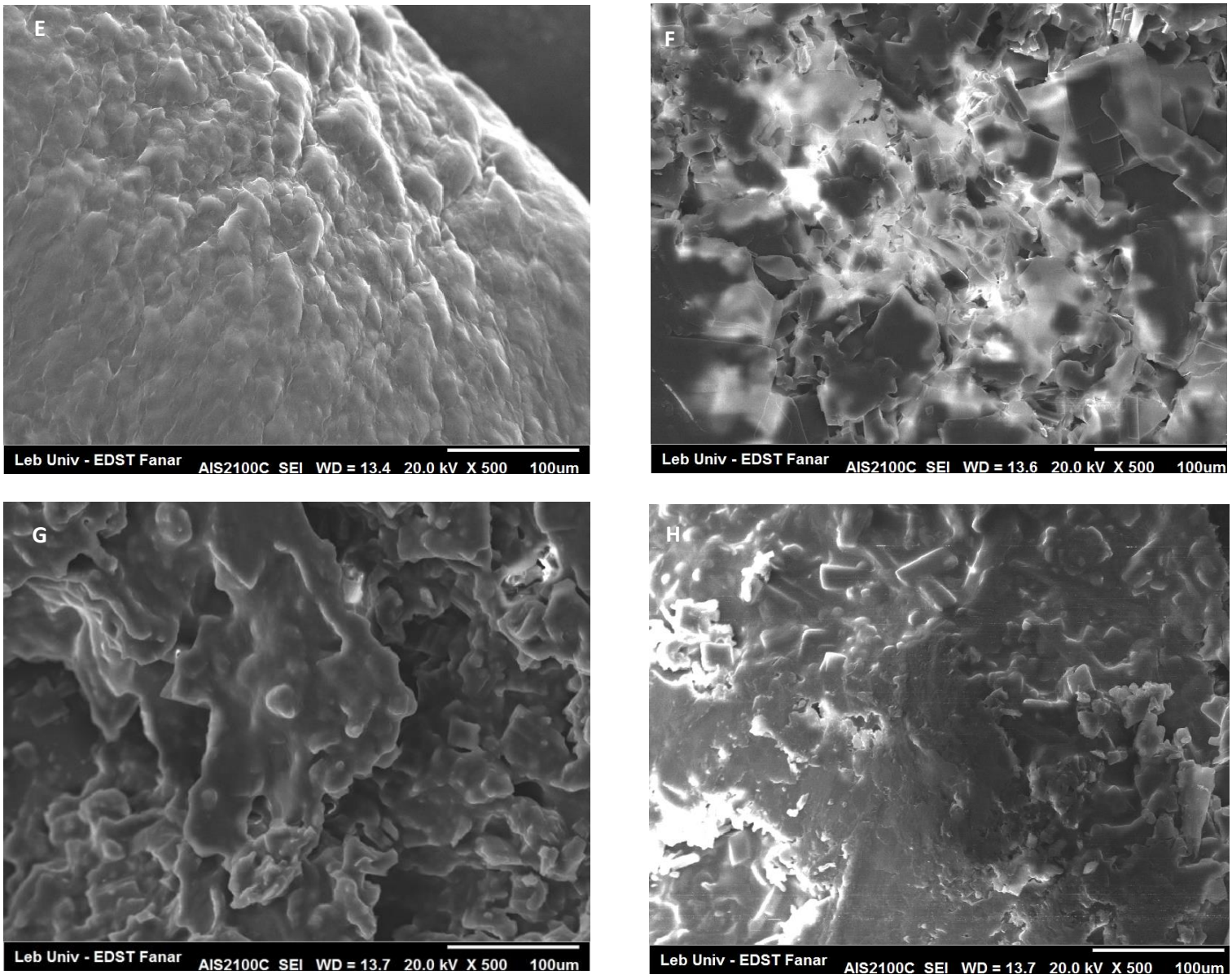

Figure S2: SEM micrographs for blank DCL of HP-β-CD concentration 25 mM (A), blank DCL of HP-β-CD concentration 75 mM (B), estragole- (C), eucalyptol- (D), isoeugenol- (E), pulegone- (F), terpineol- (G), and thymol-(H) loaded DCLs.

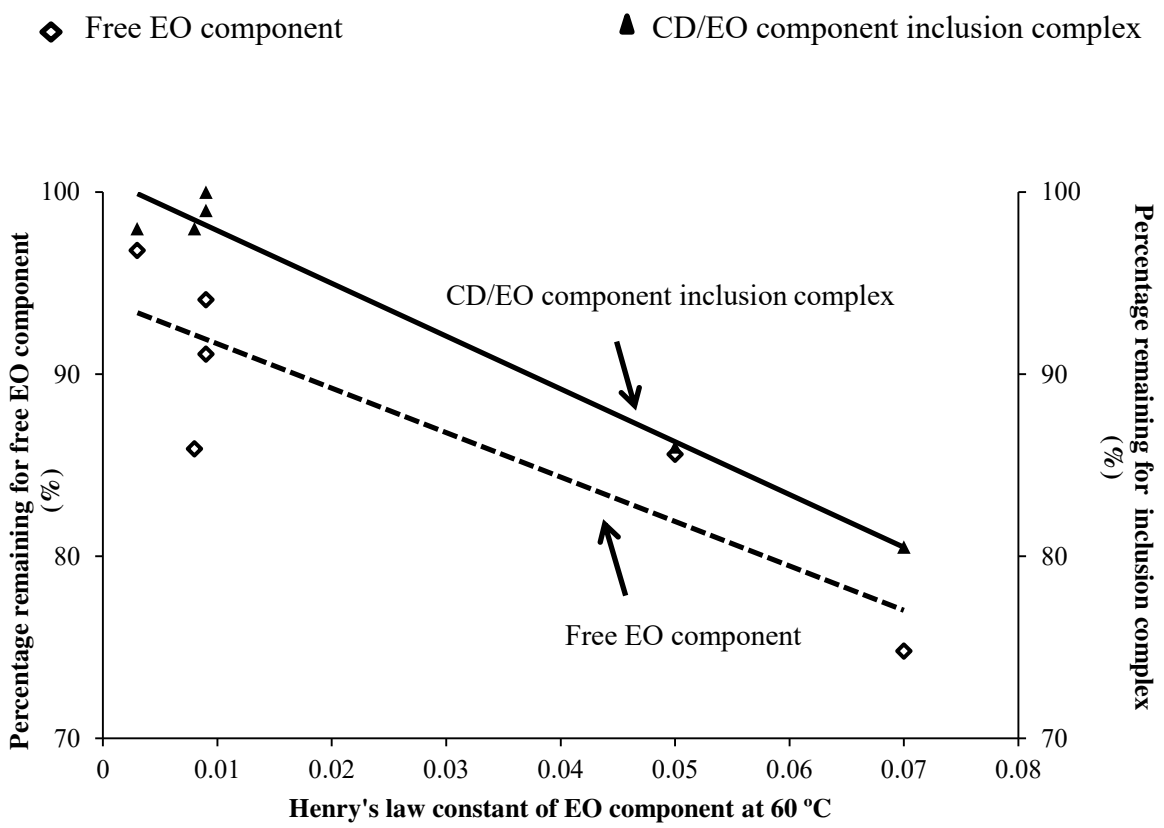

Figure S3: Relationship between the percentages of free EO component and HP-β-CD/EO component inclusion complex remaining at the last extraction step and the Henry's law constant value of EO component determined at 60 ºC.

Chapter 4

Preparation and characterization of liposomes and drug-in-cyclodextrin-in-liposomes carrying the natural bio-insecticides: α-pinene and camphor

Introduction

Several studies had focused on the use of EOs for the control of different pests. *Rosmarinus officinalis* L. oil was considered as an effective insecticide against various insect and mite species (Isman et al., 2008; Tak et al., 2016). The major components of *Rosmarinus officinalis* EO, identified by gas chromatography coupled to mass spectroscopy, were the MTs: EUC, CAM and α-PIN (Abada et al., 2019). Also, the insecticidal activity of α-PIN and CAM was investigated in several studies. For instance, the insect repellent activity of CAM was investigated against mosquitos and against the beetles *Sitophilus granarius, S. zeamais, Tribolium castaneum and Prostephanus truncates* (Obeng-Ofori et al., 1998; Seyoum et al., 2003, 2002). Besides, CAM showed contact and fumigant activity against the grain storage insects *Sitophilus oryzae* and *Rhyzopertha dominica* (Rozman et al., 2007). On the other hand, the repellent, contact and fumigant activities of α-PIN were investigated against head lice and against the maize weevil, *Sitophilus zeamai* (Dambolena et al., 2016; Langsi et al., 2020). Hence, these two MTs were selected in this work. Nevertheless, constraints related to their volatility (estimated H_c of 13×10^{-2} and 8.31×10^{-5} atm m^3/mol at 25ºC for α-PIN and CAM, respectively), readiness for oxidation and poor water solubility (2.5 and 1600 mg/L at 25 ºC for α-PIN and CAM, respectively) should be solved before their industrial application (Neeman et al., 2017; Pavlovic and Hopke, 2009; Sirtori et al., 2006). Their encapsulation is a possible solution to overcome the drawbacks related to their physicochemical properties.

According to the results discussed in the previous chapter and before conducting the experimental studies, we used to estimate the degree of encapsulation of α-PIN and CAM into Lipoid S100-CLs and DCLs based on their physiocochemical properties (log P, aquous

solubility). Briefly, we supposed that CAM will show a little retention into CLs and DCLs while α-PIN will be highly entrapped into both types of formulations.

In this work, we characterized the encapsulation of α-PIN and CAM into CLs and DCLs with the aim to select the appropriate formulation to be applied for insect pest management. In combination with CHOL, the saturated (Phospholipon 90H) or unsaturated (Lipoid S100) PLs are used for the preparation of vesicles. This chapter is presented in the form of two research articles. The first article, which is under consideration in "Processes", shows the characteristics of CLs and DCLs loading α-PIN. The second article presents the characteristics of CAM-loaded liposomes and DCLs, and is still in preparation.

The ethanol injection method was applied to prepare the vesicles. Four liposome formulations were prepared: (1) blank CLs, (2) HP-β-CD-loaded liposomes; (3) drug-loaded liposomes; (4) drug-loaded DCLs. The obtained formulations were characterized with respect to their size using laser granulometry. Also, the IR of PLs and CHOL were calculated. The EE and LR values of drugs were determined by high performance liquid chromatography (HPLC) methods. The stability of the liposome formulations was assessed after 3 months of storage at 4 ºC.

The results showed that the addition of HP-β-CD enhanced the solubility of α-PIN and CAM; the optimal solubilization occurred at HP-β-CD concentration of 50 and 75 mM for CAM and α-PIN, respectively. Compared to CLs, DCLs improved the LR of CAM; however, they did not ameliorate that of α-PIN. Furthermore, the highest encapsulation yield values for both drugs were obtained with Lipoid S100. Lipoid S100 CLs and lipoid S100 DCLs were the best systems showing efficient encapsulation of α-PIN and CAM, respectively. Finally, all formulations

composed either of saturated or unsaturated PLs effectively retained the studied insecticidal agents during 3 months of storage at 4 ºC.

References

Abada, M.B., Hamdi, S.H., Gharib, R., Messaoud, C., Fourmentin, S., Greige-Gerges, H., Jemâa, J.M.B., 2019. Post-harvest management control of Ectomyelois ceratoniae (Zeller) (Lepidoptera: Pyralidae): new insights through essential oil encapsulation in cyclodextrin. Pest Manag. Sci. 75, 2000–2008.

Dambolena, J.S.; Zunino, M.P.; Herrera, J.M.; Pizzolitto, R.P.; Areco, V.A.; Zygadlo, J.A., 2016. Terpenes: Natural Products for Controlling Insects of Importance to Human Health—A Structure-Activity Relationship Study. Psyche J. Entomol., 2016, 1–17.

Isman, M.B., Wilson, J.A., Bradbury, R., 2008. Insecticidal Activities of Commercial Rosemary Oils (Rosmarinus officinalis .) Against Larvae of Pseudaletia unipuncta . and Trichoplusia ni . in Relation to Their Chemical Compositions. Pharm. Biol. 46, 82–87.

Langsi, J.D., Nukenine, E.N., Oumarou, K.M., Moktar, H., Fokunang, C.N., Mbata, G.N., 2020. Evaluation of the Insecticidal Activities of α-Pinene and 3-Carene on Sitophilus zeamais Motschulsky (Coleoptera: Curculionidae). Insects 11, 540.

Neeman, E.M.; Avilés Moreno, J.R.; Huet, T.R, 2017. The gas phase structure of α-pinene, a main biogenic volatile organic compound. J. Chem. Phys, 147, 214305.

Obeng-Ofori, D., Reichmuth, C.H., Bekele, A.J., Hassanali, A., 1998. Toxicity and protectant potential of camphor, a major component of essential oil of Ocimum kilimandscharicum, against four stored product beetles. Int. J. Pest Manag. 44, 203–209.

Pavlovic, J.; Hopke, P.K, 2009. Technical Note: Detection and identification of radical species formed from α-pinene/ozone reaction using DMPO spin trap. Atmospheric Chem. Phys. Discuss 9, 23695–23717.

Rozman, V., Kalinovic, I., Korunic, Z., 2007. Toxicity of naturally occurring compounds of Lamiaceae and Lauraceae to three stored-product insects. J. Stored Prod. Res. 43, 349–355.

Seyoum, A., Killeen, G.F., Kabiru, E.W., Knols, B.G.J., Hassanali, A., 2003. Field efficacy of thermally expelled or live potted repellent plants against African malaria vectors in western Kenya. Trop. Med. Int. Health 8, 1005–1011.

Seyoum, A., Pålsson, K., Kung'a, S., Kabiru, E.W., Lwande, W., Killeen, G.F., Hassanali, A., Knots, B.G.J., 2002. Traditional use of mosquito-repellent plants in western Kenya and their evaluation in semi-field experimental huts against Anopheles gambiae: ethnobotanical studies and application by thermal expulsion and direct burning. Trans. R. Soc. Trop. Med. Hyg. 96, 225–231.

Sirtori, C., Altvater, P., Freitas, A., Peraltazamora, P., 2006. Degradation of aqueous solutions of camphor by heterogeneous photocatalysis. J. Hazard. Mater. 129, 110–115.

Tak, J.H., Jovel, E., Isman, M.B., 2016. Comparative and synergistic activity of Rosmarinus officinalis L. essential oil constituents against the larvae and an ovarian cell line of the cabbage looper, Trichoplusia ni (Lepidoptera: Noctuidae): Activity of rosemary essential oil constituents against cabbage looper larvae and ovarian cells. Pest Manag. Sci. 72, 474–480.

Article 1

Encapsulation of α-pinene, a natural bio-insecticide, in delivery systems based on liposomes and drug-in-cyclodextrin-in-liposomes

Zahraa Hammoud[1,2], Maya Kayouka[1], Adriana Trifan[3], Elwira Sieniawska[4], Łukasz Świątek[5], Jouda Mediouni Ben Jemâa[6], Abdelhamid Elaissari[2], Hélène Greige-Gerges[1*]

[1]Bioactive Molecules Research Laboratory, Doctoral School of Sciences and Technologies, Faculty of Sciences, Section II, Lebanese University, Lebanon

[2]Univ Lyon, University Claude Bernard Lyon-1, CNRS, LAGEP-UMR 5007, F-69622 Lyon, France

[3]Department of Pharmacognosy, Faculty of Pharmacy, Grigore T. Popa University of Medicine and Pharmacy of Iasi, Iasi, Romania

[4]Department of Pharmacognosy, Medical University of Lublin, 20-093, Lublin, Poland

[5]Department of Virology, Medical University of Lublin, 20-093, Lublin, Poland

[6]Laboratory of Biotechnology Applied to Agriculture, National Agricultural Research Institute of Tunisia (INRAT), University of Carthage, Tunisia

Abstract

The essential oil component α-pinene was reported as bio-insecticide. However, its application in agriculture and food industries is limited owing to its volatility, low aqueous solubility, and chemical instability. For the aim of improving its physicochemical properties, α-pinene was encapsulated in conventional liposomes (CLs) and drug-in-cyclodextrin-in-liposomes (DCLs). Hydroxypropyl-β-cyclodextrin/α-pinene (HP-β-CD/α-pinene) inclusion complexes were prepared in aqueous solution, and the optimal solubilization of α-pinene occurred at 7.5:1 (HP-β-CD:α-pinene) molar ratio. Ethanol-injection method was applied to produce the various formulations using saturated (Phospholipon 90H) or unsaturated (Lipoid S100) phospholipids in combination with cholesterol. The size, the phospholipid and cholesterol incorporation rates, the encapsulation efficiency (EE) and the loading rate (LR) of α-pinene, and the storage stability of liposomes were characterized. The results showed that α-pinene was efficiently entrapped in CLs and DCLs with high EE values. Moreover, Lipoid S100 CLs displayed the highest LR (22.9 ± 2.2%) of α-pinene compared to Lipoid S100 DCLs, Phospholipon 90H CLs, and Phospholipon 90H DCLs. Finally, it was found that all formulations were stable after 3 months of storage at 4 ºC since considerable amounts of α-pinene were retained in the liposome suspensions after 3 months with respect to α-pinene concentrations determined on the day of preparation.

Keywords: α-pinene; drug-in-cyclodextrin-in-liposomes; hydroxypropyl-β-cyclodextrin; insecticide; liposomes.

1. Introduction

Bio-pesticides (including insecticides, herbicides, and fungicides) play an important role in agriculture to improve crop yields and ensure a sustainable food supply [1]. In recent years, various essential oils have been reported as bio-pesticides due to their eco-friendly and biodegradable nature, effectiveness, multiple modes of action, and low toxicity to non-target organisms [2,3]. Alpha-pinene, also called 2,6,6-trimethylbicyclo [3.1.1] hept-2-ene, is a natural bicyclic monoterpene [4]. It is a component of the essential oils of rosemary (genus *Rosmarinus*, species *Rosmarinus officinalis L.*) and several coniferous trees from Pinaceae (genus *Pinus*) and Lamiaceae family (e.g., lavender, genus *Lavandula*) [5,6]. It has been demonstrated that α-pinene possesses insecticidal [7], antioxidant [8], anti-microbial [9,10], anti-inflammatory [11], and anti-tumor [12] effects. In addition, α-pinene is generally recognized as safe (GRAS) by the Food and Drug Administration and other regulatory agencies [13]. Thus, it can be used in the preparation of a wide range of value-added products in the agricultural and food sectors.

The low aqueous solubility (about 2.5 mg/L at 25 ºC), high photosensitivity, and high volatility restrict the application of α-pinene in the control of agricultural pests [14–16]. For instance, Chen et al. (2010) investigated that the photooxidation of α-pinene mainly produced pinocamphone, 3-hydroxy-α-pinene, acetaldehyde, acetone, acetic acid, and carbon dioxide. The authors also demonstrated that the rate of photodegradation increased as the relative humidity level of air (2-3%, 35-40%, and 75-80%) and residence time (18, 45 and 90 s) increased [17].

The development of encapsulation systems loading α-pinene can be utilized to improve the physicochemical properties of the compound and to allow its controlled release from the fabricated matrices [18]. Attempts were made to improve the solubility and the stability of α-

pinene through encapsulation in solid lipid nanoparticles [4], chitosan:gum Arabic microcapsules [19], or cyclodextrins (CDs) [20–22]. CDs, non-toxic cyclic oligosaccharides having a basket-shaped structure with a hydrophilic outer surface and a hydrophobic cavity, increased the solubility and the stability of α-pinene by forming CD/α-pinene inclusion complexes. Compared to α-CD and γ-CD, β-CD and its derivatives (hydroxypropyl-ß-cyclodextrin (HP-β-CD), randomly methylated-β-cyclodextrin, and a low methylated-β-cyclodextrin) were shown to be very effective for α-pinene encapsulation. Alpha-CD and γ-CD exhibit generally lower stability constants and complexation efficiencies with α-pinene compared to β-CD and its derivatives. Moreover, the complexation efficiency of native β-CD is close to that of β-CD derivatives [20].

In parallel, liposomes are specialized delivery vehicles that serve multiple roles in improving the effectiveness of bioactive molecules. They are non-toxic microscopic vesicles with concentric phospholipid bilayers surrounding an inner aqueous core. This structure makes liposomes suitable for entrapping lipophilic, hydrophilic, and amphiphilic substances [23].

The drug-in-cyclodextrin-in-liposomes (DCLs) system is based on the entrapment of lipophilic drugs in the aqueous compartment of liposomes in the form of CD/drug inclusion complexes. This system combines the relative advantages of both carriers [24]. DCLs improved the encapsulation of essential oil components such as eugenol [25], *trans*-anethole [26], estragole [27,28], and thymol [28], delayed drug release [27–29], and prolonged the biological effect of the encapsulated compounds [30,31] in comparison to conventional liposomes.

CDs are capable of removing phospholipids and cholesterol from liposomal membrane, thereby perturbing some of its properties such as its permeability and fluidity [32–34]. The impact of CD on lipid membranes is mediated by several factors including membrane structure and

composition as well as the CD type and the CD concentration [35–37]. HP-β-CD, that was used in the present study to prepare the CD/α-pinene inclusion complex, does not influence the integrity of liposome membranes compared to other CD types [38,39].

In this study, we aimed to develop an appropriate formulation for the effective delivery of α-pinene. For this purpose, α-pinene was encapsulated into CL and DCL systems composed of hydrogenated (Phospholipon 90H) or non-hydrogenated (Lipoid S100) phospholipids using the ethanol-injection method. All the formulations were characterized with respect to their size using laser granulometry. Also, the incorporation rate of phospholipids and cholesterol as well as the encapsulation efficiency and the loading rate of α-pinene were calculated. The stability of the liposome formulations in aqueous solutions was assessed after 3 months of storage at 4 ºC.

2. Results and discussion

2.1. Determination of α-pinene concentration in HP-β-CD/α-pinene inclusion complex solutions

HP-β-CD/α-pinene inclusion complexes were prepared in aqueous solution, and the optimal HP-β-CD:α-pinene molar ratio was determined. Figure 1 shows the variation of α-pinene concentration in HP-β-CD/α-pinene complex solutions at various HP-β-CD concentrations (0-100 mM). In the absence of HP-β-CD, the concentration of α-pinene was 3.2 ± 0.1 µg/mL. This value is in accordance with the value of aqueous solubility found in the literature (2.5 µg/mL) [40]. The addition of HP-β-CD leads to an enhancement of α-pinene solubility up to 366 times at HP-β-CD concentration of 75 mM. CE values permitted the evaluation of the optimal HP-β-CD:α-pinene molar ratio. The CE of α-pinene into HP-β-CD was determined as explained in equation 1. The results are reported in Table 1. The CE of α-pinene was 14.3 ± 1.3% at HP-β-CD:α-pinene molar ratio of 1:1, and the CE increased to 80.6 ± 7.7% at HP-β-CD:α-pinene

molar ratio of 7.5:1. Nevertheless, further increase in HP-β-CD concentration did not improve the CE of α-pinene. Consequently, the HP-β-CD/α-pinene inclusion complex prepared at HP-β-CD:α-pinene molar ratio of 7.5:1 was selected as the aqueous phase for the preparation of DCL batches.

Table 1: The complexation efficiency of α-pinene into HP-β-CD as a function of HP-β-CD:α-pinene molar ratio

HP-β-CD:α-pinene molar ratio	CE (%)
1:1	14.3 ± 1.3
2.5:1	40.6 ± 3.5
5:1	65.4 ± 6.2
7.5:1	80.6 ± 7.7
10:1	76.9 ± 3.8

Figure 1: The variation of α-pinene concentration in the filtrate as a function of HP-β-CD concentration.

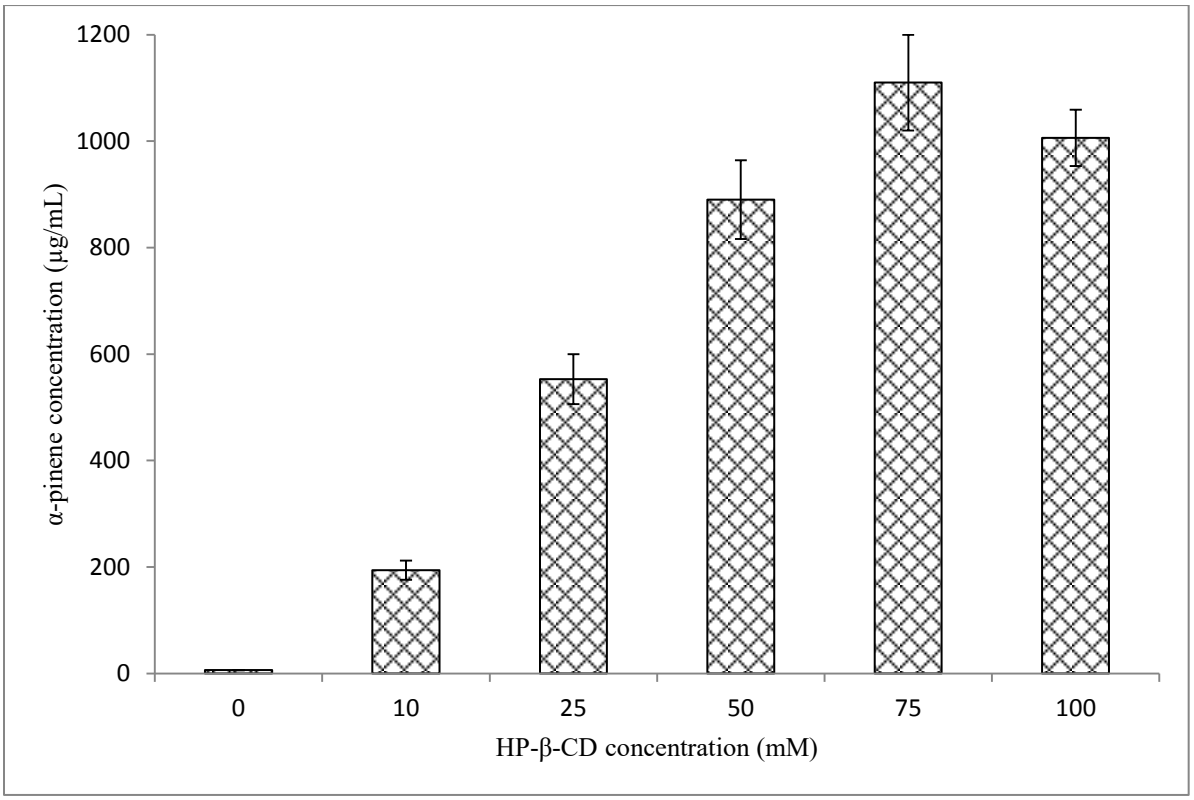

2.2. Characterization of liposome formulations

2.2.1. Determination of liposome particle size

The particle size of the liposomal batches was measured using a laser granulometer. Table 2 represents the percentage distribution and the mean particle size of the populations in each formulation.

Blank Phospholipon 90H:Chol CLs presented two distinct populations: a nanometric sized population with a mean size of 150 ± 0.0 nm and a micrometric sized population with a mean size of 6.2 ± 0.9 µm; the percentage of nanometric population was 87.7 ± 6.7%. The results are in good agreement with the results of Azzi et al. (2018) [41]. Moreover, it was found that the incorporation of α-pinene in Phospholipon 90H:Chol liposome did not affect the mean vesicle size and the size distribution of the blank batch.

For blank Lipoid S100:Chol CLs, two populations with nanometric (166 ± 33.3 nm) and micrometric (6.7 ± 0.0 µm) sizes were observed. The micrometric population was the major one since it represents 83.0 ± 1.4% of the vesicles. The results are in accordance with our previous study [42]. Compared to blank Lipoid S100:Chol CLs, α-pinene boosted the formation of larger micrometric vesicles. The accumulation of α-pinene in Lipoid S100 liposome membrane may affect the interactions between the acyl chains of phospholipids and induce swelling of the membrane, causing the formation of giant particles [43]. Rodriguez et al. (2018) reported that the incorporation of α-pinene in DPPC lipid membrane induced an increase in the membrane surface pressure and the area per lipid due to the interaction of α-pinene with the acyl chain of lipids forming lipid-α-pinene complex [44]. It is noteworthy that many other essential oil components

induce an increase in liposome particle size like eugenol [25], nerolidol [29], isoeugenol, and thymol [42].

The addition of HP-β-CD and HP-β-CD/α-pinene inclusion complex did not significantly influence the mean vesicle size of blank Phospholipon 90H:Chol formulation, which is in agreement with other studies [26,27,30,31].

HP-β-CD modified the size distribution of blank Lipoid S100:Chol liposomes. A larger population was obtained after the addition of HP-β-CD to lipoid S100 liposomes that is in accordance with our previous results obtained at HP-β-CD concentration of 25 and 75 mM [28]. Also, it was previously demonstrated that the addition of HP-β-CD induced an increase in the fluidity of liposome membrane composed of unsaturated phospholipids and Chol (Lipoid S100:Chol liposomes) while did not influence that of membranes composed of saturated phospholipid and Chol (Phospholipon 80H:Chol and Phospholipon 90H:Chol liposomes) [45]. Alpha-pinene-DCLs had smaller particle size compared to α-pinene-CLs and HP-β-CD-loaded liposomes. When α-pinene was entrapped in HP-β-CD core, the effects of both constituents (α-pinene and HP-β-CD) on liposome membrane were reduced. Same results were reported for the encapsulation of HP-β-CD/eugenol [25], HP-β-CD/isoeugenol, and HP-β-CD/thymol inclusion complexes [28] in liposomes when compared to free HP-β-CD and free guests.

2.2.2. Determination of phospholipid:Chol:α-pinene molar ratio

Phospholipids and Chol IR values, α-pinene EE, and α-pinene LR into the various liposome formulations were determined. Table 2 summarizes the obtained results.

2.2.2.1. Phospholipid incorporation rate

The dosage of phospholipids proved a high IR for Phospholipon 90H (89.5 ± 6.3%) and Lipoid S100 (95.9 ± 1.5%) in blank liposomes. The addition of α-pinene did not greatly influence the loading of Phospholipon 90H in liposome membrane while it reduced that of Lipoid S100. The difference could be attributed to the amount of α-pinene loaded in liposome membrane; the LR value of α-pinene was 0.2 ± 0.01% into Phospholipon 90H vesicles and 22.9 ± 2.2% into Lipoid S100 vesicles.

In the presence of HP-β-CD, the IR of Phospholipon 90H and Lipoid S100 in liposomes markedly decreased compared to the blank formulations, which is in agreement with our previous investigations [28]. This finding might be explained by the ability of CDs to interact with lipid bilayers and to mediate the desorption of lipid components from membranes [32].

In comparison to the blank batches, we noticed that HP-β-CD/α-pinene inclusion complex did not greatly impact the incorporation of phospholipids (either Phospholipon 90H or Lipoid S100) in liposome membranes. This finding implies that α-pinene is completely loaded into the lipophilic core of HP-β-CD, thereby reducing the interactions of both α-pinene and HP-β-CD with the liposome membrane.

2.2.2.2. Cholesterol incorporation rate

Chol quantification assay showed that the IR values of Chol into blank Phospholipon 90H liposomes and blank Lipoid S100 liposomes were 75.9 ± 3.5% and 71.2 ± 5.4%, respectively. These values are approximately consistent with recently published data: 84.2 ± 3.8% into Phospholipon 90H liposomes [41] and 77.6 ± 1.18% into Lipoid S100 liposomes [28,42]. Alpha-

pinene did not modify the Chol content of Phospholipon 90H and Lipoid S100 liposome membranes.

A remarkable decrease in the Chol IR was obtained upon the addition of HP-β-CD to Phospholipon 90H liposomes in comparison to empty vesicles (Table 2). This is determined for the first time in literature. Furthermore, the addition of HP-β-CD did not significantly influence the retention of Chol into Lipoid S100 liposomes in agreement with our previously published data [28]. On the other hand, the loading of HP-β-CD/α-pinene inclusion complex into liposome cavity lowered Chol entrapment in Phospholipon 90H liposomes while it didn't drastically impact the Chol content of Lipoid S100 liposomes in comparison to the blank liposomes. Hence, HP-β-CD may extract Chol molecules from the membrane of Phospholipon 90H:Chol vesicles forming soluble inclusion complexes out of the membrane, while no effect was exerted on Lipoid S100 vesicles. Yancey et al., (1996) proposed that the CD-mediated Chol extraction occurs by Chol desorption from the surface directly into CD hydrophobic core [46]. In addition, Steck et al. (2002) suggested that Chol efflux induced by CDs takes place through an activation-collision mechanism where the reversible partial projection of Chol molecules out of the erythrocyte lipid bilayer precedes their collisional capture by CD [47]. On the other hand, the position and orientation of Chol in saturated and unsaturated lipid bilayers has been widely studied in literature [48–50]. A common conclusion is that in saturated bilayers, Chol is found in traditional "upright" positions with the hydroxyl group oriented towards lipid head-groups, while in unsaturated bilayers, Chol is relatively often found in a "flipped" configuration with the hydroxyl group oriented towards the membrane middle plane. Furthermore, Chol molecules in unsaturated bilayers are often found to form head-to-tail contacts which may lead to specific

clustering behavior. For that, CD-mediated Chol extraction is easier from saturated Phospholipon 90H:Chol membranes compared to unsaturated Lipoid S100:Chol membranes.

2.2.2.3. α-pinene encapsulation efficiency and loading rate

Due to the fact that α-pinene is a highly lipophilic drug, it should be entrapped in the lipid membrane of liposomes. Therefore, the strength of interaction of α-pinene with lipid membrane of liposomes influences its incorporation in vesicles. Also, if we suppose that the hydrophobic compartments of DCLs (CD core and liposome membrane) retain the hydrophobic EO components, the parameters that modulate α-pinene entrapment into DCL vesicles are those related to CD-α-pinene interaction and lipid membrane-α-pinene interaction. The EE and LR of α-pinene into CLs and DCLs were determined, and the results are summarized in Table 2.

Alpha-pinene was highly encapsulated into all CL and DCL formulations. EE values of 100% were obtained for all CL formulations and for Lipoid S100-DCLs; the EE of α-pinene into Phospholipon 90H-DCLs was 72.9 ± 6.8%. The high affinity of α-pinene for both components (CDs and lipid bilayers) could explain the findings; the interaction of α-pinene with CD and lipid bilayer is strong enough to inhibit the release of α-pinene to the outer extracellular medium of CL and DCL systems. Indeed, it was reported that α-pinene possesses a high affinity for DPPC lipid membrane due to its high hydrophobicity and chemical structure that does not contain polar groups. Thus, α-pinene cannot interact directly with the DPPC polar head but it is able to interact with the hydrophobic tails of the lipids. Namely, this small hydrophobic compound adopts a position in the acyl region of the membrane rather than at the lipid-water interface [44]. Besides, it was investigated that the loading of hydrophobic drugs into liposomes increases as the hydrophobicity of the drug increases [42,51]. On the other hand, the strength of CD-guest

interaction depends mainly on the polarity and geometric accommodation between CD cavity and guest [52]. Here, the low molecular weight (136.23 g/mol) and the high hydrophobicity of α-pinene could explain the strong interaction of α-pinene with CD. Moreover, it should be noted that the stability of the inclusion complexes modulate the retention of EO components into DCLs. The formation constant (K_f) values reported in literature for HP-β-CD/α-pinene inclusion complex were 1637 M^{-1} [20] and 2000 M^{-1} [22].

Among both types of phospholipids, the highest LR value was obtained with Lipoid S100, where the LR value of α-pinene into Lipoid S100 liposomes (22.9 ± 2.2 %) was approximately 100 times higher than that of Phospholipon 90H liposomes (0.2 ± 0.02 %). Lipid bilayers composed of Lipoid S100 (unsaturated phospholipid) are less densely packed and more flexible compared to those composed of Phospholipon 90H (saturated phospholipid), leading to greater entrapment of α-pinene into liposome membrane [53]. Also, Lipoid S100 liposomes were fabricated at room temperature while the preparation of Phospholipon 90H liposomes requires heating at 55 ºC, thus promoting the loss of volatile α-pinene.

When compared to α-pinene-Phospholipon 90H CLs, the DCL carrier system did not ameliorate the LR of α-pinene. Additionally, concerning Lipoid S100 formulations, the LR value of α-pinene into DCLs was lower than that of CLs. The LR values into CLs and DCLs were 22.9 ± 2.2% and 0.6 ± 0.02%, respectively (Table 2). Although this result does not corroborate the previous studies where DCL improved the loading of essential oil components compared to CLs [25,26,54,55], it lies with the encapsulation of risperidone into similar formulations (same lipid composition and CD type) where CL proved better encapsulation than DCL [56].

The final liposome composition (phospholipid:Chol:α-pinene molar ratio) was 124:98:0.36, 118:82:0.31, 61:93:42 and 111:92:1 for phospholipon 90H-CLs, phospholipon 90H-DCLs, Lipoid S100-CLs, and Lipoid S100-DCLs, respectively. Based on the characteristics of CLs and DCLs, Lipoid S100:Chol-CL was the best encapsulating system for α-pinene compared to the other formulations. This explains the greatest effect of α-pinene on Lipoid S100-CL membrane compared to other formulations.

The release of various hydrophobic drugs, including EO components, from CLs and DCLs was studied in literature. Most of the studies demonstrated that DCLs are more effective in reducing the release of hydrophobic drugs in comparison to CLs [23]. Also, in a previous work, we showed that the size of liposomes, IR of Chol into vesicles and the LR of EO components are the key factors modulating EOs release from lipoid S-100 liposomes [42].

Table 2: Characteristics of blank CLs, α-pinene-CLs, blank DCLs, and α-pinene-DCLs prepared with Phospholipon 90H or Lipoid S100. The values of size in italic are those obtained after 3 months of storage at 4 ºC.

	Size distribution						Vesicle characterization				
Sample	Population 1		Population 2		Population 3		IR of PL (%)	IR of Chol (%)	EE of α-pinene (%)	LR of α-pinene (%)	Final PL:Chol:α-pinene molar ratio
	%	Mean size (nm)	%	Mean size (μm)	%	Mean size (μm)					
Phospholipon 90H:Chol formulations											
Blank CLs	87.7 ± 6.7 *87.3 ± 6.5*	150 ± 0.0 *150 ± 0.0*	12.3 ± 6.7 *12.7 ± 6.5*	6.2 ± 0.9 *6.2 ± 0.5*	-	-	89.5 ± 6.3	75.9 ± 3.5	-	-	122:98:0
α-pinene-CLs	84.3 ± 7.2 *82.5 ± 11.6*	140 ± 13.4 *123 ± 25.4*	15.7 ± 7.2 *17.5 ± 11.6*	7.7 ± 0.0 *7.7 ± 0.0*	-	-	88.6 ± 6.0	76.3 ± 4.3	100.0 ± 0.0	0.2 ± 0.01	124:98:0.36
Blank DCLs	72.3 ± 7.3 *61.0 ± 5.8*	140 ± 10.9 *131 ± 0.0*	27.7 ± 7.3 *17.7 ± 1.3*	6.1 ± 0.8 *6.6 ± 0.2*	- *21.3 ± 7.1*	- *48.3 ± 4.8*	66.5 ±3.9	41.1 ± 1.3	-	-	90:59:0
α-pinene-DCLs	82.5 ± 1.9 *74.3 ± 2.2*	140 ± 10.9 *115 ± 17.8*	17.5 ± 1.9 *10.8 ± 1.3*	5.7 ± 0.4 *5.8 ± 0.6*	- *14.9 ± 2.0*	- *83.5 ± 3.5*	87.8 ± 3.8	63.2 ± 3.1	72.9 ± 6.8	0.2 ± 0.02	118:82:0.31
Lipoid S100:Chol formulations											
Blank CLs	17.0 ± 1.4 *14.2 ± 0.3*	166 ± 33.3 *172 ± 41.1*	83.0 ± 1.4 *85.8 ± 0.3*	6.7 ± 0.0 *8.4 ± 2.9*	-	-	95.9 ± 1.5	71.2 ± 5.4	-	-	119:92:0
α-pinene-CLs	-	-	33.4 ± 5.3 *12.3 ± 2.5*	9.7 ± 0.7 *10.6 ± 0.8*	66.6 ± 5.3 *87.6 ± 2.5*	83.5 ± 8.7 *84.8 ± 6.4*	48.6 ± 2.4	66.4 ± 4.9	100.0 ± 0.0	22.9 ± 2.2	61:93:42
Blank DCLs	-	-	-	-	100 ± 0.0 *100 ± 0.0*	26.1 ± 0.0 *34.2 ± 4.7*	83.1 ± 0.7	74.5 ± 1.7	-	-	103:100:0
α-pinene-DCLs	34.0 ± 0.0 *18.5 ± 2.2*	131 ± 8.3 *296 ± 9.7*	66.0 ± 0.0 *61.0 ± 2.0*	6.8 ± 2.9 *7.7 ± 1.9*	- *20.5 ± 1.4*	- *29.9 ± 1.8*	89.2 ± 1.4	71.2 ± 1.3	100.0 ± 0.0	0.6 ± 0.02	111:92:1

2.2.3. Storage stability

The storage stability of the various nanoparticles was evaluated after storage for 3 months at 4 °C in terms of size and percentage of remaining α-pinene in the whole suspension. All of the prepared batches, except the blank and α-pinene-Phospholipon 90H CLs, presented an increase in the liposome particle size and in the percentage of the largest population after 3 months (Table 2). The aggregation of particles during storage cannot be excluded. This could be attributed to the low colloidal stability of liposomes. The presence of surface charge prevents aggregation due to electrostatic repulsion, and the more neutral net charge resulted in the formation of aggregates [57]. The magnitude of zeta potential, which gives a prediction of the colloidal stability, was previously determined for blank Phospholipon 90H and Lipoid S100 liposomes. The authors demonstrated that both types of formulations possessed a low zeta potential value, and thereby are susceptible to aggregate [53].

Additionally, the total α-pinene concentration in the liposome suspensions was determined after 3 months by HPLC, and the values were compared to those obtained on the day of preparation. The percentage of remaining α-pinene was 42.9 ± 4.9%, 74.4 ± 0.2%, 75.4 ± 4.3%, and 83.1 ± 5.1% in Phospholipon 90H CLs, Phospholipon 90H DCLs, Lipoid S100 CLs, and Lipoid S100 DCLs, respectively. Hence, α-pinene was still satisfactorily incorporated into liposomes after 3 months, and the DCL carrier system was more effective in retaining α-pinene during the storage in comparison to CLs.

3. Material and methods

3.1. Materials

Alpha-pinene was purchased from Acros Organics, Germany; cholesterol (Chol) (94%) from Acros organics, Belgium; and p-cymene from Fluka, Switzerland. HP-ß-CD (DS=5.6) was supplied by Roquette (Lestrem, France). Ammonium molybdate and potassium phosphate monobasic (KH_2PO_4)

were purchased from Sigma-Aldrich, Germany; methanol HPLC grade from Sigma-Aldrich, France; and triton X-100 from Sigma–Aldrich, USA. Sulfuric acid and Absolute ethanol were obtained from VWR Pro-labo chemicals, France; 4-amino-3-hydroxy-1-naphthalenesulfonic acid from Fluka, India; and hydrogen peroxide from Fisher Scientific, UK. Chol CHOD-POD kit was purchased from Spin react Company, Spain. Phospholipon 90H (90% soybean PC, 4% lysoPC, 2% triglycerides, 2% water, 0.5% ethanol, iodine value 1) and Lipoid S100 (94% soybean phosphatidylcholine, 3% lysophosphatidylcholine, 0.5% N-acyl phosphatidylethanolamine, 0.1% phosphatidylethanolamine, 0.1% phosphatidylinositol, 0.2% ethanol, 2% water) were supplied by Lipoid GmbH, Germany.

3.2. HPLC analysis of α-pinene

Stock solutions of α-pinene (1 mg/mL) and of the internal standard, p-cymene (1 mg/mL), were prepared in methanol. The stock solution of α-pinene was diluted to obtain final concentrations in the range of 1-100 µg/mL. The diluted solution of p-cymene (10 µg/mL) was also prepared in methanol. For HPLC analysis, 100 µL of each α-pinene solution was added to a solution of p-cymene (100 µL) and methanol (200 µL). The analysis was performed using an Agilent HPLC column (C18, 15 cm x 4.6 mm, 5 µm). The mobile phase was a mixture of methanol and water (85:15). The flow rate was fixed at 1 mL/min, and the injection volume was 20 µL. The detection was set at 204 nm.

The HPLC method was validated in terms of linearity, repeatability, and limit of detection. The retention times of p-cymene and α-pinene were 5.7 and 9.5 min, respectively. The calibration curve was constructed by plotting $\frac{\mathrm{AUC}_{\alpha-\mathrm{pinene}}}{\mathrm{AUC}_{\mathrm{p-cymene}}}$ against the concentration of α-pinene in µg/mL. The linear relationships were evaluated by regression analysis with the least-squares method, and the correlation coefficient ranged between 0.994 and 0.999.

3.3. Determination of the optimal HP-β-CD concentration for α-pinene solubilization

Excess amount of α-pinene (6.81 mg) was added to 5 mL of HP-β-CD solutions (0, 10, 25, 50, 75, 100 mM) yielding different HP-β-CD:α-pinene molar ratios (1:1, 2.5:1, 5:1, 7.5:1 and 10:1). The mixtures were shaken at a stirring rate of 125 rpm for 24 h at 26 °C. Then, to remove the un-dissolved α-pinene, the solutions were filtered through a 0.45 µm membrane filter. The amount of solubilized α-pinene was determined in the filtrate by HPLC analysis. The complexation efficiency (CE) was calculated using the following equation:

$$CE\ (\%) = \frac{m_{exp}}{m_{the}} \times 100 \qquad \text{(Equation 1)}$$

in which m_{exp} is the mass of α-pinene experimentally determined in the filtrate by HPLC. m_{the} is the mass of α-pinene initially used to prepare the inclusion complexes.

3.4. Preparation of HP-β-CD/α-pinene inclusion complex for DCL preparations

HP-β-CD/α-pinene inclusion complex of 7.5:1 (HP-β-CD:α-pinene) molar ratio was prepared by adding α-pinene (6.81 mg) to the HP-β-CD aqueous solution of 75 mM concentration. The mixture was stirred at a stirring rate of 125 rpm for 24 h at 26 °C. It was then filtered using a 0.45 µm cellulose filter. The filtrate was used for DCL preparation. Also, the HP-β-CD aqueous solution of 75 mM concentration was used for the fabrication of blank DCLs.

3.5. Preparation of liposomes

The liposomes were prepared by the ethanol-injection method. The appropriate amounts of phospholipids (Phospholipon 90H or Lipoid S100) (10 mg/mL) and Chol (5 mg/mL) were dissolved in absolute ethanol (10 mL) by stirring. The resulting organic phase was then injected into an aqueous solution (20 mL) using a syringe pump (Fortuna optima, GmbH-Germany) at an injection flow rate of 1 mL/min, under magnetic stirring (400 rpm) and at a temperature above the transition temperature of

phospholipids: 55 °C for Phospholipon 90H and room temperature for Lipoid S100. The liposomal suspensions were then maintained for 15 min under stirring (400 rpm) at room temperature. Finally, ethanol was evaporated under reduced pressure at 40 °C (Heidolph instruments GmbH, Germany).

Four liposomal batches were produced: (1) blank conventional liposomes (blank CLs), (2) blank DCLs, in which HP-β-CD (75 mM) was dissolved in the aqueous phase; (3) α-pinene-loaded liposomes (α-pinene-CLs), where α-pinene was dissolved in the organic phase at a concentration of 2.5 mg/mL; (4) HP-β-CD/α-pinene inclusion complex-loaded liposomes (α-pinene-DCLs), where a solution containing the HP-β-CD/α-pinene inclusion complex of 7.5:1 (HP-β-CD:α-pinene) molar ratio was used as the aqueous phase. Each batch was prepared in triplicate.

3.6. Characterization of liposomes

3.6.1. Particle size analysis

Laser granulometry (Partica Laser scattering, LA-950V2 particle size distribution analyser, HORIBA, Japan) was used to determine the diameter and size distribution of particles. This instrument is designed for measuring particle sizes ranging from 0.01 μm to 3000 μm.

3.6.2. Determination of phospholipid:Chol:α-pinene molar ratio in the formulations

The concentrations of phospholipids, Chol, and α-pinene embedded in the lipid vesicles were calculated by subtracting the free concentrations of compounds from their total concentrations determined in the liposome suspensions. Liposome suspensions were centrifuged at 21382 g and 4 ºC for 1 hour using a Vivaspin 500 centrifugal concentrator (Sartorius Stedim Biotech, Germany, MW cut off=10,000 Da). The filtrate contains the unloaded (free) compounds. For each formulation, the final liposomal composition (phospholipid:Chol:α-pinene molar ratio) was determined.

3.6.2.1. Determination of phospholipid incorporation rate

The total and the unloaded phospholipid concentrations in the various liposome formulations were quantified according to Bartlett's method as described in our previous studies [28,42]. Standard aqueous solutions of phosphorus were prepared. The organic phosphate in the samples (0.5 mL from liposome suspension and filtrate) was digested by sulfuric acid and then was oxidized to inorganic phosphate through incubating the samples in the presence of H_2O_2. The phosphomolybdic complex was formed upon interaction with ammonium molybdate. The complex was then reduced to a blue compound through interaction with 4-amino-3-hydroxy-1-naphthalenesulfonic acid. The absorbance of the blue compound was recorded at a wavelength of 815 nm. The following equation was used to calculate the incorporation rate (IR) of phospholipids:

$$IR_{PO_4^{3-}}\ (\%) = \frac{m_{PO_4^{3-}\ T} - m_{PO_4^{3-}\ F}}{m_{PO_4^{3-}\ \text{organic phase}}} \times 100 \qquad \text{(Equation 2)}$$

where $m_{PO_4^{3-}\ T}$ and $m_{PO_4^{3-}\ F}$ correspond to the total and free masses of phospholipids in the liposome suspension, respectively. $m_{PO_4^{3-}\ \text{organic phase}}$ is the mass of phospholipids initially added to the organic phase during the fabrication of liposomes.

3.6.2.2. Determination of cholesterol incorporation rate

Chol dosage in the liposome formulations was performed using Chol CHOD-POD kit as previously described [28,42]. Briefly, 1 mL of the standard kit was added to 10 µL of each sample (Chol standards prepared in triton X-100, liposome suspension, and filtrate). The absorbance of the colored complex was measured at 505 nm. This equation was used to determine the IR of Chol:

$$IR_{CHO}\ (\%) = \frac{m_{CHO\ T} - m_{CHO\ F}}{m_{CHO\ \text{organic phase}}} \times 100 \qquad \text{(Equation 3)}$$

where $m_{CHO\ T}$ is the mass of Chol in the liposome suspension, $m_{CHO\ F}$ is the mass of Chol in the filtrate, and $m_{CHO\ organic\ phase}$ is the mass of Chol initially added to the organic phase during liposome production.

3.6.2.3. Quantification of α-pinene in the formulations

The total and free concentrations of α-pinene in the formulations were determined by the HPLC method described above. The encapsulation efficiency (EE) and loading rate (LR) values of α-pinene were calculated as follows:

$$EE\ (\%) = \frac{[\alpha\text{-pinene}]_{total} - [\alpha\text{-pinene}]_{free}}{[\alpha\text{-pinene}]_{total}} \times 100 \qquad \text{(Equation 4)}$$

where $[\alpha - pinene]_{total}$ and $[\alpha - pinene]_{free}$ correspond to the total and free α-pinene concentrations in liposomal suspension, respectively.

$$LR\ (\%) = \frac{m_{liposomal\ suspension} - m_{filtrate}}{m_{initial}} \times 100 \qquad \text{(Equation 5)}$$

where $m_{liposomal\ suspension}$ stands for the mass of α-pinene in the liposomal suspension (total), and $m_{filtrate}$ stands for the mass of α-pinene in the liposomal filtrate (free). For α-pinene-CLs, $m_{initial}$ is the initial mass of α-pinene added to the organic phase during the fabrication of vesicles. For α-pinene-DCLs, $m_{initial}$ is the initial mass of α-pinene used to prepare the HP-β-CD/α-pinene inclusion complex.

3.6.3. Storage stability

The stability of the various nanoparticles was investigated by assessing their mean particle size after 3 months of storage at 4 °C. Additionally, the percentage of remaining α-pinene in the whole suspensions was calculated after 3 months by the following equation:

Percentage of remaining α-pinene $= \frac{[\alpha-\text{pinene}]_{3\ \text{months}}}{[\alpha-\text{pinene}]_{t_0}} \times 100$ (Equation 6)

in which $[\alpha - \text{pinene}]_{t_0}$ and $[\alpha - \text{pinene}]_{3\ \text{months}}$ correspond to the total concentration of α-pinene in the liposome suspension determined immediately after preparation and after storage for 3 months at 4 ºC, respectively.

3.7. Statistical analysis

Statistical analysis was performed using the Student's t-test. All assays were carried out in triplicate. The results are expressed as the mean values ± standard deviation. The significance level was set at $p \leq 0.05$.

Conclusion

In this paper, we studied the encapsulation of the bio-insecticide, α-pinene, into CLs and DCLs using hydrogenated (Phospholipon 90H) or non-hydrogenated (Lipoid S100) phospholipids and Chol. The size, the IR of phospholipids and Chol, the EE and LR of α-pinene, and the storage stability of the different formulations were characterized. Incorporation of α-pinene was more efficient in Lipoid S100-CLs compared to the other formulations, and this is associated with a greater effect of α-pinene on lipid bilayer and particle size. In addition, the various CL and DCL batches were stable after 3 months of storage at 4 ºC. Finally, it would be valuable to study the insecticidal effect of the α-pinene-loaded liposome and DCL formulations for their application in agriculture and food products.

Author contributions. Z. Hammoud realized the experiments and wrote the original draft with support from M. Kayouka, A. Elaissari and H. Greige-Gerges; A.Trifan, J. Mediouni, E. Sieniawska and Ł. Świątek critically revised and edited the manuscript; H. Greige-Gerges formulated the research idea.

Acknowledgements

This research study was supported by the "Agence Universitaire de la Francophonie, Projet de Coopération Scientifique Inter-Universitaire 2018-2020" and by "DS26 project of the Medical University of Lublin".

References:

1. Hoi, P.V.; Mol, A.P.J.; Oosterveer, P.; van den Brink, P.J.; Huong, P.T.M. Pesticide use in Vietnamese vegetable production: a 10-year study. *Int. J. Agric. Sustain.* **2016**, *14*, 325–338, doi:10.1080/14735903.2015.1134395.
2. Pavela, R.; Benelli, G. Essential Oils as Ecofriendly Biopesticides? Challenges and Constraints. *Trends Plant Sci.* **2016**, *21*, 1000–1007, doi:10.1016/j.tplants.2016.10.005.
3. Prajapati, V.; Tripathi, A.; Aggarwal, K.; Khanuja, S. Insecticidal, repellent and oviposition-deterrent activity of selected essential oils against , and. *Bioresour. Technol.* **2005**, *96*, 1749–1757, doi:10.1016/j.biortech.2005.01.007.
4. Zielińska, A.; Ferreira, N.R.; Durazzo, A.; Lucarini, M.; Cicero, N.; Mamouni, S.E.; Silva, A.M.; Nowak, I.; Santini, A.; Souto, E.B. Development and Optimization of Alpha-Pinene-Loaded Solid Lipid Nanoparticles (SLN) Using Experimental Factorial Design and Dispersion Analysis. *Molecules* **2019**, *24*, 2683, doi:10.3390/molecules24152683.
5. Carrasco, A.; Martinez-Gutierrez, R.; Tomas, V.; Tudela, J. Lavandula angustifolia and Lavandula latifolia Essential Oils from Spain: Aromatic Profile and Bioactivities. *Planta Med.* **2015**, *82*, 163–170, doi:10.1055/s-0035-1558095.
6. Wang, W.; Li, N.; Luo, M.; Zu, Y.; Efferth, T. Antibacterial Activity and Anticancer Activity of Rosmarinus officinalis L. Essential Oil Compared to That of Its Main Components. *Molecules* **2012**, *17*, 2704–2713, doi:10.3390/molecules17032704.
7. Dambolena, J.S.; Zunino, M.P.; Herrera, J.M.; Pizzolitto, R.P.; Areco, V.A.; Zygadlo, J.A. Terpenes: Natural Products for Controlling Insects of Importance to Human Health—A Structure-Activity Relationship Study. *Psyche J. Entomol.* **2016**, *2016*, 1–17, doi:10.1155/2016/4595823.
8. Bouzenna, H.; Hfaiedh, N.; Giroux-Metges, M.-A.; Elfeki, A.; Talarmin, H. Potential protective effects of alpha-pinene against cytotoxicity caused by aspirin in the IEC-6 cells. *Biomed. Pharmacother.* **2017**, *93*, 961–968, doi:10.1016/j.biopha.2017.06.031.
9. Dai, J.; Zhu, L.; Yang, L.; Qiu, J. Chemical composition, antioxidant and antimicrobial activities of essential oil from Wedelia prostrata. *EXCLI J.* **2013**, *12*, 479–490.
10. Sieniawska, E.; Los, R.; Baj, T.; Malm, A.; Glowniak, K. Antimicrobial efficacy of Mutellina purpurea essential oil and α-pinene against Staphylococcus epidermidis grown in planktonic and biofilm cultures. *Ind. Crops Prod.* **2013**, *51*, 152–157, doi:10.1016/j.indcrop.2013.09.001.
11. Kim, D.-S.; Lee, H.-J.; Jeon, Y.-D.; Han, Y.-H.; Kee, J.-Y.; Kim, H.-J.; Shin, H.-J.; Kang, J.; Lee, B.S.; Kim, S.-H.; et al. Alpha-Pinene Exhibits Anti-Inflammatory Activity Through the Suppression of MAPKs and the NF-κB Pathway in Mouse Peritoneal Macrophages. *Am. J. Chin. Med.* **2015**, *43*, 731–742, doi:10.1142/S0192415X15500457.

12. Chen, W.; Liu, Y.; Li, M.; Mao, J.; Zhang, L.; Huang, R.; Jin, X.; Ye, L. Anti-tumor effect of α-pinene on human hepatoma cell lines through inducing G2/M cell cycle arrest. *J. Pharmacol. Sci.* **2015**, *127*, 332–338, doi:10.1016/j.jphs.2015.01.008.
13. Hao, D.C.; Gu, X.-J.; Xiao, P.G. Phytochemical and biological research of Cannabis pharmaceutical resources. In *Medicinal Plants*; Elsevier, 2015; pp. 431–464 ISBN 978-0-08-100085-4.
14. Neeman, E.M.; Avilés Moreno, J.R.; Huet, T.R. The gas phase structure of α-pinene, a main biogenic volatile organic compound. *J. Chem. Phys.* **2017**, *147*, 214305, doi:10.1063/1.5003726.
15. Pavlovic, J.; Hopke, P.K. Technical Note: Detection and identification of radical species formed from α-pinene/ozone reaction using DMPO spin trap. *Atmospheric Chem. Phys. Discuss.* **2009**, *9*, 23695–23717, doi:10.5194/acpd-9-23695-2009.
16. Pinho, P.G.; Pio, C.A.; Carter, W.P.L.; Jenkin, M.E. Evaluation of α- and β-pinene degradation in the detailed tropospheric chemistry mechanism, MCM v3.1, using environmental chamber data. *J. Atmospheric Chem.* **2007**, *57*, 171–202, doi:10.1007/s10874-007-9071-0.
17. Chen, J.-M.; Cheng, Z.-W.; Jiang, Y.-F.; Zhang, L.-L. Direct VUV photodegradation of gaseous α-pinene in a spiral quartz reactor: Intermediates, mechanism, and toxicity/biodegradability assessment. *Chemosphere* **2010**, *81*, 1053–1060, doi:10.1016/j.chemosphere.2010.09.060.
18. de Oliveira, J.L.; Campos, E.V.R.; Bakshi, M.; Abhilash, P.C.; Fraceto, L.F. Application of nanotechnology for the encapsulation of botanical insecticides for sustainable agriculture: Prospects and promises. *Biotechnol. Adv.* **2014**, *32*, 1550–1561, doi:10.1016/j.biotechadv.2014.10.010.
19. Wang, D.; Chi, D.F. Morphology and Release Profile of Microcapsules Encapsulated Alpha-Pinene by Complex Coacervation. *Adv. Mater. Res.* **2012**, *602–604*, 1285–1288, doi:10.4028/www.scientific.net/AMR.602-604.1285.
20. Ciobanu, A.; Landy, D.; Fourmentin, S. Complexation efficiency of cyclodextrins for volatile flavor compounds. *Food Res. Int.* **2013**, *53*, 110–114, doi:10.1016/j.foodres.2013.03.048.
21. Kfoury, M.; Pipkin, J.D.; Antle, V.; Fourmentin, S. Captisol®: an efficient carrier and solubilizing agent for essential oils and their components. *Flavour Fragr. J.* **2017**, *32*, 340–346, doi:10.1002/ffj.3395.
22. Kfoury, M.; Auezova, L.; Fourmentin, S.; Greige-Gerges, H. Investigation of monoterpenes complexation with hydroxypropyl-β-cyclodextrin. *J. Incl. Phenom. Macrocycl. Chem.* **2014**, *80*, 51–60, doi:10.1007/s10847-014-0385-7.
23. Gharib, R.; Greige-Gerges, H.; Fourmentin, S.; Charcosset, C.; Auezova, L. Liposomes incorporating cyclodextrin–drug inclusion complexes: Current state of knowledge. *Carbohydr. Polym.* **2015**, *129*, 175–186, doi:10.1016/j.carbpol.2015.04.048.
24. McCormack, B.; Gregoriadis, G. Drugs-in-cyclodextrins-in liposomes: a novel concept in drug delivery. *Int. J. Pharm.* **1994**, *112*, 249–258, doi:10.1016/0378-5173(94)90361-1.
25. Sebaaly, C.; Charcosset, C.; Stainmesse, S.; Fessi, H.; Greige-Gerges, H. Clove essential oil-in-cyclodextrin-in-liposomes in the aqueous and lyophilized states: From laboratory to large scale using a membrane contactor. *Carbohydr. Polym.* **2016**, *138*, 75–85, doi:10.1016/j.carbpol.2015.11.053.
26. Gharib, R.; Auezova, L.; Charcosset, C.; Greige-Gerges, H. Drug-in-cyclodextrin-in-liposomes as a carrier system for volatile essential oil components: Application to anethole. *Food Chem.* **2017**, *218*, 365–371, doi:10.1016/j.foodchem.2016.09.110.
27. Gharib, R.; Haydar, S.; Charcosset, C.; Fourmentin, S.; Greige-Gerges, H. First study on the release of a natural antimicrobial agent, estragole, from freeze-dried delivery systems based on cyclodextrins and liposomes. *J. Drug Deliv. Sci. Technol.* **2019**, *52*, 794–802, doi:10.1016/j.jddst.2019.05.032.
28. Hammoud, Z.; Gharib, R.; Fourmentin, S.; Elaissari, A.; Greige-Gerges, H. Drug-in-hydroxypropyl-β-cyclodextrin-in-lipoid S100/cholesterol liposomes: Effect of the characteristics of essential oil components on their encapsulation and release. *Int. J. Pharm.* **2020**, *579*, 119151, doi:10.1016/j.ijpharm.2020.119151.

29. Azzi, J.; Auezova, L.; Danjou, P.-E.; Fourmentin, S.; Greige-Gerges, H. First evaluation of drug-in-cyclodextrin-in-liposomes as an encapsulating system for nerolidol. *Food Chem.* **2018**, *255*, 399–404, doi:10.1016/j.foodchem.2018.02.055.
30. Bragagni, M.; Maestrelli, F.; Mennini, N.; Ghelardini, C.; Mura, P. Liposomal formulations of prilocaine: effect of complexation with hydroxypropyl-ß-cyclodextrin on drug anesthetic efficacy. *J. Liposome Res.* **2010**, *20*, 315–322, doi:10.3109/08982100903544169.
31. Maestrelli, F.; González-Rodríguez, M.L.; Rabasco, A.M.; Ghelardini, C.; Mura, P. New "drug-in cyclodextrin-in deformable liposomes" formulations to improve the therapeutic efficacy of local anaesthetics. *Int. J. Pharm.* **2010**, *395*, 222–231, doi:10.1016/j.ijpharm.2010.05.046.
32. Hammoud, Z.; Khreich, N.; Auezova, L.; Fourmentin, S.; Elaissari, A.; Greige-Gerges, H. Cyclodextrin-membrane interaction in drug delivery and membrane structure maintenance. *Int. J. Pharm.* **2019**, *564*, 59–76, doi:10.1016/j.ijpharm.2019.03.063.
33. Hatzi, P.; Mourtas, S.; G. Klepetsanis, P.; Antimisiaris, S.G. Integrity of liposomes in presence of cyclodextrins: Effect of liposome type and lipid composition. *Int. J. Pharm.* **2007**, *333*, 167–176, doi:10.1016/j.ijpharm.2006.09.059.
34. Puglisi, G.; Fresta, M.; Ventura, C.A. Interaction of Natural and Modified β-Cyclodextrins with a Biological Membrane Model of Dipalmitoylphosphatidylcholine. *J. Colloid Interface Sci.* **1996**, *180*, 542–547, doi:10.1006/jcis.1996.0335.
35. Denz, M.; Haralampiev, I.; Schiller, S.; Szente, L.; Herrmann, A.; Huster, D.; Müller, P. Interaction of fluorescent phospholipids with cyclodextrins. *Chem. Phys. Lipids* **2016**, *194*, 37–48, doi:10.1016/j.chemphyslip.2015.07.017.
36. Milles, S.; Meyer, T.; Scheidt, H.A.; Schwarzer, R.; Thomas, L.; Marek, M.; Szente, L.; Bittman, R.; Herrmann, A.; Günther Pomorski, T.; et al. Organization of fluorescent cholesterol analogs in lipid bilayers - lessons from cyclodextrin extraction. *Biochim. Biophys. Acta* **2013**, *1828*, 1822–1828, doi:10.1016/j.bbamem.2013.04.002.
37. Ohvo-Rekilä, H.; Akerlund, B.; Slotte, J.P. Cyclodextrin-catalyzed extraction of fluorescent sterols from monolayer membranes and small unilamellar vesicles. *Chem. Phys. Lipids* **2000**, *105*, 167–178.
38. Nishijo, J.; Shiota, S.; Mazima, K.; Inoue, Y.; Mizuno, H.; Yoshida, J. Interactions of cyclodextrins with dipalmitoyl, distearoyl, and dimyristoyl phosphatidyl choline liposomes. A study by leakage of carboxyfluorescein in inner aqueous phase of unilamellar liposomes. *Chem. Pharm. Bull. (Tokyo)* **2000**, *48*, 48–52.
39. Piel, G.; Piette, M.; Barillaro, V.; Castagne, D.; Evrard, B.; Delattre, L. Study of the relationship between lipid binding properties of cyclodextrins and their effect on the integrity of liposomes. *Int. J. Pharm.* **2007**, *338*, 35–42, doi:10.1016/j.ijpharm.2007.01.015.
40. Li, j; Perdue, E.M. Physicochemical Properties of Selected Monoterpenes. In *Preprints of Papers Presented at the 209th ACS National Meeting. Anaheim, CA*; 1995; pp. 134–137.
41. Azzi, J.; Jraij, A.; Auezova, L.; Fourmentin, S.; Greige-Gerges, H. Novel findings for quercetin encapsulation and preservation with cyclodextrins, liposomes, and drug-in-cyclodextrin-in-liposomes. *Food Hydrocoll.* **2018**, *81*, 328–340, doi:10.1016/j.foodhyd.2018.03.006.
42. Hammoud, Z.; Gharib, R.; Fourmentin, S.; Elaissari, A.; Greige-Gerges, H. New findings on the incorporation of essential oil components into liposomes composed of lipoid S100 and cholesterol. *Int. J. Pharm.* **2019**, *561*, 161–170, doi:10.1016/j.ijpharm.2019.02.022.
43. Sikkema, J.; de Bont, J.A.; Poolman, B. Mechanisms of membrane toxicity of hydrocarbons. *Microbiol. Rev.* **1995**, *59*, 201–222.
44. Rodriguez, S.A.; Pinto, O.A.; Hollmann, A. Interaction of semiochemicals with model lipid membranes: A biophysical approach. *Colloids Surf. B Biointerfaces* **2018**, *161*, 413–419, doi:10.1016/j.colsurfb.2017.11.002.

45. Gharib, R.; Fourmentin, S.; Charcosset, C.; Greige-Gerges, H. Effect of hydroxypropyl-β–cyclodextrin on lipid membrane fluidity, stability and freeze-drying of liposomes. *J. Drug Deliv. Sci. Technol.* **2018**, *44*, 101–107, doi:10.1016/j.jddst.2017.12.009.
46. Yancey, P.G.; Rodrigueza, W.V.; Kilsdonk, E.P.; Stoudt, G.W.; Johnson, W.J.; Phillips, M.C.; Rothblat, G.H. Cellular cholesterol efflux mediated by cyclodextrins. Demonstration Of kinetic pools and mechanism of efflux. *J. Biol. Chem.* **1996**, *271*, 16026–16034.
47. Steck, T.L.; Ye, J.; Lange, Y. Probing red cell membrane cholesterol movement with cyclodextrin. *Biophys. J.* **2002**, *83*, 2118–2125, doi:10.1016/S0006-3495(02)73972-6.
48. Ermilova, I.; Lyubartsev, A.P. Cholesterol in phospholipid bilayers: positions and orientations inside membranes with different unsaturation degrees. *Soft Matter* **2019**, *15*, 78–93, doi:10.1039/C8SM01937A.
49. Harroun, T.A.; Katsaras, J.; Wassall, S.R. Cholesterol Hydroxyl Group Is Found To Reside in the Center of a Polyunsaturated Lipid Membrane. *Biochemistry* **2006**, *45*, 1227–1233, doi:10.1021/bi0520840.
50. Marquardt, D.; Heberle, F.A.; Greathouse, D.V.; Koeppe, R.E.; Standaert, R.F.; Van Oosten, B.J.; Harroun, T.A.; Kinnun, J.J.; Williams, J.A.; Wassall, S.R.; et al. Lipid bilayer thickness determines cholesterol's location in model membranes. *Soft Matter* **2016**, *12*, 9417–9428, doi:10.1039/C6SM01777K.
51. Zhigaltsev, I.V.; Maurer, N.; Akhong, Q.-F.; Leone, R.; Leng, E.; Wang, J.; Semple, S.C.; Cullis, P.R. Liposome-encapsulated vincristine, vinblastine and vinorelbine: A comparative study of drug loading and retention. *J. Controlled Release* **2005**, *104*, 103–111, doi:10.1016/j.jconrel.2005.01.010.
52. Marques, H.M.C. A review on cyclodextrin encapsulation of essential oils and volatiles. *Flavour Fragr. J.* **2010**, *25*, 313–326, doi:10.1002/ffj.2019.
53. Sebaaly, C.; Greige-Gerges, H.; Stainmesse, S.; Fessi, H.; Charcosset, C. Effect of composition, hydrogenation of phospholipids and lyophilization on the characteristics of eugenol-loaded liposomes prepared by ethanol injection method. *Food Biosci.* **2016**, *15*, 1–10, doi:10.1016/j.fbio.2016.04.005.
54. Piel, G.; Piette, M.; Barillaro, V.; Castagne, D.; Evrard, B.; Delattre, L. Betamethasone-in-cyclodextrin-in-liposome: The effect of cyclodextrins on encapsulation efficiency and release kinetics. *Int. J. Pharm.* **2006**, *312*, 75–82, doi:10.1016/j.ijpharm.2005.12.044.
55. Qiu, N.; Cai, L.; Wang, W.; Wang, G.; Cheng, X.; Xu, Q.; Wen, J.; Liu, J.; Wei, Y.; Chen, L. Barbigerone-in-hydroxypropyl-β-cyclodextrin-liposomal nanoparticle: preparation, characterization and anti-cancer activities. *J. Incl. Phenom. Macrocycl. Chem.* **2015**, *82*, 505–514, doi:10.1007/s10847-015-0533-8.
56. Wang, W.-X.; Feng, S.-S.; Zheng, C.-H. A comparison between conventional liposome and drug-cyclodextrin complex in liposome system. *Int. J. Pharm.* **2016**, *513*, 387–392, doi:10.1016/j.ijpharm.2016.09.043.
57. Wiącek, A.; Chibowski, E. Zeta potential, effective diameter and multimodal size distribution in oil/water emulsion. *Colloids Surf. Physicochem. Eng. Asp.* **1999**, *159*, 253–261, doi:10.1016/S0927-7757(99)00281-2.

Article 2

Development of formulations to improve the controlled release of the insecticidal agent, camphor

Zahraa Hammoud[1,2], Jouda Mediouni Ben Jemâa[3], Abdelhamid Elaissari[2], Hélène Greige-Gerges[1]

[1]Bioactive Molecules Research Laboratory, Doctoral School of Sciences and Technologies, Faculty of Sciences, Section II, Lebanese University, Lebanon

[2]Univ Lyon, University Claude Bernard Lyon-1, CNRS, LAGEP-UMR 5007, F-69622 Lyon, France

[3]Laboratory of Biotechnology Applied to Agriculture, National Agricultural Research Institute of Tunisia (INRAT), University of Carthage, Tunisia

Abstract

The monoterpene, camphor, is known as bio-insecticide. However, limitations in its application were reported because of its volatility and chemical instability. Therefore, its encapsulation is an important strategy that can be used to increase its stability and efficiency in integrated pest management. In this study, conventional liposomes (CLs) and drug-in-cyclodextrin-in-liposomes (DCLs) loading camphor were prepared and characterized with respect to their size, phospholipid and cholesterol incorporation rates, camphor encapsulation efficiency, camphor loading rate, and storage stability. Ethanol injection method was applied to produce the liposomes using saturated (Phospholipon 90H) or unsaturated (Lipoid S100) phospholipids in combination with cholesterol. The results showed that the incorporation of camphor was more efficient in DCLs composed of Lipoid S100 compared to the other formulations. Furthermore, it was found that all CL and DCL formulations were stable after 3 months of storage at 4 ºC (> 80% of initial camphor concentration was incorporated after 3 months). Therefore, DCLs are promising carriers for new applications of camphor in the agricultural and food industries.

Keywords: camphor, drug-in-cyclodextrin-in-liposomes; hydroxypropyl-β-cyclodextrin; insecticide; liposomes

1. Introduction

Camphor ($C_{10}H_{16}O$) is a naturally occurring cyclic monoterpenoid. It is a volatile, white, crystalline and waxy solid substance with a pleasant odor and sour taste. Camphor is derived from the wood of *Cinnamomum camphora*, a large evergreen tree seen in Asia (Rahnama-Moghadam et al., 2015; Sikka and Bartolome, 2018). It is a common component of several essential oils including rosemary, thyme, lavender, and chicory (Brenes and Roura, 2010; Shahabi et al., 2014) essential oils.

Camphor has been widely used as a fragrance in cosmetics, food flavorings, scenting agent in a variety of household products such as soap and detergent, and intermediate in the synthesis of perfume chemicals (Reed, 2005). Additionally, it has various biological activities including antimicrobial, antiviral, analgesic, anticancer, and antitussive properties (Chen et al., 2013). Camphor also presents insect repellent properties. For instance, the insect repellent activity of camphor was investigated against four beetles (*Sitophilus granarius, S. zeamais, Tribolium castaneum and Prostephanus truncatus*) with overall repellency ranging between 80 and 98%, and the repellency was dosage-dependent with the dose of 100 mg evoking over 94% repellency against the beetle species tested (Obeng-Ofori et al., 1998). Various studies proved that camphor acts as a mosquito repellent (Ansari and Razdan, 1995; Seyoum et al., 2003, 2002). Besides, camphor showed contact and fumigant activity against *Sitophilus oryzae* and *Rhyzopertha dominica* (Rozman et al., 2007). However, the application of camphor in agriculture turns out to be unsuccessful due to its volatility (estimated Henry's Law constant of 8.31×10^{-5} atm m^3/mol at 25ºC) and poor water solubility (1600 mg/L at 25ºC) (Celebioglu et al., 2018). In addition, it was reported that external factors such as temperature, light and accessibility to atmospheric oxygen influence the stability of essential oils (Turek and Stintzing, 2013). Namely, the photodegradation of camphor produced ortho-mentha-1(7)8-dien-3-ol, 3-cyclopentene-1-acetaldehyde,2,2,3-trimethyl, and cyclopentanol,3-methyl-2-(2-pentenyl) (Sirtori et al., 2006). As a result, it is necessary to develop

formulations for improving the handling of camphor. Efforts have been made to improve the physicochemical properties of camphor or camphor oil through encapsulation in gelatin-gum Arabic microcapsules (Chang et al., 2006), in porous starch microspheres (Glenn et al., 2010), in nanoemulsion (Halim Moss et al., 2017), or in cyclodextrins (CDs) (Celebioglu et al., 2018; Ciobanu et al., 2013; Tanaka et al., 1996). It was proved that CDs enhance the solubility of camphor, protect it from chemical degradation, and prolong its release.

CDs are cyclic oligosaccharides formed by the enzymatic degradation of starch. The most common native CDs are α-, β- and γ-CDs and are composed of six, seven and eight glucosyl units, respectively. They have a truncated shape with a hydrophilic surface and a hydrophobic cavity where hydrophobic guests are located inside the CD cavities forming inclusion complexes (Hammoud et al., 2019b; Szejtli, 1998). To improve the solubility of native CDs, many CD derivatives like hydroxypropyl-β-cyclodextrin (HP-β-CD) were synthesized.

In parallel, liposomes, safe and effective drug carrier systems, are spherical microscopic vesicles comprising a central aqueous compartment surrounded by a membrane composed mainly of phospholipids. During vesicle formation, the water soluble molecules are encapsulated into the aqueous core of vesicles, whereas the lipid-soluble molecules are embedded within the liposome bilayers. They represent an efficient approach for incorporating natural compounds, such as essential oil components, through improving their solubility and chemical stability (Sherry et al., 2013). Nevertheless, it was demonstrated that the incorporation of a variety of essential oil components into liposomes can destabilize liposome membrane (Gharib et al., 2017b, 2018), leading to the rapid release of the molecule from the bilayer (Gharib et al., 2017b; Kirby and Gregoriadis, 1983; Takino et al., 1994). In an attempt to overcome this problem, McCormack and Gregoriadis, 1994 suggested the possibility of forming a combined system of CDs and liposomes called drug-in-cyclodextrin-in-liposomes (DCLs) system. DCLs

are able to combine the ability of CDs to form CD/drug inclusion complexes with the use of liposomes as shuttle systems. The DCLs have been applied to encapsulate a large series of natural hydrophobic drugs comprising essential oils. Compared to conventional liposomes (CLs), this system was shown to improve the encapsulation and prolong the release of several lipophilic drugs (Azzi et al., 2018a; Chen et al., 2007; Gharib et al., 2017a, 2019; Hammoud et al., 2020; Piel et al., 2006; Sebaaly et al., 2016).

In this study, the encapsulation of camphor into CLs and DCLs is studied. The ethanol injection method was applied to prepare the CLs and DCLs using hydrogenated (Phospholipon 90H) or non-hydrogenated (Lipoid S100) phospholipids and cholesterol (Chol). All liposome formulations were characterized with respect to their size, camphor encapsulation efficiency, and camphor loading rate. The incorporation rates of phospholipids and Chol were also determined. The stability of the liposome formulations in aqueous solutions was assessed after 3 months of storage at 4 ºC.

2. Materials and methods

2.1. Materials

Camphor was purchased from Sigma–Aldrich, China; linalool from Sigma–Aldrich, Switzerland; ammonium molybdate and potassium phosphate monobasic (KH_2PO_4) from Sigma-Aldrich, Germany; triton X-100 from Sigma–Aldrich, USA; and methanol HPLC grade from Sigma-Aldrich, France. HP-β-CD (DS=5.6) was obtained from Roquette (Lestrem, France). Chol CHOD-POD kit was provided by Spin react Company, Spain. Absolute ethanol and sulfuric acid were purchased from VWR Pro-labo chemicals, France; hydrogen peroxide from Fisher Scientific, UK; 4-amino-3-hydroxy-1-naphthalenesulfonic acid from Fluka, India; and Chol (94%) from Acros organics, Belgium. Phospholipon 90H (90 % soybean PC, 4 % lysoPC, 2 % triglycerides, 2 % water, 0.5 % ethanol, iodine value 1) and Lipoid S100 (94% soybean phosphatidylcholine, 3% lysophosphatidylcholine, 0.5% N-acyl

phosphatidylethanolamine, 0.1% phosphatidylethanolamine, 0.1% phosphatidylinositol, 2% water, 0.2% ethanol) were supplied by Lipoid GmbH, Germany.

2.2. HPLC assay of camphor

The concentration of camphor in the formulations was determined by reversed phase HPLC method. Stock solutions of camphor (1 mg/mL) and of the internal standard, linalool (1 mg/mL), were prepared in methanol. Aliquots were removed from camphor stock solution and diluted in methanol to obtain final concentrations of camphor ranging from 7.5 to 1000 µg/mL. The diluted solution of linalool (10 µg/mL) was also prepared in methanol. For HPLC analysis, 100 µL of each camphor solution was added to a solution of linalool (100 µL) and methanol (200 µL). HPLC analysis was conducted using an analytic column C18 15 cm x 4.6 mm, 5 µm, (Agilent Technologies). The mobile phase was a mixture of methanol and water (70/30). The flow rate was fixed at 1 mL/min, and the detection was set at 206 nm. The injection volume was 20 µL.

The HPLC method was validated in terms of linearity, repeatability, and limit of detection. The retention times of linalool and camphor were 6.9 and 4.6 min, respectively. The calibration curve was constructed by plotting $\frac{\mathrm{AUC_{camphor}}}{\mathrm{AUC_{linalool}}}$ against the concentration of camphor in µg/mL. The linear relationships were evaluated by regression analysis with the least-squares method, and the correlation coefficient ranged between 0.995 and 0.998.

2.3. Optimization of camphor:HP-β-CD molar ratio for inclusion complex preparation

HP-β-CD/camphor inclusion complexes were prepared in aqueous solutions. Excess amount of camphor (19.03 mg) was added to 5 mL of HP-β-CD solutions (0, 10, 25, 50, 75, and 100 mM). The mixtures were shaken at a stirring rate of 125 rpm for 24 h at 26 °C, and then were filtered through a 0.45 µm

membrane filter to eliminate the un-dissolved camphor. The concentration of camphor was determined in the filtrate by the HPLC method. The complexation efficiency (CE) was calculated using the following equation:

$$CE\ (\%) = \frac{m_{exp}}{m_{the}} \times 100 \qquad \text{(Equation 1)}$$

in which m_{exp} is the mass of camphor experimentally determined by HPLC in the filtrate of the inclusion complex solutions. m_{the} represents the theoretical mass of camphor initially used to prepare the inclusion complexes.

2.4. Preparation of HP-β-CD/camphor inclusion complex for DCL preparations

HP-β-CD (50 mM) was dissolved in ultrapure water, and the required amount of camphor (25 mM) was added to obtain camphor:HP-β-CD molar ratio of 1:2. HP-β-CD/camphor inclusion complex solution was prepared as described above, and the obtained solution was used for DCLs preparation. Additionally, free HP-β-CD (50 mM) was dissolved in water and used for the preparation of blank DCLs.

2.5. Preparation of liposomes

Among the different methods used for liposome preparation, the ethanol injection was chosen in our study. The phospholipids (Phospholipon 90H or Lipoid S100) (10 mg/mL) and Chol (5 mg/mL) were dissolved in absolute ethanol (10 mL). The resulting organic phase was later injected into an aqueous solution (20 mL) using a syringe pump (Fortuna optima, GmbH-Germany) at an injection flow rate of 1 mL/min and under magnetic stirring (400 rpm). The preparation of Lipoid S100-based liposomes was carried out at room temperature while the preparation of Phospholipon 90H-based liposomes was performed at a temperature above the transition temperature of the phospholipid (~ 55 °C). Spontaneous

liposome formation occurred as soon as the ethanol solution was in contact with the aqueous phase. The liposomal suspensions were then left for 15 min under stirring (400 rpm) at room temperature. Finally, ethanol was removed by rotary evaporation (Heidolph instruments GmbH, Germany) under reduced pressure at 40 °C. The liposomal formulations were stored at 4 °C prior to analysis.

Different liposome formulations were prepared: (1) blank conventional liposomes (blank CLs); (2) blank DCLs, in which HP-β-CD was dissolved in the aqueous phase at a concentration of 50 mM; (3) camphor-loaded liposomes (camphor-CLs), where camphor was dissolved in the organic phase at a concentration of 7.5 mg/mL; (4) HP-β-CD/camphor inclusion complex-loaded liposomes (camphor-DCLs), where a solution containing the HP-β-CD/camphor inclusion complex was used as the aqueous phase during DCL preparation. Each batch was prepared in triplicate and underwent characterization as described below.

2.6. Characterization of liposomes

2.6.1. Particle size measurement

The diameter and size distribution of liposomes were determined by laser granulometry using a Partica LA-950V2 laser diffraction particle size distribution analyzer (Horiba, Japan). This instrument enables the measurement of particle sizes ranging from 0.01 μm to 3000 μm.

2.6.2. Determination of the yield of the process

The liposomal suspensions were subjected to centrifugation at 21382 g and 4 ºC for 1 hour using a Vivaspin 500 centrifugal concentrator (Sartorius Stedim Biotech, Germany, MW cut off=10,000 Da) to separate the un-retained (free) liposomal components (phospholipids, Chol, camphor) from the retained ones. Aliquots were removed from the filtrates to determine the concentrations of the unloaded constituents. Also, aliquots were removed from the liposome suspensions, sonicated for 10 min in ice,

and used to determine the total concentrations of the constituents. The concentrations of phospholipids, Chol, and camphor embedded in the lipid vesicles were calculated by subtracting the free concentrations of constituents from their total concentrations.

The incorporation rates of phospholipids and Chol were calculated according to the following formula:

$$IR\ (\%) = \frac{m_T - m_F}{m_{organic\ phase}} \times 100 \qquad \text{(Equation 2)}$$

in which m_T is the mass of the specific lipid in the liposome suspension, m_F is the mass of the lipid in the filtrate, and $m_{organic\ phase}$ is the initial mass of the lipid added to the organic phase during liposome preparation.

The EE of camphor was calculated as follows:

$$EE\ (\%) = \frac{[camphor]_{total} - [camphor]_{free}}{[camphor]_{total}} \times 100 \qquad \text{(Equation 3)}$$

where $[camphor]_{total}$ and $[camphor]_{free}$ correspond to the total and free concentrations of camphor determined in the liposomal suspension, respectively.

The LR of camphor was calculated as follows:

$$LR\ (\%) = \frac{m_{liposomal\ suspension} - m_{filtrate}}{m_{initial}} \times 100 \qquad \text{(Equation 4)}$$

where $m_{liposomal\ suspension}$ is the mass of camphor in the liposomal suspension (total), and $m_{filtrate}$ is the mass of camphor in the liposomal filtrate (free). For CLs, $m_{initial}$ is the initial camphor mass added to the organic phase during the preparation of liposomes. For DCLs, $m_{initial}$ is the mass of camphor initially used to prepare the inclusion complex.

2.6.2.1. Phospholipids quantification assay

The quantification of free and total phospholipids concentration in the various formulations was performed by Bartlett's method as described in our previous studies (Hammoud et al., 2020, 2019a). Standard aqueous solutions of phosphorus were prepared. The organic phosphate in the samples (liposome suspension and filtrate) was digested by sulfuric acid, and the samples were incubated in the presence of H_2O_2 to allow the oxidation of organic phosphates to inorganic phosphates. Then, the phosphomolybdic complex was formed upon interaction with ammonium molybdate. This was followed by its reduction to a blue product through interaction with 4-amino-3-hydroxy-1-naphthalenesulfonic acid. The absorbance of the blue compound was recorded at a wavelength of 815 nm.

2.6.2.2. Cholesterol quantification assay

The enzymatic colorimetric method was utilized to determine the total and the free concentrations of Chol in the suspensions (Hammoud et al., 2019b, 2020). In brief, 1 mL of a Chol CHOD-POD kit was added to the samples (Chol standard solutions prepared in triton X-100, filtrates, CL and DCL suspensions). The absorbance of the colored complex was measured at 505 nm.

2.6.2.3. Quantification of camphor

The concentration of camphor in the liposomal suspensions (total concentration) and filtrates (free concentration) was determined using the HPLC method described above.

2.6.3. Stability study of liposomes

The stability of the liposomal formulations was investigated by assessing their mean particle size after 3 months of storage at 4 °C. Additionally, the percentage of remaining camphor in the whole suspensions was determined after 3 months according the following equation:

$$\text{Percentage of remaining camphor} = \frac{[\text{camphor}]_{3\ \text{months}}}{[\text{camphor}]_{t_0}} \times 100 \qquad \text{(Equation 5)}$$

where $[\text{camphor}]_{t_0}$ and $[\text{camphor}]_{3\ \text{months}}$ correspond to the total concentration of camphor determined in the liposome suspensions on the day of preparation and after 3 months of storage at 4 ºC, respectively.

2.7. Statistical analysis

Statistical analysis was performed using the two samples Student's t-test. The results are expressed as the mean values ± standard deviation. The significance level was set at $*p \leq 0.05$.

3. Results and discussion

3.1. Determination of camphor concentration in HP-β-CD/camphor inclusion complex solutions

The concentration of camphor solubilized by HP-β-CD using different HP-β-CD concentrations (0-100 mM) was determined by HPLC, and the results are shown in Figure 1. The concentration of camphor in the absence of HP-β-CD was 1406.2 ± 90.7 µg/mL. This value is consistent with the aqueous solubility value found in literature (1600 µg/mL) (Yalkowsky et al., 2010). The addition of HP-β-CD enhanced the solubility of camphor, and the optimal solubilization occurred at HP-β-CD concentration of 50 mM. The camphor concentration in the filtrate was of 3666 µg/mL (24.1 mM). Therefore, the HP-β-CD/camphor inclusion complex was prepared at camphor:HP-β-CD molar ratio of 1:2 and used as the aqueous phase during DCLs preparation. The CE of camphor into HP-β-CD was calculated using equation 1, and the results are reported in Table 1. The CE value of camphor at the optimal HP-β-CD concentration (50 mM) was 96.3 ± 2.4%.

In the present study, HP-β-CD was selected due to its high aqueous solubility (> 500 mg/mL), low toxicity, and strong complexing ability with camphor. In earlier reports, different types of CDs were

used to prepare CD/camphor inclusion complexes. Ciobanu et al., (2013) determined the stability constant and the complexation efficiency of complexes formed between camphor and α-CD, β-CD, γ-CD, HP-β-CD, randomly methylated-β-cyclodextrin (RAMEB), and a low methylated-β-cyclodextrin (CRYSMEB). The authors proved that the stability constant was in the order of β-CD > CRYSMEB > HP-β-CD > RAMEB > γ-CD > α-CD. Furthermore, Tanaka et al., (1996) reported that HP-β-CD significantly increased the solubility of camphor, and the stability constant of HP-β-CD/camphor inclusion complex was higher than that of HP-α-CD/camphor and HP-γ-CD/camphor complexes.

Figure 1: The concentration of camphor solubilized in the filtrate of HP-β-CD/camphor complex solution at different HP-β-CD concentrations.

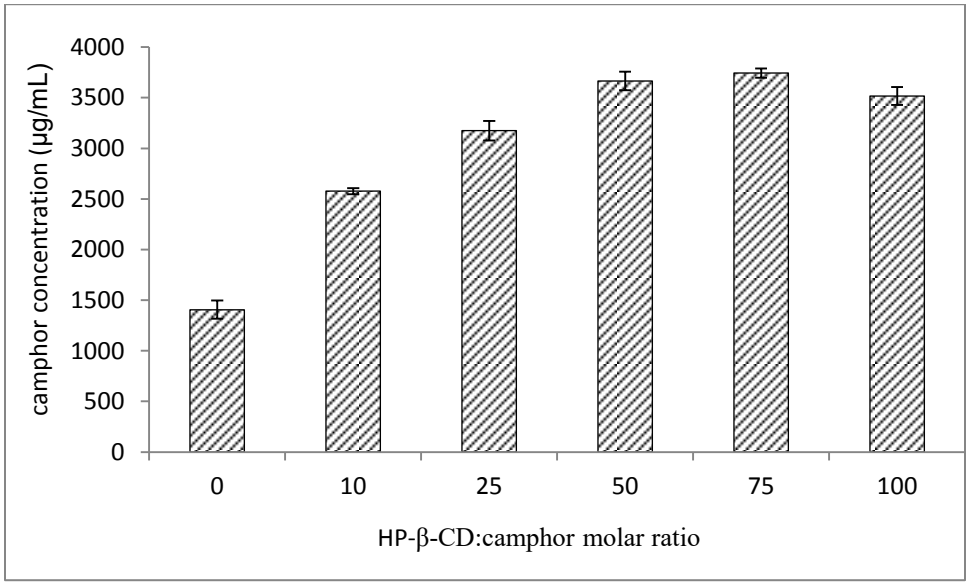

Table 2: The complexation efficiency of camphor into HP-β-CD as a function of HP-β-CD concentration.

HP-β-CD concentration (mM)	CE (%)
10	67.7 ± 0.8
25	90.6 ± 2.5
50	96.3 ± 2.4
75	98.4 ± 1.2
100	93.4 ± 3.6

3.2. Characterization of liposomes formulations

3.2.1. Particle size determination

The particle size distributions of CLs and DCLs were assessed by a laser granulometer on the day of preparation and after 3 months of storage at 4 °C. Table 2 presents the percentage distribution of nanometric and micrometric particles in each formulation.

Table 2: Percentage distribution and mean particle size of populations for blank- and camphor-loaded CLs and DCLs determined on the day of preparation and after 3 months of storage at 4 °C. The values in italic are those obtained after 3 months of storage at 4 ºC.

Sample	Population 1		Population 2		Population 3	
	(%)	Mean size (nm)	(%)	Mean size (µm)	(%)	Mean size (µm)
Phospholipon 90H:Chol formulations						
Blank CLs	98.8 ± 0.9 *98.4 ± 0.8*	150 ± 0.0 *150 ± 0.0*	1.2 ± 0.9 *1.6 ± 0.8*	5.9 ± 1.4 *5.1 ± 0.8*	-	-
Camphor-CLs	92.5 ± 2.9 *63.1 ± 3.1*	137 ± 10.9 *137 ± 10.9*	7.5 ± 2.9 *36.9 ± 3.1*	6.2 ± 0.9 *9.1 ± 0.9*	-	-
Blank DCLs	55.1 ± 4.5 *53.9 ± 0.9*	131 ± 0.0 *140± 3.3*	17.6 ± 4.5 *18.9 ± 0.4*	4.9 ± 0.4 *4.6 ± 0.9*	27.3 ± 8.7 *27.2 ± 0.5*	82.7 ± 11.6 *77.3 ± 0.0*
Camphor-DCLs	53.5 ± 0.8 *48.2 ± 0.8*	131 ± 0.0 *140 ± 1.1*	16.2 ± 2.0 *17.2 ± 1.4*	6.4 ± 0.5 *7.3 ± 2.1*	30.3 ± 2.3 *35.1 ± 2.8*	46.0 ± 1.2 *44.9 ± 3.9*
Lipoid S100:Chol formulations						
Blank CLs	17.4 ± 0.7 *16.4 ± 1.7*	172 ± 0.0 *172 ± 0.0*	82.6 ± 0.7 *83.6 ± 1.7*	6.4 ± 0.7 *7.8 ± 0.8*	-	-
Camphor-CLs	13.3 ± 2.6 *5.2 ± 1.1*	172 ± 0.0 *243 ± 13.3*	86.7 ± 2.6 *94.8 ± 1.1*	6.8 ± 0.0 *8.1 ± 0.0*	-	-
Blank DCLs	-	-	100 ± 0.0 *100 ± 0.0*	16.2 ± 1.5 18.7 ± 1.8	-	-
Camphor-DCLs	13.1 ± 2.5 *10.9 ± 2.3*	216 ± 15.0 *226 ± 0.0*	86.9 ± 2.5 *89.1 ± 2.3*	17.4 ± 2.3 *16.3 ± 1.5*	-	-

For blank Phospholipon 90H:Chol CLs, two distinct populations with nanometric (150 ± 0.0 nm) and micrometric (5.9 ± 1.4 µm) sizes appeared; the percentage of nanometric population was of 98.8 ± 0.9%.

Blank Lipoid S100:Chol liposomes presented two populations with nanometric (172 ± 0.0 nm) and micrometric (6.4 ± 0.7 µm) sizes. The micrometric population was the major one since it represents 82.6 ± 0.7% of the vesicles. The results are in good agreement with the results obtained in previous studies (Azzi et al., 2018b; Hammoud et al., 2019a). In addition, for both phospholipid types, the presence of camphor did not significantly affect the size distribution of blank liposomes.

In comparison to the blank Phospholipon 90H formulations, the incorporation of HP-β-CD reduced the percentage of nanometric population, and accordingly boosted the production of larger micrometric vesicles. Also, we can notice a significant decrease in the percentage of nanometric population in presence of HP-β-CD/camphor inclusion complex compared to the blank batch. Indeed, this result does not corroborate other literature studies where HP-β-CD does not affect Phospholipon 90H particle size (Gharib et al., 2017a; Sebaaly et al., 2016). This difference can be ascribed to the different methods used for size characterization. Most studies in literature used dynamic light scattering where the detection could be limited to submicron size range populations (Storti and Balsamo, 2010). However, the laser granulometry technique used in this study is designed for measuring particle sizes between 0.01 and 3000 µm. The aggregation of smaller particles into large vesicles could explain the appearance of giant particles in HP-β-CD-loaded liposomes and camphor-DCLs composed of Phospholipon 90H and Chol (Domazou and Luigi Luisi, 2002; Puskás and Csempesz, 2007). Phospholipon 90H liposomes presented a negative surface charge, resulting from the phosphatidylcholine head group present at the surface of vesicles, with the phosphate group located above the choline group plane (Ascenso et al., 2013; Gharib et al., 2017a; Sebaaly et al., 2016). Moreover, a previous study investigated that the presence of HP-β-CD induced a decrease in surface charge of Phospholipon 90H where CDs may produce changes in phosphatidylcholine head group orientation at the surface of vesicles, allowing exposure of positively

charged choline to the surface (Gharib et al., 2017a). Namely, the repulsive force between particles decreases in the presence of CDs; therefore, the vesicles would be more susceptible to aggregate.

For Lipoid S100 liposomes, HP-β-CD shifted the size distribution in favor of the micrometric liposomes; the percentage of micrometric population was 82.6 ± 0.7% for blank liposomes while it markedly increased to 100 ± 0.0% in the presence of HP-β-CD. The results are in accordance with our previous results obtained at HP-β-CD concentration of 25 and 75 mM (Hammoud et al., 2020). Additionally, HP-β-CD-loaded liposomes and camphor-DCLs had larger particle size compared to camphor-CLs and blank CLs, which is in agreement with the results of Maestrelli et al., (2006) and Cavalcanti et al., (2011) who showed that the HP-β-CD/guest-loaded liposomes possessed a larger diameter than the guest-loaded vesicles.

3.2.2. Determination of phospholipid:Chol:camphor molar ratio

The IR values of phospholipids and Chol as well as the EE and LR values of camphor in the various CL and DCL formulations were determined. The results are shown in Table 3.

Table 3: Phospholipid (PL) and cholesterol (Chol) incorporation rates (IR), camphor encapsulation efficiency (EE), camphor loading rate (LR), and PL:Chol:camphor molar ratio for the various liposome formulations.

Sample (PL:Chol:camphor molar ratio)	IR of PL (%)	IR of Chol (%)	EE of camphor (%)	LR of camphor (%)	Final PL:Chol:camphor molar ratio
Phospholipon 90H:Chol formulations					
Blank CLs (1:1:0)	86.6 ± 2.9	79.8 ± 1.8	-	-	1:1:0
Camphor-CLs (1:1:4)	87.9 ± 4.9	85.4 ± 3.7	62.1 ± 4.9	1.9 ± 0.4	1:1:0.08
Blank DCLs (1:1:0)	51.4 ± 7.1	64.8 ± 4.4	-	-	1:1:0
Camphor-DCLs (1:1:5)	58.4 ± 4.1	61.9 ± 5.1	56.9 ± 3.3	8.9 ± 1.7	1:1:0.5
Lipoid S100:Chol formulations					
Blank CLs (1:1:0)	93.3 ± 1.3	80.8 ± 1.4	-	-	1:1:0
Camphor-CLs (1:1:4)	92.4 ± 2.5	72.8 ± 3.6	66.2 ± 5.5	4.7 ± 0.3	1:1:0.25
Blank DCLs (1:1:0)	85.5 ± 2.5	75.2 ± 4.8	-	-	1:1:0
Camphor-DCLs (1:1:5)	86.7 ± 3.1	69.2 ± 2.7	68.4 ± 1.0	54.9 ± 2.5	1:0.75:2

3.2.2.1. Phospholipid:Chol:camphor molar ratio

The IR values of Phospholipon 90H (86.6 ± 2.9%) and Lipoid S100 (93.3 ± 1.3%) in blank liposomes were high, indicating that a small loss of phospholipids occurred during liposome preparation. The addition of camphor did not significantly affect the incorporation of Phospholipon 90H and Lipoid S100 in liposomes. Additionally, compared to empty vesicles, the loading of free HP-β-CD and HP-β-CD/camphor inclusion complex into liposome aqueous phase lowered the entrapment of both phospholipid types in liposome. This finding might be explained by the ability of CDs to interact with lipid bilayers and to extract lipid components from biomimetic and biological membranes (Hammoud et al., 2019b).

Chol quantification assay showed that the IR values of Chol were 79.8 ± 1.8% and 80.8 ± 1.4% into blank Phospholipon 90H liposomes and blank Lipoid S100 liposomes, respectively. These values are approximately consistent with recently published data: 84.2 ± 3.8% into Phospholipon 90H liposomes (Azzi et al., 2018b) and 77.6 ± 1.18% into Lipoid S100 liposomes (Hammoud et al., 2020, 2019a). Camphor did not modify the Chol content of Phospholipon 90H and Lipoid S100 liposome membranes. Furthermore, the addition of HP-β-CD and HP-β-CD/camphor complex didn't drastically impact the incorporation of Chol into Lipoid S100 liposomes. However, in the presence of HP-β-CD, the IR of Chol into phospholipon 90H liposomes markedly decreased compared to the blank formulations. Hence, HP-β-CD effectively extracted Chol from Phospholipon 90H liposome membranes, forming soluble inclusion complexes out of the membrane matrix, while no effect was exerted on Lipoid S100 vesicles. It might be that CD-mediated Chol extraction is easier from saturated Phospholipon 90H:Chol membranes compared to unsaturated Lipoid S100:Chol membranes, in agreement with our previous studies (Hammoud et al., 2020; Hammoud et al. 2020, submitted).

In terms of LR value, the DCL carrier system significantly improved the encapsulation of camphor. Likewise, literature studies showed that the DCL system represents a better encapsulation system than CLs for numerous drugs including *trans*-anethole (Gharib et al., 2017a), estragole, pulegone, thymol (Hammoud et al., 2020), celecoxib (Jain et al., 2007) and betamethasone (Piel et al., 2006). Additionally, the LR values were higher in liposomes composed of Lipoid S100 compared to those composed of Phospholipon 90H. Lipid bilayers composed of Lipoid S100 (unsaturated phospholipid) are less densely packed and more flexible compared to those composed of Phospholipon 90H (saturated phospholipid), leading to higher camphor incorporation in liposomes. Also, Lipoid S100 liposomes were fabricated at room temperature while the preparation of Phospholipon 90H liposomes requires heating at 55 ºC, thus promoting the loss of volatile camphor.

The EE values of camphor were below 70% in all CL and DCL formulations. It was reported that camphor, bearing a carbonyl group, interacts with the polar head group of phospholipids constituting stratum corneum lipid bilayer, leading to an increase in membrane fluidity and permeability (Cui et al., 2011). Furthermore, in our previous study, we investigated that the incorporation in liposomes was more efficient for the essential oil components exhibiting low aqueous solubility (Hammoud et al. 2019a); thus, the moderate incorporation in liposomes may be due to the high aqueous solubility of camphor compared to other essential oil components. On the other hand, it is noteworthy that the retention of EO components into DCLs strongly depends on the stability of the inclusion complexes. It might be that the interaction of camphor with CD is not strong enough to inhibit the release of camphor. In general, the main forces involved in the inclusion complex formation are weak non-ionic interactions, such as van der Waal forces, hydrophobic bonding and hydrogen bonding between the CD's cavity and drug molecules. CD inclusion complex formation is a dynamic equilibrium process, whereby the drug molecules continuously associate and dissociate from the CD cavity. Molecular modeling studies

showed that camphor fits in the edge of the wider rim of HP-β-CD, leading to its easier release from the cavity of HP-β-CD compared to other CD types (Celebioglu et al., 2018). In addition, the stability constant values reported in literature for HP-β-CD/camphor inclusion complex were 1280 M^{-1} (Ciobanu et al., 2013) and 1530 M^{-1} (Tanaka et al., 1996). The affinity of camphor for CD could also explain the IR values of phospholipid and Chol into camphor-DCLs and blank-DCLs. We noticed in Table 3 that the incorporation of camphor into CD cavity did not limit the effect of CD on Phospholipon 90H- and Lipoid S100 liposome membrane. Hence, it is possible that, during the preparation or storage of DCLs, lipid components, especially Chol, may enter the CD cavity and replace camphor (Chen et al., 2014). As drug molecule leaks out of CD cavity, CDs become empty, thereby able to extract lipid components from liposome membrane (Piel et al., 2006).

Based on the characteristics of CLs and DCLs, it is obvious that the best system for camphor encapsulation is the DCL system prepared using Lipoid S100.

3.2.3. Storage stability

The stability of the various formulations was examined after 3 months of storage at 4 °C. The mean size of all batches was maintained after storage except for camphor-CLs where an increase in the particle size was observed (Table 2). In addition, the total camphor concentration in the liposome suspensions was determined after 3 months by HPLC, and the values were compared to those obtained on the day of preparation. The results showed that all formulations effectively retained camphor after storage: the percentage of remaining camphor was 90.1 ± 0.2%, 93.2 ± 3.4%, 83.8 ± 6.3%, and 90.2 ± 3.1% for Phospholipon 90H CLs, phospholipon 90H DCLs, Lipoid S100 CLs, and Lipoid S100 DCLs, respectively.

Conclusion

In the present study, the encapsulation of the bio-insecticide, camphor, into CLs and DCLs was studied using hydrogenated (Phospholipon 90H) or non-hydrogenated (Lipoid S100) phospholipids and Chol. The size, the IR of phospholipids and Chol, the EE and LR of camphor, and the storage stability of the different formulations were characterized. Lipoid S100 DCLs displayed the highest LR of camphor (54.9 ± 2.5%) compared to Phospholipon 90H CLs, Phospholipon 90H DCLs and Lipoid S100 CLs. Additionally, the various CL and DCL batches were stable after 3 months of storage at 4 ºC. Finally, it would be valuable to study the insecticidal effect of camphor-CLs and camphor-DCLs for their application in agriculture and food products.

References

Ansari, M.A., Razdan, R.K., 1995. Relative efficacy of various oils in repelling mosquitoes. Indian J. Malariol. 32, 104–111.

Ascenso, A., Cruz, M., Euletério, C., Carvalho, F.A., Santos, N.C., Marques, H.C., Simões, S., 2013. Novel tretinoin formulations: a drug-in-cyclodextrin-in-liposome approach. J. Liposome Res. 23, 211–219. https://doi.org/10.3109/08982104.2013.788026

Azzi, J., Auezova, L., Danjou, P.-E., Fourmentin, S., Greige-Gerges, H., 2018a. First evaluation of drug-in-cyclodextrin-in-liposomes as an encapsulating system for nerolidol. Food Chem. 255, 399–404. https://doi.org/10.1016/j.foodchem.2018.02.055

Azzi, J., Jraij, A., Auezova, L., Fourmentin, S., Greige-Gerges, H., 2018b. Novel findings for quercetin encapsulation and preservation with cyclodextrins, liposomes, and drug-in-cyclodextrin-in-liposomes. Food Hydrocoll. 81, 328–340. https://doi.org/10.1016/j.foodhyd.2018.03.006

Brenes, A., Roura, E., 2010. Essential oils in poultry nutrition: Main effects and modes of action. Anim. Feed Sci. Technol. 158, 1–14. https://doi.org/10.1016/j.anifeedsci.2010.03.007

Cavalcanti, I.M.F., Mendonça, E.A.M., Lira, M.C.B., Honrato, S.B., Camara, C.A., Amorim, R.V.S., Filho, J.M., Rabello, M.M., Hernandes, M.Z., Ayala, A.P., Santos-Magalhães, N.S., 2011. The encapsulation of β-lapachone in 2-hydroxypropyl-β-cyclodextrin inclusion complex into liposomes: A physicochemical evaluation and molecular modeling approach. Eur. J. Pharm. Sci. 44, 332–340. https://doi.org/10.1016/j.ejps.2011.08.011

Celebioglu, A., Aytac, Z., Kilic, M.E., Durgun, E., Uyar, T., 2018. Encapsulation of camphor in cyclodextrin inclusion complex nanofibers via polymer-free electrospinning: enhanced water solubility, high temperature stability, and slow release of camphor. J. Mater. Sci. 53, 5436–5449. https://doi.org/10.1007/s10853-017-1918-4

Chang, C.-P., Leung, T.-K., Lin, S.-M., Hsu, C.-C., 2006. Release properties on gelatin-gum arabic microcapsules containing camphor oil with added polystyrene. Colloids Surf. B Biointerfaces 50, 136–140. https://doi.org/10.1016/j.colsurfb.2006.04.008

Chen, H., Gao, J., Wang, F., Liang, W., 2007. Preparation, Characterization and Pharmacokinetics of Liposomes-Encapsulated Cyclodextrins Inclusion Complexes for Hydrophobic Drugs. Drug Deliv. 14, 201–208. https://doi.org/10.1080/10717540601036880

Chen, J., Lu, W.-L., Gu, W., Lu, S.-S., Chen, Z.-P., Cai, B.-C., Yang, X.-X., 2014. Drug-in-cyclodextrin-in-liposomes: a promising delivery system for hydrophobic drugs. Expert Opin. Drug Deliv. 11, 565–577. https://doi.org/10.1517/17425247.2014.884557

Chen, W., Vermaak, I., Viljoen, A., 2013. Camphor—A Fumigant during the Black Death and a Coveted Fragrant Wood in Ancient Egypt and Babylon—A Review. Molecules 18, 5434–5454. https://doi.org/10.3390/molecules18055434

Ciobanu, A., Landy, D., Fourmentin, S., 2013. Complexation efficiency of cyclodextrins for volatile flavor compounds. Food Res. Int. 53, 110–114. https://doi.org/10.1016/j.foodres.2013.03.048

Cui, Y., Li, L., Zhang, L., Li, J., Gu, J., Gong, H., Guo, P., Tong, W., 2011. Enhancement and mechanism of transdermal absorption of terpene-induced propranolol hydrochloride. Arch. Pharm. Res. 34, 1477–1485. https://doi.org/10.1007/s12272-011-0909-2

Domazou, A.S., Luigi Luisi, P., 2002. SIZE DISTRIBUTION OF SPONTANEOUSLY FORMED LIPOSOMES BY THE ALCOHOL INJECTION METHOD. J. Liposome Res. 12, 205–220. https://doi.org/10.1081/LPR-120014758

Gharib, R., Auezova, L., Charcosset, C., Greige-Gerges, H., 2018. Effect of a series of essential oil molecules on DPPC membrane fluidity: a biophysical study. J. Iran. Chem. Soc. 15, 75–84. https://doi.org/10.1007/s13738-017-1210-1

Gharib, R., Auezova, L., Charcosset, C., Greige-Gerges, H., 2017a. Drug-in-cyclodextrin-in-liposomes as a carrier system for volatile essential oil components: Application to anethole. Food Chem. 218, 365–371. https://doi.org/10.1016/j.foodchem.2016.09.110

Gharib, R., Haydar, S., Charcosset, C., Fourmentin, S., Greige-Gerges, H., 2019. First study on the release of a natural antimicrobial agent, estragole, from freeze-dried delivery systems based on cyclodextrins and liposomes. J. Drug Deliv. Sci. Technol. 52, 794–802. https://doi.org/10.1016/j.jddst.2019.05.032

Gharib, R., Najjar, A., Auezova, L., Charcosset, C., Greige-Gerges, H., 2017b. Interaction of Selected Phenylpropenes with Dipalmitoylphosphatidylcholine Membrane and Their Relevance to Antibacterial Activity. J. Membr. Biol. 250, 259–271. https://doi.org/10.1007/s00232-017-9957-y

Glenn, G.M., Klamczynski, A.P., Woods, D.F., Chiou, B., Orts, W.J., Imam, S.H., 2010. Encapsulation of Plant Oils in Porous Starch Microspheres. J. Agric. Food Chem. 58, 4180–4184. https://doi.org/10.1021/jf9037826

Halim Moss, A.-T., Abdelfatta, N.A.H., Mohafrash, S.M.M., 2017. Nanoemulsion of Camphor (Eucalyptus globulus) Essential Oil, Formulation, Characterization and Insecticidal Activity against Wheat Weevil, Sitophilus granarius. Asian J. Crop Sci. 9, 50–62. https://doi.org/10.3923/ajcs.2017.50.62

Hammoud, Z., Kayouka, M., Trifan, A., Sieniawska, E., Świątek, Ł., Mediouni Ben Jemâa, J., Elaissari, A., Greige-Gerges, H., 2020. Encapsulation of α-pinene, a natural bio-insecticide, in delivery systems based on liposomes and drug-in-cyclodextrin-in-liposomes. Processes (submitted)

Hammoud, Z., Gharib, R., Fourmentin, S., Elaissari, A., Greige-Gerges, H., 2020. Drug-in-hydroxypropyl-β-cyclodextrin-in-lipoid S100/cholesterol liposomes: Effect of the characteristics of essential oil components on their encapsulation and release. Int. J. Pharm. 579, 119151. https://doi.org/10.1016/j.ijpharm.2020.119151

Hammoud, Z., Gharib, R., Fourmentin, S., Elaissari, A., Greige-Gerges, H., 2019a. New findings on the incorporation of essential oil components into liposomes composed of lipoid S100 and cholesterol. Int. J. Pharm. 561, 161–170. https://doi.org/10.1016/j.ijpharm.2019.02.022

Hammoud, Z., Khreich, N., Auezova, L., Fourmentin, S., Elaissari, A., Greige-Gerges, H., 2019b. Cyclodextrin-membrane interaction in drug delivery and membrane structure maintenance. Int. J. Pharm. 564, 59–76. https://doi.org/10.1016/j.ijpharm.2019.03.063

Jain, S.K., Gupta, Y., Jain, A., Bhola, M., 2007. Multivesicular Liposomes Bearing Celecoxib-β-Cyclodextrin Complex for Transdermal Delivery. Drug Deliv. 14, 327–335. https://doi.org/10.1080/10717540601098740

Kirby, C., Gregoriadis, G., 1983. The effect of lipid composition of small unilamellar liposomes containing melphalan and vincristine on drug clearance after injection into mice. Biochem. Pharmacol. 32, 609–615. https://doi.org/10.1016/0006-2952(83)90483-5

Maestrelli, F., González-Rodríguez, M.L., Rabasco, A.M., Mura, P., 2006. Effect of preparation technique on the properties of liposomes encapsulating ketoprofen–cyclodextrin complexes aimed for transdermal delivery. Int. J. Pharm. 312, 53–60. https://doi.org/10.1016/j.ijpharm.2005.12.047

McCormack, B., Gregoriadis, G., 1994. Drugs-in-cyclodextrins-in liposomes: a novel concept in drug delivery. Int. J. Pharm. 112, 249–258. https://doi.org/10.1016/0378-5173(94)90361-1

Obeng-Ofori, D., Reichmuth, C.H., Bekele, A.J., Hassanali, A., 1998. Toxicity and protectant potential of camphor, a major component of essential oil of Ocimum kilimandscharicum, against four stored product beetles. Int. J. Pest Manag. 44, 203–209. https://doi.org/10.1080/096708798228112

Piel, G., Piette, M., Barillaro, V., Castagne, D., Evrard, B., Delattre, L., 2006. Betamethasone-in-cyclodextrin-in-liposome: The effect of cyclodextrins on encapsulation efficiency and release kinetics. Int. J. Pharm. 312, 75–82. https://doi.org/10.1016/j.ijpharm.2005.12.044

Puskás, I., Csempesz, F., 2007. Influence of cyclodextrins on the physical stability of DPPC-liposomes. Colloids Surf. B Biointerfaces 58, 218–224. https://doi.org/10.1016/j.colsurfb.2007.03.011

Rahnama-Moghadam, S., Hillis, L.D., Lange, R.A., 2015. Environmental Toxins and the Heart, in: Heart and Toxins. Elsevier, pp. 75–132. https://doi.org/10.1016/B978-0-12-416595-3.00003-7

Reed, M.D., 2005. Poisoning & Toxicology Handbook, Third Edition. Chest 127, 1081. https://doi.org/10.1378/chest.127.3.1081

Rozman, V., Kalinovic, I., Korunic, Z., 2007. Toxicity of naturally occurring compounds of Lamiaceae and Lauraceae to three stored-product insects. J. Stored Prod. Res. 43, 349–355. https://doi.org/10.1016/j.jspr.2006.09.001

Sebaaly, C., Charcosset, C., Stainmesse, S., Fessi, H., Greige-Gerges, H., 2016. Clove essential oil-in-cyclodextrin-in-liposomes in the aqueous and lyophilized states: From laboratory to large scale using a membrane contactor. Carbohydr. Polym. 138, 75–85. https://doi.org/10.1016/j.carbpol.2015.11.053

Seyoum, A., Killeen, G.F., Kabiru, E.W., Knols, B.G.J., Hassanali, A., 2003. Field efficacy of thermally expelled or live potted repellent plants against African malaria vectors in western Kenya. Trop. Med. Int. Health 8, 1005–1011. https://doi.org/10.1046/j.1360-2276.2003.01125.x

Seyoum, A., Pålsson, K., Kung'a, S., Kabiru, E.W., Lwande, W., Killeen, G.F., Hassanali, A., Knots, B.G.J., 2002. Traditional use of mosquito-repellent plants in western Kenya and their evaluation in semi-field experimental huts against Anopheles gambiae: ethnobotanical studies and application by thermal expulsion and direct burning. Trans. R. Soc. Trop. Med. Hyg. 96, 225–231. https://doi.org/10.1016/S0035-9203(02)90084-2

Shahabi, S., Jorsaraei, S.G.A., Akbar Moghadamnia, A., Barghi, E., Zabihi, E., Golsorkhtabar Amiri, M., Maliji, G., Sohan Faraji, A., Abdi Boora, M., Ghazinejad, N., Shamsai, H., 2014. The effect of camphor on sex hormones levels in rats. Cell J. 16, 231–234.

Sherry, M., Charcosset, C., Fessi, H., Greige-Gerges, H., 2013. Essential oils encapsulated in liposomes: a review. J. Liposome Res. 23, 268–275. https://doi.org/10.3109/08982104.2013.819888

Sikka, S.C., Bartolome, A.R., 2018. Perfumery, Essential Oils, and Household Chemicals Affecting Reproductive and Sexual Health, in: Bioenvironmental Issues Affecting Men's Reproductive and Sexual Health. Elsevier, pp. 557–569. https://doi.org/10.1016/B978-0-12-801299-4.00036-0

Sirtori, C., Altvater, P., Freitas, A., Peraltazamora, P., 2006. Degradation of aqueous solutions of camphor by heterogeneous photocatalysis. J. Hazard. Mater. 129, 110–115. https://doi.org/10.1016/j.jhazmat.2005.08.017

Storti, F., Balsamo, F., 2010. Particle size distributions by laser diffraction: sensitivity of granular matter strength to analytical operating procedures. Solid Earth 1, 25–48. https://doi.org/10.5194/se-1-25-2010

Szejtli, J., 1998. Introduction and General Overview of Cyclodextrin Chemistry. Chem. Rev. 98, 1743–1754. https://doi.org/10.1021/cr970022c

Takino, T., Konishi, K., Takakura, Y., Hashida, M., 1994. Long Circulating Emulsion Carrier Systems for Highly Lipophilic Drugs. Biol. Pharm. Bull. 17, 121–125. https://doi.org/10.1248/bpb.17.121

Tanaka, M., Matsuda, H., Sumiyoshi, H., Arima, H., Hirayama, F., Uekama, K., Tsuchiya, S., 1996. 2-Hydroxypropylated Cyclodextrins as a Sustained-Release Carrier for Fragrance Materials. Chem. Pharm. Bull. (Tokyo) 44, 416–420. https://doi.org/10.1248/cpb.44.416

Turek, C., Stintzing, F.C., 2013. Stability of Essential Oils: A Review: Stability of essential oils…. Compr. Rev. Food Sci. Food Saf. 12, 40–53. https://doi.org/10.1111/1541-4337.12006

Yalkowsky, S., He, Y., Jain, P., 2010. Handbook of Aqueous Solubility Data, Second Edition. CRC Press. https://doi.org/10.1201/EBK1439802458

Discussion and Perspectives

Discussion

EOs possess antibacterial, antifungal and antiviral properties and have been investigated as a potential source of novel antimicrobial compounds, alternatives to hazardous chemical pesticides and agents promoting food preservation (Astani et al., 2010; Mossa, 2016; Pandey et al., 2017; Solórzano-Santos and Miranda-Novales, 2012). However, as previously discussed in this manuscript, it is important to encapsulate EOs in order to extend their shelf life and activities. Nanoparticles were extensively proposed for drug delivery where they allowed targeted delivery and controlled release of the drug (Rizvi and Saleh, 2018). Liposomes and DCLs were used in our studies as carriers for several EO components. Here, the ethanol injection method was applied for the preparation of liposomes. This method is simple, a one step process, inexpensive and rapid. Also, it avoids the use of harmful solvents as well as strong forces that may disrupt the liposomes and the entrapped molecules (Justo and Moraes, 2010). The liposome preparation parameters (PL concentration, CHOL concentration, stirring rate, organic phase/aqueous volume ratio, and the rate of the ethanol phase injection) were previously optimized (Sebaaly et al., 2016). In combination with CHOL, the unsaturated PL, Lipoid S100, was selected in our studies for vesicle preparation. This lipid proved a higher encapsulation of the EO component, eugenol, into liposomes compared to the saturated PLs like Phospholipon 90H and Phospholipon 80 (Sebaaly et al., 2016). Phospholipon 90H was used in this work to prepare some liposome formulations since it was previously demonstrated that liposomes composed of saturated PLs present a higher stability during storage for several months at 4°C and a better stability during freeze-drying compared to liposomes composed of unsaturated PLs (Sebaaly et al., 2016).

During my thesis, the first study was to characterize the encapsulation of the MTs: EUC, PUL, TER and THY, and the PPs, EST and ISOEUG, into CLs and DCLs composed of Lipoid S100 and CHOL. Then, the MTs α-PIN and CAM were encapsulated in CLs and DCLs using Phospholipon 90H or Lipoid S100

in combination with CHOL. Alpha-PIN and CAM were chosen in the latter study due to their interesting insecticidal properties. Although several studies investigated the encapsulation of EO components into CLs and DCLs, there is no available data on the effect of the physicochemical parameters of a drug on CL and DCL characteristics. For that, the effect of the chemical structure, aqueous solubility, log P, and Hc on the encapsulation and the release of EO components from CLs and DCLs was investigated. The structure, log P, and aqueous solubility values of the selected drugs are presented in Table 1. It is worthy to note that the Hc values of the selected drugs, except those of α-PIN and CAM, are for the first time experimentally determined at 30 and 60 °C, and the results are reported in Table 1. The experimental Hc values determined at 30 °C are in good agreement with the predicted Hc values found in the literature (Pubchem). The EE and the LR values of the chosen EO components into CLs and DCLs were calculated, and the values are represented in Table 1.

Table 1: The structure, log P, aqueous solubility, and Hc of the selected EO components, and their EE and LR values into CLs and DCLs.

EO component	Structure	Aqueous solubility (mg/L)	Log P	Hc		CLs		DCLs	
				30 ºC	60 ºC	EE (%)	LR (%)	EE (%)	LR (%)
Alpha-pinene	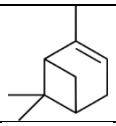	2.5	4.83	-	-	100.0 ± 0.0	22.9 ± 2.2	100.0 ± 0.0	0.6 ± 0.02
Camphor	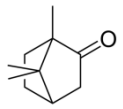	1600	2.38	-	-	66.2 ± 5.5	4.7 ± 0.3	68.4 ± 1.0	54.9 ± 2.5
Estragole	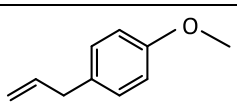	178	3.4	0.03	0.07	90.9 ± 0.74	1.1 ± 0.3	89.7 ± 3.8	10.9 ± 3.1
Eucalyptol	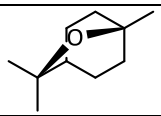	3500	2.74	0.01	0.05	61.9 ± 7.05	4.9 ± 0.1	49.4 ± 8.4	2.18 ± 0.3
Isoeugenol	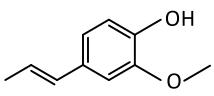	665	2.6	0.005	0.008	96.4 ± 3.25	19.9 ± 2.2	88.7 ± 0.9	13.0 ± 1.0

Pulegone	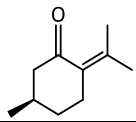	276	3.08	0.005	0.009	90.5 ± 0.32	2.9± 0.3	61.8 ± 6.7	9.33 ± 1.1
Terpineol	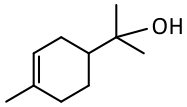	7100	2.98	0.001	0.003	73.7 ± 4.13	18.7 ± 0.6	25.3 ± 1.8	13.3 ± 1.6
Thymol	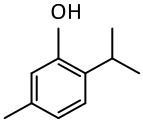	900	3.3	0.003	0.009	79.1 ± 3.86	20.5 ± 1.9	49.5 ± 4.0	23.1 ± 1.0

The aqueous solubility and log P values are from Pubchem

1. The characteristics of CLs

1.1. The influence of EO components on liposome particle size

In general, blank liposomes composed of Phospholipon 90H or Lipoid S100 in combination with CHOL represented two distinct populations: a nanometric sized population and a micrometric sized population. The nanometric population was the major population for blank phospholipon 90H particles while the micrometric population was the major population for Lipoid S100 particles. Larger vesicles were obtained in comparison to the literature and this could be related to the different methods used for size characterization. Here, the size characterization was done using the laser granulometry technique which enables measuring particle sizes between 0.01 and 3000 μm. However, most studies in literature used dynamic light scattering for size characterization where the detection could be limited to submicron size range populations (Storti and Balsamo, 2010).

The effects of EO components on the particle size of Lipoid S100 liposomes were evaluated. CAM, EUC and PUL did not influence the size distribution of Lipoid S100 liposomes. However, the EO components: α-PIN, EST, ISOEUG, TER and THY boosted the formation of larger vesicles in comparison to blank Lipoid S100 liposomes. Based on these results, we can propose that the degree of drug incorporation into liposomes control their effect on particle size where drugs with high LR into

liposomes showed a greater effect on particle size distribution. The accumulation of lipophilic drugs in the hydrophobic part of the membrane may affect the interactions between the acyl chains of PLs and induces swelling of the membrane, leading to the formation of larger vesicles (Sikkema et al., 1995). Moreover, giant particles could be clusters or aggregates of smaller particles (Domazou and Luigi Luisi, 2002). It is noteworthy to mention that many other EO components induce an increase in liposome particle size like eugenol (Sebaaly et al., 2015) and nerolidol (Azzi et al., 2018). Here, the morphological characterization using scanning electron microscope was performed confirming the broad size distribution of Lipoid S100 formulations (drug-loaded-, CD-loaded-, and CD/drug inclusion complex-loaded liposomes). The results proved that aggregation/fusion of batches during preparation or storage cannot be excluded.

1.2. The influence of EO components on the membrane composition of liposomes

The selected EO components exert different effects on the membrane composition of Lipoid S100 liposomes. Alpha-PIN, ISOEUG, PUL and THY significantly reduced PL retention while the other EO components did not greatly influence the loading of PLs into vesicles. It might be that the degree of encapsulation of EOs in liposomes modulates the extent of interaction of EOs with membrane phospholipids where a decrease in the PL IR was demonstrated for liposomes exhibiting a high LR of drugs, except for PUL. The interaction of the studied EO components (except CAM) with DPPC liposome membranes was previously studied (Cristani et al., 2007; Gharib et al., 2018a, 2017b; Rodriguez et al., 2018). It was proved that the selected components interact with the polar head groups and the hydrophobic acyl chains of PLs, producing a membrane fluidizing effect. Moreover, it was demonstrated that the EO components, except EUC, act as substitution impurities, taking place of lipid molecules, while EUC acts as an interstitial impurity and intercalates in the bilayer.

On the other hand, the incorporation of EUC, ISOEUG, PUL and THY reduced CHOL entrapment into liposomes. The other EO components did not modify the CHOL content of vesicles. Fang et al., (2001) reported that certain lipid soluble drugs compete with CHOL molecules for the hydrophobic space in the liposomal membrane.

1.3.The factors influencing the incorporation of EO components into CLs

The entrapment of drugs into liposomes, generally evaluated by their EE and LR values, depends on the studied EO components. The EE values into CLs were higher for EO components exhibiting lower aqueous solubility (α-PIN, EST, ISOEUG and PUL) compared to those exhibiting higher aqueous solubility values (CAM, EUC, TER and THY). Moreover, it was investigated that manifesting a high Hc value could be a factor that reduces the liposomal incorporation of EO components. In addition, bearing a hydroxyl group in the chemical structure of EO components (ISOEUG, TER and THY) seems to enhance their incorporation into CLs, as evidenced by their LR values. This was probably due to the interaction of hydroxyl groups of drugs with the membrane components of liposomes (PLs, CHOL) (Cristani et al., 2007). The non-hydroxylated EO component α-PIN presents a high LR value into CLs, and this was attributed to the high affinity of α-PIN for lipid membranes due to its high hydrophobicity and chemical structure that does not contain polar groups (Rodriguez et al., 2018). Besides, it is worthy to mention that all these factors modulate the retention of CAM in Lipoid S100-CLs which was characterized in a separate study during my thesis.

1.4.The factors influencing the release of EO components from CLs

The release of the studied EO components (α-PIN and CAM were not included due to unfavorable circumstances in the last year of my thesis) in free form or when encapsulated into CLs was studied using multiple headspace extraction, and the parameters that influence their release were estimated. In

their free form, EO components presented different release rates; the Hc value of EO component was shown to control its release as revealed by plotting the release percentage as a function of Hc value. However, Hc did not influence the release of components from liposomes. Liposomes efficiently retained EO components, thereby reducing their volatility. The factors that affect the release rate of EO components from CLs are the size of liposomal batches (slower release for liposomes of larger size), IR of CHOL into liposomes (the slow release of pulegone was ascribed to the low CHOL content of pulegone-loaded vesicles), LR of EO components (slower release for components possessing a high LR into liposomes), and the location of components within the lipid bilayer (the deep insertion of components in lipid bilayers caused their slower release from liposomes).

2. The effect of CDs on particle size and membrane composition of liposomes

For the first time in literature, the effect of HP-β-CD on liposome size and liposome membrane composition (PL and CHOL IR values) was investigated using various HP-β-CD concentrations (25, 50, 75 mM). Table 2 presents the size and membrane composition of blank- and HP-β-CD-loaded liposomes (blank DCLs) prepared with Phospholipon 90H or Lipoid S100 in combination with CHOL.

Table 2: The size distribution and membrane composition of blank and HP-β-CD-loaded liposomes prepared with Phospholipon 90H or Lipoid S100 in combination with cholesterol.

sample	Size distribution						Membrane composition	
	Population 1		population 2		population 3		IR of PL (%)	IR of CHOL (%)
	%	Mean size (nm)	%	Mean size (μm)	%	Mean size (μm)		
Phospholipon 90H:CHOL formulations								
Blank liposome	93.2 ± 3.8	150 ± 0.0	6.8 ± 3.8	6.1 ± 1.1	-	-	88.1 ± 4.6	77.8 ± 2.6
Blank DCL (HP-β-CD 50 mM)	55.1 ± 4.5	131 ± 0.0	17.6 ± 4.5	4.9 ± 0.4	27.3 ± 8.7	82.7 ± 11.6	51.4 ± 7.1	64.8 ± 4.4
Blank DCL (HP-β-CD 75 mM)	72.3 ± 7.3	140 ± 10.9	27.7 ± 7.3	6.1 ± 0.8	-	-	66.5 ± 3.9	41.1 ± 1.3
Lipoid S100:CHOL formulations								
Blank liposome	17.2 ± 0.9	169 ± 16.6	82.8 ± 0.9	6.5 ± 0.3	-	-	94.4 ± 3.1	76.5 ± 2.6
Blank DCL (HP-β-CD 25 mM)	-	-	75.5 ± 6.4	12.1 ± 0.9	24.5 ± 6.4	63.2 ± 6.1	82.7 ± 0.7	77.3 ± 1.0
Blank DCL (HP-β-CD 50 mM)	-	-	100 ± 0.0	16.2 ± 1.5	-	-	85.5 ± 2.5	75.2 ± 4.8
Blank DCL (HP-β-CD 75 mM)	-	-	67.5 ± 4.9	7.7 ± 0.1	32.5 ± 4.9	78.0 ± 14.9	82.1 ± 2.5	75.6 ± 3.2

Note: The values presented in this table consider the results of all studies; the values are expressed as mean values of all results ± SD.

As explained above, two populations of nanometric and micrometric sizes were obtained with blank Lipoid S100 and Phospholipon 90H liposomes (Table 2). The addition of HP-β-CD (25, 50 and 75 mM) to Lipoid S100:CHOL liposomes promoted the formation of larger vesicles. HP-β-CD interacts with the acyl chains of Lipoid S100 constituting liposome membrane; the packing of the acyl chains is reduced, and this leads to membrane swelling and particle size enlargement (Gharib et al., 2018b). Similarly, the addition of HP-β-CD (50 and 75 mM) to Phospholipon 90H:CHOL liposomes reduced the percentage of nanometric population, and accordingly boosted the production of larger micrometric vesicles. In comparison to blank liposomes, the aggregation of smaller particles into large vesicles could explain the appearance of giant particles in Phospholipon 90H:CHOL and Lipoid S100:CHOL liposomes carrying HP-β-CD. The presence of surface charge prevents aggregation due to electrostatic repulsion, and the

more neutral net charge results in the formation of aggregates (Wiącek and Chibowski, 1999). The magnitude of zeta potential, which is a parameter that characterizes the particles surface charge, was previously determined for blank Phospholipon 90H and Lipoid S100 liposomes (Gharib et al., 2017a). The authors demonstrated that both types of formulations present a negative surface charge, resulting from the phosphatidylcholine head group orientation at the surface of vesicles, with the phosphate group located above the choline group plane. Besides, HP-β-CD decreased the zeta potential value (surface charge) of Phospholipon 90H liposomes; CDs may produce changes in phosphatidylcholine head group orientation at the surface of vesicles, allowing exposure of positively charged choline to the surface (Gharib et al., 2017a).

At all the tested CD concentrations, HP-β-CD reduced the incorporation of PLs into Phospholipon 90H and Lipoid S100 liposome membrane compared to blank liposomes. This finding was explained by the ability of CDs to extract lipid components from lipid membranes (Denz et al., 2016; Ohtani et al., 1989). Moreover, in comparison to the blank batches, HP-β-CD lowered CHOL entrapment in Phospholipon 90H liposomes while it didn't markedly influence the retention of CHOL in Lipoid S100 lipid vesicles. Hence, HP-β-CD may extract CHOL molecules from Phospholipon 90H:CHOL liposome membrane while no effect was exerted on Lipoid S100 membranes. Literature studies demonstrated that CD-mediated CHOL extraction occurs through CHOL desorption from the surface directly into CD hydrophobic core (Yancey et al., 1996). Also, it was investigated that in saturated bilayers, CHOL is found in traditional "upright" positions with the hydroxyl group oriented towards lipid head-groups, while in unsaturated bilayers, CHOL is relatively often found in a "flipped" configuration with the hydroxyl group oriented towards the membrane middle plane (Ermilova and Lyubartsev, 2019; Harroun et al., 2006). The different orientation of CHOL may explain the variability of the effect of CD on both membranes.

To conclude, HP-β-CD interacts with liposome membrane, and the formation of HP-β-CD/PL and HP-β-CD/CHOL inclusion complexes cannot be excluded. However, as noticed in Table 2, the effect of HP-β-CD on liposome membranes is not concentration dependent in the studied CD concentration range.

3. Characteristics of DCLs

3.1. The effect of inclusion complex on the particle size and the membrane composition of liposomes

Previous studies investigated the formation of inclusion complexes between HP-β-CD and the selected EO components where the formation constant (K_f) values were determined (Table 3). Here, the concentration of EO components solubilized in the presence of different HP-β-CD concentrations (0–100 mM) was studied. The optimal CD concentration allowing efficient solubilization of drugs was determined (Table 3). During DCL preparation, the HP-β-CD/EO inclusion complex was prepared using the optimal HP-β-CD concentration.

Table 3: The CD concentration used in the preparation of the inclusion complexes, the K_f of the various inclusion complexes, and the effect of inclusion complexes on the Lipoid S100 liposome size and the membrane composition.

Inclusion complex	k_f (M^{-1})	Used CD concentration (mM)	Effect on size distribution	Effect on PL IR	Effect on CHOL IR
α-pinene	1637[a]; 2000[b]	75	Abolished the formation of large vesicles	No effect	No effect
Camphor	1280[a], 1530[c]	50	No significant effect	No effect	No effect
Estragole	1581[d]	75	Boosted the formation of large vesicles	Reduced	Reduced
Eucalyptol	334[d]; 1200[b]; 1112[b]	25	Boosted the formation of large vesicles	No effect	Reduced
Isoeugenol	441[d]	25	Abolished the formation of large vesicles	No effect	Reduced
Pulegone	676[d]; 867[b];798[b]	25	Abolished formation of large vesicles	Reduced	Reduced
Terpineol	761[d]	25	Boosted formation of large vesicles	No effect	No effect
Thymol	806[d]; 1400[b];1313[b]	75	Abolished formation of large vesicles	No effect	Reduced

a: (Ciobanu et al., 2013); b: (Kfoury et al., 2014);c : (Tanaka et al., 1996) ; d: (Kfoury et al., 2016)
Note: The effect of inclusion complex is based on comparison of size and membrane composition of Lipoid S100:CHOL drug-loaded DCLs with the respective blank DCLs.

In comparison to blank DCLs, the effect of the inclusion complexes on Lipoid S100-liposome particle size and membrane composition was examined. These effects are summarized in Table 3. Briefly, most

of inclusion complexes lowered the incorporation of PLs or CHOL into liposomes compared to blank DCLs. Hence, we suppose that the inclusion complexes may be dissociated during DCL preparation, leading to the liberation of the EO component from HP-β-CD core. CD inclusion complex formation is a dynamic equilibrium process, whereby the drug molecules continuously associate and dissociate from CD cavity. As drug molecules leak out of CD cavity, CDs become empty, thereby able to extract lipid components from liposome membranes (Piel et al., 2006). Also, some of the EO components, when released from the CD cavity, may interact with the liposome lipid bilayer, thereby minimizing the incorporation of PL or CHOL into the vesicles. The probability of drug release from CD cavity depends mainly on the strength of CD-guest interaction and on the stability of the inclusion complex, determined by its K_f value. The strength of interaction depends on the polarity and the geometric accommodation between CD cavity and guest (Marques, 2010).

3.2.The factors affecting the incorporation of EO components into DCLs

Variable factors control the loading of EO components into DCLs. If we suppose that the hydrophobic compartments of DCLs (CD core and liposome membrane) retain the hydrophobic EO components, the parameters that modulate EO entrapment into DCL vesicles are those related to CD-EO component interaction and lipid membrane-EO component interaction. First, it was found that the EE of PPs into DCLs was higher than that of MTs, except for α-PIN. This was associated with the greater increase in the liposome membrane fluidity and disorder demonstrated in the presence of PPs compared to MTs (Gharib et al., 2018a, 2017b). Also, it might be that the allyl chain of PPs remains outside the cavity of HP-β-CD and interacts with the hydroxypropyl moieties present on CD ring. This leads to an increase in the stability of HP-β-CD/PP inclusion complex compared to HP-β-CD/MT inclusion complex (Jug et al., 2010). Additionally, a negative relationship was found between the EE of EO components into DCLs (α-PIN is not included) and the CHOL content of formulations. CHOL molecules accommodate within the

free space that was formed due to the kink in the chain of unsaturated lipids, causing a decrease in the flexibility of the surrounding lipid chains (Monteiro et al., 2014); therefore, the loading of the inclusion complexes into liposomal aqueous phase is lowered. It should be mentioned that the EE of CAM fits in the relationship demonstrated between EE and CHOL content of DCLs. However, α-PIN exhibited a high EE into DCLs that does not fit in the relationship. It would be that the interaction of α-PIN with CD and lipid bilayer is strong enough to inhibit its release to the outer extracellular medium of DCL. As explained before, α-PIN has a high affinity for lipid membranes. Also, the strong interaction between α-PIN and CD may be attributed to the higher hydrophobicity (higher log P value) of α-PIN compared to the other selected EO components (Kfoury et al., 2014). Hence, the high hydrophobicity of α-PIN could explain the peculiar characteristics of α-PIN-loaded DCLs when compared to DCLs carrying the other EO components.

In this work, a linear increase in the LR of MTs into DCLs was observed with the increases in log P value of compounds. This was ascribed to the strong positive correlation between log P of MTs and the K_f value of HP-β-CD/MT inclusion complex (Kfoury et al., 2014). The HP-β-CD/MT inclusion complex with a greater K_f value (complex entrapping MT with greater log P) presented an improved retention of MT into HP-β-CD cavity; thus, the loading of MT into DCL would further increase. Nevertheless, this relationship was not maintained when dealing with α-PIN and CAM. Namely, α-PIN that possesses a high logP value demonstrated a low LR into DCLs and CAM that exhibits a low logP value demonstrated a high LR into DCLs. A few studies investigated the effect of co-solvents, including ethanol, on the formation of inclusion complexes between CD and various guest molecules. And the literature data regarding the effect of co-solvents and CDs on the solubility improvement of a drug are controversial. Some studies proved that the presence of a co-solvent facilitates the complex formation by dissolving the guest before entering the CD cavity. In addition, the co-solvent could dissolve the excess

guest molecules which are not incorporated into the CDs cavity (Charumanee et al., 2016). However, a destabilizing effect on CDs complexation, caused by co-solvents, has also been reported; cosolvents induced a decrease in complexation efficiency and K_f of inclusion complexes (Nakhle et al., 2020). In this case, two mechanisms have been discussed: First, at a certain concentration of the cosolvent, the environment became more hydrophobic and the guests tend to dissolve in the surrounding medium rather than entering the CD cavity. This hampered the driving forces of the complex formation (Loftsson and Brewster, 2012). Secondly, the co-solvent can compete with a drug molecule to occupy the space in the CDs cavity (Boonyarattanakalin, 2015). Namely, adding co-solvents, like ethanol, to complexing media (CD and guest) can help the formation of drug-CD-cosolvent ternary complex or can be harmful to the formation of CD/drug binary complex. The effectiveness of CD in solvent/water mixtures depended on several factors like the type of CD, the guest structure and the characteristics of the medium (solvent type and percentage, hydrophobicity, etc.) (Charumanee et al., 2016; Li et al., 2009; Nakhle et al., 2020). As shown in Table 1, α-PIN exhibits a very low aqueous solubility value compared to the other EO components which means that the interaction between α-PIN and ethanol is stronger than the interaction between the other selected EO components and ethanol; the existence of ethanol may lead to the dissociation of HP-β-CD/ α-PIN inclusion complex rather than the formation of α-PIN – HP-β-CD–ethanol ternary complex. Therefore, it could be suitable to analyze the stability of inclusion complex in the presence of ethanol. On the other hand, to our knowledge, the literature lacks noticeable data on the interaction of camphor with lipid membranes. For that, the factors that induced its high loading into DCLs cannot be estimated from literature data. However, it might be that one of the major interactions responsible for retaining CAM into DCLs is a strong hydrogen bonding between carbonyl group of CAM (hydrogen bond acceptor group) and any hydrogen bond donor group in lipid membranes (such as CHOL hydroxyl group, NH^+_3 group of phosphatiylethanolamine head group, etc.) or in HP-β-

CD. As HP-β-CD contains 25- and 39- hydrogen bond donor and acceptor groups, respectively (Saokham et al., 2018), the formation of hydrogen bonds between the carbonyl group of CAM and CD would also take place. Moreover, it may be that adding ethanol to complexing media (HP-β-CD and CAM) induced forming CAM–HP-β-CD–ethanol ternary complex rather than distabilizing HP-β-CD/CAM inclusion complex (CAM interaction with ethanol is weaker compared to the other EO components).

3.3. The factors affecting the release of EO components from DCLs

The release of the EO components from CD/drug inclusion complex and from DCL was analyzed investigating the factors that influence this release. Hc was demonstrated as a key factor controlling the release of EO components from HP-β-CD/EO component inclusion complex. The release of components from DCLs was not affected by their Hc; thus the release mechanism of EO components from DCLs is more complex in comparison to HP-β-CD as additional parameters modulate their release from DCLs. The EE of EO components was shown to influence their release from the DCL vesicles, in accordance with Piel et al. (2006) who demonstrated a direct correlation between the EE of betamethasone into DCLs and their release rate from vesicles using different CD types (HP-β-CD, randomly methylated β-CD, partially methylated crystallized-β-CD, HP-γ-CD) and CD concentrations (10, 40 mM).

As a conclusion, liposomes and DCLs could be useful for the encapsulation of EO components, extending their various applications. The results obtained in this work may allow estimating the capability of lipoid S100-CLs and DCLs to entrap an EO component based on its physiochemical properties. Furthermore, the developed formulations may be suitable for preventing microbial spoilage of various food, cosmetics and pharmaceutical products during storage.

4. CLs versus DCLs

In my thesis, we demonstrated that DCLs significantly improved the LR of CAM, EST, PUL, and THY compared to CLs. Literature studies showed that the incorporation of several hydrophobic drugs including *trans*-anethole, which is an isomer of EST (Gharib et al., 2017a), and betamethasone (Piel et al., 2006) into liposomes in the form of CD/drug inclusion complex resulted in an improvement of drug encapsulation compared to CLs. DCLs did not ameliorate the LR of α-PIN, EUC, ISOEUG, and TER, in accordance with Wang et al., (2016) who proved, using the same lipid composition and CD type used here, that CL caused better encapsulation for risperidone than DCL.

The storage stability of the various CL and DCL formulations was evaluated: after 10 months of storage at 4 ºC for EST, EUC, ISOEUG, PUL, TER and THY; after 3 months of storage for α-PIN and CAM. In general, most of the prepared CLs and DCLs were stable after storage where the retention of EO components in the various formulations is satisfactory, and the DCL carrier system was more effective in reducing EO component release with respect to CL.

The characteristics (size, PL IR, CHOL IR, drug EE, drug LR, and storage stability) of α-PIN- and CAM-loaded CLs and DCLs were analyzed using Lipoid S100 and Phospholipon 90H in combination with CHOL. It was found that Lipoid S100-CL was the best encapsulating system for α-PIN compared to the other formulations. Lipoid S100-DCL was the best system for CAM encapsulation. The encapsulation of the insecticidal agent EUC into Phospholipon 90H:CHOL-liposomes and DCLs was previously characterized before and after freeze-drying. These results revealed that freeze-dried DCL presented better retention of EUC compared to CLs (Gharib et al., 2020). The best encapsulation system for α-PIN, CAM and EUC could be later selected for its potential use in agriculture and food products.

Perspectives

Future studies could be conducted to test the effectiveness of CLs and DCLs loading EUC, α-PIN- and CAM as well as the free EOs on different species of pests, namely: *Ectomyelois ceratoniae, Ephestia kuehniella, Tribolium castaneum and Carpophilus hemipterus* which are considered among the most destructive species of dates and other stored food. To increase their shelf life, it is necessary to freeze-dry the CL and DCL formulations containing α-PIN- and CAM before their applications, and the stability of the formulations during freeze drying should be assessed. Additionally, the stability of the various CD/drug inclusion complexes in the presence of ethanol could be analyzed for determining the factors (drug structure and physicochemical properties) that influence the stability of CD/drug inclusion complex in ethanol/water mixtures. In light of the results obtained in this work, fluorescent CDs could be used to track the location (aqueous phase or membrane) of CDs and CD/drug inclusion complexes in liposomes. Moreover, by conjugating a fluorescent dye to an EO component, the forms and the locations of the drug in DCL vesicles (inside or outside the particles, as free drug in membrane or aqueous phase, as inclusion complex in membrane or aqueous phase) could be monitored to get solid evidence on DCL structure and properties.

References:

Astani, A., Reichling, J., Schnitzler, P., 2010. Comparative study on the antiviral activity of selected monoterpenes derived from essential oils: ANTIVIRAL ACTIVITY OF MONOTERPENES DERIVED FROM ESSENTIAL OILS. Phytother. Res. 24, 673–679. https://doi.org/10.1002/ptr.2955

Azzi, J., Auezova, L., Danjou, P.-E., Fourmentin, S., Greige-Gerges, H., 2018. First evaluation of drug-in-cyclodextrin-in-liposomes as an encapsulating system for nerolidol. Food Chem. 255, 399–404. https://doi.org/10.1016/j.foodchem.2018.02.055

Boonyarattanakalin, K., 2015. Influence of Ethanol as Co-Solvent in Cyclodextrin Inclusion Complexation: A Molecular Dynamics Study. Sci. Pharm. 83, 387–399. https://doi.org/10.3797/scipharm.1412-08

Charumanee, S., Okonogi, S., Sirithunyalug, J., Wolschann, P., Viernstein, H., 2016. Effect of Cyclodextrin Types and Co-Solvent on Solubility of a Poorly Water Soluble Drug. Sci. Pharm. 84, 694–704. https://doi.org/10.3390/scipharm84040694

Ciobanu, A., Landy, D., Fourmentin, S., 2013. Complexation efficiency of cyclodextrins for volatile flavor compounds. Food Res. Int. 53, 110–114. https://doi.org/10.1016/j.foodres.2013.03.048

Cristani, M., D'Arrigo, M., Mandalari, G., Castelli, F., Sarpietro, M.G., Micieli, D., Venuti, V., Bisignano, G., Saija, A., Trombetta, D., 2007. Interaction of Four Monoterpenes Contained in Essential Oils with Model Membranes: Implications for Their Antibacterial Activity. J. Agric. Food Chem. 55, 6300–6308. https://doi.org/10.1021/jf070094x

Denz, M., Haralampiev, I., Schiller, S., Szente, L., Herrmann, A., Huster, D., Müller, P., 2016. Interaction of fluorescent phospholipids with cyclodextrins. Chem. Phys. Lipids 194, 37–48. https://doi.org/10.1016/j.chemphyslip.2015.07.017

Domazou, A.S., Luigi Luisi, P., 2002. SIZE DISTRIBUTION OF SPONTANEOUSLY FORMED LIPOSOMES BY THE ALCOHOL INJECTION METHOD. J. Liposome Res. 12, 205–220. https://doi.org/10.1081/LPR-120014758

Ermilova, I., Lyubartsev, A.P., 2019. Cholesterol in phospholipid bilayers: positions and orientations inside membranes with different unsaturation degrees. Soft Matter 15, 78–93. https://doi.org/10.1039/C8SM01937A

Fang, J.-Y., Hong, C.-T., Chiu, W.-T., Wang, Y.-Y., 2001. Effect of liposomes and niosomes on skin permeation of enoxacin. Int. J. Pharm. 219, 61–72. https://doi.org/10.1016/S0378-5173(01)00627-5

García, M., Donadel, O.J., Ardanaz, C.E., Tonn, C.E., Sosa, M.E., 2005. Toxic and repellent effects ofBaccharis salicifolia essential oil onTribolium castaneum. Pest Manag. Sci. 61, 612–618. https://doi.org/10.1002/ps.1028

Gharib, R., Auezova, L., Charcosset, C., Greige-Gerges, H., 2018a. Effect of a series of essential oil molecules on DPPC membrane fluidity: a biophysical study. J. Iran. Chem. Soc. 15, 75–84. https://doi.org/10.1007/s13738-017-1210-1

Gharib, R., Auezova, L., Charcosset, C., Greige-Gerges, H., 2017a. Drug-in-cyclodextrin-in-liposomes as a carrier system for volatile essential oil components: Application to anethole. Food Chem. 218, 365–371. https://doi.org/10.1016/j.foodchem.2016.09.110

Gharib, R., Fourmentin, S., Charcosset, C., Greige-Gerges, H., 2018b. Effect of hydroxypropyl-β–cyclodextrin on lipid membrane fluidity, stability and freeze-drying of liposomes. J. Drug Deliv. Sci. Technol. 44, 101–107. https://doi.org/10.1016/j.jddst.2017.12.009

Gharib, R., Greige-Gerges, H., Fourmentin, S., Charcosset, C., Auezova, L., 2015. Liposomes incorporating cyclodextrin–drug inclusion complexes: Current state of knowledge. Carbohydr. Polym. 129, 175–186. https://doi.org/10.1016/j.carbpol.2015.04.048

Gharib, R., Jemâa, J.M.B., Charcosset, C., Fourmentin, S., Greige-Gerges, H., 2020. Retention of Eucalyptol, a Natural Volatile Insecticide, in Delivery Systems Based on Hydroxypropyl-β-Cyclodextrin and Liposomes. Eur. J. Lipid Sci. Technol. 122, 1900402. https://doi.org/10.1002/ejlt.201900402

Gharib, R., Najjar, A., Auezova, L., Charcosset, C., Greige-Gerges, H., 2017b. Interaction of Selected Phenylpropenes with Dipalmitoylphosphatidylcholine Membrane and Their Relevance to Antibacterial Activity. J. Membr. Biol. 250, 259–271. https://doi.org/10.1007/s00232-017-9957-y

Harroun, T.A., Katsaras, J., Wassall, S.R., 2006. Cholesterol Hydroxyl Group Is Found To Reside in the Center of a Polyunsaturated Lipid Membrane. Biochemistry 45, 1227–1233. https://doi.org/10.1021/bi0520840

Jug, M., Mennini, N., Melani, F., Maestrelli, F., Mura, P., 2010. Phase solubility, 1H NMR and molecular modelling studies of bupivacaine hydrochloride complexation with different cyclodextrin derivates. Chem. Phys. Lett. 500, 347–354. https://doi.org/10.1016/j.cplett.2010.10.046

Justo, O.R., Moraes, Ã.M., 2010. Economical Feasibility Evaluation of an Ethanol Injection Liposome Production Plant. Chem. Eng. Technol. 33, 15–20. https://doi.org/10.1002/ceat.200800502

Kfoury, M., Auezova, L., Fourmentin, S., Greige-Gerges, H., 2014. Investigation of monoterpenes complexation with hydroxypropyl-β-cyclodextrin. J. Incl. Phenom. Macrocycl. Chem. 80, 51–60. https://doi.org/10.1007/s10847-014-0385-7

Kfoury, M., Hădărugă, N.G., Hădărugă, D.I., Fourmentin, S., 2016. Cyclodextrins as encapsulation material for flavors and aroma, in: Encapsulations. Elsevier, pp. 127–192. https://doi.org/10.1016/B978-0-12-804307-3.00004-1

Li, R., Quan, P., Liu, D.-F., Wei, F.-D., Zhang, Q., Xu, Q.-W., 2009. The Influence of Cosolvent on the Complexation of HP-β-cyclodextrins with Oleanolic Acid and Ursolic Acid. AAPS PharmSciTech 10, 1137. https://doi.org/10.1208/s12249-009-9317-z

Loftsson, T., Brewster, M.E., 2012. Cyclodextrins as Functional Excipients: Methods to Enhance Complexation Efficiency. J. Pharm. Sci. 101, 3019–3032. https://doi.org/10.1002/jps.23077

Marques, H.M.C., 2010. A review on cyclodextrin encapsulation of essential oils and volatiles. Flavour Fragr. J. 25, 313–326. https://doi.org/10.1002/ffj.2019

Monteiro, N., Martins, A., Reis, R.L., Neves, N.M., 2014. Liposomes in tissue engineering and regenerative medicine. J. R. Soc. Interface 11, 20140459–20140459. https://doi.org/10.1098/rsif.2014.0459

Moretti, M.D.L., Sanna-Passino, G., Demontis, S., Bazzoni, E., 2002. Essential oil formulations useful as a new tool for insect pest control. AAPS PharmSciTech 3, 64–74. https://doi.org/10.1208/pt030213

Mossa, A.-T.H., 2016. Green Pesticides: Essential Oils as Biopesticides in Insect-pest Management. J. Environ. Sci. Technol. 9, 354–378. https://doi.org/10.3923/jest.2016.354.378

Nakhle, L., Kfoury, M., Greige-Gerges, H., Fourmentin, S., 2020. Effect of dimethylsulfoxide, ethanol, α- and β-cyclodextrins and their association on the solubility of natural bioactive compounds. J. Mol. Liq. 310, 113156. https://doi.org/10.1016/j.molliq.2020.113156

Ohtani, Y., Irie, T., Uekama, K., Fukunaga, K., Pitha, J., 1989. Differential effects of alpha-, beta- and gamma-cyclodextrins on human erythrocytes. Eur. J. Biochem. 186, 17–22.

Pandey, A.K., Kumar, P., Singh, P., Tripathi, N.N., Bajpai, V.K., 2017. Essential Oils: Sources of Antimicrobials and Food Preservatives. Front. Microbiol. 7. https://doi.org/10.3389/fmicb.2016.02161

Piel, G., Piette, M., Barillaro, V., Castagne, D., Evrard, B., Delattre, L., 2006. Betamethasone-in-cyclodextrin-in-liposome: The effect of cyclodextrins on encapsulation efficiency and release kinetics. Int. J. Pharm. 312, 75–82. https://doi.org/10.1016/j.ijpharm.2005.12.044

Rizvi, S.A.A., Saleh, A.M., 2018. Applications of nanoparticle systems in drug delivery technology. Saudi Pharm. J. 26, 64–70. https://doi.org/10.1016/j.jsps.2017.10.012

Rodriguez, S.A., Pinto, O.A., Hollmann, A., 2018. Interaction of semiochemicals with model lipid membranes: A biophysical approach. Colloids Surf. B Biointerfaces 161, 413–419. https://doi.org/10.1016/j.colsurfb.2017.11.002

Saokham, P., Muankaew, C., Jansook, P., Loftsson, T., 2018. Solubility of Cyclodextrins and Drug/Cyclodextrin Complexes. Molecules 23, 1161. https://doi.org/10.3390/molecules23051161

Sebaaly, C., Greige-Gerges, H., Stainmesse, S., Fessi, H., Charcosset, C., 2016. Effect of composition, hydrogenation of phospholipids and lyophilization on the characteristics of eugenol-loaded liposomes prepared by ethanol injection method. Food Biosci. 15, 1–10. https://doi.org/10.1016/j.fbio.2016.04.005

Sebaaly, C., Jraij, A., Fessi, H., Charcosset, C., Greige-Gerges, H., 2015. Preparation and characterization of clove essential oil-loaded liposomes. Food Chem. 178, 52–62. https://doi.org/10.1016/j.foodchem.2015.01.067

Sikkema, J., de Bont, J.A., Poolman, B., 1995. Mechanisms of membrane toxicity of hydrocarbons. Microbiol. Rev. 59, 201–222.

Solórzano-Santos, F., Miranda-Novales, M.G., 2012. Essential oils from aromatic herbs as antimicrobial agents. Curr. Opin. Biotechnol. 23, 136–141. https://doi.org/10.1016/j.copbio.2011.08.005

Storti, F., Balsamo, F., 2010. Particle size distributions by laser diffraction: sensitivity of granular matter strength to analytical operating procedures. Solid Earth 1, 25–48. https://doi.org/10.5194/se-1-25-2010

Tanaka, M., Matsuda, H., Sumiyoshi, H., Arima, H., Hirayama, F., Uekama, K., Tsuchiya, S., 1996. 2-Hydroxypropylated Cyclodextrins as a Sustained-Release Carrier for Fragrance Materials. Chem. Pharm. Bull. (Tokyo) 44, 416–420. https://doi.org/10.1248/cpb.44.416

Wang, W.-X., Feng, S.-S., Zheng, C.-H., 2016. A comparison between conventional liposome and drug-cyclodextrin complex in liposome system. Int. J. Pharm. 513, 387–392. https://doi.org/10.1016/j.ijpharm.2016.09.043

Wiącek, A., Chibowski, E., 1999. Zeta potential, effective diameter and multimodal size distribution in oil/water emulsion. Colloids Surf. Physicochem. Eng. Asp. 159, 253–261. https://doi.org/10.1016/S0927-7757(99)00281-2

Yancey, P.G., Rodrigueza, W.V., Kilsdonk, E.P., Stoudt, G.W., Johnson, W.J., Phillips, M.C., Rothblat, G.H., 1996. Cellular cholesterol efflux mediated by cyclodextrins. Demonstration Of kinetic pools and mechanism of efflux. J. Biol. Chem. 271, 16026–16034.